

**GUANIDINE CATALYZED ENANTIOSELECTIVE  
MANNICH REACTION: TOWARDS THE SYNTHESIS  
OF  $\beta$ -AMINO ACIDS**

**PAN YUANHANG**

**NATIONAL UNIVERSITY OF SINGAPORE**

**2011**

**GUANIDINE CATALYZED ENANTIOSELECTIVE  
MANNICH REACTION: TOWARDS THE SYNTHESIS  
OF  $\beta$ -AMINO ACIDS**

**PAN YUANHANG**

*(BSc., Zhejiang University)*

**A THESIS SUBMITTED**

**FOR THE DEGREE OF DOCTOR OF PHILOSOPHY**

**DEPARTMENT OF CHEMISTRY**

**NATIONAL UNIVERSITY OF SINGAPORE**

*To my parents  
for their love, support, and encouragement*

## Acknowledgements

I would like to take this opportunity to thank my supervisor, Associate Professor Tan Choon-Hong, for his guidance and encouragement during my PhD research and study. It is my honour to work with him, and his suggestions, especially his optimistic attitude to research and life, are valuable to me, not only for my PhD study, but also for my future career life.

I would like to thank all my labmates for creating such a harmonious, encouraging, and helpful working environment. My special thanks go to Dr Jiang Zhiyong, for his great help throughout my two projects and my life; Mr. Kee Choon Wee for his kind discussion and collaboration on the decarboxylation project; Mr. Zhao Yujun, for his collaboration on the fluorocarbon nucleophile project; Mr. Liu Hongjun, Ma Ting and Yang Yuanyong for their kind suggestions. I also must thank all of the former and TCH group members for their collaboration and helpful discussions.

I thank Mdm Han Yanhui and Mr. Wong Chee Ping for their assistance in NMR analysis, Mdm Wong Lai Kwai and Mdm Lai Hui Ngee for their assistance in Mass analysis. I also owe my thanks to many other people in NUS chemistry department, for their help and assistance from time to time.

Last but not least, I also would like to take this opportunity to thank all my friends who have shared or is sharing the happy time with me in Singapore. Singapore is a wonderful place and I enjoy my life here.

## Thesis Declaration

The work in this thesis is the original work of Pan Yuanhang, performed independently under the supervision of Associate Professor Tan Choon-Hong, (in TCH laboratory), Chemistry Department, National University of Singapore, between 2007 and 2011.

The content of the thesis has been partly published in:

- 1) *Chem. Eur. J.* **2011**, *17*, 8363.
- 2) *Chem. Eur. J.* **2010**, *16*, 779.

---

Name

---

Signature

---

Date

# Table of Contents

**Summary**

**List of Schemes**

**List of Tables**

**List of Figures**

**List of Abbreviations**

## **Chapter 1**

Biomimetic Decarboxylative Reactions

1.1 Introduction-----	2
1.2 Decarboxylative Reactions Catalyzed by Metal Complexes-----	2
1.2.1 Condensation Reaction-----	2
1.2.2 Aldol Reaction-----	4
1.2.3 1,4-Addition-----	8
1.3 Organocatalytic Decarboxylative Reactions-----	10
1.3.1 Condensation Reaction-----	10
1.3.2 Aldol Reaction-----	11
1.3.3 1,4-Addition-----	13
1.3.4 Mannich Reaction-----	15
1.3.5 Protonation-----	19
1.4 Summary-----	21

## Chapter 2

### Bicyclic Guanidine Catalyzed Enantioselective Decarboxylative Mannich and Amination Reactions

2.1 Introduction-----	26
2.2 Enantioselective Decarboxylative Mannich Reaction-----	30
2.2.1 Synthesis of Malonic Acid Half Thioesters (MAHTs)-----	30
2.2.2 Synthesis of <i>N</i> -Sulfonyl Imines-----	31
2.2.3 Synthesis of Chiral Bicyclic Guanidine-----	31
2.2.4 Decarboxylative Mannich Reaction of MAHTs-----	32
2.3 Enantioselective Decarboxylative Amination Reaction-----	37
2.4 Summary-----	40
2.5 Experimental Section-----	41

## Chapter 3

### Mechanistic Studies of Guanidine Catalyzed Decarboxylative Mannich Reaction

3.1 Introduction-----	76
3.2 NMR Study of the Reaction Profile-----	78
3.3 Mass Spectrometry Study of the Reaction Profile-----	80
3.4 DFT Calculation-----	81
3.5 Proposed Mechanism-----	84
3.6 Summary-----	86
3.7 Experimental Section-----	87

## **Chapter 4**

### Bicyclic Guanidine Catalyzed Enantioselective Mannich Reaction of Fluorocarbon Nucleophiles

4.1 Fluorocarbon Nucleophiles-----	92
4.2 Enantioselective Mannich Reaction of Fluorocarbon Nucleophiles-----	98
4.2.1 Synthesis of Fluorocarbon Nucleophiles-----	98
4.2.2 Synthesis of <i>N</i> -Carbonyl Imines-----	99
4.2.3 Mannich Reaction of Fluorinated $\beta$ -keto Acetyloxazolidinone-----	100
4.2.4 Selectively Deacylation/Decarboxylation-----	103
4.2.5 Mannich Reaction of other Fluorocarbon Nucleophiles-----	106
4.3 Experimental Section-----	108
<b>Appendix</b> -----	149
<b>Publications</b> -----	221

## Summary

The aim of this study is to develop guanidine catalyzed highly enantioselective Mannich reactions.

Inspired by nature, we developed chiral bicyclic guanidine catalyzed biomimetic decarboxylative Mannich reaction of malonic acid half thioesters. Moderate to good yields (up to 85% yield) and high enantioselectivities (up to 98% *ee*) were achieved with various malonic acid half thioesters including  $\alpha$ -alkyl substituted malonic acid half thioesters which were developed for the first time. The decarboxylative amination reaction also showed good yields (up to 90% yield) and high *ee* values (up to 90% *ee*). This methodology provided the synthetic route towards both  $\beta$ -amino acid derivatives and  $\alpha$ -amino acid derivatives.

Mechanistically, based on the experimental characterization of intermediates and theoretical calculations, we proposed that the decarboxylative Mannich reaction underwent a fast nucleophilic addition followed by a slow decarboxylation. The rate-determining step was the slow decarboxylation.

In addition, we have developed a highly enantio- and diastereoselective guanidine-catalyzed Mannich reaction with  $\alpha$ -fluoro- $\beta$ -keto acyloxazolidinone as the fluorocarbon nucleophile (up to 99% yield, up to 99:1 *dr*, up to >99% *ee*).  $\alpha$ -Fluoro- $\beta$ -amino acid derivatives with chiral fluorinated carbon were obtained *via* selective deacylation or decarboxylation reaction. A transient enolate was obtained *via* retro-Claisen or decarboxylation followed by protonation to give enantiopure fluorinated compounds.

## List of Schemes

- Scheme 1.1** Claisen condensation in polyketide biosynthesis
- Scheme 1.2** Biomimetic decarboxylative Claisen condensation
- Scheme 1.3** Catalytic decarboxylative aldol reaction of benzol MAHT with various aldehydes
- Scheme 1.4** Enantioselective decarboxylative aldol reaction of MeMAHT with various aldehydes
- Scheme 1.5** Two proposed mechanisms of decarboxylative reactions
- Scheme 1.6** The deprotonation of MeMAHT-Cu complex
- Scheme 1.7** Asymmetric synthesis of antidepressant (*S*)-rolipram
- Scheme 1.8** Self-condensation of MAHOs promoted by TSTU.
- Scheme 1.9** Decarboxylative aldol reaction of MAHO/MAHT with ethyl pyruvate
- Scheme 1.10** Proposed mechanism of Et<sub>3</sub>N-catalyzed decarboxylative aldol reaction
- Scheme 1.11** Catalyst design for decarboxylative 1,4-addition of MAHT to nitro-olefins
- Scheme 1.12** Proposed mechanism of asymmetric decarboxylative Mannich reaction
- Scheme 1.13** Et<sub>3</sub>N promoted decarboxylative Mannich reaction
- Scheme 1.14** Proposed mechanism for decarboxylative protonations
- Scheme 1.15** Brunner's observation of decarboxylative protonation of MAHO
- Scheme 1.16** Enantioselective decarboxylative protonation of acyclic *N*-MAHO

- Scheme 1.17** Highly enantioselective decarboxylative protonation of cyclic *N*-MAHO
- Scheme 2.1** Direct Michael addition between trifluoroethyl thioester and  $\alpha,\beta$ -unsaturated aldehydes
- Scheme 2.2** Asymmetric Mannich reaction of phenylacetate thioesters by soft enolization
- Scheme 2.3** Cross-aldol reaction of isatins and ketones
- Scheme 2.4** Synthesis of MAHTs started from diethyl malonate
- Scheme 2.5** Synthesis of *N*-sulfonyl imines
- Scheme 2.6** Synthesis of bicyclic guanidine
- Scheme 2.7** Proposed model of biomimetic decarboxylative Mannich reaction
- Scheme 2.8** Highly enantioselective decarboxylative Mannich reaction between MAHT **83b** and imines
- Scheme 2.9** Highly enantioselective decarboxylative Mannich reaction between  $\alpha$ -alkyl MAHTs and imines
- Scheme 2.10** Decarboxylative amination reaction of  $\alpha$ -alkyl MAHTs
- Scheme 2.11** Highly enantioselective decarboxylative Mannich reaction between  $\alpha$ -alkyl MAHTs and imines
- Scheme 3.1** Decarboxylative Aldol reaction of MAHO and MAHT
- Scheme 3.2** Reaction of MAHT **83b** with imine **86a** monitored by  $^1\text{H}$  NMR in THF- $d_8$
- Scheme 3.3** Reaction of MAHT **83** with imine **86** catalyzed by guanidine **92**
- Scheme 3.4** Proposed mechanism of decarboxylative Mannich reaction
- Scheme 4.1** Protocols to construct chiral C-F bond

- Scheme 4.2** Asymmetric Mannich reaction catalyzed by tryptophan-derived catalyst **109**
- Scheme 4.3** Asymmetric alkylation of  $\alpha$ -fluoro- $\beta$ -ketoesters under phase transfer conditions
- Scheme 4.4** Asymmetric conjugate addition of  $\alpha$ -fluoro- $\beta$ -ketoesters catalyzed by bicyclic guanidine
- Scheme 4.5** Preparation of  $\alpha$ -fluoro- $\beta$ -keto acyloxazolidinones
- Scheme 4.6** Synthesis of *N*-carbonyl imines
- Scheme 4.7** Highly enantioselective and diastereoselective reactions between  $\beta$ -keto acetyloxazolidinone **1c** and *N*-Eoc imines
- Scheme 4.8** Useful transformations of the Mannich product
- Scheme 4.9** Proposed mechanism of deacylation of Mannich product **129g**
- Scheme 4.10** Proposed mechanism of decarboxylation of Mannich product **129g**
- Scheme 4.11** Cleavage of *N*-Eoc imine under acidic condition
- Scheme 4.12** Asymmetric Mannich reaction of FPSO and FNSM

## List of Tables

- Table 1.1** Catalytic Doebner-Knoevenagel condensations between MAHT **7** and various aldehydes
- Table 1.2** Catalytic asymmetric decarboxylative 1,4-addition of MAHT **7** to nitro-olefins
- Table 1.3** A practical synthesis of  $\alpha,\beta$ -unsaturated esters from aldehydes
- Table 1.4** Scope of the decarboxylative 1,4-addition of MAHT to nitro-olefins
- Table 1.5** Asymmetric decarboxylative Mannich reaction of MAHT with imines
- Table 2.1** Optimization of decarboxylative Mannich reaction between MAHTs and imine **86a**
- Table 2.2** Optimization of decarboxylative Mannich reaction between MeMAHT **83c** and imine **86a**
- Table 4.1** Highly enantioselective and diastereoselective Mannich reactions of fluorocarbon nucleophiles

## List of Figures

- Figure 1.1** Structures of compounds **46** and **47**
- Figure 1.2** Monitoring of the reaction in DMF-*d*<sub>7</sub> as a function of time at room temperature
- Figure 2.1** p*K*<sub>a</sub> values of α-protons of nucleophiles in DMSO
- Figure 3.1** Characterization of intermediate **102a** and **102b** via <sup>1</sup>H NMR
- Figure 3.2** Monitoring the reaction mixture at 10 °C in THF-*d*<sub>8</sub>
- Figure 3.3** Detection of counter-anions of **102a** or **102b** by direct injection ESI-MS
- Figure 3.4** DFT calculation results
- Figure 3.5** Stationary points
- Figure 4.1** Two possible transition state models

## List of Abbreviations

MAHT	malonic acid half thioester
MAHO	malonic acid half oxyester
MeMAHT	methyl malonic acid half thioester
FBSM	1-Fluoro-bis(phenylsulfonyl)methane
FSM	fluoro(phenylsulfonyl) methane
<i>N</i> -Eoc	<i>N</i> -3-ethylpentan-3-yloxycarbonyl
FSPO	1-fluoro-1-(phenylsulfonyl)propan-2-one
FNSM	$\alpha$ -Fluoro- $\alpha$ -nitro-(phenylsulfonyl)methane
AcOH	acetic acid
Ac	acetyl
$[\alpha]$	optical rotation
aq.	aqueous
Ar	aryl
Bn	benzyl
Boc	<i>tert</i> -Butyloxycarbonyl
<i>t</i> Bu	<i>tert</i> -butyl
c	concentration
cat.	catalyst
<i>m</i> CPBA	<i>meta</i> -Chloroperoxybenzoic acid
Cbz	Carbobenzyloxy
CDI	1,1'-carbonyldiimidazole

°C	degrees (Celcius)
δ	chemical shift in parts per million
DCM	dichloromethane
DFT	density functional theory
DMAP	4-dimethylaminopyridine
DMSO	dimethyl sulfoxide
<i>dd</i>	doublet of doublet
dr	diastereomeric ratio
<i>ee</i>	enantiomeric excess
EI	electron impact ionization
ESI	electro spray ionization
Et	ethyl
Et <sub>3</sub> N	triethylamine
Eoc	ethoxycarbonyl
FAB	fast atom bombardment ionization
FTIR	fourier transformed infrared spectroscopy
g	grams
ΔG	Gibbs free energy
h	hour(s)
HPLC	high pressure liquid chromatography
HRMS	high resolution mass spectroscopy
Hz	hertz

i.d.	internal diameter
IR	infrared
<i>J</i>	coupling constant
LRMS	low resolution mass spectroscopy
Me	methyl
MeCN	acetonitrile
MeOH	methanol
mg	milligram
MHz	megahertz
min.	minute(s)
ml	milliliter
μl	microliter
mmol	millimole
MS	mass spectroscopy
MeNO <sub>2</sub>	nitromethane
NMR	nuclear magnetic resonance
NC	not checked
ppm	parts per million
<i>i</i> Pr	isopropyl
Ph	phenyl
PTC	phase transfer catalyst
rt	room temperature

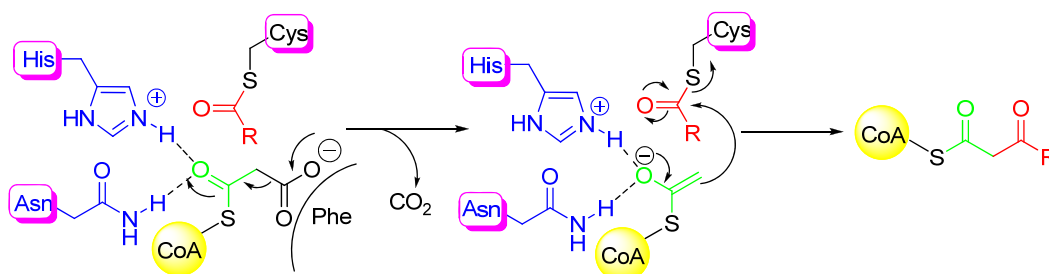
<i>rac</i>	racemic
TBD	1,5,7-Triazabicyclo[4.4.0]dec-5-ene
TBAF	tetrabutylammonium fluoride
TFA	trifluoroacetic acid
TFAA	trifluoroacetic anhydride
THF	tetrahydrofuran
TLC	thin layer chromatography
TMSI	iodotrimethylsilane
TMSOTf	Trimethylsilyl trifluoromethanesulfonate
TS	transition state
TsCl	<i>para</i> -toluenesulfonyl chloride
Ts	<i>para</i> -toluenesulfonyl
TsOH	<i>para</i> -toluenesulfonic acid
M	mol·l <sup>-1</sup>
TSTU	<i>O</i> -( <i>N</i> -Succinimidyl)- <i>N,N,N,N</i> -tetramethyluroniumtetra-fluoroborate
Tol	toluene
d	day

***Chapter 1***

***Biomimetic Decarboxylative Reactions***

## 1.1 Introduction

Nature's ability to form carbon-carbon bonds under mild conditions has been an inspiration and motivation for synthetic chemists. For example, the biosynthesis of polyketides required the generation of ester enolates under physiological conditions, which forbidden the use of strong bases.<sup>1</sup> This feat is achieved through decarboxylation of malonic acid half thioester (MAHT), a process catalyzed by polyketide synthase (PKS). His and Asn of PKS activate MAHT towards decarboxylation and the resulting thioester enolate undergoes electrophilic trapping with an acyl unit to furnish the Claisen condensation product (Scheme 1.1).<sup>1c</sup> The attention of chemists is drawn towards such strategy and the use of MAHTs and malonic acid half oxyesters (MAHOs) as precursors of ester enolates.



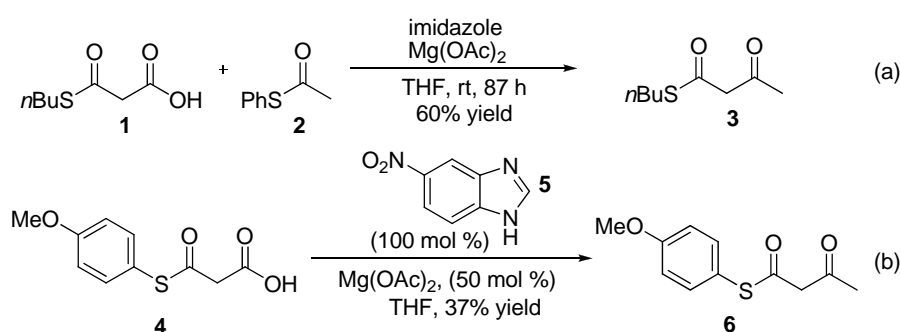
**Scheme 1.1** Claisen condensation in polyketide biosynthesis

The decarboxylative reactions of MAHTs and MAHOs have been investigated by many generations of chemists. Both asymmetric and non-asymmetric decarboxylative reactions have been reported. This chapter reviews catalytic decarboxylative reactions of MAHTs and MAHOs mediated by metal complexes and organocatalysts as well as those using stoichiometric amount of promoters.

## 1.2 Decarboxylative Reactions Catalyzed by Metal Complexes

### 1.2.1 Condensation Reaction

More than 30 years ago, Kobuke first demonstrated that decarboxylative Claisen condensation can be promoted in an enzyme free condition with magnesium acetate (Scheme 1.2a).<sup>2</sup> The formation of *n*-butyl thioester **3** indicated that the nucleophile originated from *n*-butyl MAHT **1** rather than thioacetate **2**.



**Scheme 1.2** Biomimetic decarboxylative Claisen condensation

This method is significant as it may lead to better design of artificial polyketide synthase (PKS). Many histidine-rich organic structures with esterase and/or phosphatase activity have been elegantly devised over the past few decades. However, this condition is incompatible with Claisen self-condensation, required for the oligomerizations, which leads to polyketides. The self-condensation of *n*-butyl MAHT **1** or phenyl thioacetate **2** was impossible due to the poor leaving group of *n*-butylthiolate or lack of access to activated carbanion intermediates *via* decarboxylation, respectively. Later, Matile solved this problem by tuning the properties of the thiolate leaving group and the catalyst.<sup>3</sup> When *para*-methoxyl phenyl MAHT **4** was used as the substrate, and 5-nitro-benzimidazole **5** as the

catalyst, the self-condensation product **6** was obtained while the yield was only 37% (Scheme 1.2b).

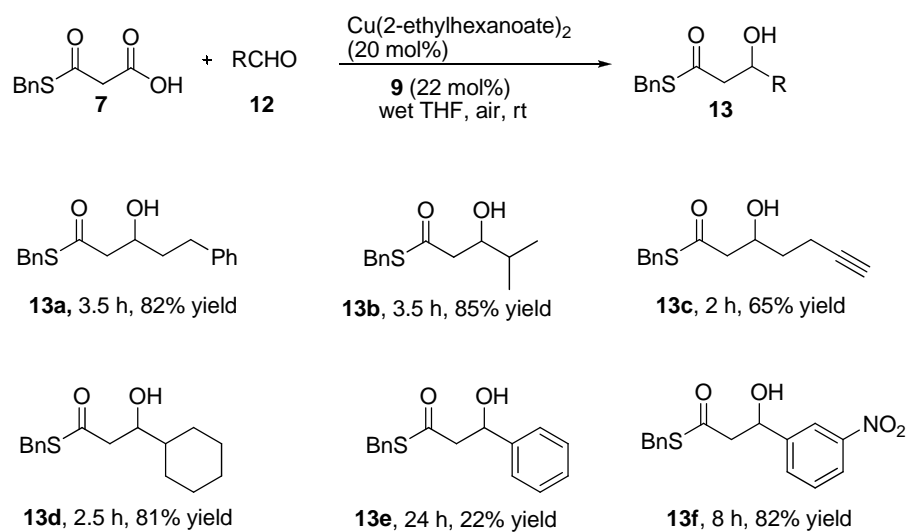
Along a similar thread, Thomas reported the decarboxylative Doebner-Knoevenagel condensation in 2007 (Table 1.1).<sup>4</sup> This reaction offers a route to iterative metal-catalyzed condensations of thioesters, affording complex polyketides. Most of the aldehydes tested showed excellent regio- and stereoselectivities. However, aliphatic aldehydes gave low yields and needed improvement before they are useful.

**Table 1.1** Catalytic Doebner-Knoevenagel condensations between MAHT **7** and various aldehydes

Entry	R	Yield (%)	<b>10</b> : <b>11</b>
1	C <sub>6</sub> H <sub>5</sub>	75	<5 : >95
2	2-NO <sub>2</sub> -C <sub>6</sub> H <sub>4</sub>	91	30 : 70
3	H	34	>95 : <5
4	Me	35	>95 : <5
5	<i>n</i> -pent	32	>95 : <5

## 1.2.2 Aldol Reaction

The aldol reaction is recognized as one of the most important tools for the construction of carbon–carbon bonds in organic chemistry.<sup>5</sup> The first biomimetic decarboxylative aldol reaction was reported by Shair in 2003 (Scheme 1.3).<sup>6</sup>



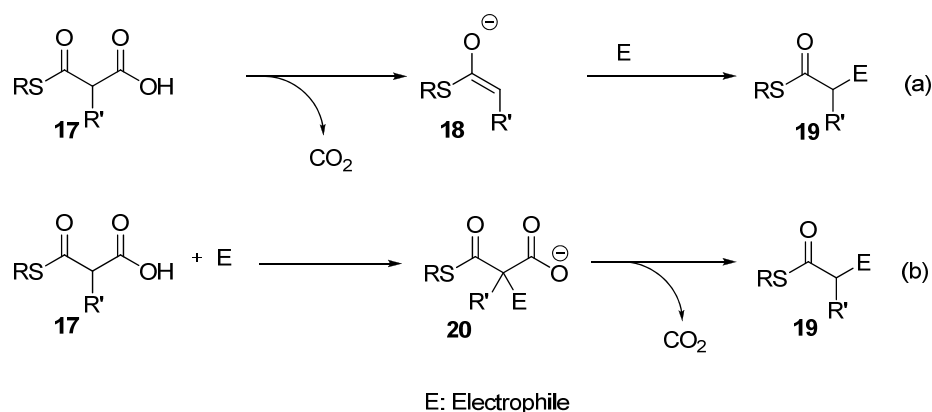
**Scheme 1.3** Catalytic decarboxylative aldol reaction of benzol MAHT with various aldehydes

The Cu(II)-catalyzed decarboxylative aldol reaction was conducted in an exceptionally mild condition. It can be performed in an open-air environment and in wet THF at room temperature, with reagents added in any order. This reaction is typically run in an open vial, using TG grade acetone or EtOAc as solvent, which are often used to wash glasswares. Aliphatic aldehydes, which are typically poor substrates in catalytic aldol reaction due to enolization and self-condensation, were demonstrated to be good substrates for this mild reaction. Electron deficient aromatic aldehydes gave better yields than electron rich ones. It is noteworthy that MAHOs was not discussed in this report, probably due to their low reactivity.

Cozzi attempted an enantioselective version of the decarboxylative aldol reaction with MAHTs.<sup>7a</sup> Various bases and ligands were screened with moderate success. The best result was an enantioselectivity of 39% *ee* with 41% yield. Shair

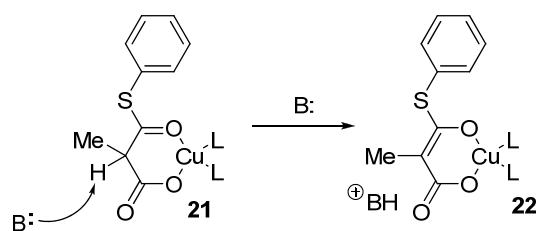


A decarboxylation/nucleophilic addition pathway in which MAHT/MAHO undergoes decarboxylation first to form an enolate **18** (a) and a nucleophilic addition/decarboxylation mechanism in which nucleophilic addition precedes decarboxylation (b).



**Scheme 1.5** Two proposed mechanisms of decarboxylative reactions

Based on the kinetic and isotope labelling experiments, Shair proposed that nucleophilic addition precedes decarboxylation in decarboxylative aldol reaction of MeMAHT **14**.<sup>8</sup> A 13 mol% of the chiral ligand **15** was used and Cu(OTf)<sub>2</sub> was used in 10 mol%. The excess 3 mol% of chiral ligand thus functioned as a chiral base to de-protonate the MeMAHT-Cu complex (Scheme 1.6). The bidentate coordination of MeMAHT **14** by Cu(II) orients the C-2 proton orthogonal to the system, allowing deprotonation but not decarboxylation. This led to species **22**, which would undergo nucleophilic addition.

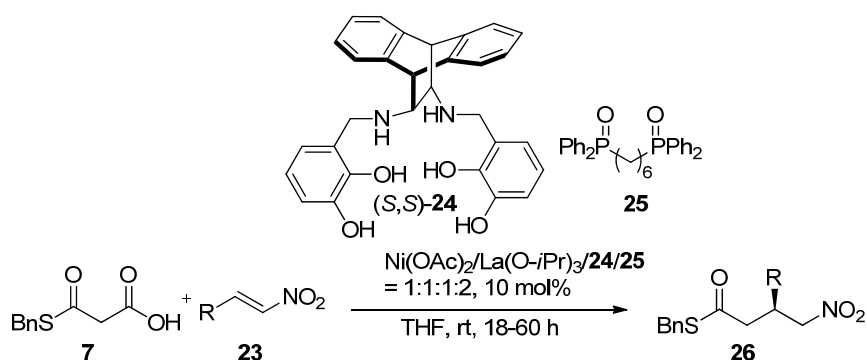


**Scheme 1.6** The deprotonation of MeMAHT-Cu complex

### 1.2.3 1,4-Addition

One of the most common approaches towards C-C or C-X bond formation is the conjugate addition of nucleophiles to electron-deficient alkenes.<sup>9</sup> In 2010, the Shibasaki group reported a heterobimetallic Ni/La-salan complex catalyzed decarboxylative Michael reaction of MAHT **7**.<sup>10</sup> Excellent *ee* values were obtained with  $\beta$ -aryl nitro-olefins (Table 1.2, entries 1-9). However, the  $\beta$ -alkyl nitro-olefins gave moderate yields and enantioselectivities (Table 1.2, entries 10-12).

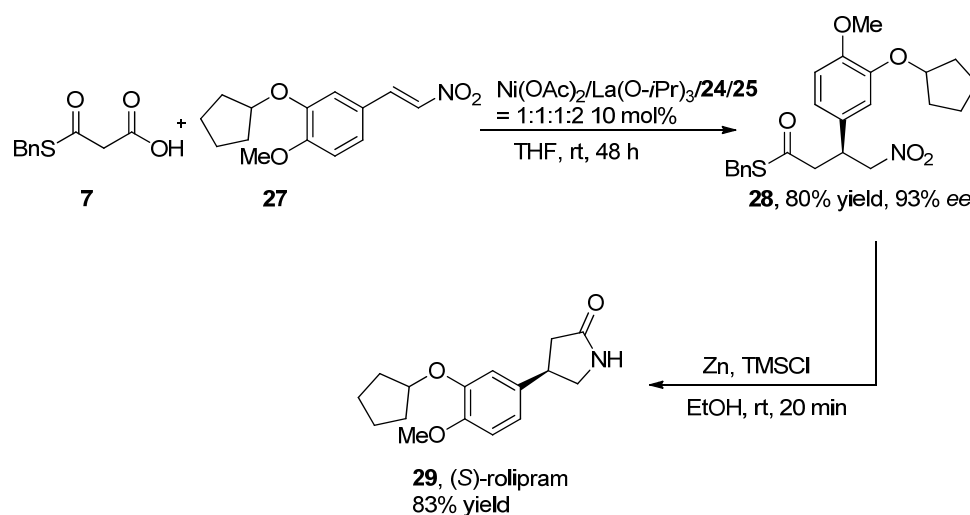
**Table 1.2** Catalytic asymmetric decarboxylative 1,4-addition of MAHT **7** to nitro-olefins



Entry	R	Yield (%)	<i>ee</i> (%)
1	Ph	92	91
2	4-Cl-C <sub>4</sub> H <sub>4</sub>	99	91

3	4-Br-C <sub>6</sub> H <sub>4</sub>	99	91
4	3-Br-C <sub>6</sub> H <sub>4</sub>	98	90
5	4-Me- C <sub>6</sub> H <sub>4</sub>	91	92
6	4-OMe- C <sub>6</sub> H <sub>4</sub>	92	91
7	2-furyl	96	90
8	2-thienyl	96	94
9	3-thienyl	92	90
10	PhCH <sub>2</sub> CH <sub>2</sub>	71	71
11	<i>i</i> -Bu	54	66
12	<i>c</i> -hex	40	66

This method was successfully applied to the synthesis of (*S*)-rolipram **29**, an antidepressant (Scheme 1.7). Catalytic asymmetric decarboxylative 1,4-addition of MAHT **7** to a substituted nitro-olefin gave the adduct **27** in 80% yield and 93% *ee*. The nitro group of **27** was reduced to amine by the treatment of Zn and TMSCl. This was followed by cyclization during work-up to give (*S*)-rolipram in 83% yield.



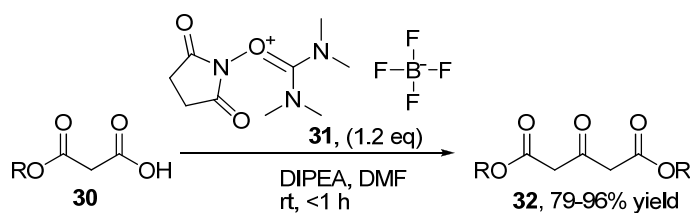
**Scheme 1.7** Asymmetric synthesis of antidepressant (*S*)-rolipram

## 1.3 Organocatalytic Decarboxylative Reactions

Asymmetric transformations based on the direct addition of simple ester and amide remains a challenging problem in organic synthesis. The difficulty is due to the relatively high  $pK_a$  values of the  $\alpha$ -protons of these carbonyl compounds.<sup>11</sup> Physiological conditions forbid the use of strong bases, but nature has provided an elegant solution - the decarboxylation pathway using only weak base.

### 1.3.1 Condensation Reaction

The first organo-base promoted self-condensation reaction of MAHOs was reported by Scott in 2003.<sup>12</sup> The author found that the use of a slight excess of *O*-(*N*-succinimidyl)-*N,N,N,N*-tetramethyluroniumtetra-fluoroborate (TSTU) **31** with *N,N*-diisopropylethylamine (DIPEA) in DMF provided the self-condensation product in good to excellent yields (Scheme 1.8).



**Scheme 1.8** Self-condensation of MAHOs promoted by TSTU

In 2005, List developed the organocatalytic Doehner-Knoevenagel reaction of MAHO **33**.<sup>13</sup> It was catalyzed by 4-dimethylaminopyridine (DMAP) in DMF. Both aliphatic and aromatic aldehydes gave excellent regio- and stereoselectivities

(Table 1.3). This mild reaction is particularly useful to prepare  $\alpha,\beta$ -unsaturated carbonyl compounds.

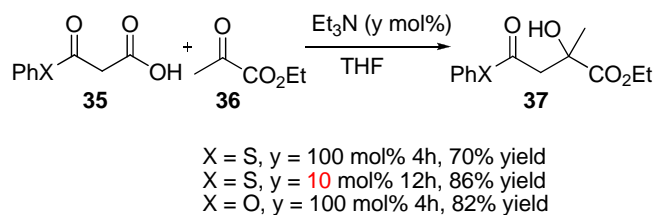
**Table 1.3** A practical synthesis of  $\alpha,\beta$ -unsaturated ester from aldehydes



Entry	R	Yield (%)	E:Z
1	<i>n</i> -Bu	91	95:5
2	<i>n</i> -hex	95	96:4
3	PhCH <sub>2</sub> CH <sub>2</sub>	91	95:5
4	<i>i</i> -Pr	96	> 99:1
5	<i>c</i> -hex	96	98:2
6	<i>t</i> -Bu	92	> 99:1
7	Ph	92	> 99:1
8	1-naphthyl	92	> 99:1
9	2-furyl	90	> 99:1
10	4-OMe-C <sub>6</sub> H <sub>4</sub>	99	> 99:1

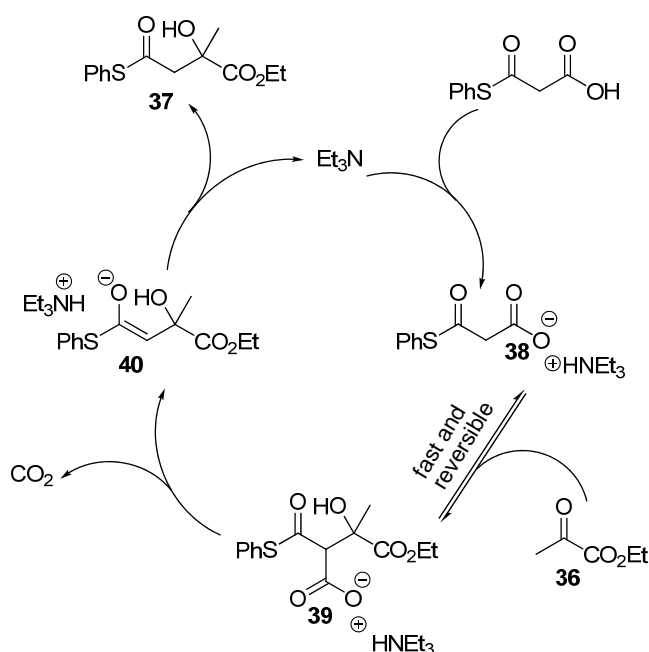
### 1.3.2 Aldol Reaction

Fagnou and co-workers reported that both MAHOs and MAHTs add smoothly to ethyl pyruvate **36** in the presence of Et<sub>3</sub>N at room temperature (Scheme 1.9).<sup>14</sup> For MAHT **35a**, catalytic amount of Et<sub>3</sub>N is sufficient to ensure that the reaction goes to completion with no loss of the yield. This observation gave an early indication that organocatalytic decarboxylative enantioselective aldol reaction may be possible when a chiral Brønsted base is used.



**Scheme 1.9** Decarboxylative aldol reaction of MAHO/MAHT with ethyl pyruvate

Using DOSY NMR, the nucleophilic addition intermediate **39** was observed and characterized (Scheme 1.10). Competition experiment revealed that nucleophilic addition step was reversible and the decarboxylation step was irreversible. By monitoring the reaction profile with  $^1\text{H}$  NMR, rate constants for each of the bond forming/bond breaking steps in the reaction pathway were determined. The data supported that the first nucleophilic addition step was much faster than the decarboxylation step. Based on the experimental data, a mechanism for the  $\text{Et}_3\text{N}$  catalyzed decarboxylative aldol reaction was proposed; nucleophilic addition was determined to precede decarboxylation (Scheme 1.10).



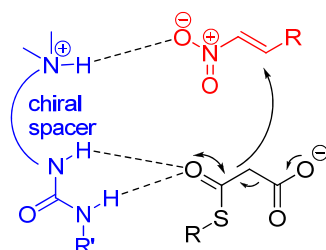
**Scheme 1.10** Proposed mechanism of Et<sub>3</sub>N-catalyzed decarboxylative aldol reaction

### 1.3.3 1,4-Addition

By mimicking the activation mode of MAHT in the polyketide synthesis, Wennemers and co-workers designed the enantioselective decarboxylative Michael reaction of MAHT to nitro-olefins. The reaction was catalyzed by *Cinchona* alkaloid derivatives.<sup>15</sup>

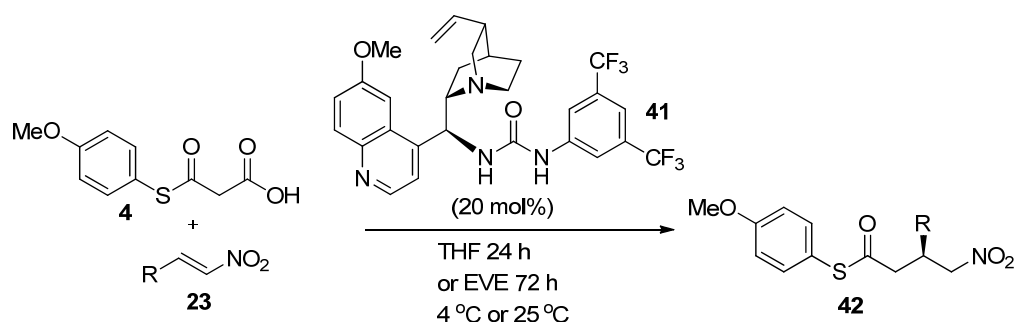
Since the PKS accomplishes the activation of MAHT with the assistance of His and Asn, a bifunctional base containing a basic site and a coordination site may be suitable to mimic this process. *Cinchona* alkaloid urea/thiourea derivatives were chosen as catalysts for this decarboxylative reaction. The tertiary amine of the catalyst is able to deprotonate the MAHT and the urea/thiourea moiety should

provide hydrogen bonding opportunity for the orientation of the MAHT and the nitroolefin in a chiral environment (Scheme 1.11).



**Scheme 1.11** Catalyst design for decarboxylative 1,4-addition of MAHT to nitro-olefins

After screening several catalysts, *Cinchona* alkaloid urea derivative **41** was found to provide good level of selectivity. Good to excellent yields were obtained when *para*-methoxyphenyl MAHT **4** adds to both aryl- and alkyl-nitroolefins **23** in THF. However, the *ee* values were moderate. Higher *ee* values but lower yields were obtained when the reaction was conducted in ethyl vinyl ether (EVE) (Table 1.4). The result demonstrated that MAHTs can be utilized as ester enolate equivalents in organic synthesis.

**Table 1.4** Scope of the decarboxylative 1,4-addition of MAHT to nitro-olefins

Entry	R	THF 24h		EVE 72h	
		Yield (%)	<i>ee</i> (%)	Yield (%)	<i>ee</i> (%)
1	Ph	94	63	57	88
2	4-Cl-C <sub>6</sub> H <sub>4</sub>	96	61	41	79
3	4-NO <sub>2</sub> -C <sub>6</sub> H <sub>4</sub>	94	55	61	82
4	2-NO <sub>2</sub> -C <sub>6</sub> H <sub>4</sub>	99	67	51	90
5	2-CF <sub>3</sub> -C <sub>6</sub> H <sub>4</sub>	89	65	36	86
6	2-thienyl	93	61	13	73
7	4-OMe-C <sub>6</sub> H <sub>4</sub>	78	66	97	75
8	<i>n</i> -pent	71	57	43	79
9	<i>c</i> - hex	16	63	23	78

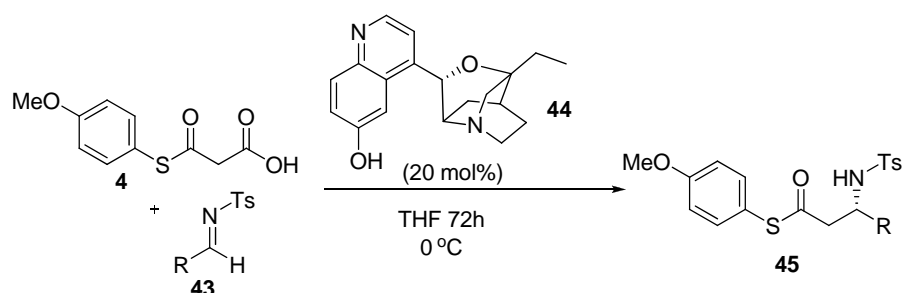
### 1.3.4 Mannich Reaction

As potential precursors for  $\beta$ -lactams, various strategies for the stereoselective synthesis of  $\beta$ -amino acids have been reported.<sup>16</sup> Amongst these, the most robust and powerful method is attributed to the asymmetric Mannich reaction, of which several organocatalytic versions have been developed over the past few years.<sup>17</sup>

In 2007, the first decarboxylative Mannich reaction was reported by Ricci using a *Cinchona* alkaloid derivative as catalyst.<sup>18</sup> The reaction proceeded rather slowly

and moderate to good yields were obtained after 3 days using 20 mol% of catalyst **44** (Table 1.5).  $\beta$ -Amino thioesters **45** were obtained with enantiomeric excesses of up to 79%.

**Table 1.5** Asymmetric decarboxylative Mannich reaction of MAHT to imines

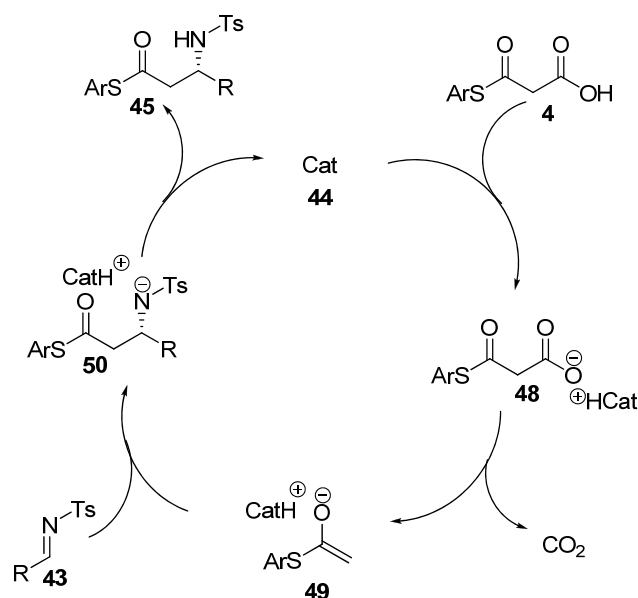


Entry	R	Yield (%)	ee (%)
1	C <sub>6</sub> H <sub>5</sub>	61	69
2	4-MeO-C <sub>6</sub> H <sub>4</sub>	52	68
3	1-naphthyl	76	64
4	PhCH <sub>2</sub> CH <sub>2</sub>	42	79
5	2-Br-C <sub>6</sub> H <sub>4</sub>	66	38
6	<i>c</i> -hex	41	60

Methyl thioester malonate **46** add to imines sluggishly in the presence of catalyst **44**. Acid **47** did not react with imine and only unproductive decarboxylation occurs (Figure 1.1). Ricci and co-workers proposed that decarboxylation preceded nucleophilic addition (Scheme 1.12). The catalyst deprotonated MAHT and the resulting carboxylate underwent decarboxylation to form a thioacetate enolate. The enolate, being in close proximity to the catalyst as an ion-pair, trapped the imine to form the final product.



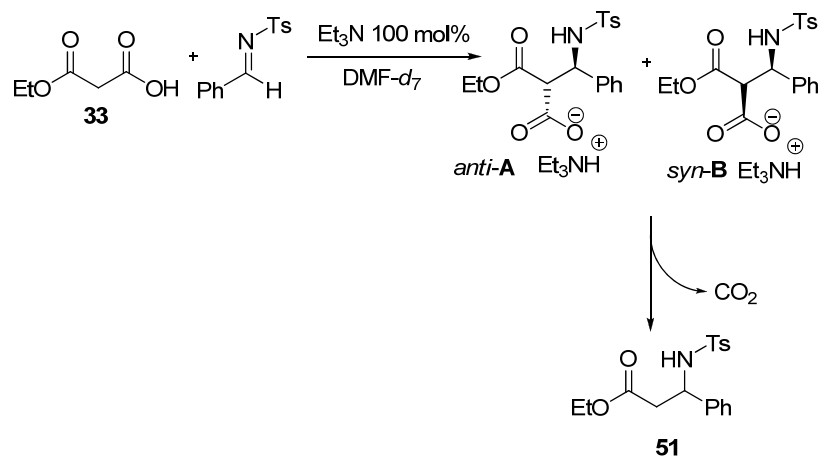
**Figure 1.1** Structures of compounds **46** and **47**



**Scheme 1.12** Proposed mechanism of asymmetric decarboxylative Mannich reaction

To gain more insight into the organocatalytic decarboxylative Mannich reaction, Rouden and co-workers monitored the  $\text{Et}_3\text{N}$  promoted Mannich reaction of MAHO **33** to imine in  $\text{DMF-}d_7$  (Scheme 1.13).<sup>19</sup> The results supported the mechanism that nucleophilic addition precedes decarboxylation, which differs from Ricci's proposed mechanism.<sup>18</sup> It is, however, similar to Fagnou's proposal in  $\text{Et}_3\text{N}$ -catalyzed decarboxylative aldol reaction.<sup>14</sup> The two diastereoisomers **A** and **B** of the nucleophilic addition carboxylates were characterized *in situ* by  $^1\text{H}$  NMR at  $-20\text{ }^\circ\text{C}$ . It was shown clearly that during the course of the reaction, the

ratio of both diastereoisomers remained constants (Figure 1.2). This could be explained by the reversibility of the first nucleophilic addition and the stability of intermediates.



**Scheme 1.13** Et<sub>3</sub>N promoted decarboxylative Mannich reaction

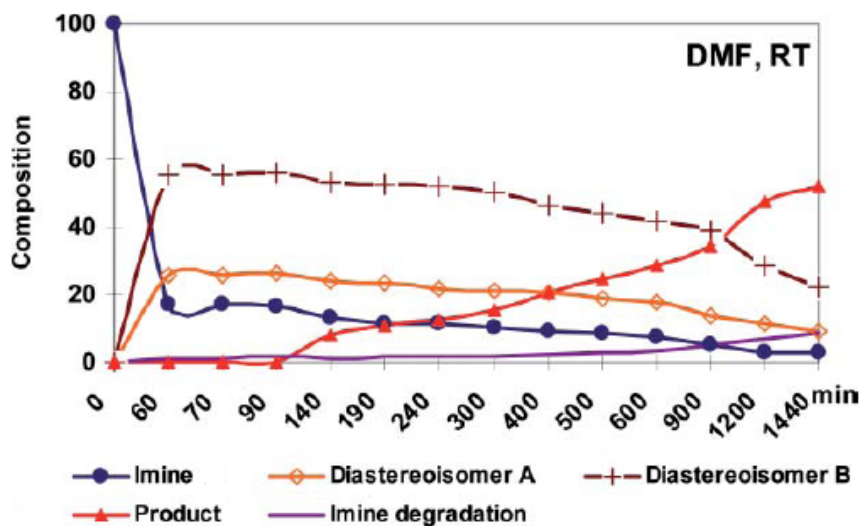


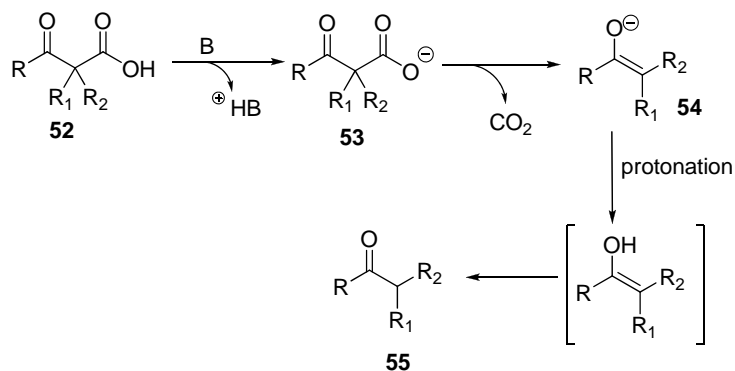
**Figure 1.2** Monitoring the reaction in DMF-*d*<sub>7</sub> as a function of time at room temperature<sup>19</sup>

### 1.3.5 Protonation

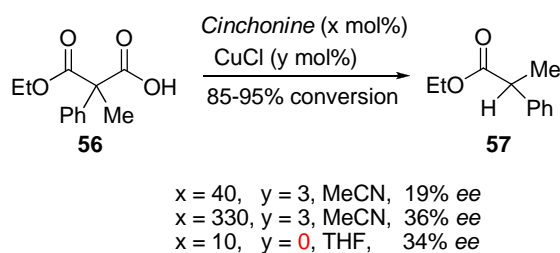
The enantioselective protonation is an attractive and efficient approach for the preparation of chiral carbonyl compounds with an  $\alpha$  stereogenic center.<sup>20</sup> It has been documented that catalytic amount of base is enough to conduct the decarboxylative protonation reaction (Scheme 1.14).<sup>21,22</sup> A fully substituted MAHO or MAHT **52** is deprotonated by a base, followed by the loss of CO<sub>2</sub> to form the enolate **54**. If the enolate is protonated in a chiral environment in the form of a chiral Brønsted base, the final carbonyl compound can be enantio-enriched. In the first step of the reaction, the base is protonated and should form an ion pair with the enolate due to the electrostatic effect. However, the concentration of this complex should be low as the catalyst is present in sub-stoichiometric amount. The pK<sub>a</sub> of the substrate is usually lower than the protonated base; the enolate thus may abstract the proton directly from the substrate leading to racemic product. To prevent the enolate protonation from the substrate and ensure high enantioselective induction, stoichiometric amount of base was often used.

The first enantioselective protonation was investigated by Maumy<sup>23</sup> and subsequently by Brunner<sup>21,24</sup> using racemic MAHOs. *Cinchona* alkaloids in the presence of copper chloride were used as the catalysts. Brunner found that the additive CuCl was not essential for enantioselectivity and reactivity (Scheme 1.15). When the decarboxylative protonation reaction of MAHO **56** was catalyzed

by *Cinchonine* and CuCl in MeCN, 36% *ee* was obtained. Alternatively, catalytic amount of base can be used without CuCl and 34% *ee* was obtained.

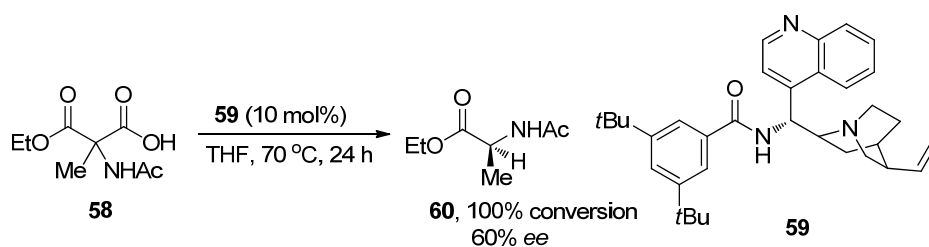


**Scheme 1.14** Proposed mechanism for decarboxylative protonations



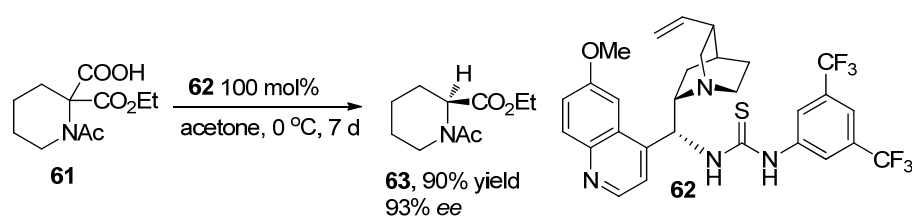
**Scheme 1.15** Brunner's observation of decarboxylative protonation of MAHO

In 2003, Brunner reported the catalytic enantioselective decarboxylative protonation of acyclic aminohemimalonate (*N*-MAHOs).<sup>25</sup> *N*-MAHO **58** was subjected to the reaction in THF at 70 °C for 24 h (Scheme 1.16). Modified *Cinchona* derivative **59** gave decarboxylated adduct **60** with 60% *ee* while natural *Cinchona* alkaloids typically showed low enantioselectivities (< 10% *ee*).



**Scheme 1.16** Enantioselective decarboxylative protonation of acyclic *N*-MAHO

More recently, Rouden reported the enantioselective decarboxylative protonation of cyclic *N*-MAHOs.<sup>26</sup> Good to excellent *ee* values were obtained using stoichiometric amount of *Cinchona* thiourea derivative **62** (Scheme 1.17). This is the first example of enantioselective decarboxylative protonation achieving more than 90% *ee* values. The reaction required 1.0 equivalent of the catalyst and the reaction took 7 days to complete. This new methodology provides a valuable alternative to the asymmetric protonation of lithium enolates and it is useful to prepare optically pure  $\alpha$ -amino acids.



**Scheme 1.17** Highly enantioselective decarboxylative protonation of cyclic *N*-MAHO

## 1.4 Summary

Since the first asymmetric decarboxylation described by Marckwald in 1904,<sup>27</sup>

this reaction has passed through a century of development. While several successful reactions have been developed, more investigations are still required to design practical methods to full use of these reactions. Examples with high level of enantiomeric inductions are still rare and the substrate scopes of many reactions are still limited.

The organocatalytic version of this reaction is particularly attractive as they are environmentally benign with CO<sub>2</sub> as the only side product. The organocatalytic decarboxylation also offers an elegant solution to circumvent the high p*K*<sub>a</sub> problem of simple ester and amide. We will describe the enantioselective decarboxylative Mannich and amination reactions of MAHTs catalyzed by bicyclic guanidine in the following chapters. The mechanistic study of the decarboxylative Mannich reaction will also be discussed.

---

**References:**

---

- (1) (a) O'Hagan, D. *The polyketide metabolites* (ED.: Horwood, E.), Chichester, UK **1991**. (b) Heath, R. J.; Rock, R. O. *Nat. Prod. Rep.* **2002**, *19*, 581. (c) Austin, M. B.; Izumikawa, M.; Bowman, M. E.; Udworthy, D. W.; Ferrer, J.-L.; Moore, B. S.; Noel, J. P. *J. Biol. Chem.* **2004**, *279*, 45162.
- (2) Kobuke, Y.; Yoshida, J.-i. *Tetrahedron Lett.* **1978**, *19*, 367.
- (3) Sakai, M.; Sordé, N.; Matile, S. *Molecules* **2001**, *6*, 845.
- (4) Berru , F.; Antoniotti, S.; Thomas, O. P.; Amade, P. *Eur. J. Org. Chem.* **2007**, 1743.
- (5) (a) Machajewski, T. D.; Wong, C.-H. *Angew. Chem. Int. Ed.* **2000**, *39*, 1352. (b) Palomo, C.; Oiarbide, M.; Garcia, J. M. *Chem. Soc. Rev.* **2004**, *33*, 65. (c) Schetter, B.; Mahrwald, R. *Angew. Chem. Int. Ed.* **2006**, *45*, 7506.
- (6) Lalic, G.; Aloise, A. D.; Shair, M. D. *J. Am. Chem. Soc.* **2003**, *125*, 2852.
- (7) (a) Orlandi, S.; Benaglia, M.; Cozzi, F. *Tetrahedron Lett.* **2004**, *45*, 1747. (b) Magdziak, D.; Lalic, G.; Lee, H. M.; Fortner, K. C.; Aloise, A. D.; Shair, M. D. *J. Am. Chem. Soc.* **2005**, *127*, 7284.
- (8) Fortner, K. C.; Shair, M. D. *J. Am. Chem. Soc.* **2007**, *129*, 1032.
- (9) Sibi, M. P.; Manyem, S. *Tetrahedron* **2000**, *56*, 8033.
- (10) Furutachi, M.; Mouri, S.; Matsunaga, S.; Shibasaki, M. *Chem. Asian J.* **2010**, *5*, 2351.
- (11) (a) Bordwell, F. G.; Fried, H. E. *J. Org. Chem.* **1981**, *46*, 4327. (b) Bordwell, F. G.; Fried, H. E. *J. Org. Chem.* **1991**, *56*, 4218
- (12) Ryu, Y.; Scott, A. I. *Tetrahedron Lett.* **2003**, *44*, 7499.
- (13) List, B.; Doehring, A.; Fonseca, M.; Wobser, K.; van Thienen, H.; Torres, R.; Galilea, P. *Adv. Synth. Catal.* **2005**, *347*, 1558.
- (14) Blaquiere, N.; Shore, D. G.; Rousseaux, S.; Fagnou, K. *J. Org. Chem.* **2009**, *74*, 6190.
- (15) Lubkoll, J.; Wennemers, H. *Angew. Chem., Int. Ed.* **2007**, *46*, 6841.

- (16)(a) *Enantioselective Synthesis of  $\beta$ -Amino Acids, Second Edition* (Eds.: E. Juaristi, V. A. Soloshonok), Wiley, **2005**. (b) Liu, M.; Sibi, M. P. *Tetrahedron* **2002**, *58*, 7991.
- (17)(a) Ting, A.; Schaus, S. E. *Eur. J. Org. Chem.* **2007**, 5797. (b) Verkade, J. M. M.; Hermert, L. J. C. v.; Quaedflieg, P. J. L. M.; Rutjes, F. P. J. T.; *Chem. Soc. Rev.* **2008**, *37*, 29.
- (18) Ricci, A.; Petterson, D.; Bernardi, L.; Fini, F.; Fochi, M.; Perez Herrera, R.; Sgarzani, V. *Adv. Synth. Catal.* **2007**, *349*, 1037.
- (19) Banchet, J.; Lefebvre, P.; Legay, R.; Lasne, M.-A.; Rouden, J. *Green Chem.* **2010**, *12*, 252.
- (20)(a) Fehr, C. *Angew. Chem. Int. Ed.* **1996**, *35*, 2566. (b) Duhamel, L.; Duhamel, P.; Plaquevent, J.-C. *Tetrahedron: Asymmetry* **2004**, *15*, 3653.
- (21) Brunner, H.; Müller, J.; Spitzer, J. *Monatsh. Chem.* **1996**, *127*, 845.
- (22) Banchet, J.; Baudoux, J.; Amere, M.; Lasne, M.-A.; Rouden, J. *Eur. J. Org. Chem.* **2008**, 5493.
- (23) Toussaint, O.; Capdevielle, P.; Maumy, M. *Tetrahedron Lett.* **1987**, *28*, 539.
- (24) Brunner, H.; Kurzwart, M. *Monatsh. Chem.* **1992**, *123*, 121.
- (25) Brunner, H.; Baur, M. A. *Eur. J. Org. Chem.* **2003**, 2854.
- (26)(a) Rogers, L. M.-A.; Rouden, J.; Lecomte, L.; Lasne, M.-C. *Tetrahedron Lett.* **2003**, *44*, 3047. (b) Seitz, T.; Baudoux, J.; Bekolo, H.; Cahard, D.; Plaquevent, J.-C. Lasne, M.-C. Rouden, J. *Tetrahedron* **2006**, *62*, 6155. (c) Amere, M.; Lasne, M.-C.; Rouden, J. *Org. Lett.* **2007**, *9*, 2621.
- (27)(a) Marckwald, W. *Ber. Dtsch. Chem. Ges.* **1904**, *37*, 349. (b) Marckwald, W. *Ber. Dtsch. Chem. Ges.* **1904**, *37*, 1368.

*Chapter 2*

*Bicyclic Guanidine  
Catalyzed Enantioselective  
Decarboxylative Mannich and Amination Reactions*

## 2.1 Introduction

Asymmetric transformations based on the direct addition of simple ester or amide nucleophiles remain a challenging problem in organic synthesis. The difficulty is due to the relatively high  $pK_a$  values of the  $\alpha$ -protons of these carbonyl compounds.<sup>1</sup> Typically, strong base is necessary to activate this position or through metal-catalyzed reactions.<sup>2</sup> Unlike simple ketones and aldehydes, it is not possible to activate esters through the enamine catalytic pathway.<sup>3</sup>

In organocatalysis, diethyl malonate **64** with a  $pK_a$  value of 16.4 can be activated by amine bases to act as a nucleophile in asymmetric reactions (Figure 2.1). However, ketones or oxyesters can not be activated by amine bases. Although the change from oxyester to thioester results a  $pK_a$  reduction approximately 2 units, it still cannot be fully deprotonated by amine bases.

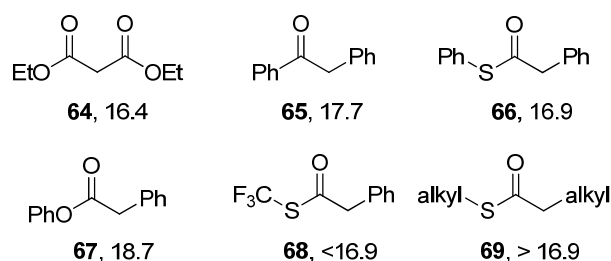
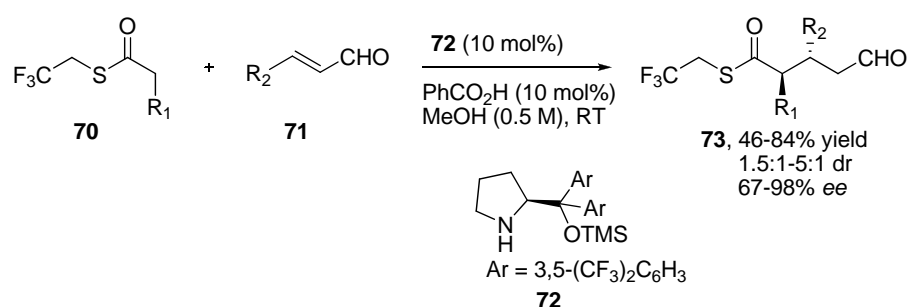


**Figure 2.1**  $pK_a$  values of  $\alpha$ -protons of nucleophiles in DMSO

During the course of searching lower  $pK_a$  value simple ester equivalent nucleophiles, trifluoroethyl thioesters, with  $pK_a$  less than 16.9, which is very close to malonate diester ( $pK_a = 16.4$ ) has recently been applied as nucleophile in organocatalytic reactions. In 2008, Barbas and co-workers reported direct Michael addition with trifluoroethyl thioesters **70** and  $\alpha,\beta$ -unsaturated aldehydes **71** via

secondary amine catalyst **72** (Scheme 2.1).<sup>4</sup> Moderate to good yields and *ee* values were obtained while the diastereoselectivities were not good. Low *ee* value was observed when R<sub>2</sub> was alkyl group. They also demonstrated trifluoroethyl thioester system worked well in nitroolefin-based Michael, aldol, amination and Mannich reactions.

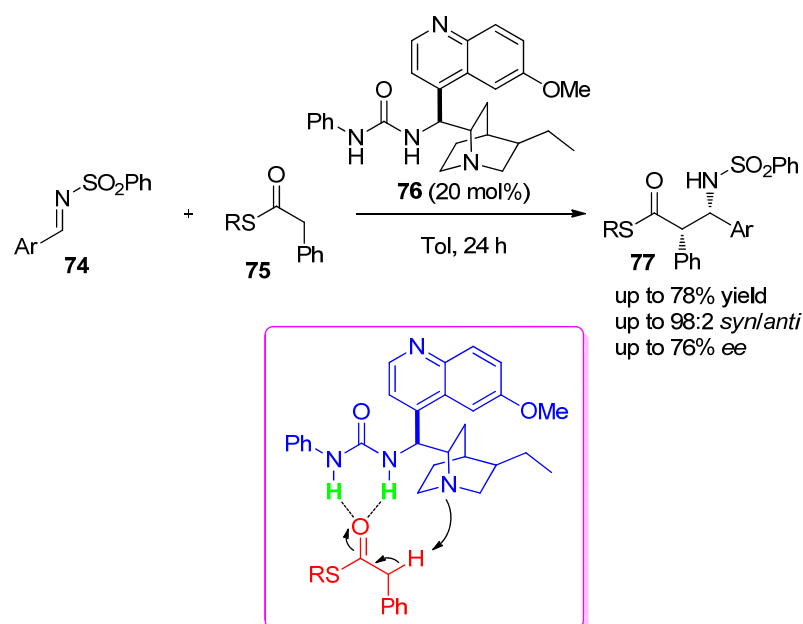


**Scheme 2.1** Direct Michael addition between trifluoroethyl thioester and α,β-unsaturated aldehydes

Although trifluoroethyl thioester **68** as ester nucleophile works well in some reactions, augmenting reactivity by only relying on electronic activation of the thioester is inherently limited. At some point, as the thiol component of the thioester is made increasingly electron withdrawing, competing reactions such as ketene formation and acyl transfer will likely arise, precluding this approach as a general enolization technique.

On the contrary, soft enolization occurs when a relatively weak base and a carbonyl-activating component act in a concert manner, together with close proximity to affect reversible deprotonation. One example of this strategy was reported by Coltart and co-workers in an asymmetric Mannich reaction of phenylacetate thioesters **75** using *Cinchona* alkaloid-based urea catalyst **76**

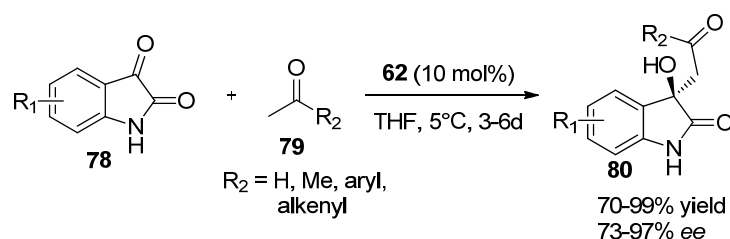
(Scheme 2.2).<sup>5</sup> Moderate yields and *ee* values were obtained with 20 mol% catalyst loading. The carbonyl activating component of thioester is realized by hydrogen bonding interaction by urea moiety. Such interaction facilitates deprotonation kinetically relative to intermolecular processes. The enolate that forms should also be more stable thermodynamically, due to the cooperative internal stabilization of the hydrogen bonding and resulting ammonium moieties. Thus this method opens the door to the development of a general mode of enolization-based organocatalysis of mono-carbonyl compounds. However, the big drawback of this method is that the phenyl group of phenylacetate thioesters is crucial to lower the *pK<sub>a</sub>* value. Therefore the substrate scope is very limited.



**Scheme 2.2** Asymmetric Mannich reaction of phenylacetate thioesters by soft enolization

Zhao and co-workers reported cross-aldol reaction of isatins **78** and ketones **79** catalyzed by catalyst **62** (Scheme 2.3).<sup>6</sup> Not only acetone, acetophenones, but also

cyclic ketones gave good results. Interestingly, acetaldehyde also participated in this reaction with 82% yield and 73% *ee* value. The authors proposed that acetone was fully deprotonated by quinidine thiourea catalyst **62**. However, one can argue that the deprotonation of acetone by amine base is not thermodynamically favorable due to the high *pK<sub>a</sub>* value. We believe that the reaction probably underwent a soft enolization mechanism. Acetone was partially deprotonated by amine base with assistance of hydrogen bond interaction between the carbonyl group of acetone and the thiourea moiety of catalyst **62**.

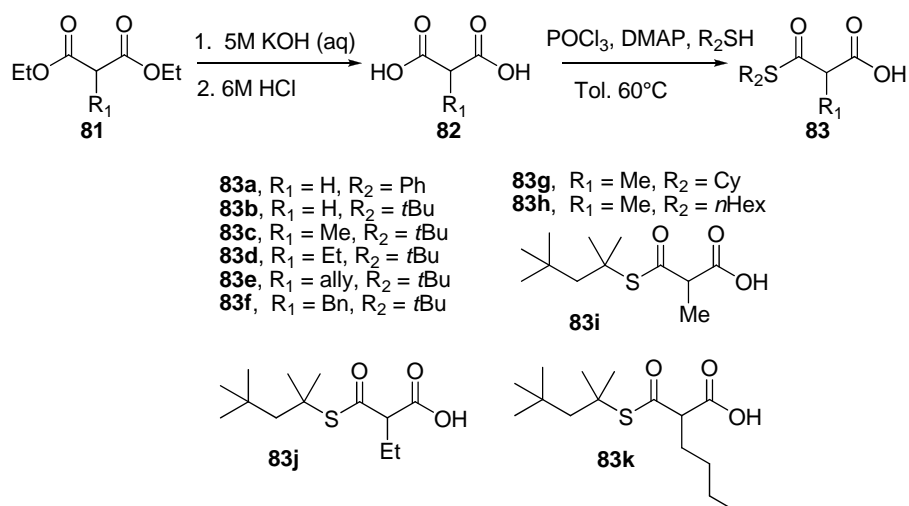


**Scheme 2.3** Cross-aldol reaction of isatins and ketones

Besides these strategies discussed above, another important strategy is attributed to decarboxylative reactions using malonic acid half thioesters (MAHTs) as ester equivalent nucleophiles. This method is inspired from nature's polyketide biosynthesis and has been fully reviewed in Chapter 1. Although the first decarboxylative reaction was discovered more than hundred years ago, the progress in organocatalytic field is very slow. In the following sections, we will describe bicyclic guanidine catalyzed biomimetic decarboxylative Mannich and amination reactions.

## 2.2 Enantioselective Decarboxylative Mannich Reaction

### 2.2.1 Synthesis of Malonic Acid Half Thioesters (MAHTs)

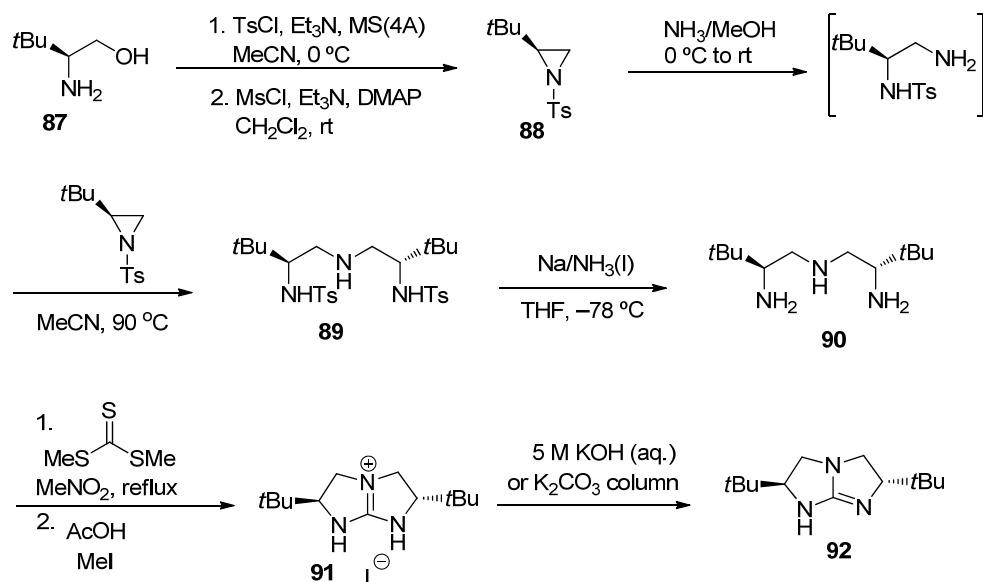


**Scheme 2.4** Synthesis of MAHTs from diethyl malonates

Take the advantage of esterification using the combination of phosphoryl chloride ( $\text{POCl}_3$ ) and 4-Dimethylaminopyridine (DMAP), we found that MAHTs **83** can be obtained by mono-esterification of different malonic acids **82**, where malonic acids can be either purchased or hydrolyzed from diethyl malonates **81** (Scheme 2.4). This method has a large substrate scope.  $R_1$  can be H, aryl, alkyl, allyl and even hetero atoms such as F, Cl.  $R_2$  can be aryl and alkyl groups regardless of the steric hindrance. However, it was inevitable that both mono-esterification product and bis-esterification product were observed. In some case, the consumption of **82** was incomplete. Due to the similar polarity of **82** and **83**, it was difficult to separate them. Because of these two facts, the yield of **83** was about 30-70%.



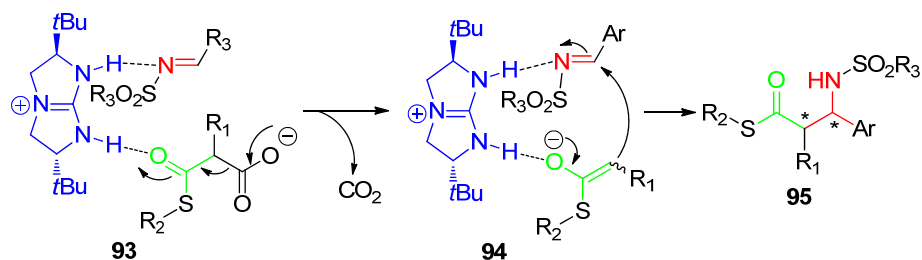
KOH aqueous solution or solid  $K_2CO_3$  column to give the chiral bicyclic guanidine catalyst **92**.



**Scheme 2.6** Synthesis of bicyclic guanidine

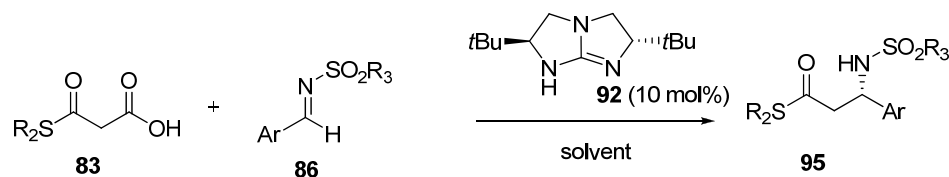
## 2.2.4 Decarboxylative Mannich Reaction of MAHTs

According to the bio-activation model of decarboxylation in Scheme 1.1, catalytic amount of organic base is sufficient to promote the decarboxylation process. Hence, we proposed that the bifunctional nature of bicyclic guanidine<sup>9</sup> catalyst **92** should be appropriate for proximity-assisted decarboxylative strategy. Catalyst **92** is able to deprotonate MAHT **83** to form intermediate **93** with hydrogen bond interaction between imine **86**, deprotonated MAHT and protonated guanidine. The hydrogen bond interaction would assist the decarboxylation to generate thioester enolate which can be trapped by imine to release the Mannich product. In the whole process, protonated guanidine provides hydrogen bonding opportunity for the orientation of the MAHT and imine in a chiral environment.



**Scheme 2.7** Proposed model of biomimetic decarboxylative Mannich reaction

To document our proposed protocol, *N*-tosyl (Ts) imine **86a** was chosen as the model acceptor for the decarboxylative Mannich reaction of MAHTs (Table 2.1). The reaction between MAHT **83a** and imine **86a** proceeded smoothly with excellent yield in the presence of 10 mol% of bicyclic guanidine **92** in THF at room temperature. However, only 15% enantiomeric excess was obtained. A much higher *ee* value was obtained when *t*-butyl substituted MAHT **83b** (entry 2) was applied as donor. Solvent screening revealed that diethyl ether showed the best *ee* value but low yield of the adduct was obtained (entry 4). Lowering the reaction temperature to 0 °C did not improve the enantioselectivity significantly (entries 7-9). As a compromise between yield and *ee* values, we chose THF as solvent for the screening of different imines. Several imines were tested, unfortunately none of them could provide high *ee* values at 0 °C (entries 9-12). Fortunately, when the temperature was decreased to -10 °C, 92% *ee* was observed when MAHT **83b** was reacted with *N*-tosyl (Ts) imine **86a** (entry 13). The yield reached 72% after 96 hours. We attributed the moderate yield to a competing reaction: the unproductive decarboxylation of MAHTs. This side reaction cannot be eliminated even at low reaction temperature.

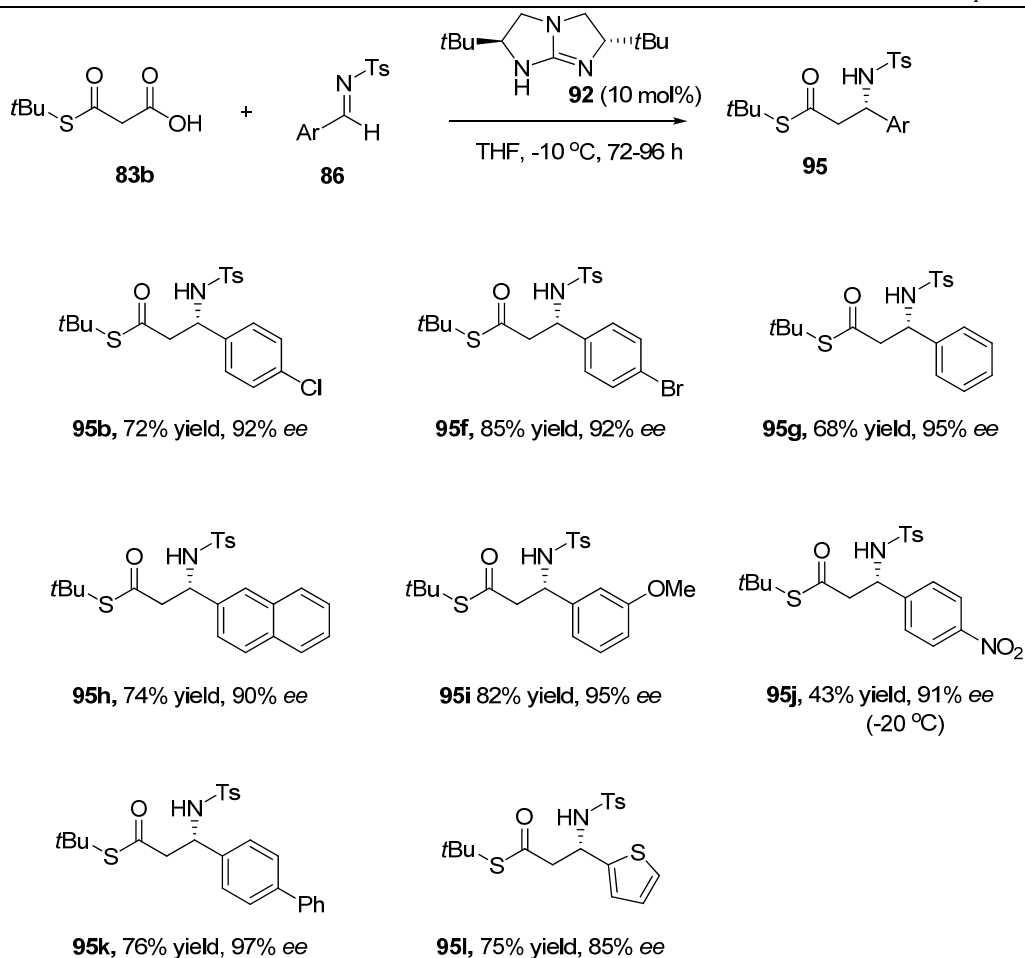
**Table 2.1** Optimization of decarboxylative Mannich reaction between MAHTs and imine **86a**<sup>a</sup>

Entry	<b>83</b>	<b>86</b>	T(°C)	t (h)	Solvent	<b>95</b>	Yield <sup>b</sup>	ee (%) <sup>c</sup>
1	<b>83a</b>	<b>86a</b>	25	24	THF	<b>95a</b>	>95	15
2	<b>83b</b>	<b>86a</b>	25	30	THF	<b>95b</b>	89	57
3	<b>83b</b>	<b>86a</b>	25	30	Et <sub>2</sub> O	<b>95b</b>	30	80
4	<b>83b</b>	<b>86a</b>	25	30	TBME	<b>95b</b>	40	77
5	<b>83b</b>	<b>86a</b>	25	30	Toluene	<b>95b</b>	62	40
6	<b>83b</b>	<b>86a</b>	25	30	CH <sub>2</sub> Cl <sub>2</sub>	<b>95b</b>	23	32
7	<b>83b</b>	<b>86a</b>	0	96	Et <sub>2</sub> O	<b>95b</b>	33	80
8	<b>83b</b>	<b>86a</b>	0	96	TBME	<b>95b</b>	34	82
9	<b>83b</b>	<b>86a</b>	0	48	THF	<b>95b</b>	60	65
10	<b>83b</b>	<b>86b</b>	0	48	THF	<b>95c</b>	45	60
11	<b>83b</b>	<b>86c</b>	0	48	THF	<b>95d</b>	50	77
12	<b>83b</b>	<b>86d</b>	0	48	THF	<b>95e</b>	57	77
13	<b>83b</b>	<b>86a</b>	-10	96	THF	<b>95b</b>	72	92
14	<b>83b</b>	<b>86d</b>	-10	96	THF	<b>95e</b>	48	80

<sup>a</sup>The reaction was performed with 1.5 equiv. of MAHT and 1.0 equiv. of **86**.

<sup>b</sup>Yield of isolated product. <sup>c</sup>Determined by HPLC.

With the optimal reaction condition developed, the substrate scope was evaluated (Scheme 2.8). We examined the performance of MAHT **83b** with a series of *N*-Ts imines in the presence of 10 mol% catalyst **92**. Good yields and excellent *ee* values were obtained with imines bearing both electron-withdrawing and electron-donating aryl groups as well as hetero-aryl group (up to 85% yield, up to 97% *ee*).



**Scheme 2.8** Highly enantioselective decarboxylative Mannich reaction between MAHT **83b** and imines

Different  $\alpha$ -alkyl-substituted MAHTs were prepared using our own method (Scheme 2.4) and tested in the decarboxylative Mannich reaction with *N*-Ts imines **86a** (Table 2.2). Excellent conversion and Good *ee* value were obtained when MeMAHT **83c** reacted with imine **86a** under the previous established condition while the diastereoselectivity was only 3:2 (entry 1). The reaction became sluggish when lowering the temperature to 0 °C (entry 2). TBME provided excellent *ee* value of the *anti* isomer. Catalyst loading screening showed that 10 mol% catalyst was sufficient to promote the reaction (entries 3-6). Diethyl ether and 2-isopropoxypropane also gave excellent *ee* value while the reaction took a

long time to complete (entries 8, 9). Although excellent *ee* value of *anti* isomer can be obtained, attempt to improve the diastereoselectivity failed. The two diastereoisomers can be easily separated using flash column chromatography.

**Table 2.2** Optimization of decarboxylative Mannich reaction between MeMAHT **83c** and imine **86a**<sup>a</sup>

Entry	Solvent	x	t (h)	Conv. (%) <sup>b</sup>	<i>anti/syn</i> <sup>c</sup>	<i>ee</i> (%) <sup>d</sup>
1	THF	10	48	95	3:2	83, 59
2 <sup>e</sup>	THF	10	96	< 20	5:1	n.d.
3	TBME	20	28	89	2:1	95, 70
4	TBME	15	48	89	7:3	96, 73
5	TBME	10	60	88	7:3	96, 68
6	TBME	5	96	86	7:3	92, 70
7 <sup>e</sup>	TBME	10	96	< 20	n.d.	n.d.
8	Et <sub>2</sub> O	10	96	95	2.8:1	92, 70
9	<i>i</i> Pr <sub>2</sub> O	10	96	95	2.8:1	93, 70

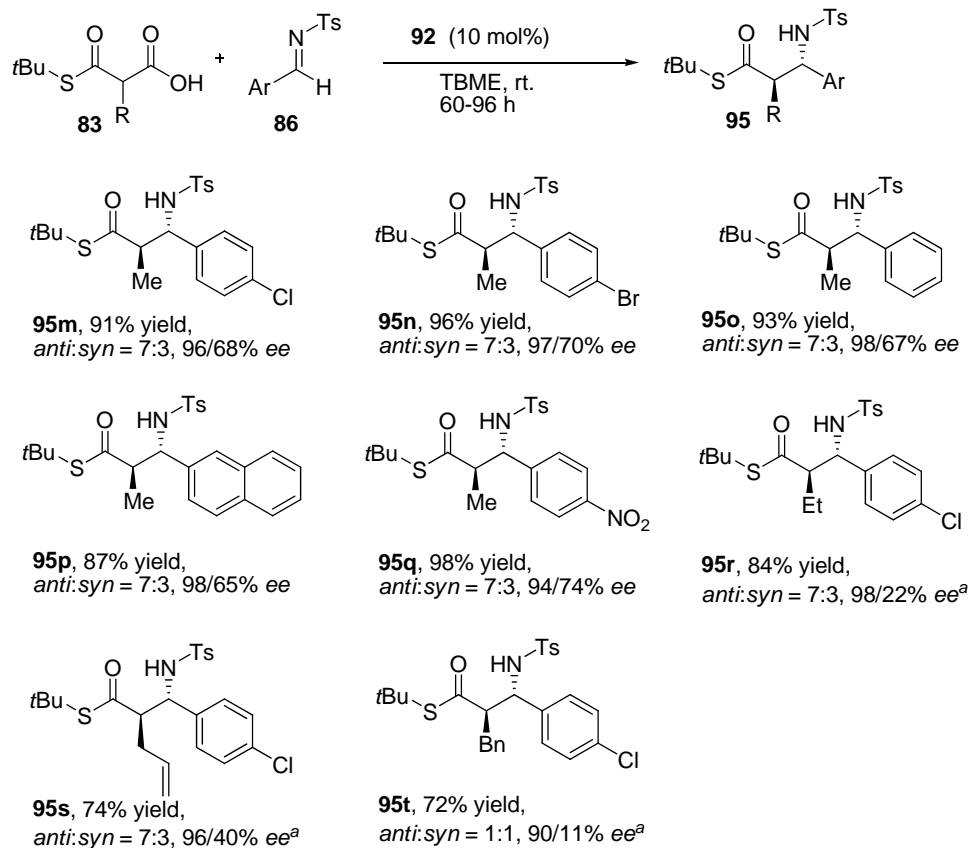
<sup>a</sup>The reaction was performed with 1.5 equiv. of **83c** and 1.0 equiv. of **86a**.

<sup>b</sup>Determined by crude NMR. <sup>c</sup>Determined by crude NMR. <sup>d</sup>Determined by HPLC.

<sup>e</sup>Reaction was performed at 0 °C.

With the established condition in hand, we evaluate the substrate scope of different  $\alpha$ -alkyl MAHTs and imines as shown in Scheme 2.9. Good to excellent yields were obtained and the *ee* value of the *anti* isomers were excellent. 20 mol% of catalyst **92** was necessary to ensure the reaction rate when  $\alpha$ -alkyl group become bulkier (**95r**, **s**, **t**). The drawback of this reaction is that the diastereoselectivity was low and the *ee* value of the *syn* isomer was moderate. However, to the best of our knowledge, this is the first example of

decarboxylative Mannich reaction using  $\alpha$ -alkyl-substituted MAHTs. The relative and absolute stereochemistries was determined from X-ray analysis of **95n**.

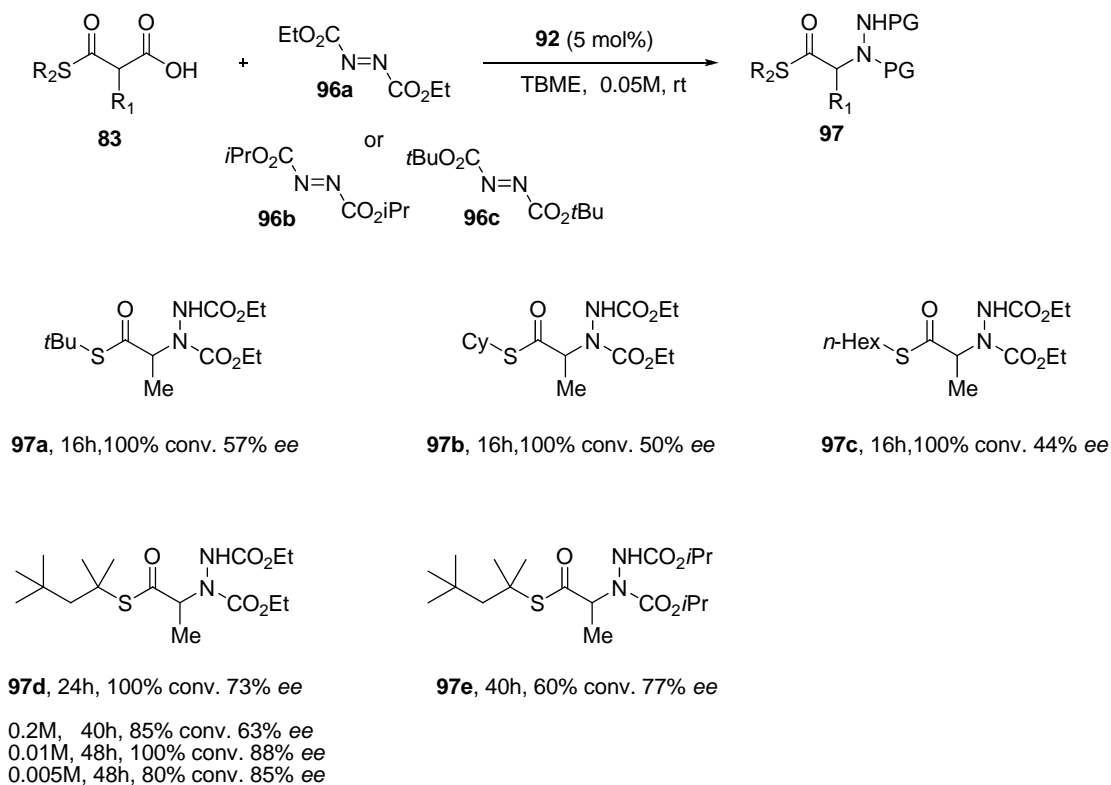


**Scheme 2.9** Highly enantioselective decarboxylative Mannich reaction between  $\alpha$ -alkyl MAHTs and imines. <sup>a</sup>20 mol% of **92** was used.

### 2.3 Enantioselective Decarboxylative Amination Reaction

$\beta$ -amino acid derivatives are useful building blocks in the preparation of natural products, pharmaceutical targets, and polypeptides with unique structural properties. The decarboxylative Mannich reaction we described allows access to valuable enantiopure  $\beta$ -amino thioesters. On the contrary, proteinogenic  $\alpha$ -amino acid derivatives, which are constituents of all enzymes which control metabolism in the living system, play an essential role for life. Hence, We

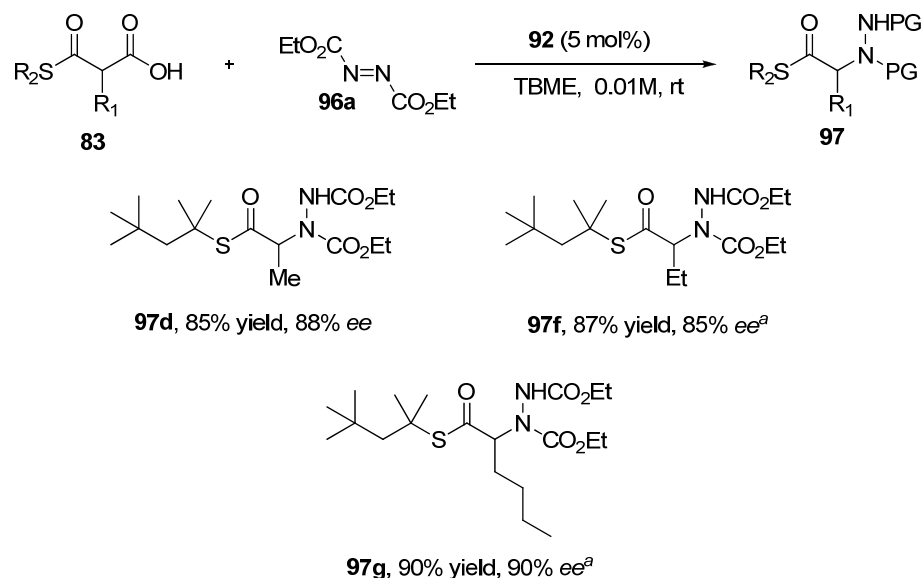
realized that decarboxylative  $\alpha$ -amination,<sup>10</sup> if successful, would lead to the complementary  $\alpha$ -amino thioesters.



**Scheme 2.10** Decarboxylative amination reaction of  $\alpha$ -alkyl MAHTs.

Decarboxylative amination between MeMAHT **83c** and diethyl azodicarboxylate **96a** in the presence of 5 mol% bicyclic guanidine catalyst **92** gave alkyl-substituted  $\alpha$ -amino thioester **97a** with 57% *ee* after 16 hours (Scheme 2.10). However, increasing the catalyst loading to 10 mol% also gave the same result. Changing the thioester part to cyclohexyl or *n*-hexyl did not improve the *ee* value. Due to its lower *pK<sub>a</sub>* value and high steric hindrance, S,S-bis(2,4,4-trimethylpentan-2-yl) propanebis(thioate) was proved to be a very efficient nucleophile in guanidine catalyzed conjugate addition reactions.<sup>11</sup> Take the advantage of (2,4,4-trimethylpentan-2-yl) thioester, MAHT **83i** was prepared

using our own method and tested for the decarboxylative amination reaction. 73% *ee* was obtained with full conversion after 36 hours. Changing the azodicarboxylate to bulkier one **96b** led to lower reaction rate although the *ee* value improved slightly. Di-tert-butyl azodicarboxylate **96c** did not participate in this reaction. Concentration showed a big influence in this amination reaction. *ee* value of **97d** dropped to 63% when the concentration was increased to 0.2 M. The optimal concentration would be 0.01 M as 88% *ee* was obtained with full conversion after 48 h.



**Scheme 2.11** High enantioselective decarboxylative Mannich reaction between  $\alpha$ -alkyl MAHTs and imines. <sup>a</sup>20 mol% of **92** was used.

Alkyl-substituted  $\alpha$ -amino thioesters were obtained with good yields and *ee* values when  $\alpha$ -alkyl substituted MAHTs **83i-k** added to diethyl azodicarboxylate **96a** in the presence of 5 or 20 mol% of catalyst **92** (Scheme 2.11). Typically MAHT **83k**, 90% yield and 90% *ee* value of  $\alpha$ -amino thioester **97g** which was difficult to be obtained using traditional methods. With simple deprotection and

hydrolysis of product **97d-g**, alkyl-substituted  $\alpha$ -amino acids can be obtained easily. This method could provide a new synthetic route toward unnatural  $\alpha$ -amino acids.

## **2.4 Summary**

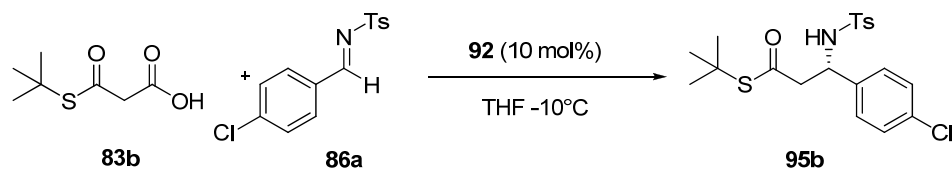
We have developed bicyclic guanidine-catalyzed enantioselective biomimetic decarboxylative Mannich and decarboxylative amination reactions. Good yields and excellent enantioselectivities (up to 98% yield, up to 98% *ee*) were obtained with a wide range of MAHTs. Both  $\beta$ -amino acid derivatives and  $\alpha$ -amino acid derivatives can be obtained using this methodology.

## 2.5 Experimental Section

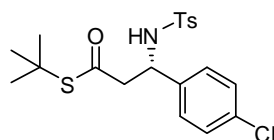
### 2.5.1 General Procedures and Methods

$^1\text{H}$  and  $^{13}\text{C}$  NMR spectra were recorded on a Bruker ACF300 (300MHz), Bruker DPX300 (300MHz) DRX500 (500MHz) or AMX500 (500MHz) spectrometer. Chemical shifts are reported in parts per million (ppm). The residual solvent peak was used as an internal reference. Low resolution mass spectra were obtained on a Finnigan/MAT LCQ spectrometer in ESI mode and a Finnigan/MAT 95XL-T mass spectrometer in FAB mode. All high resolution mass spectra were obtained on a Finnigan/MAT 95XL-T spectrometer. Enantiomeric excess values were determined by chiral HPLC analysis on Dionex Ultimate 3000 HPLC units, including a Ultimate 3000 Pump, Ultimate 3000 variable Detectors. Optical rotations were recorded on Jasco DIP-1000 polarimeter. Melting points were determined on a BÜCHI B-540 melting point apparatus. Analytical thin layer chromatography (TLC) was performed with Merck pre-coated TLC plates, silica gel 60F-254, layer thickness 0.25 mm. Flash chromatography separations were performed on Merck 60 (0.040 - 0.063mm) mesh silica gel. THF and TBME (*tert*-butyl methyl ether) were distilled from sodium/benzophenone and stored under  $\text{N}_2$  atmosphere. Other reagents and solvents were commercial grade and used as supplied without further purification, unless otherwise stated.

## 2.5.2 Typical experimental procedure for the reaction between MAHT **83b** and *N*-Tosyl imine **86a** catalyzed by **92**



*N*-Tosyl imine **86a** (22.0 mg, 0.075 mmol, 1.5 equiv.) and **92** (1.12 mg, 0.005 mmol, 0.1 equiv.) were dissolved in THF (0.5 ml). The mixture was cooled down to -10 °C. 15 min later, MAHT **83b** (8.8 mg, 0.05 mmol, 1.0 equiv.) was added. The reaction mixture was stirred at -10 °C. After 96 hours, the reaction solvent was removed *in vacuo* and the crude product was directly loaded onto a short silica gel column, followed by gradient elution with hexane/EA mixtures (20/1 - 6/1 ratio). After removing the solvent, product **95b** (15.3 mg) was obtained as a white solid in 72% yield.



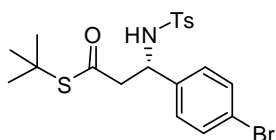
### (S)-S-*tert*-butyl

### 3-(4-chlorophenyl)-3-(4-methylphenylsulfonamido)propanethioate (**95b**)

White solid, Mp: 132 – 134 °C. 92% *ee*,  $[\alpha]_D^{20} = -39.3$  (*c* 0.62, CHCl<sub>3</sub>). <sup>1</sup>H NMR (500 MHz, CDCl<sub>3</sub>, ppm) δ 7.56 (d, *J* = 8.2 Hz, 2H), 7.20 – 7.09 (m, 4H), 7.02 (d, *J* = 8.5 Hz, 2H), 5.84 (d, *J* = 7.0 Hz, 1H), 4.66 (dd, *J* = 12.8, 6.5 Hz, 1H), 2.85 (dd, *J* = 15.2, 6.6 Hz, 1H), 2.76 (dd, *J* = 15.3, 5.8 Hz, 1H), 2.38 (s, 3H), 1.34

(s, 9H).  $^{13}\text{C}$  NMR (75.5 MHz,  $\text{CDCl}_3$ , ppm)  $\delta$  198.0, 143.6, 137.9, 137.4, 133.7, 129.7, 128.7, 128.3, 127.3, 54.8, 50.0, 49.2, 29.7, 21.7. LRMS (ESI)  $m/z$  448.0 ( $\text{M} + \text{Na}^+$ ), HRMS (ESI)  $m/z$  448.0765 ( $\text{M} + \text{Na}^+$ ), calc. for  $\text{C}_{20}\text{H}_{24}\text{ClNO}_3\text{S}_2\text{Na}$  448.0778.

The *ee* was determined by HPLC analysis. CHIRALPAK IA (4.6 mm i.d. x 250 mm); Hexane/2-propanol = 70/30; flow rate 1.0 ml/min; 25 °C; 230 nm; retention time: 9.0 min (major), 12.1 min (minor).

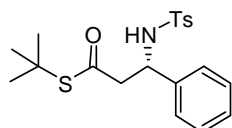


**(S)-S-tert-butyl**

**3-(4-bromophenyl)-3-(4-methylphenylsulfonamido)propanethioate (95f)**

White solid, Mp: 144 – 146 °C. 92% *ee*,  $[\alpha]_{\text{D}}^{20} = -38.6$  (*c* 0.69,  $\text{CHCl}_3$ );  $^1\text{H}$  NMR (500 MHz,  $\text{CDCl}_3$ , ppm)  $\delta$  7.55 (d,  $J = 8.0$  Hz, 2H), 7.28 (d,  $J = 8.2$  Hz, 2H), 7.16 (d,  $J = 7.9$  Hz, 2H), 6.96 (d,  $J = 8.2$  Hz, 2H), 5.85 (d,  $J = 6.9$  Hz, 1H), 4.65 (dd,  $J = 12.8, 6.4$  Hz, 1H), 2.84 (dd,  $J = 15.3, 6.6$  Hz, 1H), 2.76 (dd,  $J = 15.3, 5.7$  Hz, 1H), 2.38 (s, 3H), 1.34 (s, 9H).  $^{13}\text{C}$  NMR (75.5 MHz,  $\text{CDCl}_3$ , ppm)  $\delta$  198.1, 143.6, 138.4, 137.4, 131.7, 129.7, 128.6, 127.3, 121.9, 54.9, 49.9, 49.2, 29.7, 21.7. LRMS (ESI)  $m/z$  492.0 ( $\text{M} + \text{Na}^+$ ), HRMS (ESI)  $m/z$  492.0270 ( $\text{M} + \text{Na}^+$ ), calc. for  $\text{C}_{20}\text{H}_{24}\text{BrNO}_3\text{S}_2\text{Na}$  492.0273.

The *ee* was determined by HPLC analysis. CHIRALPAK IA (4.6 mm i.d. x 250 mm); Hexane/2-propanol = 70/30; flow rate 1.0 ml/min; 25 °C; 254 nm; retention time: 9.7 min (major), 13.6 min (minor).

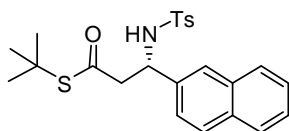


**(S)-S-tert-butyl 3-(4-methylphenylsulfonamido)-3-phenylpropanethioate**

**(95g)**

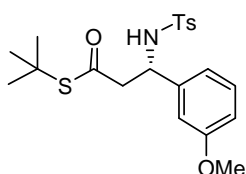
White solid, Mp: 118 – 120 °C. 95% *ee*,  $[\alpha]_D^{29} = -22.1$  (*c* 0.60, CHCl<sub>3</sub>); <sup>1</sup>H NMR (500 MHz, CDCl<sub>3</sub>, ppm) δ 7.59 (d, *J* = 8.2 Hz, 2H), 7.23 – 7.12 (m, 5H), 7.11 – 7.01 (m, 2H), 5.66 (d, *J* = 6.8 Hz, 1H), 4.68 (dd, *J* = 12.8, 6.5 Hz, 1H), 2.90 (dd, *J* = 15.2, 6.7 Hz, 1H), 2.80 (dd, *J* = 15.2, 5.8 Hz, 1H), 2.37 (s, 3H), 1.34 (s, 9H). <sup>13</sup>C NMR (75.5 MHz, CDCl<sub>3</sub>, ppm) δ 198.2, 143.4, 139.3, 137.6, 129.6, 128.7, 127.9, 127.4, 126.8, 55.4, 50.3, 49.0, 29.7, 21.7. LRMS (ESI) *m/z* 414.0 (M + Na<sup>+</sup>), HRMS (ESI) *m/z* 414.1167 (M + Na<sup>+</sup>), calc. for C<sub>20</sub>H<sub>26</sub>NO<sub>3</sub>S<sub>2</sub>Na 414.1168.

The *ee* was determined by HPLC analysis. CHIRALPAK IA (4.6 mm i.d. x 250 mm); Hexane/2-propanol = 70/30; flow rate 1.0 ml/min; 25 °C; 230 nm; retention time: 7.6 min (major), 9.0 min (minor).

**(S)-S-tert-butyl****3-(4-methylphenylsulfonamido)-3-(naphthalen-2-yl)propanethioate (95h)**

White solid, Mp: 134 – 136 °C. 90% *ee*,  $[\alpha]_D^{29} = -59.5$  (*c* 0.67, CHCl<sub>3</sub>). <sup>1</sup>H NMR (500 MHz, CDCl<sub>3</sub>, ppm) 7.84 – 7.60 (m, 1H), 7.54 (d, *J* = 8.2 Hz, 2H), 7.50 – 7.40 (m, 3H), 7.24 – 7.15 (m, 1H), 7.00 (d, *J* = 8.0 Hz, 2H), 5.85 (d, *J* = 6.9 Hz, 1H), 4.87 (dd, *J* = 12.8, 6.5 Hz, 1H), 2.99 (dd, *J* = 15.2, 6.7 Hz, 1H), 2.89 (dd, *J* = 15.2, 5.8 Hz, 1H), 2.22 (s, 3H), 1.33 (s, 9H). <sup>13</sup>C NMR (75.5 MHz, CDCl<sub>3</sub>, ppm) δ 198.2, 143.4, 137.5, 136.4, 133.2, 133.0, 129.5, 128.6, 128.1, 127.7, 127.3, 126.4, 126.3, 126.1, 124.4, 55.7, 50.2, 49.1, 29.7, 21.5. LRMS (ESI) *m/z* 464.0 (M + Na<sup>+</sup>), HRMS (ESI) *m/z* 464.1311 (M + Na<sup>+</sup>), calc. for C<sub>24</sub>H<sub>27</sub>NO<sub>3</sub>S<sub>2</sub>Na 464.1315.

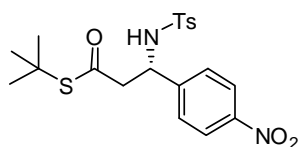
The *ee* was determined by HPLC analysis. CHIRALPAK IA (4.6 mm i.d. x 250 mm); Hexane/2-propanol = 70/30; flow rate 1.0 ml/min; 25 °C; 254 nm; retention time: 9.5 min (major), 10.6 min (minor).



**(S)-S-tert-butyl****3-(3-methoxyphenyl)-3-(4-methylphenylsulfonamido)propanethioate (95i)**

White solid, Mp: 98 – 100 °C. 95% *ee*,  $[\alpha]_D^{29} = -27.1$  (*c* 0.78, CHCl<sub>3</sub>); <sup>1</sup>H NMR (500 MHz, CDCl<sub>3</sub>, ppm) δ 7.59 (d, *J* = 8.2 Hz, 2H), 7.16 (d, *J* = 8.0 Hz, 2H), 7.10 (t, *J* = 7.9 Hz, 1H), 6.75 – 6.65 (m, 2H), 6.57 (s, 1H), 5.68 (d, *J* = 6.8 Hz, 1H), 4.66 (q, *J* = 6.5 Hz, 1H), 3.68 (s, 3H), 2.89 (dd, *J* = 15.2, 6.7 Hz, 1H), 2.80 (dd, *J* = 15.2, 5.8 Hz, 1H), 2.36 (s, 3H), 1.35 (s, 9H). <sup>13</sup>C NMR (75.5 MHz, CDCl<sub>3</sub>, ppm) δ 198.2, 159.8, 143.4, 140.9, 137.6, 129.7, 129.6, 127.4, 119.1, 113.7, 112.2, 55.4, 55.3, 50.3, 49.0, 29.8, 21.6. LRMS (ESI) *m/z* 444.1 (M + Na<sup>+</sup>), HRMS (ESI) *m/z* 444.1266 (M + Na<sup>+</sup>), calc. for C<sub>21</sub>H<sub>27</sub>NO<sub>4</sub>S<sub>2</sub>Na 444.1274.

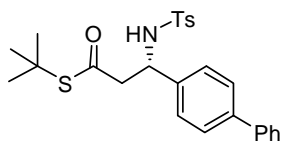
The *ee* was determined by HPLC analysis. CHIRALPAK AD-H (4.6 mm i.d. x 250 mm); Hexane/2-propanol = 70/30; flow rate 1.0 ml/min; 25 °C; 254 nm; retention time: 10.3 min (major), 11.2 min (minor).

**(S)-S-tert-butyl****3-(4-methylphenylsulfonamido)-3-(4-nitrophenyl)propanethioate (95j)**

White solid, Mp: 145 – 147 °C. 91% *ee*,  $[\alpha]_D^{29} = -31.4$  (*c* 0.27, CHCl<sub>3</sub>). <sup>1</sup>H NMR (500 MHz, CDCl<sub>3</sub>, ppm) δ 8.05 (d, *J* = 8.7 Hz, 2H), 7.59 (d, *J* = 8.2 Hz, 2H), 7.32 (d, *J* = 8.6 Hz, 2H), 7.18 (d, *J* = 8.0 Hz, 2H), 6.03 (d, *J* = 6.8 Hz, 1H), 4.77

(dd,  $J = 12.4, 6.4$  Hz, 1H), 2.86 (dd,  $J = 15.4, 6.6$  Hz, 1H), 2.78 (dd,  $J = 15.4, 5.4$  Hz, 1H), 2.37 (s, 3H), 1.33 (s, 9H).  $^{13}\text{C}$  NMR (75.5 MHz,  $\text{CDCl}_3$ , ppm)  $\delta$  197.8, 147.5, 146.8, 144.0, 137.2, 129.8, 127.8, 127.3, 123.8, 54.8, 49.5, 49.5, 29.7, 21.7. LRMS (ESI)  $m/z$  459.0 ( $\text{M} + \text{Na}^+$ ), HRMS (ESI)  $m/z$  459.1014 ( $\text{M} + \text{Na}^+$ ), calc. for  $\text{C}_{20}\text{H}_{24}\text{N}_2\text{O}_5\text{S}_2\text{Na}$  459.1019.

The *ee* was determined by HPLC analysis. CHIRALPAK IA (4.6 mm i.d. x 250 mm); Hexane/2-propanol = 70/30; flow rate 1.0 ml/min; 25 °C; 254 nm; retention time: 15.4 min (major), 16.8 min (minor).

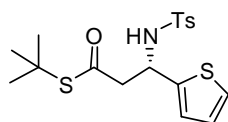


**(S)-S-*tert*-butyl**

**3-(biphenyl-4-yl)-3-(4-methylphenylsulfonamido)propanethioate (95k)**

White solid, Mp: 137 – 139 °C. 97% *ee*,  $[\alpha]_{\text{D}}^{20} = -37.3$  ( $c$  0.84,  $\text{CHCl}_3$ );  $^1\text{H}$  NMR (500 MHz,  $\text{CDCl}_3$ , ppm)  $\delta$  7.60 (d,  $J = 8.1$  Hz, 2H), 7.51 (d,  $J = 7.6$  Hz, 2H), 7.47 – 7.37 (m, 4H), 7.37 – 7.30 (m, 1H), 7.23 – 7.12 (m, 4H), 5.78 (d,  $J = 6.9$  Hz, 1H), 4.75 (dd,  $J = 12.8, 6.5$  Hz, 1H), 2.94 (dd,  $J = 15.3, 6.8$  Hz, 1H), 2.85 (dd,  $J = 15.3, 5.7$  Hz, 1H), 2.34 (s, 3H), 1.36 (s, 9H).  $^{13}\text{C}$  NMR (75.5 MHz,  $\text{CDCl}_3$ , ppm)  $\delta$  198.2, 143.4, 140.8, 140.7, 138.3, 137.6, 129.6, 129.0, 127.6, 127.4, 127.3, 127.2, 55.2, 50.2, 49.0, 29.8, 21.6. LRMS (ESI)  $m/z$  490.1 ( $\text{M} + \text{Na}^+$ ), HRMS (ESI)  $m/z$  490.1480 ( $\text{M} + \text{Na}^+$ ), calc. for  $\text{C}_{26}\text{H}_{29}\text{NO}_3\text{S}_2\text{Na}$  490.1481.

The *ee* was determined by HPLC analysis. CHIRALPAK IA (4.6 mm i.d. x 250 mm); Hexane/2-propanol = 80/20; flow rate 1.0 ml/min; 25 °C; 254 nm; retention time: 16.7 min (major), 18.5 min (minor).



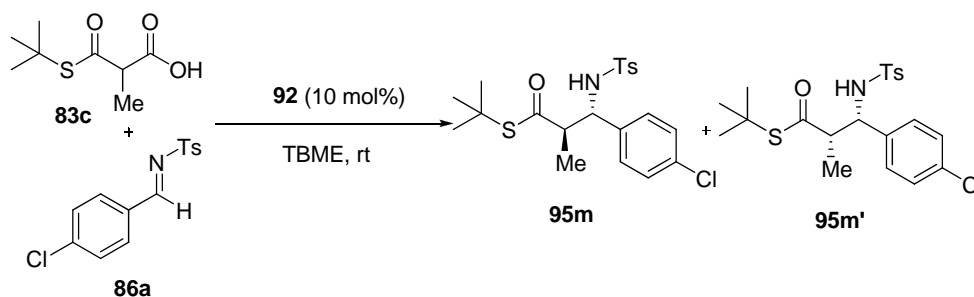
**(S)-S-*tert*-butyl**

**3-(4-methylphenylsulfonamido)-3-(thiophen-2-yl)propanethioate (95I)**

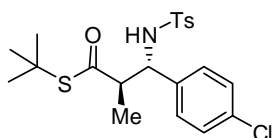
White solid, Mp: 97 – 99 °C. 85% *ee*,  $[\alpha]_D^{29} = -25.6$  (*c* 0.78, CHCl<sub>3</sub>); <sup>1</sup>H NMR (500 MHz, CDCl<sub>3</sub>, ppm) δ 7.66 (d, *J* = 8.2 Hz, 2H), 7.21 (d, *J* = 8.0 Hz, 2H), 7.11 (dd, *J* = 5.0, 1.1 Hz, 1H), 6.83 – 6.78 (m, 1H), 6.78 – 6.74 (m, 1H), 5.72 (d, *J* = 7.9 Hz, 1H), 4.99 (dd, *J* = 13.4, 5.8 Hz, 1H), 3.02 (dd, *J* = 15.7, 5.6 Hz, 1H), 2.93 (dd, *J* = 15.7, 5.9 Hz, 1H), 2.39 (s, 3H), 1.38 (s, 9H). <sup>13</sup>C NMR (75.5 MHz, CDCl<sub>3</sub>, ppm) δ 198.0, 143.5, 143.2, 137.6, 129.7, 127.3, 126.8, 125.4, 125.4, 51.1, 50.3, 49.1, 29.8, 21.7. LRMS (ESI) *m/z* 420.0 (M + Na<sup>+</sup>), HRMS (ESI) *m/z* 420.0733 (M + Na<sup>+</sup>), calc. for C<sub>18</sub>H<sub>23</sub>NO<sub>3</sub>S<sub>3</sub>Na 420.0732.

The *ee* was determined by HPLC analysis. CHIRALPAK IA (4.6 mm i.d. x 250 mm); Hexane/2-propanol = 70/30; flow rate 1.0 ml/min; 25 °C; 230 nm; retention time: 8.5 min (major), 10.3 min (minor).

### 2.5.3 Typical experimental procedure for the reaction between MAHT **83c** and *N*-Tosyl imine **86a** catalyzed by **92**



*N*-Tosyl imine **86a** (14.6 mg, 0.05 mmol, 1.0 equiv.) and **92** (1.12 mg, 0.005 mmol, 0.1 equiv) were dissolved in TBME (1.0 ml). The mixture stirred at room temperature for 10 min, followed by adding MAHT **83c** (14.3 mg, 0.075 mmol, 1.5 equiv.). The reaction mixture was stirred at room temperature and monitored by TLC. After 96 hours, upon complete consumption of **86a**, the reaction solvent was removed *in vacuo* and the crude product was directly loaded onto a short silica gel column, followed by gradient elution with hexane/EA mixtures (20/1 - 6/1 ratio). After removing the solvent, products **95m** and **95m'** (totally 20.2 mg) were obtained as white solid in 92% yield. **95m** and **95m'** were separated by flash chromatography.

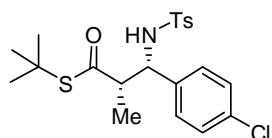


(*2R,3S*)-*S*-*tert*-butyl

3-(4-chlorophenyl)-2-methyl-3-(4-methylphenylsulfonamido)propanethioate

(**95m**)

White solid, Mp: 144 –146 °C. 96% *ee*,  $[\alpha]_{\text{D}}^{29} = -117.2$  (*c* 1.09, CHCl<sub>3</sub>); <sup>1</sup>H NMR (500 MHz, CDCl<sub>3</sub>, ppm) δ 7.48 (d, *J* = 8.2 Hz, 2H), 7.13 – 7.03 (m, 4H), 6.94 (d, *J* = 8.3 Hz, 2H), 6.05 (d, *J* = 8.3 Hz, 1H), 4.46 (dd, *J* = 8.1, 5.9 Hz, 1H), 2.83 – 2.73 (m, 1H), 2.34 (s, 3H), 1.34 (s, 9H), 1.14 (d, *J* = 7.0 Hz, 3H). <sup>13</sup>C NMR (75.5 MHz, CDCl<sub>3</sub>, ppm) δ 203.7, 143.3, 138.0, 137.8, 133.4, 129.42, 128.5, 128.3, 127.1, 77.6, 77.2, 76.8, 60.3, 53.4, 49.1, 29.6, 21.6, 16.5. LRMS (ESI) *m/z* 462.0 (M + Na<sup>+</sup>), HRMS (ESI) *m/z* 462.0932 (M + Na<sup>+</sup>), calc. for C<sub>21</sub>H<sub>26</sub>ClNO<sub>3</sub>S<sub>2</sub>Na 460.0935.



**(2*S*,3*S*)-*S*-*tert*-butyl**

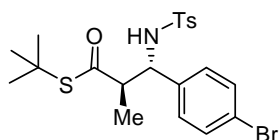
**3-(4-chlorophenyl)-2-methyl-3-(4-methylphenylsulfonamido)propanethioate**

**(95*m*<sup>?</sup>)**

Colorless oil; 68% *ee*,  $[\alpha]_{\text{D}}^{29} = -6.0$  (*c* 0.71, CHCl<sub>3</sub>); <sup>1</sup>H NMR (500 MHz, CDCl<sub>3</sub>, ppm) δ 7.50 (d, *J* = 8.0 Hz, 2H), 7.14 – 7.03 (m, 4H), 6.93 (d, *J* = 8.2 Hz, 2H), 5.57 (d, *J* = 7.6 Hz, 1H), 4.40 (t, *J* = 7.5 Hz, 1H), 2.84 – 2.70 (m, 1H), 2.36 (s, 3H), 1.26 (s, 9H), 1.18 (d, *J* = 7.0 Hz, 3H). <sup>13</sup>C NMR (75.5 MHz, CDCl<sub>3</sub>, ppm) δ 202.1, 143.6, 137.2, 137.0, 133.6, 129.6, 129.0, 128.4, 127.4, 59.9, 54.1, 48.6, 29.6, 21.6, 14.4. LRMS (ESI) *m/z* 462.0 (M + Na<sup>+</sup>).

The *ee* was determined by HPLC analysis. CHIRALPAK AD-H (4.6 mm i.d. x 250 mm); Hexane/2-propanol = 75/25; flow rate 1.0 ml/min; 25 °C; 230 nm;

retention time: *anti* isomer: 10.9 min (major), 24.3 min (minor); *syn* isomer: 6.6 min (minor), 8.1 min (major).

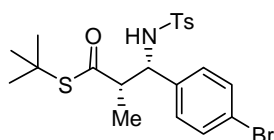


**(2*R*,3*S*)-*S*-tert-butyl**

**3-(4-bromophenyl)-2-methyl-3-(4-methylphenylsulfonamido)propanethioate**

**(95n)**

White solid, Mp: 145 –147 °C. 97% *ee*,  $[\alpha]_D^{29} = -108.6$  (*c* 0.96, CHCl<sub>3</sub>); <sup>1</sup>H NMR (500 MHz, CDCl<sub>3</sub>, ppm) δ 7.48 (d, *J* = 8.3 Hz, 2H), 7.26 – 7.22 (m, 2H), 7.08 (d, *J* = 8.0 Hz, 2H), 6.87 (d, *J* = 8.3 Hz, 2H), 6.01 (d, *J* = 8.3 Hz, 1H), 4.43 (dd, *J* = 8.2, 5.7 Hz, 1H), 2.85 – 2.73 (m, 1H), 2.35 (s, 3H), 1.34 (s, 9H), 1.15 (d, *J* = 7.0 Hz, 3H). <sup>13</sup>C NMR (75.5 MHz, CDCl<sub>3</sub>, ppm) δ 203.8, 143.3, 138.4, 138.0, 131.5, 129.4, 128.7, 127.1, 121.6, 60.4, 53.3, 49.1, 29.7, 21.6, 16.5. LRMS (ESI) *m/z* 506.0 (M + Na<sup>+</sup>), HRMS (ESI) *m/z* 506.0427 (M + Na<sup>+</sup>), calc. for C<sub>21</sub>H<sub>26</sub>BrNO<sub>3</sub>S<sub>2</sub>Na 506.0430.



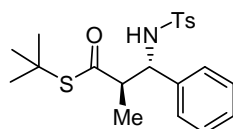
**(2*S*,3*S*)-*S*-tert-butyl**

**3-(4-bromophenyl)-2-methyl-3-(4-methylphenylsulfonamido)propanethioate**

**(95n')**

Colorless oil; 70% *ee*,  $[\alpha]_D^{29} = -20.0$  (*c* 0.68, CHCl<sub>3</sub>); <sup>1</sup>H NMR (500 MHz, CDCl<sub>3</sub>, ppm) δ 7.49 (d, *J* = 8.2 Hz, 2H), 7.24 (d, *J* = 8.5 Hz, 2H), 7.11 (d, *J* = 8.0 Hz, 2H), 6.88 (d, *J* = 8.4 Hz, 2H), 5.40 (d, *J* = 6.6 Hz, 1H), 4.39 (t, *J* = 6.1 Hz, 1H), 2.83 – 2.70 (m, 1H), 2.37 (s, 3H), 1.28 (s, 9H), 1.16 (d, *J* = 7.0 Hz, 3H). <sup>13</sup>C NMR (75.5 MHz, CDCl<sub>3</sub>, ppm) δ 202.2, 143.6, 137.4, 137.2, 131.4, 129.6, 129.4, 127.4, 77.65, 77.2, 76.8, 59.9, 53.9, 48.7, 29.6, 21.7, 14.2. LRMS (ESI) *m/z* 506.0 (M + Na<sup>+</sup>).

The *ee* was determined by HPLC analysis. CHIRALPAK AD-H (4.6 mm i.d. x 250 mm); Hexane/2-propanol = 75/25; flow rate 1.0 ml/min; 25 °C; 230 nm; retention time: *anti* isomer: 12.2 min (major), 29.2 min (minor); *syn* isomer: 7.4 min (minor), 9.1 min (major).

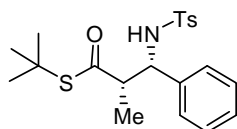


**(2*R*,3*S*)-*S*-*tert*-butyl**

**2-methyl-3-(4-methylphenylsulfonamido)-3-phenylpropanethioate (95o)**

White solid, Mp: 179 –181 °C. 98% *ee*,  $[\alpha]_D^{29} = -93.3$  (*c* 1.10, CHCl<sub>3</sub>); <sup>1</sup>H NMR (500 MHz, CDCl<sub>3</sub>, ppm) δ 7.49 (d, *J* = 8.2 Hz, 2H), 7.16 – 7.09 (m, 3H), 7.05 (d, *J* = 8.1 Hz, 2H), 7.02 – 6.97 (m, 2H), 5.97 (d, *J* = 8.4 Hz, 1H), 4.49 (dd, *J* = 8.4, 5.9 Hz, 1H), 2.87 – 2.79 (m, 1H), 2.31 (s, 3H), 1.34 (s, 9H), 1.14 (d, *J* = 7.0 Hz, 3H). <sup>13</sup>C NMR (126 MHz, CDCl<sub>3</sub>, ppm) δ 203.7, 142.9, 139.3, 138.3, 129.3, 128.40, 127.6, 127.2, 126.9, 60.9, 53.8, 48.9, 29.7, 21.6, 16.4. LRMS (ESI) *m/z* 428.1 (M + Na<sup>+</sup>), HRMS (ESI) *m/z* 428.1318 (M + Na<sup>+</sup>), calc. for

$C_{21}H_{27}NO_3S_2Na$ , 428.1325.

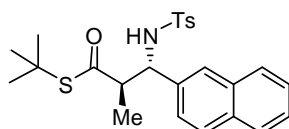


**(2*S*,3*S*)-*S*-tert-butyl**

**2-methyl-3-(4-methylphenylsulfonamido)-3-phenylpropanethioate (95o')**

White solid, Mp: 142 –143 °C. 67% *ee*,  $[\alpha]_D^{29} = -25.4$  (*c* 0.42,  $CHCl_3$ );  $^1H$  NMR (500 MHz,  $CDCl_3$ , ppm)  $\delta$  7.51 (d, *J* = 8.1 Hz, 2H), 7.16 – 7.05 (m, 5H), 7.02 – 6.95 (m, 2H), 5.41 (d, *J* = 7.7 Hz, 1H), 4.43 (t, *J* = 7.6 Hz, 1H), 2.87 – 2.77 (m, 1H), 2.33 (s, 3H), 1.25 (s, 9H), 1.20 (d, *J* = 7.0 Hz, 3H).  $^{13}C$  NMR (126 MHz,  $CDCl_3$ , ppm)  $\delta$  202.2, 143.3, 138.6, 137.5, 129.5, 128.3, 127.7, 127.5, 127.4, 60.6, 54.4, 48.4, 29.6, 21.6, 14.4. LRMS (ESI) *m/z* 428.1 (*M* +  $Na^+$ ).

The *ee* was determined by HPLC analysis. Lux 5u Cellulose-2 (4.6 mm i.d. x 250 mm); Hexane/2-propanol = 90/10; flow rate 1.0 ml/min; 25 °C; 230 nm; retention time: *anti* isomer: 17.2 min (minor), 21.4 min (major); *syn* isomer: 19.0 min (minor), 28.1 min (major).

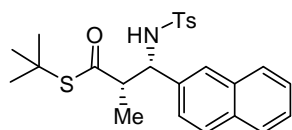


**(2*R*,3*S*)-*S*-tert-butyl**

**2-methyl-3-(4-methylphenylsulfonamido)-3-(naphthalen-2-yl)propanethioate**

**(95p)**

White solid, Mp: 136 –138 °C. 98% *ee*,  $[\alpha]_D^{29} = -108.7$  (*c* 1.31, CHCl<sub>3</sub>). <sup>1</sup>H NMR (500 MHz, CDCl<sub>3</sub>, ppm) δ 7.78 – 7.70 (m, 1H), 7.64 – 7.56 (m, 2H), 7.48 – 7.38 (m, 4H), 7.35 (s, 1H), 7.15 – 7.08 (m, 1H), 6.85 (d, *J* = 8.0 Hz, 2H), 6.06 (d, *J* = 8.4 Hz, 1H), 4.64 (dd, *J* = 8.3, 6.0 Hz, 1H), 3.03 – 2.82 (m, 1H), 2.10 (s, 3H), 1.32 (s, 9H), 1.20 (d, *J* = 7.0 Hz, 3H). <sup>13</sup>C NMR (126 MHz, CDCl<sub>3</sub>, ppm) δ 203.8, 143.0, 138.1, 136.2, 133.1, 132.86, 129.2, 128.4, 128.1, 127.7, 127.1, 126.4, 126.3, 126.1, 124.6, 61.2, 53.56, 49.0, 29.7, 21.4, 16.6. LRMS (ESI) *m/z* 478.1 (M + Na<sup>+</sup>), HRMS (ESI) *m/z* 478.1479 (M + Na<sup>+</sup>), calc. for C<sub>25</sub>H<sub>29</sub>NO<sub>3</sub>S<sub>2</sub>Na, 478.1471.



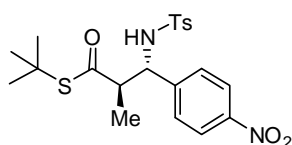
**(2*S*,3*S*)-*S*-*tert*-butyl**

**2-methyl-3-(4-methylphenylsulfonamido)-3-(naphthalen-2-yl)propanethioate**

**(95*p*'**

White solid, Mp: 130 –132 °C. 65% *ee*,  $[\alpha]_D^{29} = -7.9$  (*c* 0.84, CHCl<sub>3</sub>); <sup>1</sup>H NMR (500 MHz, CDCl<sub>3</sub>, ppm) δ 7.76 – 7.69 (m, 1H), 7.64 – 7.56 (m, 2H), 7.49 – 7.39 (m, 4H), 7.32 (s, 1H), 7.16 – 7.11 (m, 1H), 6.91 (d, *J* = 7.9 Hz, 2H), 5.46 (d, *J* = 7.4 Hz, 1H), 4.60 (t, *J* = 7.3 Hz, 1H), 2.99 – 2.89 (m, 1H), 2.14 (s, 3H), 1.24 (d, *J* = 7.0 Hz, 3H), 1.22 (s, 9H). <sup>13</sup>C NMR (126 MHz, CDCl<sub>3</sub>, ppm) δ 202.4, 143.3, 137.3, 135.4, 133.0, 132.9, 129.4, 128.2, 128.1, 127.7, 127.4, 127.2, 126.3, 126.2, 124.8, 60.8, 54.1, 48.6, 29.6, 21.4, 14.3. LRMS (ESI) *m/z* 478.1 (M + Na<sup>+</sup>).

The *ee* was determined by HPLC analysis. CHIRALPAK IA (4.6 mm i.d. x 250 mm); Hexane/2-propanol = 90/10; flow rate 1.0 ml/min; 25 °C; 254 nm; retention time: *anti* isomer: 18.4 min (major), 32.4 min (minor); *syn* isomer: 15.0 min (major), 23.2 min (minor).

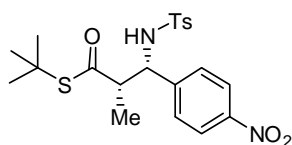


**(2*R*,3*S*)-*S*-*tert*-butyl**

**2-methyl-3-(4-methylphenylsulfonamido)-3-(4-nitrophenyl)propanethioate**

**(95q)**

White solid, Mp: 155 –157 °C. 94% *ee*,  $[\alpha]_D^{29} = -149.7$  (*c* 0.97, CHCl<sub>3</sub>). <sup>1</sup>H NMR (500 MHz, CDCl<sub>3</sub>, ppm) δ 8.01 (d, *J* = 8.7 Hz, 2H), 7.53 (d, *J* = 8.2 Hz, 2H), 7.23 (d, *J* = 8.7 Hz, 2H), 7.11 (d, *J* = 8.1 Hz, 2H), 6.25 (d, *J* = 8.3 Hz, 1H), 4.58 (dd, *J* = 8.2, 5.2 Hz, 1H), 2.87 – 2.80 (m, 1H), 2.33 (s, 3H), 1.31 (s, 9H), 1.17 (d, *J* = 7.1 Hz, 3H). <sup>13</sup>C NMR (126 MHz, CDCl<sub>3</sub>, ppm) δ 203.5, 147.4, 146.9, 143.7, 137.8, 129.59, 127.9, 127.1, 123.6, 60.2, 53.0, 49.4, 29.6, 21.6, 16.6. LRMS (ESI) *m/z* 473.0 (M + Na<sup>+</sup>), HRMS (ESI) *m/z* 473.1167 (M + Na<sup>+</sup>), calc. for C<sub>21</sub>H<sub>26</sub>N<sub>2</sub>O<sub>5</sub>S<sub>2</sub>Na, 473.1175.

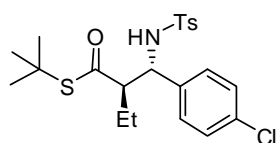


**(2*S*,3*S*)-*S*-*tert*-butyl**

**2-methyl-3-(4-methylphenylsulfonamido)-3-(4-nitrophenyl)propanethioate****(95q')**

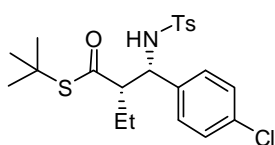
White solid, Mp: 148 –150 °C. 74% *ee*,  $[\alpha]_D^{29} = -9.4$  (*c* 0.59, CHCl<sub>3</sub>); <sup>1</sup>H NMR (500 MHz, CDCl<sub>3</sub>, ppm) δ 8.03 (d, *J* = 8.7 Hz, 2H), 7.56 (d, *J* = 8.2 Hz, 2H), 7.28 (d, *J* = 4.2 Hz, 2H), 7.15 (d, *J* = 8.0 Hz, 2H), 5.72 (d, *J* = 6.9 Hz, 1H), 4.56 (t, *J* = 7.0 Hz, 1H), 2.95 – 2.70 (m, 1H), 2.37 (s, 3H), 1.29 (s, 9H), 1.19 (d, *J* = 7.0 Hz, 3H). <sup>13</sup>C NMR (126 MHz, CDCl<sub>3</sub>, ppm) δ 201.7, 147.5, 146.0, 144.0, 137.0, 129.7, 128.7, 127.4, 123.5, 59.8, 53.7, 49.0, 29.6, 21.6, 14.1. LRMS (ESI) *m/z* 473.0 (M + Na<sup>+</sup>).

The *ee* was determined by HPLC analysis. CHIRALPAK IA (4.6 mm i.d. x 250 mm); Hexane/2-propanol = 70/30; flow rate 1.0 ml/min; 25 °C; 230 nm; retention time: *anti* isomer: 16.6 min (major), 28.6 min (minor); *syn* isomer: 7.1 min (minor), 9.2 min (major).

**(R)-S-tert-butyl****2-((S)-(4-chlorophenyl)(4-methylphenylsulfonamido)methyl)butanethioate****(95r)**

White solid, Mp: 139 –141 °C. 98% *ee*,  $[\alpha]_D^{29} = -96.0$  (*c* 0.50, CHCl<sub>3</sub>). <sup>1</sup>H NMR (500 MHz, CDCl<sub>3</sub>, ppm) δ 7.47 (d, *J* = 8.3 Hz, 2H), 7.14 – 7.00 (m, 4H), 6.90 (d, *J* = 8.4 Hz, 2H), 6.10 (d, *J* = 8.5 Hz, 1H), 4.54 (dd, *J* = 8.4, 5.0 Hz, 1H),

2.59 – 2.52 (m, 1H), 2.34 (s, 3H), 1.80 – 1.69 (m, 1H), 1.54 – 1.47 (m, 1H), 1.32 (s, 9H), 0.93 (t,  $J = 7.4$  Hz, 3H).  $^{13}\text{C}$  NMR (126 MHz,  $\text{CDCl}_3$ , ppm)  $\delta$  203.8, 143.2, 138.2, 137.9, 133.3, 129.41, 128.5, 128.2, 127.1, 60.8, 58.6, 49.3, 29.6, 24.3, 21.6, 11.9. LRMS (ESI)  $m/z$  476.1 ( $\text{M} + \text{Na}^+$ ), HRMS (ESI)  $m/z$  476.1080 ( $\text{M} + \text{Na}^+$ ), calc. for  $\text{C}_{22}\text{H}_{28}\text{ClNO}_3\text{S}_2\text{Na}$ , 476.1091.



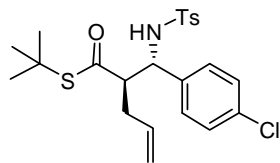
**(S)-S-tert-butyl**

**2-((S)-(4-chlorophenyl)(4-methylphenylsulfonamido)methyl)butanethioate**

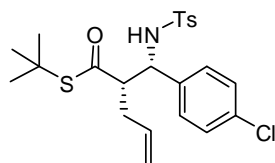
**(95r')**

Colorless oil; 22% *ee*.  $^1\text{H}$  NMR (500 MHz,  $\text{CDCl}_3$ , ppm)  $\delta$  7.48 (d,  $J = 8.0$  Hz, 2H), 7.09 (dd,  $J = 13.2, 8.1$  Hz, 4H), 6.92 (d,  $J = 8.2$  Hz, 2H), 5.30 (d,  $J = 7.2$  Hz, 1H), 4.37 (t,  $J = 7.5$  Hz, 1H), 2.64 – 2.52 (m, 1H), 2.36 (s, 3H), 1.74 – 1.64 (m, 2H), 1.23 (s, 9H), 0.88 (t,  $J = 7.4$  Hz, 3H).  $^{13}\text{C}$  NMR (75 MHz,  $\text{CDCl}_3$  ppm)  $\delta$  201.4, 143.6, 137.2, 137.1, 133.6, 129.6, 129.0, 128.4, 127.4, 61.5, 59.1, 48.9, 29.6, 22.2, 21.6, 11.8. LRMS (ESI)  $m/z$  476.0 ( $\text{M} + \text{Na}^+$ ).

The *ee* was determined by HPLC analysis. CHIRALPAK IA (4.6 mm i.d. x 250 mm); Hexane/2-propanol = 90/10; flow rate 1.0 ml/min; 25 °C; 210 nm; retention time: *anti* isomer: 14.2 min (major), 30.0 min (minor); *syn* isomer: 10.8 min (minor), 11.9 min (major).

**(R)-S-tert-butyl****2-((S)-(4-chlorophenyl)(4-methylphenylsulfonamido)methyl)pent-4-enoate (95s)**

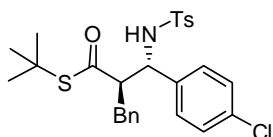
White solid, Mp: 132 –134 °C. 96% *ee*,  $[\alpha]_D^{29} = -57.4$  (*c* 0.50, CHCl<sub>3</sub>). <sup>1</sup>H NMR (500 MHz, CDCl<sub>3</sub>, ppm) δ 7.47 (d, *J* = 8.2 Hz, 2H), 7.13 – 7.01 (m, 4H), 6.89 (d, *J* = 8.4 Hz, 2H), 6.15 (d, *J* = 8.6 Hz, 1H), 5.79 – 5.64 (m, 1H), 5.14 – 5.02 (m, 2H), 4.57 (dd, *J* = 8.7, 4.7 Hz, 1H), 2.74 – 2.61 (m, 1H), 2.48 – 2.40 (m, 1H), 2.34 (s, 3H), 2.32 – 2.26 (m, 1H), 1.31 (s, 9H). <sup>13</sup>C NMR (75 MHz, CDCl<sub>3</sub>) δ 203.2, 143.3, 138.2, 137.7, 133.8, 133.4, 129.4, 128.5, 128.2, 127.1, 118.7, 58.7, 58.3, 49.5, 35.2, 29.6, 21.6. LRMS (ESI) *m/z* 488.0 (M + Na<sup>+</sup>), HRMS (ESI) *m/z* 488.1087 (M + Na<sup>+</sup>), calc. for C<sub>23</sub>H<sub>28</sub>ClNO<sub>3</sub>S<sub>2</sub>Na, 488.1091.

**(S)-S-tert-butyl****2-((S)-(4-chlorophenyl)(4-methylphenylsulfonamido)methyl)pent-4-enoate (95s')**

White solid, Mp: 131 –133 °C. 41% *ee*. <sup>1</sup>H NMR (500 MHz, CDCl<sub>3</sub>, ppm) δ 7.48 (d, *J* = 8.3 Hz, 2H), 7.16 – 7.05 (m, 4H), 6.91 (d, *J* = 8.5 Hz, 2H), 5.74 – 5.58

(m, 1H), 5.40 (d,  $J = 7.6$  Hz, 1H), 5.12 – 5.00 (m, 2H), 4.41 (t,  $J = 7.8$  Hz, 1H), 2.76 – 2.69 (m, 1H), 2.45 – 2.39 (m, 2H), 2.36 (s, 3H), 1.23 (s, 9H).  $^{13}\text{C}$  NMR (126 MHz,  $\text{CDCl}_3$  ppm)  $\delta$  200.6, 143.7, 137.2, 136.8, 134.2, 133.7, 129.6, 129.0, 128.4, 127.4, 118.2, 59.5, 59.0, 49.1, 33.5, 29.6, 21.6. LRMS (ESI)  $m/z$  488.0 ( $\text{M} + \text{Na}^+$ ).

The *ee* was determined by HPLC analysis. CHIRALPAK IA (4.6 mm i.d. x 250 mm); Hexane/2-propanol = 90/10; flow rate 1.0 ml/min; 25 °C; 230 nm; retention time: *anti* isomer: 14.7 min (major), 27.7 min (minor); *syn* isomer: 11.5 min (major), 13.2 min (minor).



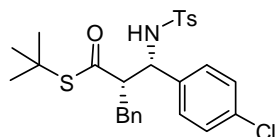
**(2*R*,3*S*)-*S*-*tert*-butyl**

**2-benzyl-3-(4-chlorophenyl)-3-(4-methylphenylsulfonamido)propanethioate**

**(95t)**

White solid, Mp: 164 –166 °C. 90% *ee*,  $[\alpha]_{\text{D}}^{20} = -19.2$  ( $c$  0.51,  $\text{CHCl}_3$ ).  $^1\text{H}$  NMR (500 MHz,  $\text{CDCl}_3$ , ppm)  $\delta$  7.46 (d,  $J = 8.2$  Hz, 2H), 7.31 –7.19 (m, 3H), 7.13 (d,  $J = 7.2$  Hz, 2H), 7.08 – 7.01 (m, 4H), 6.83 (d,  $J = 8.4$  Hz, 2H), 6.30 (d,  $J = 8.7$  Hz, 1H), 4.54 (dd,  $J = 8.7, 3.9$  Hz, 1H), 3.02 (dd,  $J = 15.8, 10.1$  Hz, 2H), 2.90 – 2.81 (m, 2H), 2.34 (s, 3H), 1.25 (s, 9H).  $^{13}\text{C}$  NMR (75 MHz,  $\text{CDCl}_3$  ppm)  $\delta$  203.6, 143.3, 138.2, 137.7, 137.6, 133.4, 129.4, 129.4, 128.8, 128.5, 128.2, 127.1, 127.0, 61.0, 58.4, 49.3, 37.1, 29.4, 21.6. LRMS (ESI)  $m/z$  538.1 ( $\text{M} + \text{Na}^+$ ), HRMS (ESI)  $m/z$  538.1240 ( $\text{M} + \text{Na}^+$ ), calc. for  $\text{C}_{27}\text{H}_{30}\text{ClNO}_3\text{S}_2\text{Na}$ ,

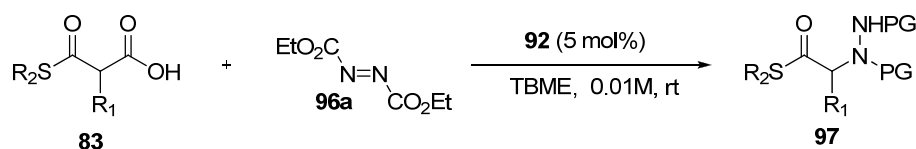
538.1248.

**(2*S*,3*S*)-*S*-tert-butyl****2-benzyl-3-(4-chlorophenyl)-3-(4-methylphenylsulfonamido)propanethioate****(95*t'*)**

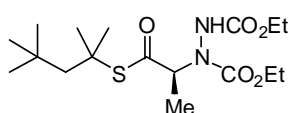
White solid, Mp: 161 –163 °C. 11% *ee*. <sup>1</sup>H NMR (500 MHz, CDCl<sub>3</sub>, ppm) δ 7.51 (d, *J* = 8.1 Hz, 2H), 7.25 – 7.08 (m, 7H), 7.02 (d, *J* = 7.4 Hz, 2H), 6.96 (d, *J* = 8.3 Hz, 2H), 5.38 (d, *J* = 7.2 Hz, 1H), 4.45 (t, *J* = 7.0 Hz, 1H), 3.02 – 2.83 (m, 3H), 2.36 (s, 3H), 1.12 (s, 9H) <sup>13</sup>C NMR (75 MHz, CDCl<sub>3</sub> ppm) δ 201.0, 143.8, 138.0, 137.0, 136.9, 133.8, 129.7, 129.4, 129.0, 128.6, 128.5, 127.5, 126.8, 61.8, 59.3, 48.8, 35.3, 29.4, 21.7. LRMS (ESI) *m/z* 538.1 (M + Na<sup>+</sup>).

The *ee* was determined by HPLC analysis. CHIRALPAK IA (4.6 mm i.d. x 250 mm); Hexane/2-propanol = 90/10; flow rate 1.0 ml/min; 25 °C; 230 nm; retention time: *anti* isomer: 26.8 min (major), 46.3 min (minor); *syn* isomer: 23.6 min (major), 34.2 min (minor).

## 2.5.4 General experimental procedure for decarboxylative amination between MAHTs **83** and diethyl azodicarboxylate **96a** catalyzed by **92**



Diethyl azodicarboxylate **96a** (23.7  $\mu$ l, 0.15 mmol, 3.0 equiv.) and **92** (0.56 mg, 0.0025 mmol, 0.05 equiv. for **83i**, 0.2 equiv. for **83j**, **83k**) were dissolved in TBME (5.0 ml), followed by adding MAHT **83** (0.05 mmol, 1.0 equiv.). The reaction mixture was stirred at room temperature and monitored by TLC. After 48 hours, upon complete consumption of **83**, the reaction solvent was removed *in vacuo* and the crude product was directly loaded onto a short silica gel column, followed by gradient elution with hexane/EA mixtures (20/1 - 6/1 ratio). After removing the solvent, product **97** was obtained as colorless oil.



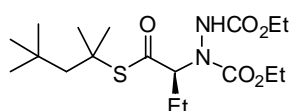
### (S)-Diethyl

### 1-(1-oxo-1-(2,4,4-trimethylpentan-2-ylthio)propan-2-yl)hydrazine-1,2-dicarboxylate (**97d**)

Colorless oil; 88% *ee*,  $[\alpha]_D^{29} = +3.9$  (*c* 1.35,  $\text{CHCl}_3$ ).  $^1\text{H}$  NMR (500 MHz,  $\text{CDCl}_3$ , ppm)  $\delta$  6.69 – 6.23 (m, 1H), 5.08 – 4.63 (m, 1H), 4.32 – 4.10 (m, 4H), 1.83 (s, 2H), 1.55 (d, *J* = 3.6 Hz, 6H), 1.44 (d, *J* = 6.2 Hz, 3H), 1.30 – 1.22 (m, 6H), 1.01

(s, 9H).  $^{13}\text{C}$  NMR (126 MHz,  $\text{CDCl}_3$  ppm)  $\delta$  200.8, 156.1, 63.2, 62.4, 53.8, 53.7, 32.9, 31.8, 29.9, 14.6. LRMS (ESI)  $m/z$  399.0 ( $\text{M} + \text{Na}^+$ ), HRMS (ESI)  $m/z$  399.1933 ( $\text{M} + \text{Na}^+$ ), calc. for  $\text{C}_{17}\text{H}_{32}\text{N}_2\text{O}_5\text{SNa}$ , 399.1924.

The *ee* was determined by HPLC analysis. CHIRALPAK IA (4.6 mm i.d. x 250 mm); Hexane/2-propanol = 92/08; flow rate 0.8 ml/min; 25 °C; 230 nm; retention time: 9.1 min (minor), 13.1 min (major).

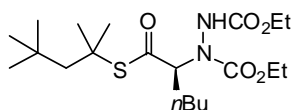


**(S)-Diethyl 1-(1-oxo-1-(2,4,4-trimethylpentan-2-ylthio)butan-2-yl)**

**hydrazine-1,2-dicarboxylate (97f)**

Colorless oil; 85% *ee*,  $[\alpha]_{\text{D}}^{29} = -4.0$  ( $c$  1.15,  $\text{CHCl}_3$ );  $^1\text{H}$  NMR (500 MHz,  $\text{CDCl}_3$ , ppm)  $\delta$  6.67 – 6.33 (m, 1H), 4.84 – 4.39 (m, 1H), 4.29 – 4.11 (m, 4H), 1.94 (br, 1H), 1.82 (s, 2H), 1.75 (br, 1H), 1.54 (s, 6H), 1.27 (t,  $J = 7.0$  Hz, 6H), 1.09 (br, 3H), 1.00 (s, 9H).  $^{13}\text{C}$  NMR (75 MHz,  $\text{CDCl}_3$  ppm)  $\delta$  200.1, 156.7, 70.5, 69.3, 63.2, 62.2, 54.0, 53.6, 32.9, 31.8, 29.9, 29.8, 22.6, 14.6, 11.3. LRMS (ESI)  $m/z$  413.0 ( $\text{M} + \text{Na}^+$ ), HRMS (ESI)  $m/z$  413.2094 ( $\text{M} + \text{Na}^+$ ), calc. for  $\text{C}_{18}\text{H}_{34}\text{N}_2\text{O}_5\text{SNa}$ , 413.2081.

The *ee* was determined by HPLC analysis. CHIRALPAK IA (4.6 mm i.d. x 250 mm); Hexane/2-propanol = 92/08; flow rate 0.8 ml/min; 25 °C; 230 nm; retention time: 7.5 min (minor), 9.5 min (major).



**(S)-Diethyl 1-(1-oxo-1-(2,4,4-trimethylpentan-2-ylthio)hexan-2-yl)**

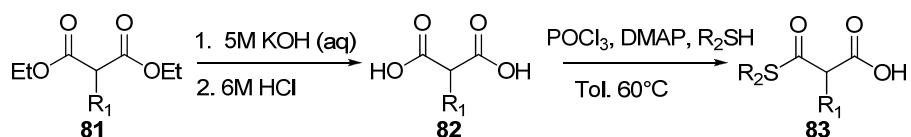
**hydrazine-1,2-dicarboxylate (97g)**

Colorless oil; 90% *ee*,  $[\alpha]_D^{29} = +3.5$  (*c* 1.42, CHCl<sub>3</sub>); <sup>1</sup>H NMR (500 MHz, CDCl<sub>3</sub>, ppm)  $\delta$  6.69 – 6.28 (m, 1H), 4.97 – 4.49 (m, 1H), 4.28 – 4.11 (m, 4H), 1.87 (br, 1H), 1.82 (s, 2H), 1.73 (br, 1H), 1.54 (s, 6H), 1.50 – 1.29 (m, 4H), 1.27 (t, *J* = 7.1 Hz, 6H), 1.00 (s, 9H), 0.90 (t, *J* = 7.3 Hz, 3H). <sup>13</sup>C NMR (75 MHz, CDCl<sub>3</sub> ppm)  $\delta$  200.4, 156.65, 68.7, 67.7, 63.2, 62.2, 54.0, 53.6, 32.9, 31.8, 29.9, 29.8, 28.8, 28.4, 22.5, 14.6, 14.0. LRMS (ESI) *m/z* 441.0 (M + Na<sup>+</sup>), HRMS (ESI) *m/z* 441.2392 (M + Na<sup>+</sup>), calc. for C<sub>20</sub>H<sub>38</sub>N<sub>2</sub>O<sub>5</sub>SNa, 441.2394.

The *ee* was determined by HPLC analysis. CHIRALPAK IA (4.6 mm i.d. x 250 mm); Hexane/2-propanol = 92/08; flow rate 0.8 ml/min; 25 °C; 230 nm; retention time: 6.7 min (minor), 8.8 min (major).

**2.5.5 Procedures for the preparation of Malonic acid half thioesters**

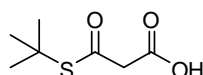
**(MAHTs)**



Substituted diethyl malonate **81** (10.0 mmol, 1.0 equiv.) and 20 ml 5M KOH (aq) was added to a 50 ml clean round bottom flask. After stirring at room temperature for 48 hours, the mixture was washed with diethyl ether (3×10 ml).

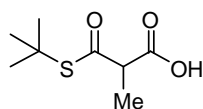
The aqueous phase was acidified with HCl (6M). The product was extracted with EA (3 x 20 ml). The combined EA fractions were dried over MgSO<sub>4</sub>. Evaporation of volatile compounds under reduced pressure gives the substituted malonic acid **82** (60-90% yield).

Substituted malonic acid **82** (5.0 mmol) and DMAP (0.5 mmol, 61 mg, 0.1 equiv.) was added to a 25 ml clean round bottom flask, followed by adding toluene (10 ml), POCl<sub>3</sub> (5.5 mmol, 512.7  $\mu$ l, 1.1 equiv) and R<sub>2</sub>SH (5.5 mmol, 1.1 equiv.). The mixture was heated to 60°C for 8 hours. The solvent was removed *in vacuo* and the crude product was directly loaded onto a silica gel column, followed by gradient elution with hexane/EA mixtures (20/1 - 4/1 ratio). After removing the solvent, product MAHT (30-70% yield) was obtained as colorless oil. Propanebis(thioate) was isolated as the side product.



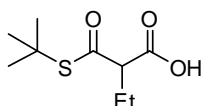
**3-(*tert*-Butylthio)-3-oxopropanoic acid (83b)**

Colorless oil. <sup>1</sup>H NMR (300 MHz, CDCl<sub>3</sub>, ppm),  $\delta$  10.58 (br, 1H), 3.47 (s, 2H), 1.41 (s, 9H). <sup>13</sup>C NMR (75 MHz, CDCl<sub>3</sub> ppm)  $\delta$  191.8, 171.7, 49.6, 49.3, 29.6. LRMS (ESI) *m/z* 175 (M – H<sup>+</sup>).



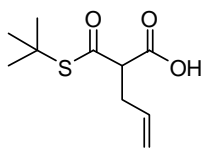
**3-(*tert*-Butylthio)-2-methyl-3-oxopropanoic acid (83c)**

Colorless oil.  $^1\text{H}$  NMR (300 MHz,  $\text{CDCl}_3$ , ppm),  $\delta$  11.25 (br, 1H), 3.50 (q,  $J = 7.2$  Hz, 1H), 1.38 (s, 9H), 1.31 (d,  $J = 7.2$  Hz, 3H).  $^{13}\text{C}$  NMR (75 MHz,  $\text{CDCl}_3$  ppm)  $\delta$  196.0, 175.5, 54.2, 48.9, 29.6, 14.1. LRMS (ESI)  $m/z$  189 ( $\text{M} - \text{H}^+$ ).



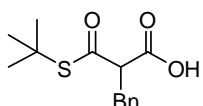
**2-(*tert*-Butylthiocarbonyl)butanoic acid (83d)**

Colorless oil.  $^1\text{H}$  NMR (300 MHz,  $\text{CDCl}_3$ , ppm),  $\delta$  11.05 (br, 1H), 3.36 (t,  $J = 7.4$  Hz, 1H), 2.01 – 1.78 (m, 2H), 1.42 (s, 9H), 0.92 (t,  $J = 7.4$  Hz, 3H).  $^{13}\text{C}$  NMR (75 MHz,  $\text{CDCl}_3$  ppm)  $\delta$  195.4, 174.9, 61.6, 49.2, 29.7, 23.2, 11.7.



**2-(*tert*-Butylthiocarbonyl)pent-4-enoic acid (83e)**

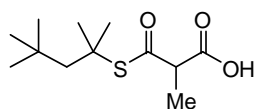
Colorless oil.  $^1\text{H}$  NMR (300 MHz,  $\text{CDCl}_3$ , ppm),  $\delta$  5.89 – 5.60 (m, 1H), 5.24 – 5.00 (m, 2H), 3.57 (t,  $J = 7.4$  Hz, 1H), 2.64 (t,  $J = 7.0$  Hz, 1H), 1.48 (s, 9H).  $^{13}\text{C}$  NMR (75 MHz,  $\text{CDCl}_3$  ppm)  $\delta$  194.8, 174.3, 133.5, 118.2, 59.7, 49.5, 33.6, 29.8. LRMS (ESI)  $m/z$  215 ( $\text{M} - \text{H}^+$ ).



**2-Benzyl-3-(*tert*-butylthio)-3-oxopropanoic acid (83f)**

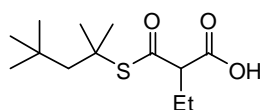
Colorless oil.  $^1\text{H}$  NMR (500 MHz,  $\text{CDCl}_3$  ppm)  $\delta$  7.31 – 7.16 (m, 5H), 3.79 (t,  $J$

= 7.5 Hz, 1H), 3.22 (d,  $J = 7.5$  Hz, 2H), 1.43 (s, 9H).  $^{13}\text{C}$  NMR (75 MHz,  $\text{CDCl}_3$  ppm)  $\delta$  194.5, 174.1, 137.2, 129.0, 128.5, 126.8, 61.6, 49.2, 35.2, 29.5. LRMS (ESI)  $m/z$  265 ( $\text{M} - \text{H}^+$ ).



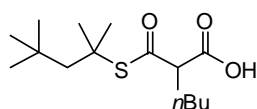
**2-Methyl-3-oxo-3-(2,4,4-trimethylpentan-2-ylthio)propanoic acid (83i)**

Colorless oil.  $^1\text{H}$  NMR (500 MHz,  $\text{CDCl}_3$  ppm)  $\delta$  9.63 (br, 1H), 3.63 – 3.52 (m, 1H), 1.84 (s, 2H), 1.57 (s, 6H), 1.42 (d,  $J = 7.1$  Hz, 3H), 1.02 (s, 9H).  $^{13}\text{C}$  NMR (126 MHz,  $\text{CDCl}_3$  ppm)  $\delta$  195.9, 175.7, 54.5, 54.1, 53.4, 32.7, 31.8, 29.6, 29.6, 14.3. LRMS (ESI)  $m/z$  245 ( $\text{M} - \text{H}^+$ ).



**2-((2,4,4-Trimethylpentan-2-ylthio)carbonyl)butanoic acid (83j)**

Colorless oil.  $^1\text{H}$  NMR (500 MHz,  $\text{CDCl}_3$  ppm)  $\delta$  10.21 (br, 1H), 3.38 (t,  $J = 7.3$  Hz, 1H), 1.94 – 1.86 (m, 2H), 1.83 – 1.78 (m, 2H), 1.54 (d,  $J = 2.6$  Hz, 6H), 0.99 (s, 9H), 0.95 (t,  $J = 7.5$  Hz, 3H).  $^{13}\text{C}$  NMR (126 MHz,  $\text{CDCl}_3$  ppm),  $\delta$  195.4, 174.7, 61.7, 54.4, 53.5, 32.8, 31.9, 29.6, 29.5, 23.3, 11.8. LRMS (ESI)  $m/z$  283 ( $\text{M} + \text{Na}^+$ ).



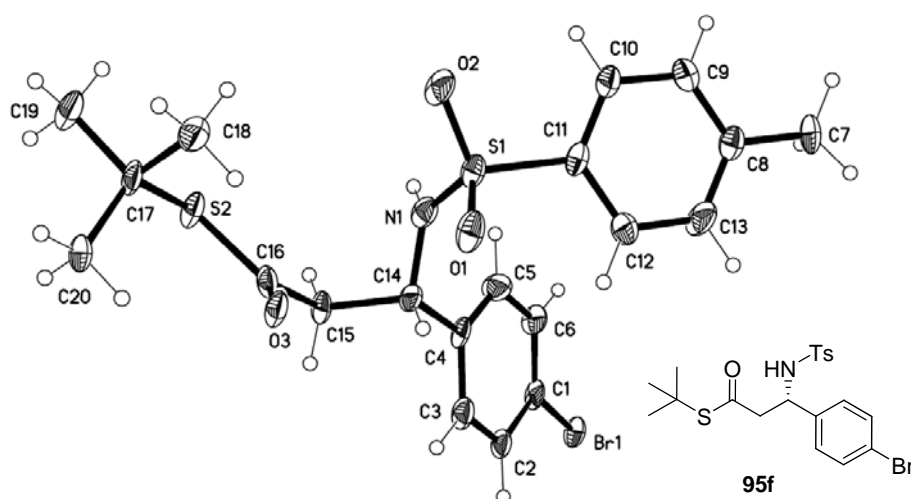
### 2-((2,4,4-Trimethylpentan-2-ylthio)carbonyl)hexanoic acid (**83k**)

Colorless oil.  $^1\text{H}$  NMR (500 MHz,  $\text{CDCl}_3$  ppm)  $\delta$  10.50 (br, 1H), 3.46 (t,  $J = 7.4$  Hz, 1H), 1.91 – 1.85 (m, 2H), 1.83 (d,  $J = 3.0$  Hz, 2H), 1.56 (d,  $J = 2.9$  Hz, 6H), 1.35 – 1.28 (m, 4H), 1.00 (s, 9H), 0.88 (t,  $J = 6.9$  Hz, 3H).  $^{13}\text{C}$  NMR (126 MHz,  $\text{CDCl}_3$  ppm),  $\delta$  195.5, 174.9, 60.2, 54.5, 53.6, 32.8, 31.8, 29.6, 29.6, 29.4, 22.5, 13.9. LRMS (ESI)  $m/z$  287 ( $\text{M} + \text{H}^+$ ).

### 2.5.6 Determination of the absolute configurations of adducts

The crystallographic coordinates of **95f** and **95n** have been deposited with the Cambridge Crystallographic Data Centre (CCDC; deposition no. 800382 and 800383). These data can be obtained free of charge from the CCDC at [www.ccdc.cam.ac.uk/data\\_request/cif](http://www.ccdc.cam.ac.uk/data_request/cif).

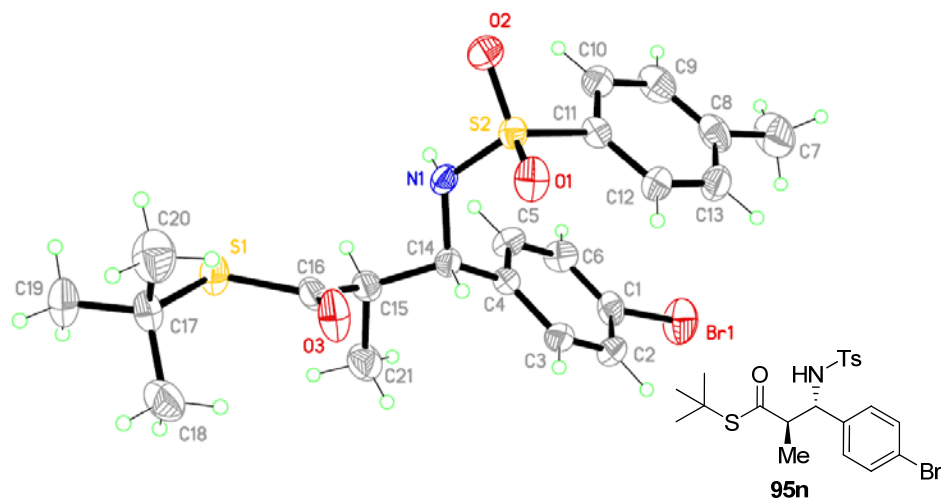
- i. Absolute configurations of **95b-l**, were determined by X-ray structure analysis of the product **95f**.



X-ray structure of **95f**

- ii. Absolute configurations of **95m-t**, were determined by X-ray structure

analysis of the product **95n**.



X-ray structure of **95n**

- iii. Absolute configurations of the *syn* isomers, **95m'-t'** were deduced by comparing the structure of compound **95n**.
- iv. Absolute configurations of compounds **97d-g** were deduced by comparing the structure of compound **95n**.

#### X-ray report of compound **95f** (A397)

The crystal is monoclinic, space group P2(1). The asymmetric unit contains one molecule of the compound  $C_{20}H_{24}NO_3S_2Br$ . As the absolute structure parameter is 0.038 with esd 0.0112, the reported structure is the correct hand. Final R values are  $R_1=0.0543$  and  $wR_2=0.1370$  for 2-theta up to  $55^\circ$

Table. Crystal data and structure refinement for A397.

Identification code a397

Empirical formula	C <sub>20</sub> H <sub>24</sub> Br N O <sub>3</sub> S <sub>2</sub>	
Formula weight	470.43	
Temperature	100(2) K	
Wavelength	0.71073 Å	
Crystal system	Monoclinic	
Space group	P2(1)	
Unit cell dimensions	a = 9.821(7) Å	α = 90°.
	b = 9.556(6) Å	β =
	106.741(13)°.	
	c = 11.956(8) Å	γ = 90°.
Volume	1074.5(12) Å <sup>3</sup>	
Z	2	
Density (calculated)	1.454 Mg/m <sup>3</sup>	
Absorption coefficient	2.127 mm <sup>-1</sup>	
F(000)	484	
Crystal size	0.60 x 0.18 x 0.16 mm <sup>3</sup>	
Theta range for data collection	2.17 to 27.46°.	
Index ranges	-12 ≤ h ≤ 12, -12 ≤ k ≤ 12, -15 ≤ l ≤ 14	
Reflections collected	7071	
Independent reflections	4394 [R(int) = 0.0369]	
Completeness to theta = 27.46°	99.3 %	

Absorption correction	Semi-empirical from equivalents
Max. and min. transmission	0.7272 and 0.3618
Refinement method	Full-matrix least-squares on F <sup>2</sup>
Data / restraints / parameters	4394 / 1 / 252
Goodness-of-fit on F <sup>2</sup>	1.078
Final R indices [I>2sigma(I)]	R1 = 0.0543, wR2 = 0.1370
R indices (all data)	R1 = 0.0591, wR2 = 0.1479
Absolute structure parameter	0.038(11)
Largest diff. peak and hole	1.901 and -1.469 e.Å <sup>-3</sup>

#### X-ray report of compound **95n** (A401)

The crystal is monoclinic, space group P2(1). The asymmetric unit contains one molecule of the compound C<sub>21</sub>H<sub>26</sub>NO<sub>3</sub>S<sub>2</sub>Br. As the absolute structure parameter is -0.0041 with esd 0.0075, the reported structure is the correct hand. Final R values are R1=0.0410 and wR2=0.0787 for 2-theta up to 55°

Table. Crystal data and structure refinement for A401.

Identification code	a401
---------------------	------

Empirical formula	C <sub>21</sub> H <sub>26</sub> Br N O <sub>3</sub> S <sub>2</sub>	
Formula weight	484.46	
Temperature	223(2) K	
Wavelength	0.71073 Å	
Crystal system	Monoclinic	
Space group	P2(1)	
Unit cell dimensions	a = 10.5875(7) Å	α = 90°.
	b = 9.8380(7) Å	β =
		99.811(2)°.
	c = 11.1154(8) Å	γ = 90°.
Volume	1140.85(14) Å <sup>3</sup>	
Z	2	
Density (calculated)	1.410 Mg/m <sup>3</sup>	
Absorption coefficient	2.005 mm <sup>-1</sup>	
F(000)	500	
Crystal size	0.60 x 0.16 x 0.14 mm <sup>3</sup>	
Theta range for data collection	1.86 to 27.50°.	
Index ranges	-11 ≤ h ≤ 13, -12 ≤ k ≤ 12, -14 ≤ l ≤ 13	
Reflections collected	8053	
Independent reflections	4898 [R(int) = 0.0319]	
Completeness to theta = 27.50°	99.7 %	

Absorption correction	Semi-empirical from equivalents
Max. and min. transmission	0.7666 and 0.3792
Refinement method	Full-matrix least-squares on F <sup>2</sup>
Data / restraints / parameters	4898 / 1 / 262
Goodness-of-fit on F <sup>2</sup>	0.933
Final R indices [I > 2σ(I)]	R1 = 0.0410, wR2 = 0.0787
R indices (all data)	R1 = 0.0515, wR2 = 0.0823
Absolute structure parameter	-0.004(8)

Largest diff. peak and hole 0.477 and -0.423 e.Å<sup>-3</sup>

**References:**

- (1) (a) Bordwell, F. G.; Fried, H. E. *J. Org. Chem.* **1981**, *46*, 4327. (b) Bordwell, F. G.; Fried, H. E. *J. Org. Chem.* **1991**, *56*, 4218
- (2) (a) Evans, D. A., Downey, C. W. & Hubbs, J. L. *J. Am. Chem. Soc.* **2003**, *125*, 8706. (b) Harada, S., Handa, S., Matsunaga, S., Shibasaki, M. *Angew. Chem. Int. Ed.* **2005**, *44*, 4365. (c) Saito, S., Kobayashi, S. *J. Am. Chem. Soc.* **2006**, *128*, 8704.
- (3) Notz, W., Tanaka, F., Barbas, C. F. *Acc. Chem. Res.* **2004**, *37*, 580. (b) Mukherjee, S., Yang, J. W., Hoffmann, S., List, B. *Chem. Rev.* **2007**, *107*, 5471.
- (4) (a) Alonso, D.; Kitagaki, S.; Utsumi, N.; Barbas, III C. F. *Angew. Chem., Int. Ed.* **2008**, *47*, 4588. (b) Utsumi, N.; Kitagaki, S.; Barbas, III C. F. *Org. Lett.* **2008**, *10*, 3405.
- (5) Kohler, M. C.; Yost, J. M.; Garnsey, M. R.; Coltart, D. M. *Org. Lett.* **2010**, *12*, 3376.
- (6) Guo, Q.; Bhanushali, M.; Zhao, C.-G. *Angew. Chem. Int. Ed.* **2010**, *49*, 9460.
- (7) Yamanaka, M.; Nishida, A.; Nakagawa, M. *J. Org. Chem.* **2003**, *68*, 3112.
- (8) Ye, W.; Leow, D.; Goh, S. L. M.; Tan, C.-T.; Chian, C.-H.; Tan, C.-H. *Tetrahedron Lett.* **2006**, *47*, 1007.
- (9) (a) Jiang, Z.; Pan, Y.; Zhao, Y.; Ma, T.; Lee, R.; Yang, Y.; Huang, K.-W.; Wong, M. W.; Tan, C.-H. *Angew. Chem. Int. Ed.* **2009**, *48*, 3627. (b) Lee, R.;

Lim, X.; Chen, T.; Tan, G.; Tan, C.-H.; Huang, K.-W.; *Tetrahedron Lett.* **2009**, *50*, 1560.

(10) For selected reviews of amination reactions: (a) Janey, J. M. *Angew. Chem. Int. Ed.* **2005**, *44*, 4292. (b) Nair, V.; Biju, A.; Mathew, S.; Babu, B. P. *Chem. Asian J.* **2008**, *3*, 810.

(11) Ye, W.; Jiang, Z.; Zhao, Y.; Goh, S. L. M.; Leow, D.; Soh, Y. T.; Tan, C.-H. *Adv. Synth. Catal.* **2007**, *349*, 2454.

***Chapter 3***

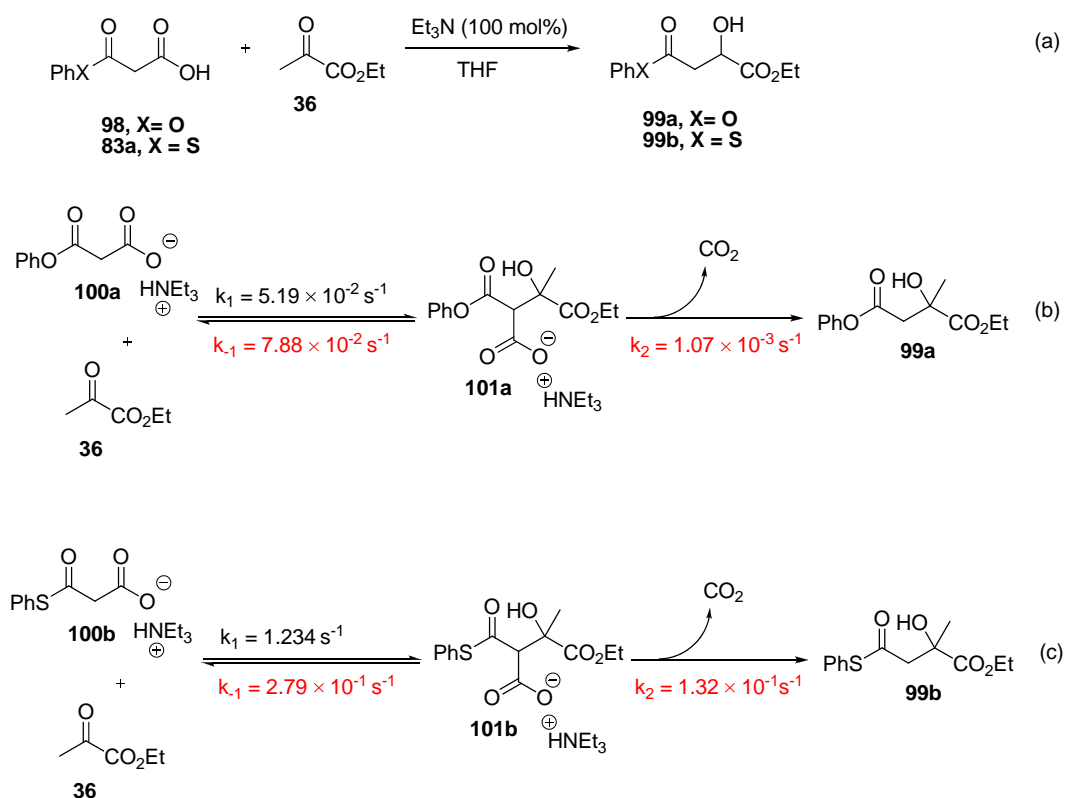
***Mechanistic Studies of Guanidine  
Catalyzed Decarboxylative Mannich Reaction***

### 3.1 Introduction

Various aspects of the mechanism of decarboxylative reactions have been discussed. The main debate is whether MAHT undergoes decarboxylation first to form the thioester enolate or it involves the formation of a nucleophilic addition carboxylate intermediate followed by loss of CO<sub>2</sub> (Scheme 1.5).

Shair and co-workers reported copper complex-catalyzed enantioselective decarboxylative aldol reaction with high enantioselectivities and good yields.<sup>1</sup> Based on the kinetic and isotope labeling experiments the predecarboxylation intermediate was proposed. Fagnou and co-workers proposed the similar intermediate **101** in triethylamine-catalyzed decarboxylative Aldol reaction by DOSY NMR (Scheme 3.1).<sup>2</sup>

By monitoring the relative concentration of MAHO **98**, intermediate **101** and product **99** in Benzene-*d*<sub>6</sub> using <sup>1</sup>H NMR, The reaction provided a close fit to the reversible model. The rate constants were calculated based on the reversible model. The constants showed that the nucleophilic addition was a faster and reversible process while the decarboxylation was irreversible and slower [Scheme 3.1 (b)]. The rate-determining step was the decarboxylation. The rate constants of decarboxylative aldol reaction of MAHT **83a** were also calculated and showed the similar results [Scheme 3.1 (c)]. Compared to the constants of MAHO and MAHT, MAHT showed higher reactivity.



**Scheme 3.1** (a) Decarboxylative Aldol reaction of MAHO and MAHT. (b) Calculated rate constants for reversible addition and irreversible decarboxylation of MAHO (c) Calculated rate constants for reversible addition and irreversible decarboxylation of MAHT

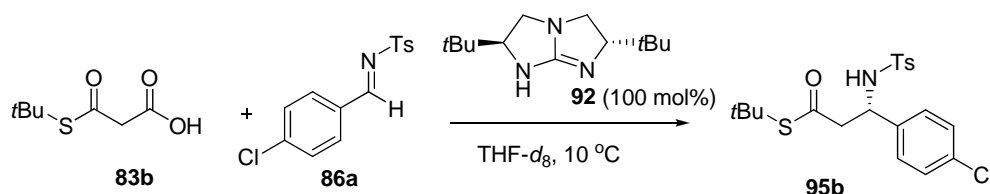
Rouden and co-workers also monitored the reaction profile of  $\text{Et}_3\text{N}$  catalyzed decarboxylative Mannich reaction and identified the nucleophilic addition intermediate.<sup>3</sup> However, on the other hand, Ricci and co-workers found Methyl thioester malonate **46** added to imines sluggishly in the presence of catalyst **44**. Acid **47** did not react with imine and only unproductive decarboxylation occurs.<sup>4</sup> Therefore they proposed that decarboxylation occurred first followed by nucleophilic addition.

Taking the advantage of previous reports, we will describe the mechanistic studies of the bicyclic guanidine catalyzed decarboxylative Mannich reaction in

the following sections.

### 3.2 NMR Study of the Reaction Profile.

Stoichiometric amount of bicyclic guanidine-catalyzed reaction between MAHT **83b** and imine **86a** in THF- $d_8$  showed the appearance of the new peaks in crude  $^1\text{H}$  NMR that were assigned as the two diastereoisomers of the nucleophilic addition carboxylate intermediates **8** (Figure 3.1).



**Scheme 3.2** Reaction of MAHT **83b** with imine **86a** monitored by  $^1\text{H}$  NMR in THF- $d_8$

$^1\text{H}$  NMR analysis revealed two key protons of intermediates **102a**, as shown in Figure 3.1, doublet at *syn*:  $\text{H}_a$ ,  $\delta = 4.63$  ppm ( $J = 8.3$  Hz),  $\text{H}_b$ ,  $\delta = 3.40$  ppm ( $J = 8.3$  Hz), and *anti*:  $\text{H}_a$ ,  $\delta = 4.59$  ppm ( $J = 9.2$  Hz),  $\text{H}_b$ ,  $\delta = 3.41$  ppm ( $J = 9.1$  Hz). This result is consistent with Rouden's observation in triethylamine-catalysed decarboxylative Mannich reactions. *N*-anionic compound bearing carboxylic acid group is difficult to detect due to the more basic site of nitrogen than oxygen. Once such compound forms, it will undergo fast intra-molecular proton transfer to form *O*-anionic compound. To our surprise, however, we also observed another pair of two key protons, *syn*:  $\text{H}_c$ ,  $\delta = 4.94$  ppm ( $J = 7.8$  Hz),  $\text{H}_d$ ,  $\delta = 3.51$  ppm ( $J = 7.8$  Hz), and *anti*:  $\text{H}_c$ ,  $\delta = 5.00$  ppm ( $J = 8.0$  Hz),  $\text{H}_d$ ,  $\delta = 3.50$  ppm ( $J = 8.1$  Hz). The new intermediate was assumed as *N*-anionic compound **102b**.

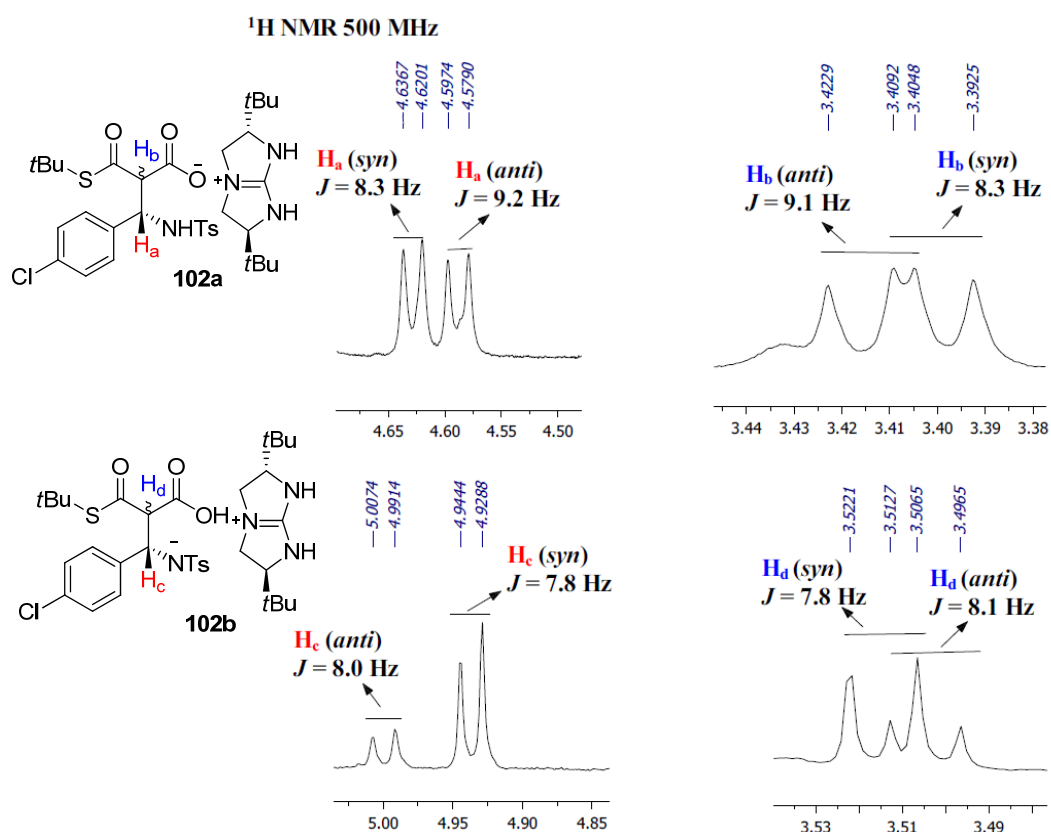


**Figure 3.1** Characterization of intermediate **102a** and **102b** via <sup>1</sup>H NMR

The reaction profile of the decarboxylative addition of MAHT **83b** to imine **86a** with stoichiometric amount of bicyclic guanidine **92** was monitored using <sup>1</sup>H NMR analysis (Figure 3.2). An internal standard pentachlorobenzene in THF-*d*<sub>8</sub> was used. It was shown in triethylamine-catalyzed decarboxylative Mannich reaction that the imine would be consumed rapidly with the slow formation of product. Once the reaction was started, the intermediate **102a**, **102b** and product **95b** appeared. The maximum concentration of intermediate **102a** observed at approximately *t* = 80 min while intermediate **102b** disappeared at *t* = 53 min.

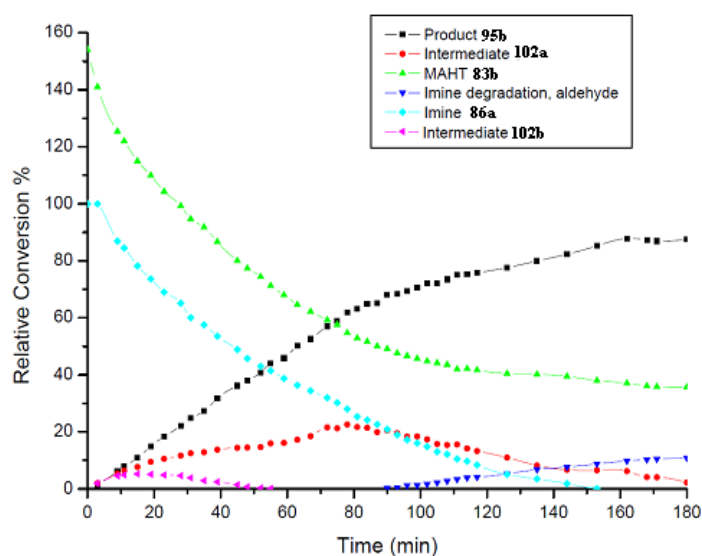


**Figure 3.2 Monitoring the reaction mixture at 10 °C in THF- $d_8$ .** The reaction species were monitored in THF- $d_8$  under stoichiometric amount of bicyclic guanidine **3** using  $^1\text{H}$  NMR. Relative conversions were measured based on an internal standard (pentachlorobenzene)

### 3.3 Mass Spectrometry Study of the Reaction Profile

Electron spray ionization mass spectrometry (ESI-MS) provides the access to the direct investigation of chemical reactions in solution. The high sensitivity of ESI-MS makes the detection possible not only for the reaction substrates and products, but also for the transient intermediates as they are present in real reaction conditions, providing new insights into the mechanism. We were pleased to discover that under standard catalytic reaction conditions, through direct injection ESI-MS analysis, the carboxylate intermediate **102a** or **102b** was successfully intercepted and characterized as its counter-anion species **103a** or **103b** (calculated  $m/z$ : 468.1, measured  $m/z$ : 468.1) (Figure 3.3). The isotope distribution analysis from the ESI-MS spectra was also consistent with **103a** or

**103b.** Such observations provided strong evidence that nucleophilic addition preceded decarboxylation.

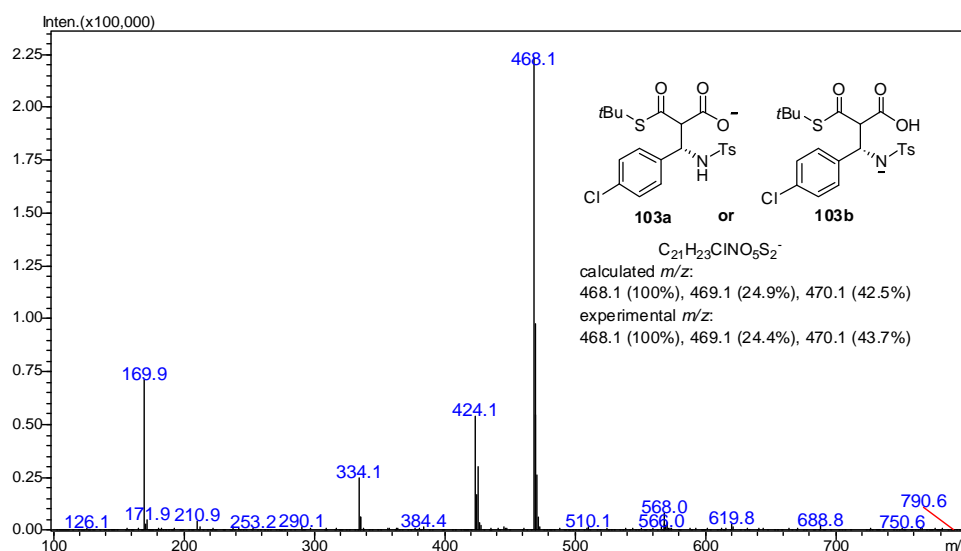


**Figure 3.3** Detection of counter-anions of **102a** or **102b** by direct injection ESI-MS

### 3.4 DFT Calculation

The observation of **102a/102b** via  $^1\text{H}$  NMR and **103a/103b** via ESI strongly supports a Nucleophilic addition/Decarboxylation mechanism. However, observation of self-decarboxylative product thioester during the course of reaction implies that the Decarboxylation/Nucleophilic addition pathway could not be conclusively ruled out. Hence, density functional theory (DFT) calculations were performed to further elucidate the mechanism. Decarboxylation of MAHT **83c** has a barrier of 18.5 kcal/mol (Figure 3.4a), which is substantially higher than both the barriers for Mannich (Figure 3.4b) and Tautomerization (Figure 3.4c). Four transition state structures (TS structure) leading to all four diastereoisomers were located for the Mannich reaction of **83c-enol** to **86a**. The pre-transition state

complexes showed that both **83c-enol** and **86a** are hydrogen-bonded to [**92+H**] (Figure 3.4b). This dual activation is expected to increase the reaction rate of the nucleophilic addition by bringing the reacting centers into close proximity and also by lowering the LUMO of **86a**. Thus, DFT calculation lends credence to the Nucleophilic addition/Decarboxylation mechanism on the basis of the lower  $\Delta G^\ddagger$  for nucleophilic addition relative to decarboxylation.

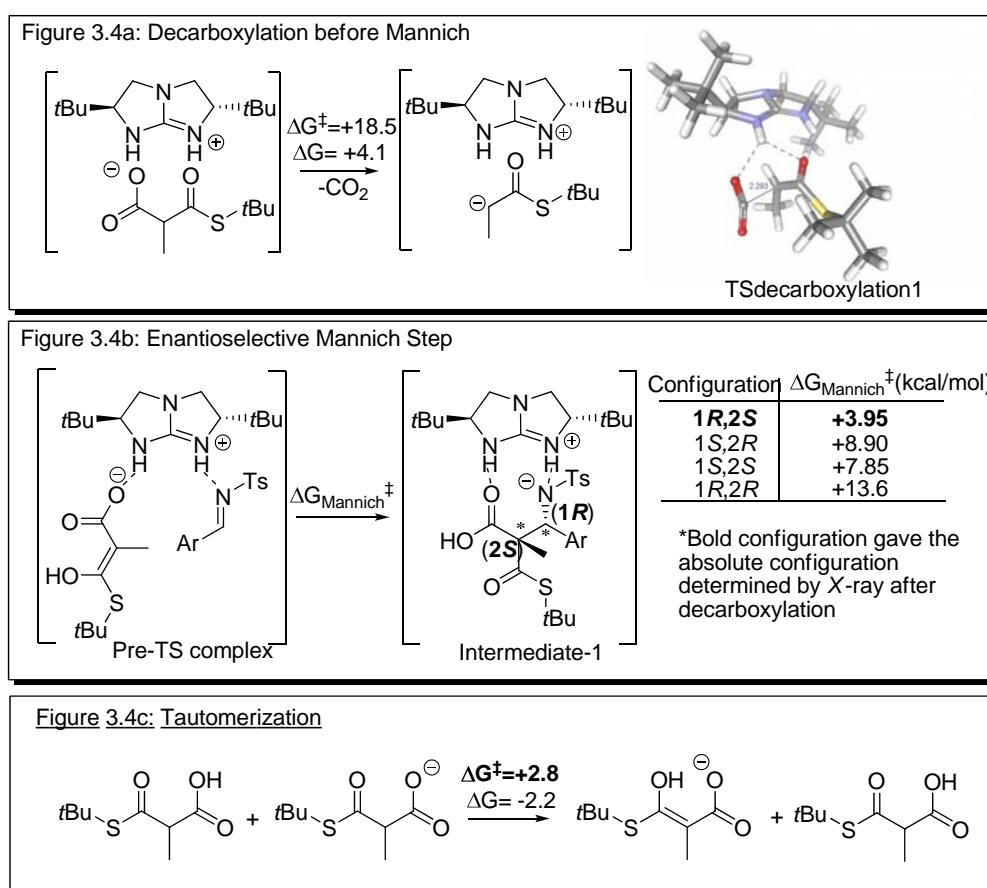


**Figure 3.4 DFT Calculation Results** Ar = 4-ClC<sub>6</sub>H<sub>4</sub>.  $\Delta G^\ddagger$  is the difference in Gibbs free energy between the transition states and the reactants.  $\Delta G$  is the difference in Gibbs free energy between the molecules on the right side of the chemical equation and those on the left. All units are given in kcal/mol.

**TS-1<sub>(1R,2S)</sub>** has the lowest Gibbs free energy among the four TS structures

located; it is 4.38 kcal/mol lower in energy compared to the next lowest energy

transition state, **TS-1**<sub>(1*S*,2*R*)</sub>. This result is consistent with both the absolute configuration observed experimentally and the high enantioselectivity observed (Scheme 2.9), which validates our theoretical calculations.

We further proposed the decarboxylation after the Mannich reaction proceeds *via* an intermediate-**3**, which is thermodynamically more stable than intermediate-**2** (Figure 3.5). The decarboxylation from intermediate-**3** has a  $\Delta G^\ddagger$  of 18.3 kcal/mol, which is of similar magnitude to the decarboxylation indicated in Figure 3.4a. This suggests that the  $\Delta G^\ddagger$  of decarboxylation is fairly unaffected by the chemical environment of the TS structures. Based on  $\Delta G^\ddagger$  in Figure 3.4, the rate-determining step is the decarboxylation, thus future attempts to increase the reaction rate should focus on tuning properties that can lower  $\Delta G^\ddagger$  of decarboxylation. Furthermore, intermediate **102a** and **102b** that was relevant to intermediate-**1** and **3** was proved in DFT calculation.

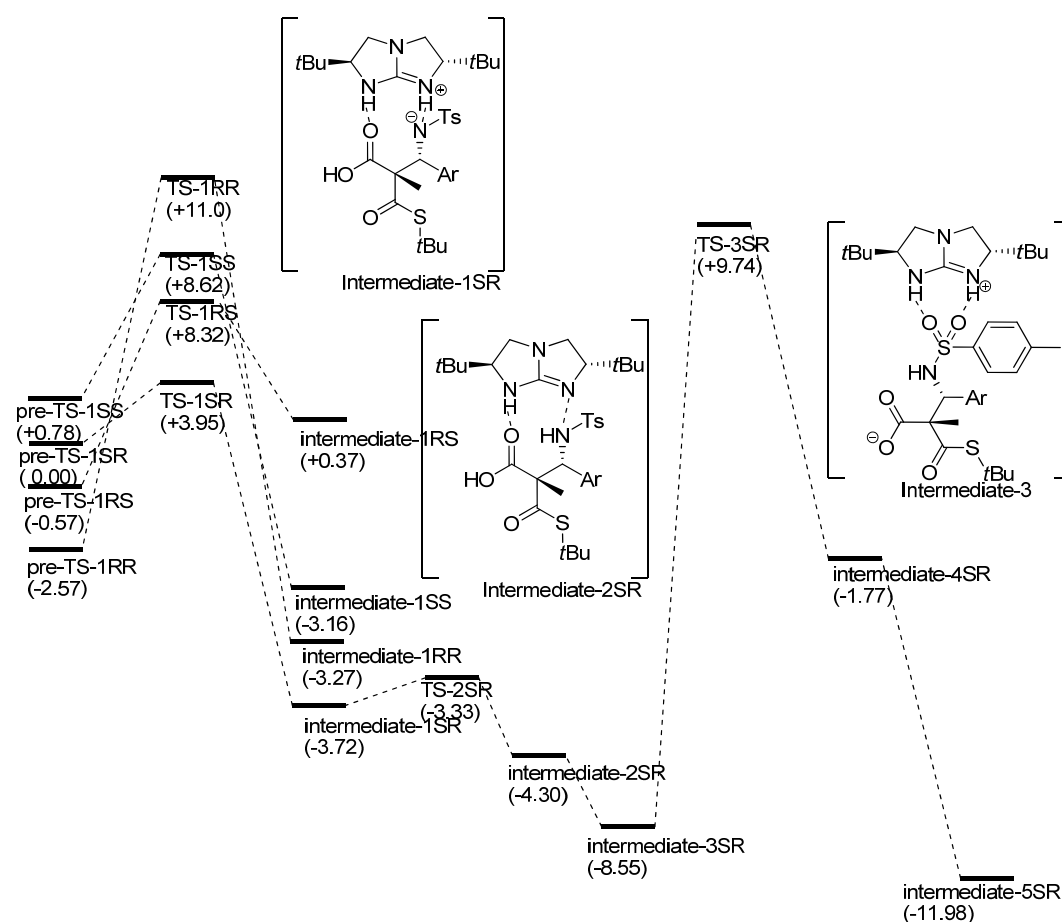
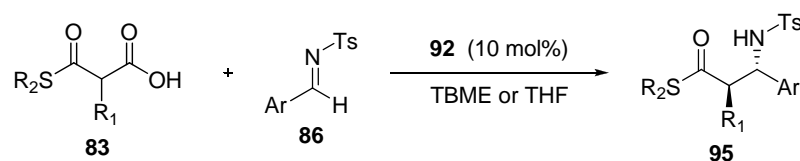


**Figure 3.5** Stationary points Ar = 4-ClC<sub>6</sub>H<sub>4</sub>. Stationary points optimized at RM06-2X/6-31G(d) on Gibbs free energy surface along the reaction coordinate. All energies are given in kcal/mol.

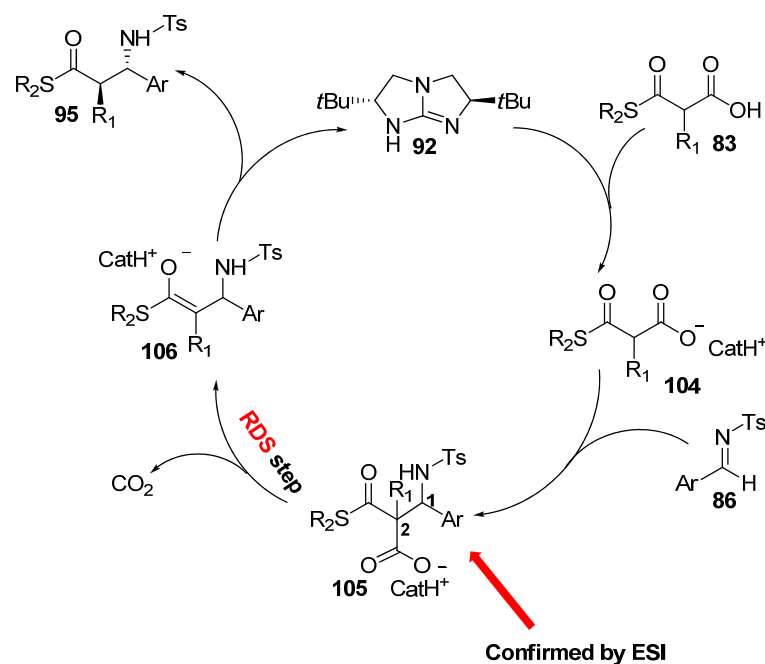
### 3.5 Proposed Mechanism



**Scheme 3.3** Reaction of MAHT **83** with imine **86** catalyzed by guanidine **92**

Based on the experimental studies and DFT calculation, we proposed the decarboxylative Mannich reaction shown in Scheme 3.3 which underwent nucleophilic addition followed by decarboxylation. As shown in Scheme 3.4, catalyst **92** deprotonated MAHT **83** and the resulting carboxylate **104** underwent

nucleophilic addition to form intermediate **105**, which was confirmed by ESI. The enantio-induction of the carbons C1 and C2 has been established at this step as 1*R*, 2*S*. Slow decarboxylation of intermediate **105** yielded enolate salt **106**, proton transfer in which then released the final product **95** and regenerated catalyst **92**. As mentioned before, the diastereoselectivity of such decarboxylative Mannich reaction was moderate. The reason was that the last step, protonation of the enolate showed low stereoselectivity. The enolate can obtain proton either from protonated **92** or MAHT **83**. Firstly, the  $pK_a$  of MAHT **83** probably was lower than the protonated **92**. Additionally, the concentration of MAHT **83** was higher than protonated **92**. Although ion pair may form between the enolate and protonated **92**; the enolate can abstract the proton directly from the substrate leading to the racemization of C2 carbon to give the low diastereoselectivity.



**Scheme 3.4** Proposed mechanism of decarboxylative Mannich reaction catalyzed by guanidine **92**.

### **3.6 Summary**

In conclusion, based on experimental characterization of intermediates and DFT calculations, we proposed that nucleophilic addition precedes decarboxylation. The nucleophilic addition step was faster while the decarboxylation step was very slower. The rate-determining step was the decarboxylation of the nucleophilic addition adduct.

## 3.7 Experimental Section

### 3.7.1 General procedures and methods

$^1\text{H}$  spectra were recorded on a DRX500 (500MHz) spectrometer. Chemical shifts are reported in parts per million (ppm). The residual solvent peak was used as an internal reference. Low resolution mass spectra were obtained on a Finnigan/MAT LCQ spectrometer in ESI mode and a Finnigan/MAT 95XL-T mass spectrometer in FAB mode.

### 3.7.2 Procedure for the Determination of Reaction Profile by $^1\text{H}$ NMR

MAHT **83b** (5.3 mg, 0.03 mmol, 1.5 equiv.) and internal standard pentachlorobenzene (4.9 mg, 0.02 mmol, 1.0 equiv.) were weighed and dissolved into 0.5 ml deuterated THF and charged into an oven-dried clean NMR tube. After the NMR tube was cooled to 10 °C, a baseline  $^1\text{H}$  NMR spectrum was obtained. A 0.25 ml deuterated THF solution of **92** (4.6 mg, 0.02 mmol, 1.0 equiv.) and *N*-Tosyl imine **86a** (5.9 mg, 0.02 mmol, 1.0 equiv.) were added. The time was noted, the tube was inverted to mix and a starting point  $^1\text{H}$  NMR spectrum was obtained.  $^1\text{H}$  NMR spectra were taken at 3 min intervals. Concentrations of reaction components at each time interval were then determined relative to internal standard.

### 3.7.3 Procedure for the determination of intermediate by ESI-MS

*N*-Tosyl imine **86a** (22.0 mg, 0.075 mmol, 1.5 equiv.) and **92** (1.12 mg, 0.005 mmol, 0.1 equiv) were dissolved in THF (0.5 ml). The mixture was cooled down to -10 °C. 15 min later, MAHT **83b** (8.8 mg, 0.05 mmol, 1.0 equiv.) was added. The reaction mixture was stirred at -10 °C. ESI-MS spectra were taken at 10 hours intervals.

### 3.7.4 Computational detail

All calculations were performed on 64-bit Linux systems in the HPC (High Performance Computing) center in NUS (National University of Singapore). Gaussian 09<sup>5</sup> was used for all calculations. Geometry optimization was performed at RM06-2X<sup>6</sup>/6-31G(d)<sup>7</sup> with tight convergence criteria *via* “opt=tight” and integration grid specified *via* “int=ultrafine”<sup>8</sup>. Frequency calculations were performed on all stationary points to verify their nature. Single point calculations (int=ultrafine option was used) on RM06-2X/6-31G(d) optimized stationary points were performed at RM06-2x/6-311++G(2df,2p)<sup>9</sup> and CPCM<sup>10</sup> solvation model was used to estimate the effect of THF on the energetic of the stationary points. Intrinsic Reaction Coordinates (IRC) calculations on all transition states were performed with the following combination of keywords “irc=(maxpoints=500,recalc=20,calcfc,maxcycle=100,tight) M062x/6-31G(d) geom=connectivity int=ultrafine”. The minima found by IRC were re-optimized and single points calculations were performed as described above.

---

**References:**

---

- (1) Fortner, K. C.; Shair, M. D. *J. Am. Chem. Soc.* **2007**, *129*, 1032.
- (2) Blaquiere, N.; Shore, D. G.; Rousseaux, S.; Fagnou, K. *J. Org. Chem.* **2009**, *74*, 6190.
- (3) Banchet, J.; Lefebvre, P.; Legay, R.; Lasne, M.-A.; Rouden, J. *Green Chem.*, **2010**, *12*, 252.
- (4) Ricci, A.; Petterson, D.; Bernardi, L.; Fini, F.; Fochi, M.; Perez Herrera, R.; Sgarzani, V. *Adv. Synth. Catal.* **2007**, *349*, 1037.
- (5) Frisch, M. J. *et al.* Gaussian 09, revision A.02; Gaussian, Inc.: Wallingford, CT, 2009.
- (6) Zhao, Y.; Truhlar, D. G. *Theor. Chem. Acc.* **2008**, *120*, 215.
- (7) (a) Ditchfield, R.; Hehre, W. J.; Pople, J. A. *J. Chem. Phys.* **1971**, *54*, 724; (b) Hehre, W. J.; Ditchfield, R.; Pople, J. A. *J. Chem. Phys.* **1972**, *56*, 2257; (c) Hariharan, P. C.; Pople, J. A. *Theor. Chim. Acta.* **1973**, *28*, 213; (d) Francl, M. M.; Pietro, W. J.; Hehre, W. J.; Binkley, J. S.; Gordon, M. S.; DeFrees, D. J.; Pople, J. A. *J. Chem. Phys.* **1982**, *77*, 3654.
- (8) For a discussion on the sensitivity of meta-hybrid functional to integration grid size: Wheeler, S. E.; Houk, K. N. *J. Chem. Theory. Comput.* **2010**, *6*, 395.

- (9) (a) Krishnan, R.; Binkley, J. S.; Seeger, R.; Pople, J. A. *J. Chem. Phys.* **1980**, 72, 650; (b) Frisch, M. J.; Pople, J. A.; Binkley, J. S. *J. Chem. Phys.* **1984**, 80, 3265; (c) McLean, A. D.; Chandler, G. S. *J. Chem. Phys.* **1980**, 72, 5639.
- (10) (a) Barone, V.; Cossi, M. *J. Phys. Chem. A* **1998**, 102, 1995; (b) Cossi, M.; Rega, N.; Scalmani, G.; Barone, V. *J. Comput. Chem.* **2003**, 24, 669.

*Chapter 4*

*Bicyclic Guanidine  
Catalyzed Enantioselective  
Mannich Reaction of Fluorocarbon Nucleophiles*

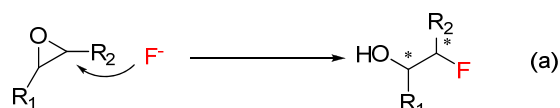
## **4.1 Fluorocarbon Nucleophiles**

Powerful probes for revealing the workings of biological systems can be prepared through the judicious replacement of hydrogen with fluorine.<sup>1</sup> The C-F bond brings about significant effect on the reactivity, stability and bioavailability of molecules. While natural organofluoro-compounds are rare, synthetic fluorinated compounds are widely used in a variety of fields because the incorporation of fluorine atom or fluorinated group often furnishes molecules with quite unique properties that cannot be replaced by any other element. Thus there is a strong demand for the expansion of the availability of versatile fluorine-containing building blocks.

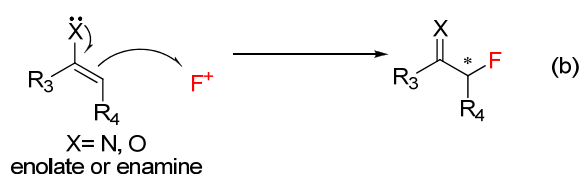
With this demand, several strategies have been developed for the construction of chiral fluorinated compounds (Scheme 4.1). Due to the small size of  $F^-$  and its low polarizability,  $F^-$  usually behaves like a base rather than a nucleophile. Hence nucleophilic fluorination always occurs in harsh conditions [Scheme 4.1 (a)].<sup>2</sup> On the other hand, with the development of various  $F^+$ -source, the electrophilic fluorination plays a key role in the formation of C-F bonds [Scheme 4.1 (b)].<sup>3</sup> However, the application is limited due to the use of  $F^+$  as the only electrophile, especially for the enantioselective cases. Recently, fluorocarbon nucleophiles have been developed to overcome the limitation of electrophilic fluorination in asymmetric synthesis [Scheme 4.1 (c)]. With the pre-installation of fluorine atom to a nucleophile, the resulted

fluorocarbon nucleophile is further activated by the fluorine atom and can be applied to traditional organic reactions, which is particularly suitable for organocatalytic transformations.

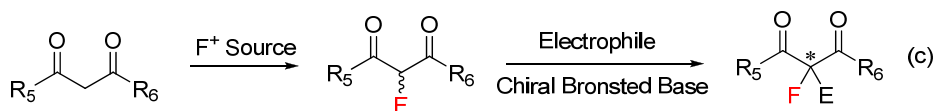
## Nucleophilic Fluorination



## Electrophilic Fluorination



## Fluorocarbon Nucleophile

**Scheme 4.1** Protocols to construct chiral C-F bond

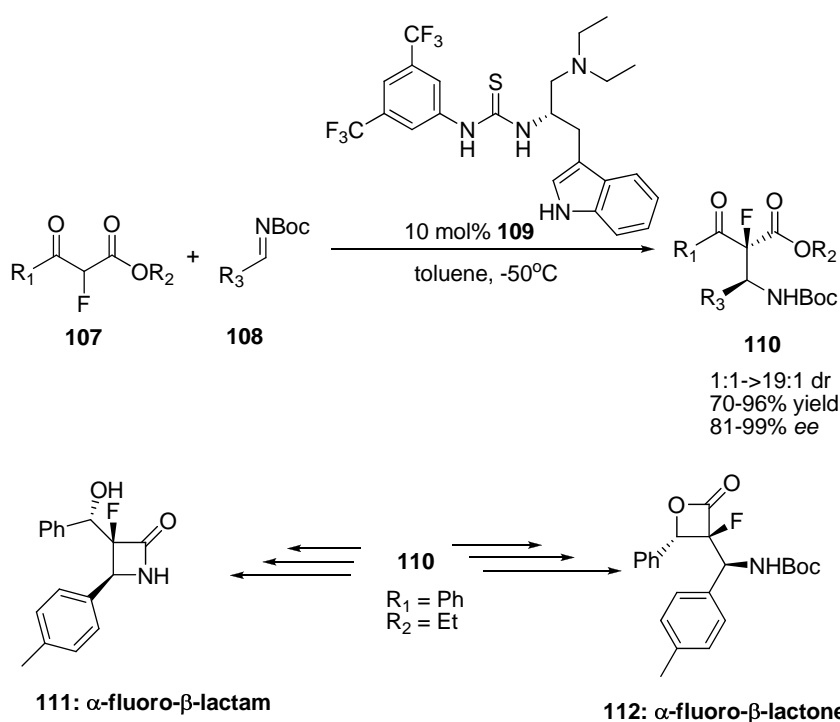
Organocatalytic enantioselective reactions with various fluorocarbon nucleophiles have been well developed during the past 5 years. 1-Fluoro-bis(phenylsulfonyl)methane (FBSM)<sup>4</sup> and fluoro(phenylsulfonyl)methane (FSM)<sup>5</sup> derivatives are effective synthetic equivalent of monofluoromethyl species in asymmetric catalysis. FBSM has been used in *Cinchona* alkaloid salt catalyzed asymmetric Mannich reaction and conjugate addition by Shibata. However, the  $\alpha$ -carbon is not chiral. FBSM is only used for the installation of fluorine atom but not the construction of chiral C-F bond.

On the other hand, fluorinated 1,3-dicarbonyl compounds are good candidates for the construction of chiral C-F bonds. 1,3-dicarbonyl compounds have already

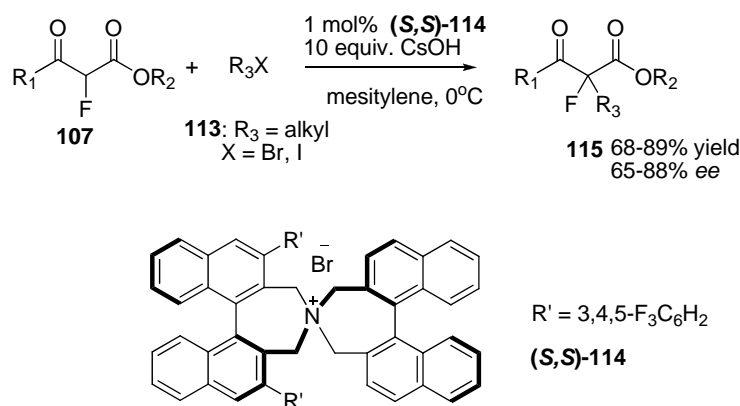
been proved as excellent nucleophiles in organocatalytic transformations. With the extra fluorine atom, the  $pK_a$  of the  $\alpha$ -carbon becomes even lower, which means fluorinated 1,3-dicarbonyl compounds can be easily activated under mild conditions. Furthermore, due to the most electron negative property of fluorine, it may affect the transition state orientation usually resulting in high diastereo- and enantioselectivity.

Several groups reported the use of fluorinated 1,3-dicarbonyl compound as nucleophiles with organocatalysts. Lu and co-workers reported asymmetric Mannich reaction of  $\alpha$ -fluoro- $\beta$ -ketoesters **107** and *N*-Boc imine **108** with a tryptophan-derived bifunctional thiourea catalyst (Scheme 4.2).<sup>6</sup> Good yields and *ee* values were obtained with moderate to good *dr*.  $\alpha$ -fluoro- $\beta$ -lactam and  $\alpha$ -fluoro- $\beta$ -lactone, which were key structures of many drug compounds, were successfully prepared in three steps from the Mannich product **110**. Catalyst **109** was first developed by them and the nitrogen atom of the indole moiety was proposed as hydrogen bond acceptor assisting the interaction between the catalyst and substrates to ensure the high enantioselectivity. The same group also reported the conjugate addition and amination of  $\alpha$ -fluoro- $\beta$ -ketoesters **107** catalyzed by *Cinchona* alkaloid derivatives.<sup>7</sup>

Besides Lu's work, Wang<sup>8a</sup> and Kim<sup>8b</sup> also reported Michael reaction using  $\alpha$ -fluoro- $\beta$ -ketoesters **107** and various nitroolefins catalyzed by *Cinchona* alkaloid derivatives respectively.



**Scheme 4.2** Asymmetric Mannich reaction catalyzed by tryptophan-derived catalyst **109**

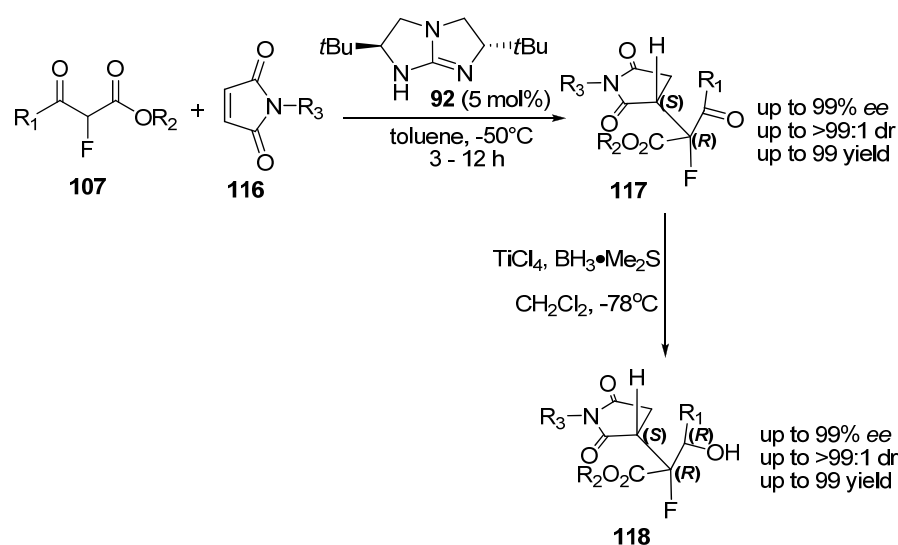


**Scheme 4.3** Asymmetric alkylation of  $\alpha$ -fluoro- $\beta$ -ketoesters under phase transfer conditions

$\alpha$ -fluoro- $\beta$ -ketoesters **107** has proven suitable substrate for phase transfer catalysis. Maruoka and co-workers reported asymmetric alkylation of  $\alpha$ -fluoro- $\beta$ -ketoesters **107** with different alkyl halides **113** catalyzed by *N*-spiro chiral quaternary ammonium bromide (*S,S*)-**114** (Scheme 4.3).<sup>9</sup> Good yields were

obtained while the best *ee* value achieved was 89%.

Almost at the same time, our group developed the conjugate addition of  $\alpha$ -fluoro- $\beta$ -ketoesters **107** with maleimides **116** catalyzed by our bicyclic guanidine **92**.<sup>10</sup> Excellent results were obtained with various  $\alpha$ -fluoro- $\beta$ -ketoesters and maleimides. The conjugate addition product **117** can be selectively reduced to provide alcohol **118** as a single diastereoisomer with 3 adjacent chiral centers.



**Scheme 4.4** Asymmetric conjugate of  $\alpha$ -fluoro- $\beta$ -ketoesters catalyzed by bicyclic guanidine

DFT calculation at the B3LYP/6-31\* level was performed to gain mechanism insight. Two possible structures for the pre-transition-state complex were hypothesized: face-on or side-on (Figure 4.1). The side-on TS was strongly preferred over the face-on TS because of the stronger hydrogen bond association between the guanidine catalyst and the maleimide carbonyl group. The DFT calculation therefore documented the bifunctionality of the bicyclic guanidine **92**.

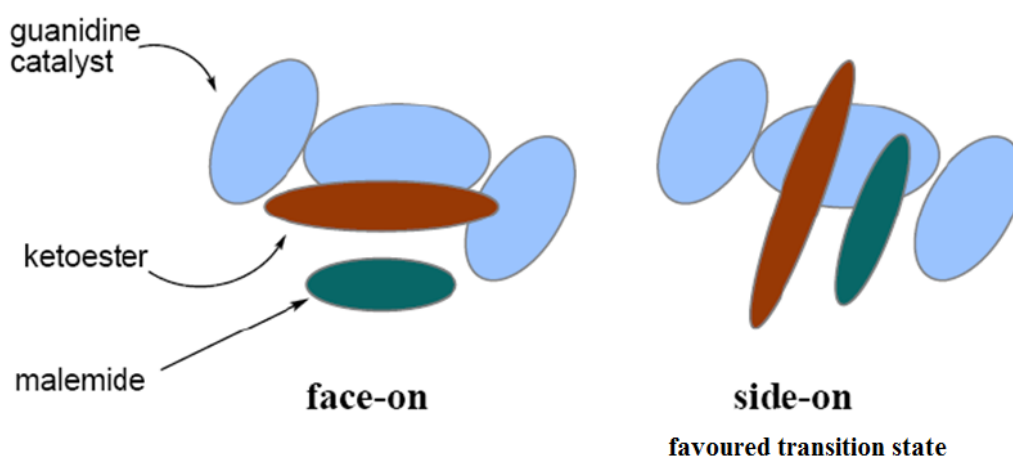
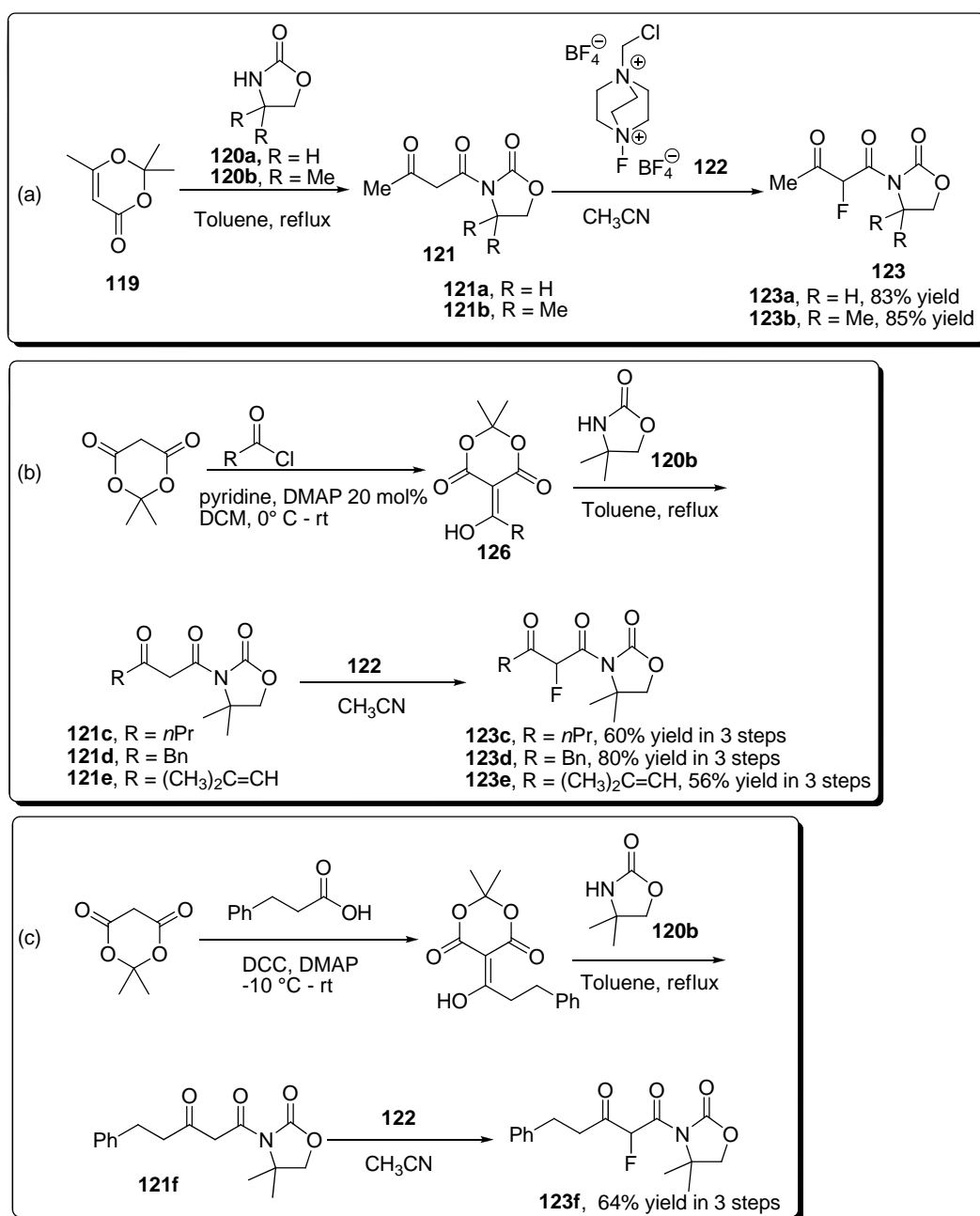


**Figure 4.1** Two possible transition state models

The fluorinated amino acids (F-AAs) impart unique properties when they were used in the modification of peptides and proteins in protein engineering.<sup>11</sup> They are also ideal intermediates for drug discovery programs and have found their way into drugs like Vaniqa (antineoplastic agent). Mannich reaction is considered as one of the most robust and powerful methods towards the synthesis of  $\beta$ -amino acids.<sup>12</sup> We will describe guanidine catalyzed asymmetric Mannich reaction with fluorinated carbon nucleophiles in the following sections.

## 4.2 Enantioselective Mannich Reaction of Fluorocarbon Nucleophiles

### 4.2.1 Synthesis of Fluorocarbon Nucleophiles

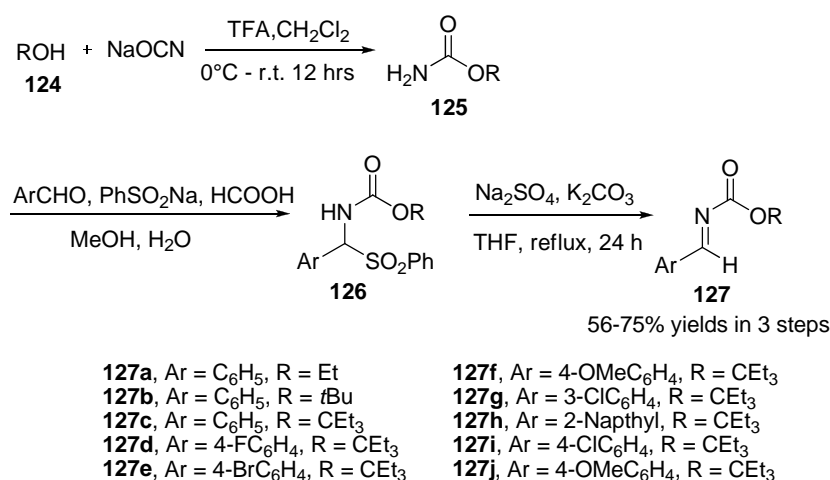


**Scheme 4.5** Preparation of  $\alpha$ -fluoro- $\beta$ -keto acyloxazolidinones

$\alpha$ -fluoro- $\beta$ -keto acyloxazolidinones can be prepared by electrophilic

fluorination of 1,3 dicarbonyl compounds **121** using Selectfluor. Compounds **123a** and **123b** were synthesized by the reaction between 2,2,6-trimethyl-4H-1,3-dioxin-4-one **119** and oxazolidinones in reflux toluene [Scheme 4.5 (a)].<sup>13</sup> On the other hand, the preparation of compounds **123c-f** started from Meldrum's acid **124** [Scheme 4.5 (b) and (c)].<sup>14</sup> Condensation of Meldrum's acid with acetyl chloride or acid followed by ring opening with oxazolidinone **120b** yielded compounds **121c-f**, which were fluorinated to give  $\alpha$ -fluoro- $\beta$ -keto acyloxazolidinones **123c-f** in good yields.

#### 4.2.2 Synthesis of *N*-carbonyl Imines



**Scheme 4.6** Synthesis of *N*-carbonyl imines

Imines **127a** and **127b** were prepared based on the literature report<sup>15</sup> starting from carbamate **125** in two steps with good yields. However, neither **127a** nor **127b** can give high diastereo- and enantioselectivity in our Mannich reaction with fluorinated carbon nucleophiles. We developed new type imines **127c-j** which are more bulky but remain the activity. The corresponding carbamates were prepared

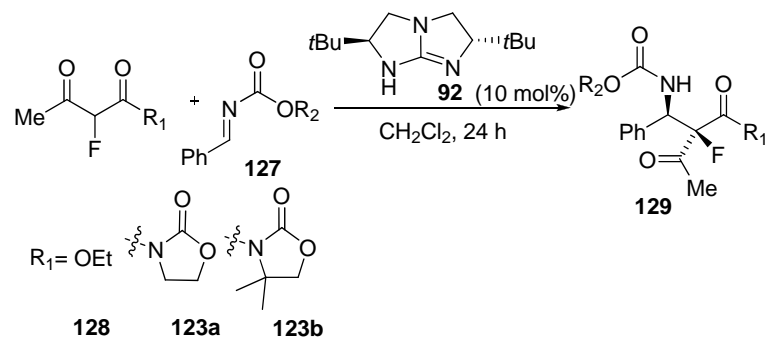
from 3-ethylpentan-3-ol with excellent yields. After following the next two reported steps, *N*-3-ethylpentan-3-yloxycarbonyl (Eoc) imine **127c-j** can be achieved with good yields.

### 4.2.3 Mannich Reaction of Fluorinated $\beta$ -keto Acetyloxazolidinone

In our preliminary studies, we obtained excellent yield of the Mannich reaction between  $\alpha$ -fluoro- $\beta$ -ketoester **128** and *N*-ethoxycarbonyl imine **127a** but the enantio- and diastereoselectivities were moderate (Table 4.1, entry 1). Based on our experiences with bicyclic guanidine-catalyzed asymmetric reactions, increasing the steric hindrance of substrates would respond positively to the diastereo- and enantioselectivity. Hence, we changed the *N*-ethoxycarbonyl imine **127a** to *N*-Boc imine **127b**. The diastereoselectivity increased slightly to 10:1 while the *ee* value decreased (Table 4.1, entry 2). With the additional carbonyl group of  $\beta$ -keto acetyloxazolidinone, it has an additional opportunity for hydrogen bonding interaction to the catalyst. We then worked on the  $\alpha$ -fluoro- $\beta$ -ketoester and replaced the ester moiety to oxazolidinone. Due to the lower reactivity of  $\beta$ -keto acetyloxazolidinones, reaction between **123a** and *N*-Boc imine **127b** had to be carried out at room temperature. Unfortunately, moderate *ee* value was obtained and the diastereoselectivity was lost (Table 4.1, entry 3). However, when  $\beta$ -keto acetyloxazolidinone **123b** was used as the donor with *N*-Boc imine **127b**, the *ee* value was increased to 95%, although the *dr* was moderate (Table 4.1,

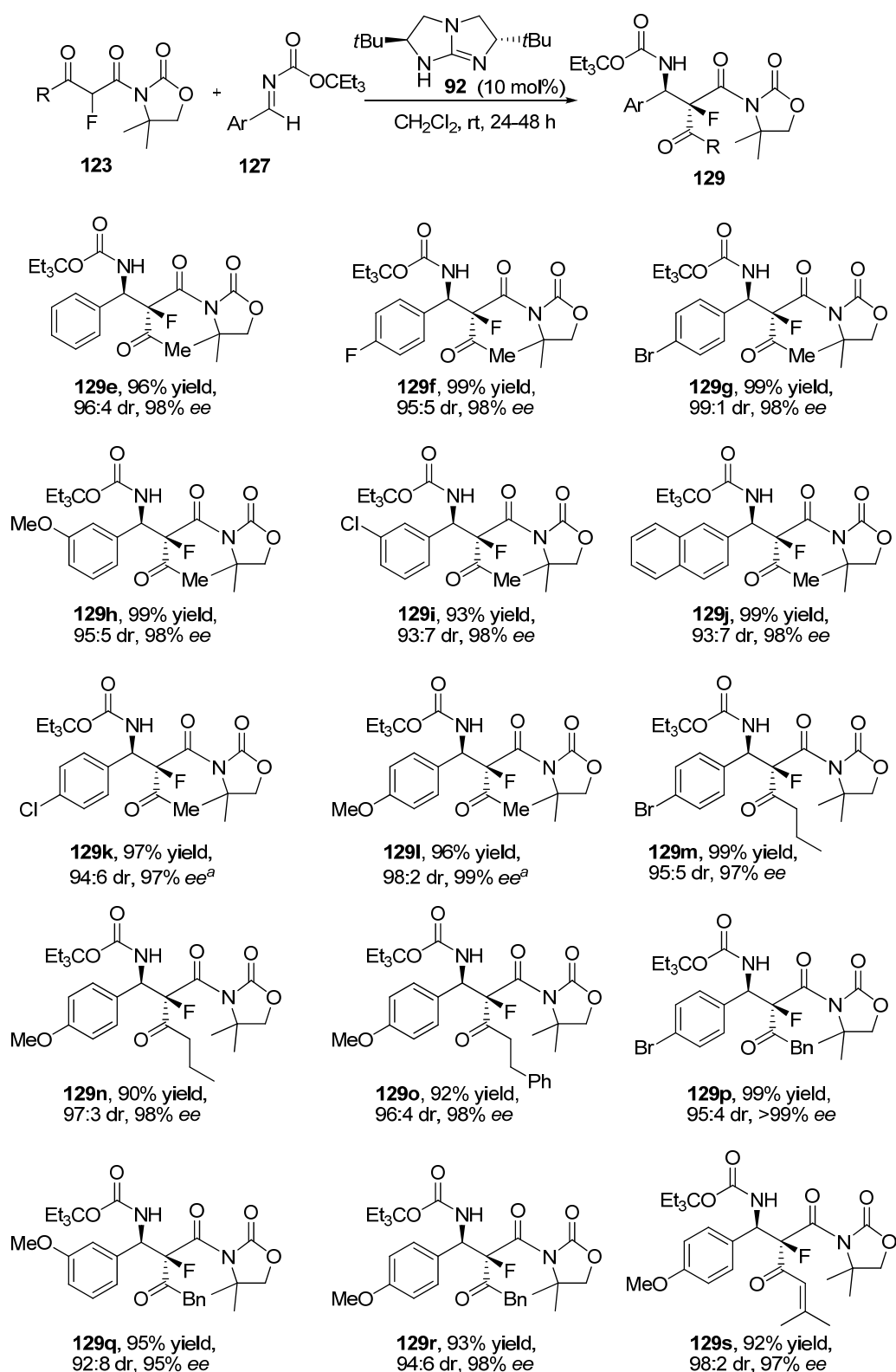
entry 4). By changing *N*-Boc imine **127b** to more bulky *N*-Eoc imine **127c**, adduct **129e** was obtained in excellent yields and excellent enantio- and diastereoselectivities (Table 4.1, entry 5).

**Table 4.1** Highly enantioselective and diastereoselective Mannich reactions of fluorocarbon nucleophiles



Entry	<b>127</b>	T [°C]	<b>129</b>	Yield (%) <sup>a</sup>	<i>dr</i> <sup>b</sup>	<i>ee</i> (%) <sup>c</sup>
1	<b>128</b> <b>127a</b>	-50	<b>129a</b>	99	9:1	84
2	<b>128</b> <b>127b</b>	-50	<b>129b</b>	90	10:1	71
3	<b>123a</b> <b>127b</b>	rt	<b>129c</b>	92	1:1	83
4	<b>123b</b> <b>127b</b>	rt	<b>129d</b>	85	4:1	95
5	<b>123b</b> <b>127c</b>	rt	<b>129e</b>	96	96:4	98

<sup>a</sup>Yield of isolated product. <sup>b</sup>Determined by HPLC analysis. <sup>c</sup>Determined by HPLC



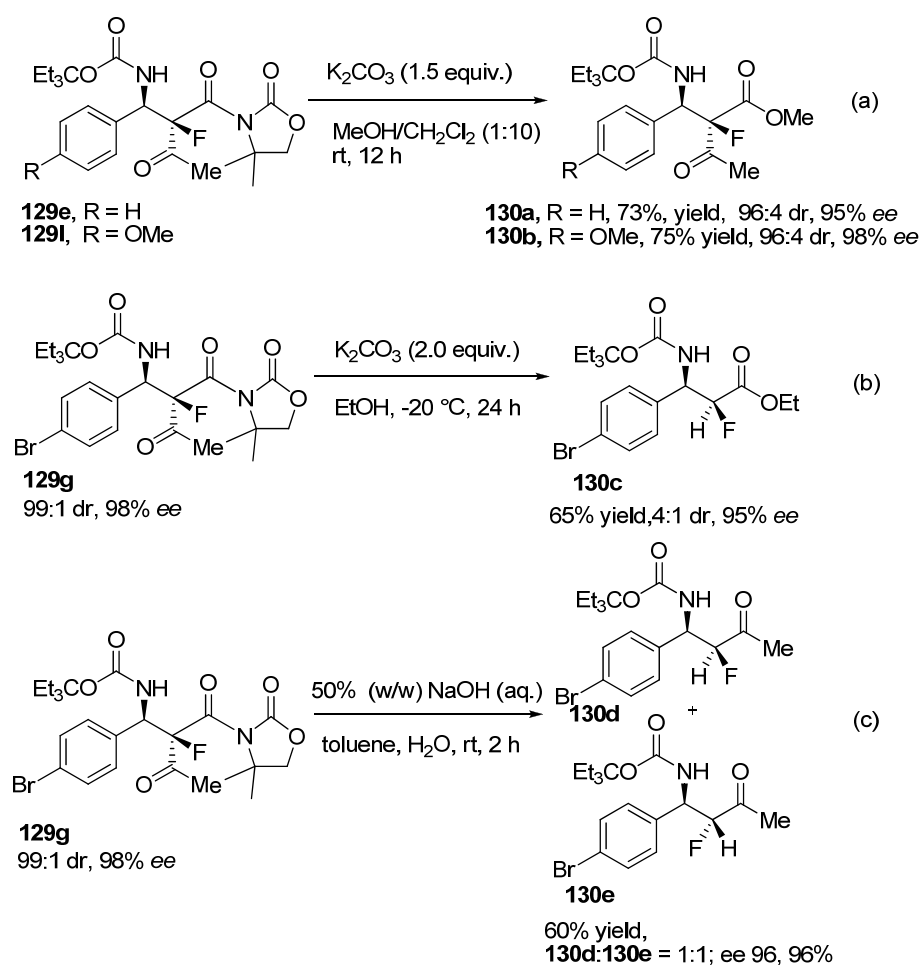
**Scheme 4.7** Highly enantioselective and diastereoselective reactions between  $\beta$ -keto acetyloxazolidinone **1c** and *N*-Eoc imines. <sup>a</sup> Toluene as solvent

#### 4.2.4 Deacylation/Decarboxylation

The ability of malonates and  $\beta$ -ketoesters to be decarboxylated *via* their corresponding acids under acidic conditions after alkylations, renders these reagents to be extremely useful and form a significant portion of undergraduate teaching on carbonyl chemistry. It is known that decarboxylation occurs through a six-membered transition state with the extrusion of a molecule of carbon dioxide. It is, however, less well known that under strongly basic conditions,  $\beta$ -ketoesters undergo deacylation reaction, cleaving the keto side, in a retro-Claisen condensation fashion. The ability of  $\alpha,\alpha$ -dichloro- $\beta$ -keto esters to react with even relatively weak nucleophiles in mild conditions to effect this deacylation reaction has also been overlooked.<sup>16</sup>

Initially, we were searching for a mild condition to modify the oxazolidinone moiety of the Mannich product. We found that oxazolidinone can be converted to a methyl ester easily using  $K_2CO_3$  under mild condition without loss of *ee* value and diastereoselectivity [Scheme 4.8 (a)]. When the amount of potassium carbonate was increased, transesterification was succeeded with deacylation reaction yielding the  $\alpha$ -fluoro- $\beta$ -amino ester **130c** [Scheme 4.8 (b)]. A round of optimization revealed that the use of ethanol at a lower temperature gave the best yield. The deacylation should proceed *via* retro-Claisen condensation<sup>17</sup> to release a neutral molecular, ethyl acetate. The resulted enolate underwent a diastereoselective protonation to give the *syn* diastereoisomer as the major product

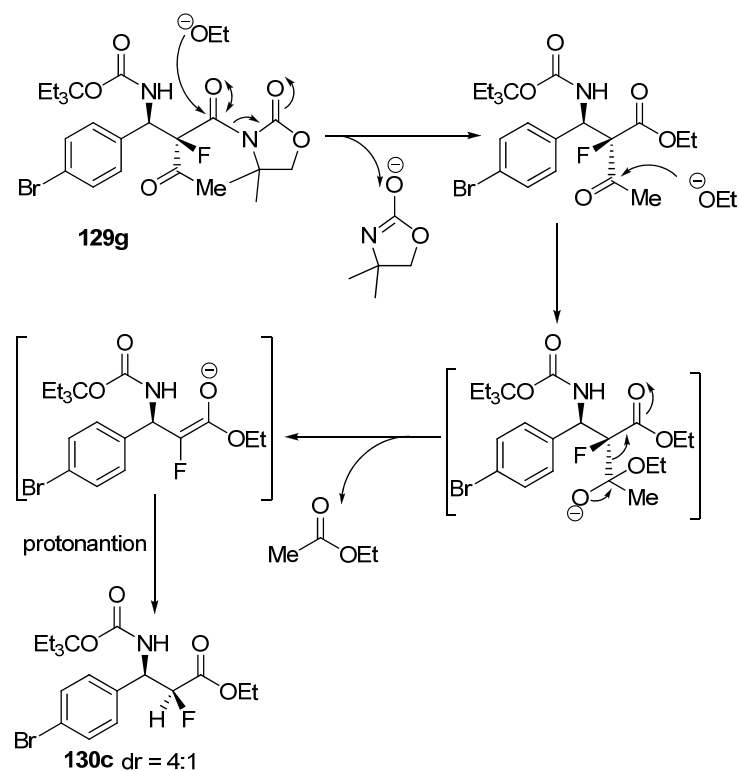
(Scheme 4.9).



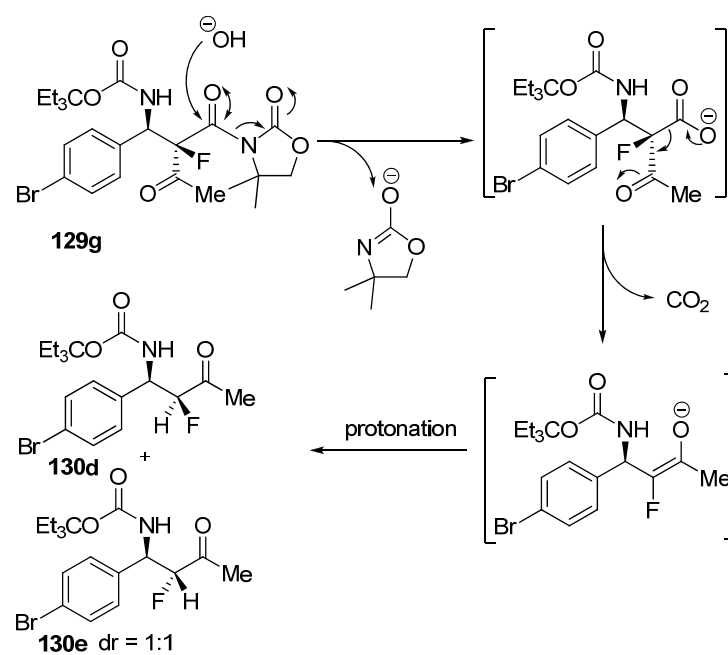
#### Scheme 4.8 Useful transformations of the Mannich product

When sodium hydroxide was used, hydroxide anion acted as a nucleophile instead of ethanolate anion. The oxazolidinone moiety was converted to the carboxylate salt which underwent decarboxylation [Scheme 4.8 (c)].<sup>18</sup> The subsequent enolate generated underwent protonation to give a 1:1 mixture of  $\alpha$ -fluoro- $\beta$ -amino ketones **130d** and **130e**, which were separated successfully using flash chromatography (Scheme 4.10). The use of such mild conditions for deacylation and decarboxylation is likely due to the inductive effect of a

neighbouring C-F bond. These unexpected results provided us an entry towards the preparation of novel, chiral  $\alpha$ -fluorinated  $\beta$ -amino acid derivatives.

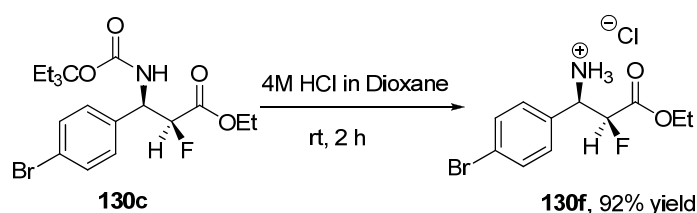


**Scheme 4.9** Proposed mechanism of deacylation of Mannich product **129g**



**Scheme 4.10** Proposed mechanism of decarboxylation of Mannich product **129g**

We have developed a highly enantio- and diastereoselective guanidine-catalyzed Mannich reaction with  $\alpha$ -fluoro- $\beta$ -keto acyloxazolidinone as the fluorocarbon nucleophile. *N*-Eoc imines were firstly prepared in our laboratory to ensure the highly enantio- and diastereoselectivities. The product can be converted to  $\alpha$ -Fluoro- $\beta$ -amino acid derivatives with chiral fluorinated carbon *via* selective deacylation or decarboxylation reaction. Similar to *N*-Boc imine, *N*-Eoc imine can be cleaved under acidic condition to give excellent yield (Scheme 4.11).

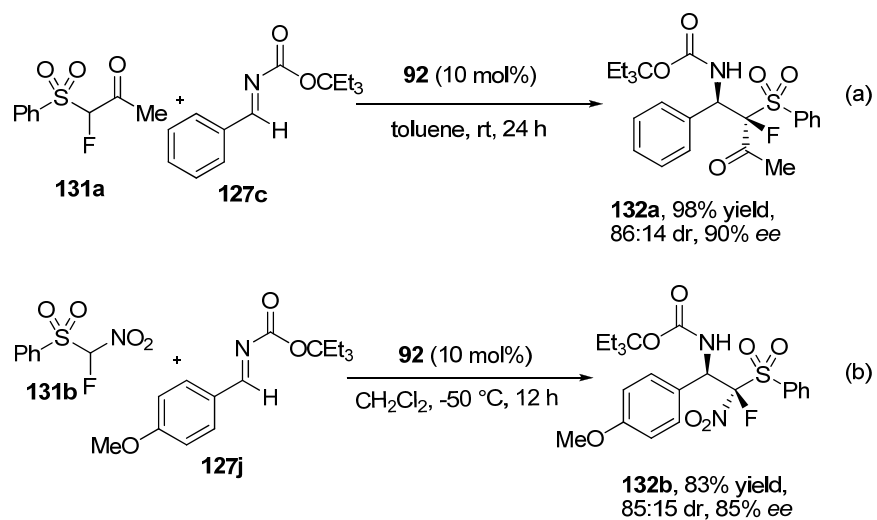


**Scheme 4.11** Cleavage of *N*-Eoc imine under acidic condition

#### 4.2.5 Mannich Reaction of other Fluorocarbon Nucleophiles

FBSM was shown to be an excellent fluorocarbon nucleophile. We prepared  $\alpha$ -fluoro- $\beta$ -ketosulfones to determine whether they are suitable for our reaction. Indeed, the Mannich reaction of 1-fluoro-1-(phenylsulfonyl)propan-2-one (FSPO) **131a** gave an adduct with high *ee* value and good diastereoselectivity [Scheme 4.12 (a)]. The preparation of  $\alpha$ -fluoro- $\alpha,\beta$ -diamines, particularly one that contains a quaternary fluorinated carbon is an attractive target.  $\alpha$ -Fluoro- $\alpha$ -nitro-(phenylsulfonyl)methane (FNSM) **131b** was very active due to the strong electron withdrawing nitro group. It was previously used by Olah in

Michael reaction with good results.<sup>5</sup> The Mannich reaction between FNSM **131b** and *N*-Eoc imine **127j** proceeded smoothly at  $-50^{\circ}\text{C}$  to give adduct **132b** in good *ee* value and diastereoselectivity [Scheme 4.12 (b)].



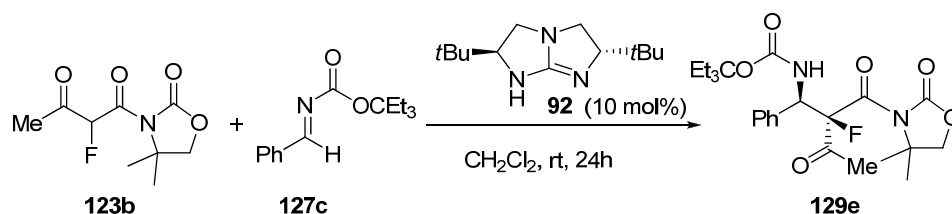
**Scheme 4.12** Asymmetric Mannich reaction of FPSO and FNSM

## **4.3 Experimental Section**

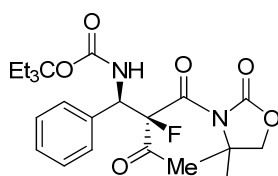
### **4.3.1 General procedures and methods**

$^1\text{H}$  and  $^{13}\text{C}$  NMR spectra were recorded on a Bruker ACF300 (300MHz), Bruker DPX300 (300MHz) or AMX500 (500MHz) spectrometer. Chemical shifts are reported in parts per million (ppm). The residual solvent peak was used as an internal reference. Low resolution mass spectra were obtained on a Finnigan/MAT LCQ spectrometer in ESI mode and a Finnigan/MAT 95XL-T mass spectrometer in FAB mode. All high resolution mass spectra were obtained on a Finnigan/MAT 95XL-T spectrometer. Infrared spectra were recorded on a BIO-RAD FTS 165 FTIR spectrometer. Enantiomeric excess values were determined by chiral HPLC analysis on Dionex Ultimate 3000 HPLC units, including a Ultimate 3000 Pump, Ultimate 3000 variable Detectors. Optical rotations were recorded on Jasco DIP-1000 polarimeter. Melting points were determined on a BÜCHI B-540 melting point apparatus. Analytical thin layer chromatography (TLC) was performed with Merck pre-coated TLC plates, silica gel 60F-254, layer thickness 0.25 mm. Flash chromatography separations were performed on Merck 60 (0.040 - 0.063mm) mesh silica gel. Toluene was distilled from sodium/benzophenone and stored under  $\text{N}_2$  atmosphere. Dichloromethane was distilled from  $\text{CaH}_2$  and stored under  $\text{N}_2$  atmosphere. Other reagents and solvents were commercial grade and were used as supplied without further purification, unless otherwise stated.

**4.3.2 Experimental procedure for the reaction between  $\alpha$ -fluoro- $\beta$ -keto acyloxazolidinone **123b** and *N*-3-ethylpentan-3-yloxycarbonyl (Eoc) imine **127c** catalyzed by **92****



*N*-3-ethylpentan-3-yloxycarbonyl (Eoc) imine **127c** (24.7 mg, 0.1 mmol, 2.0 equiv.) and **92** (1.12 mg, 0.005 mmol, 0.1 equiv.) were dissolved in dichloromethane (0.5 ml) and stirred at room temperature for 10 min, then  $\alpha$ -fluoro- $\beta$ -keto acyloxazolidinone **123b** (10.85 mg, 0.05 mmol, 1.0 equiv.) was added. The reaction mixture was stirred at room temperature and monitored by TLC. After 24 hours, upon complete consumption of **123b**, the reaction solvent was removed *in vacuo* and the crude product was directly loaded onto a short silica gel column, followed by gradient elution with hexane/EA mixtures (10/1-2/1 ratio). After removing the solvent, product **129e** (22.2 mg) was obtained as colorless oil in 96% yield.



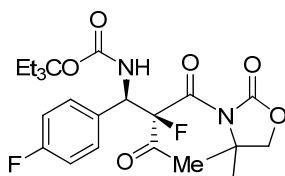
**3-ethylpentan-3-yl**

**(1*R*,2*R*)-2-(4,4-dimethyl-2-oxooxazolidine-3-carbonyl)-2-fluoro-3-oxo-1-phen**

**ylbutylcarbamate (129e)**

Colorless oil; 98% *ee*, *dr* = 96:4;  $[\alpha]_D^{29} = +120.2$  (*c* 0.78, CHCl<sub>3</sub>); <sup>1</sup>H NMR (500 MHz, CDCl<sub>3</sub>, ppm):  $\delta = 7.38 - 7.28$  (m, 5H), 5.87 (d, *J* = 4.7 Hz, 1H), 5.52 - 5.47 (m, 1H), 4.05 - 3.94 (m, 2H), 2.40, (d, *J* = 3.1 Hz, 0.1H), 2.17 (br, 2.9H), 1.79 - 1.73 (m, 6H), 1.51 - 1.44 (m, 3.5H), 1.25 - 1.21 (br, 2.5H), 0.80 - 0.67 (m, 9H); <sup>13</sup>C NMR (75.5 MHz, CDCl<sub>3</sub>, ppm):  $\delta = 200.0$  (d, *J* = 24.6 Hz), 166.7 (d, *J* = 27.3 Hz), 154.4, 152.5, 136.0, 128.8, 128.5, 128.2, 100.9 (d, *J* = 214.5 Hz), 88.0, 75.9, 61.4, 56.6 (d, *J* = 25.8), 26.9, 24.7, 24.4, 22.7, 7.5; <sup>19</sup>F NMR (282.4 MHz, CDCl<sub>3</sub>, ppm): -93.0 (d, *J* = 21.8 Hz); IR (film): 3449, 2970, 2361, 1786, 1705, 1493, 1327, 1215 cm<sup>-1</sup>; LRMS (ESI) *m/z* 487.0 (M + Na<sup>+</sup>), HRMS (ESI) *m/z* 487.2216 (M + Na<sup>+</sup>), calc. for C<sub>24</sub>H<sub>33</sub>FN<sub>2</sub>O<sub>6</sub><sup>23</sup>Na 487.2215.

The *ee* was determined by HPLC analysis. CHIRALCEL IA (4.6 mm i.d. x 250 mm); Hexane/2-propanol = 85/15; flow rate 1.0 ml/min; 25°C; 210 nm; retention time: major isomer: 7.8 min (minor), 11.5 min (major); minor isomer: 13.4 min (minor), 29.4 min (major).

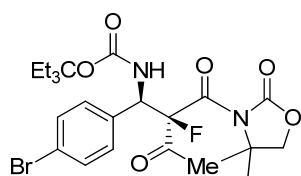
**3-ethylpentan-3-yl**

**(1R,2R)-2-(4,4-dimethyl-2-oxooxazolidine-3-carbonyl)-2-fluoro-1-(4-fluorophenyl)-3-oxobutylcarbamate (129f)**

**enyl)-3-oxobutylcarbamate (129f)**

Colorless oil; 98% *ee*, *dr* = 95:5;  $[\alpha]_D^{29} = +57.1$  (*c* 2.55, CHCl<sub>3</sub>); <sup>1</sup>H NMR (500 MHz, CDCl<sub>3</sub>, ppm): δ = 7.38 - 7.30 (m, 2H), 7.04 – 6.98 (m, 2H), 5.87 – 5.86 (m, 1H), 5.48 - 5.43 (m, 1H), 4.05 – 3.94 (m, 2H), 2.38, (d, *J* = 2.7 Hz, 0.16H), 2.22 (d, *J* = 3.4 Hz, 2.85H), 1.80 – 1.71 (m, 6H), 1.55 -1.44 (m, 3H), 1.25 - 1.21 (br, 2H), 0.80 – 0.68 (m, 9H); <sup>13</sup>C NMR (75.5 MHz, CDCl<sub>3</sub>, ppm): δ = 199.9 (d, *J* = 24.8 Hz), 166.7 (d, *J* = 23.4 Hz), 162.6 (d *J* = 247.1 Hz), 154.4, 152.4, 131.9, 130.3 (d, *J* = 7.0 Hz), 115.1 (d, *J* = 21.4 Hz), 100.6 (d, *J* = 212.6 Hz), 88.2, 75.9, 61.5, 56.0 (d, *J* = 26.4 Hz), 26.9, 24.6, 24.4, 22.7, 7.5; <sup>19</sup>F NMR (282.4 MHz, CDCl<sub>3</sub>, ppm): –37.9, –93.1 (d, *J* = 24.6 Hz); IR (film): 2970, 2372, 1786, 1705, 1508, 1330, 1223 cm<sup>-1</sup>; LRMS (ESI) *m/z* 505.0 (M + Na<sup>+</sup>), HRMS (ESI) *m/z* 505.2134 (M + Na<sup>+</sup>), calc. for C<sub>24</sub>H<sub>32</sub>F<sub>2</sub>N<sub>2</sub>O<sub>6</sub><sup>23</sup>Na 505.2121.

The *ee* was determined by HPLC analysis. CHIRALCEL IA (4.6 mm i.d. x 250 mm); Hexane/2-propanol = 90/10; flow rate 1.0 ml/min; 25°C; 210 nm; retention time: major isomer: 9.1 min (minor), 16.0 min (major); minor isomer: 18.7 min (minor), 35.2 min (major).

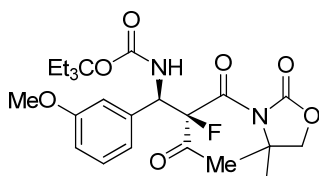


### 3-ethylpentan-3-yl

**(1*R*,2*R*)-1-(4-bromophenyl)-2-(4,4-dimethyl-2-oxooxazolidine-3-carbonyl)-2-fluoro-3-oxobutylcarbamate (129g)**

White solid, Mp: 59.5°C. 98% *ee*, *dr* = 99:1;  $[\alpha]_D^{20} = +86.3$  (*c* 0.38, CHCl<sub>3</sub>); <sup>1</sup>H NMR (500 MHz, CDCl<sub>3</sub>, ppm): δ = 7.45 (d, *J* = 8.5 Hz, 2H), 7.28 - 7.18 (m, 2H), 5.87 (d, *J* = 9.0 Hz, 1H), 5.44 - 5.39 (m, 1H), 4.04 - 3.95 (m, 2H), 2.36, (br, 0.2H), 2.17 (br, 2.9H), 1.82 - 1.75 (m, 6H), 1.54 - 1.43 (m, 3.3H), 1.25 - 1.21 (br, 2.8H), 0.85 - 0.69 (m, 9H); <sup>13</sup>C NMR (75.5 MHz, CDCl<sub>3</sub>, ppm): δ = 199.7 (d, *J* = 24.0 Hz), 166.6 (d, *J* = 25.3 Hz), 154.4, 152.3, 135.2, 131.3, 130.3, 122.3, 100.3 (d, *J* = 211.7 Hz), 88.3, 75.9, 61.5, 56.0 (d, *J* = 26.7), 26.9, 24.6, 24.3, 22.7, 7.5; <sup>19</sup>F NMR (282.4 MHz, CDCl<sub>3</sub>, ppm): -93.0 (d, *J* = 21.3 Hz); IR (film): 2970, 2360, 1786, 1732, 1705, 1489, 1327 cm<sup>-1</sup>; LRMS (ESI) *m/z* 564.9, 566.9 (M + Na<sup>+</sup>), HRMS (ESI) *m/z* 565.1334 (M + Na<sup>+</sup>), calc. for C<sub>24</sub>H<sub>32</sub>F<sup>79</sup>BrN<sub>2</sub>O<sub>6</sub><sup>23</sup>Na 565.1344, *m/z* 567.1305 (M + Na<sup>+</sup>), calc. for C<sub>24</sub>H<sub>32</sub>F<sup>81</sup>BrN<sub>2</sub>O<sub>6</sub><sup>23</sup>Na 567.1300.

The *ee* was determined by HPLC analysis. CHIRALCEL IA (4.6 mm i.d. x 250 mm); Hexane/2-propanol = 80/20; flow rate 0.8 ml/min; 25°C; 230 nm; retention time: major isomer: 8.4 min (minor), 13.8 min (major); minor isomer: 12.4 min (major), 17.8 min (minor).

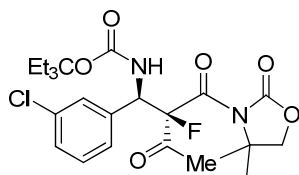


### 3-ethylpentan-3-yl

**(1*R*,2*R*)-2-(4,4-dimethyl-2-oxooxazolidine-3-carbonyl)-2-fluoro-1-(3-methoxyphenyl)-3-oxobutylcarbamate (129h)**

Colorless oil; 98% *ee*, *dr* = 95:5;  $[\alpha]_{\text{D}}^{29} = +174.0$  (*c* 0.91,  $\text{CHCl}_3$ );  $^1\text{H}$  NMR (500 MHz,  $\text{CDCl}_3$ , ppm):  $\delta = 7.23$  (t,  $J = 8.0$  Hz, 1H), 6.96 – 6.81 (m, 3H), 5.82 (br, 1H), 5.50 - 5.44 (m, 1H), 4.05 – 3.94 (m, 2H), 3.79 (s, 3H), 2.38, (br, 0.2H), 2.16 (br, 3.0H), 1.82 – 1.69 (m, 6H), 1.58 -1.45 (m, 3.9H), 1.25 (br, 2.2H), 0.85 – 0.69 (m, 9H);  $^{13}\text{C}$  NMR (75.5 MHz,  $\text{CDCl}_3$ , ppm):  $\delta = 200.0$  (d,  $J = 23.3$  Hz), 166.6 (d,  $J = 22.5$  Hz), 159.4, 154.4, 152.5, 137.6, 129.2, 120.7, 114.3, 113.7, 100.9 (d,  $J = 212.7$  Hz), 88.0, 75.9, 61.5, 56.5 (d,  $J = 25.1$  Hz), 55.3, 26.9, 24.7, 24.4, 22.7, 7.5;  $^{19}\text{F}$  NMR (282.4 MHz,  $\text{CDCl}_3$ , ppm):  $-92.4$  (d,  $J = 22.4$  Hz); IR (film): 2970, 1782, 1705, 1492, 1327  $\text{cm}^{-1}$ ; LRMS (ESI)  $m/z$  517.0 ( $\text{M} + \text{Na}^+$ ), HRMS (ESI)  $m/z$  517.2314 ( $\text{M} + \text{Na}^+$ ), calc. for  $\text{C}_{25}\text{H}_{35}\text{FN}_2\text{O}_7^{23}\text{Na}$  517.2321.

The *ee* was determined by HPLC analysis. CHIRALCEL IC (4.6 mm i.d. x 250 mm); Hexane/2-propanol = 80/20; flow rate 1.0 ml/min; 25°C; 210 nm; retention time: major isomer: 8.2 min (minor), 11.4 min (major); minor isomer: 13.3 min (minor), 17.2 min (major).



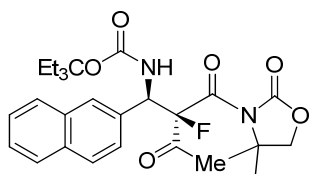
### 3-ethylpentan-3-yl

### (1*R*,2*R*)-1-(3-chlorophenyl)-2-(4,4-dimethyl-2-oxooxazolidine-3-carbonyl)-2-fluoro-3-oxobutylcarbamate (129i)

Colorless oil; 98% *ee*, *dr* = 93:7;  $[\alpha]_{\text{D}}^{29} = +88.6$  (*c* 2.01,  $\text{CHCl}_3$ );  $^1\text{H}$  NMR (500

MHz, CDCl<sub>3</sub>, ppm):  $\delta$  = 7.40 - 7.18 (m, 4H), 5.89 (d,  $J$  = 9.5 Hz, 1H), 5.43 (q, 10.4 Hz, 1H), 4.04 - 3.95 (m, 2H), 2.38, (br, 0.2H), 2.27 (br, 2.8H), 1.83 - 1.72 (m, 6H), 1.58 - 1.42 (m, 3.8H), 1.25 - 1.21 (br, 2.4H), 0.85 - 0.68 (m, 9H); <sup>13</sup>C NMR (75.5 MHz, CDCl<sub>3</sub>, ppm):  $\delta$  = 199.6 (d,  $J$  = 24.6 Hz), 166.7 (d,  $J$  = 26.3 Hz), 154.4, 152.3, 138.2, 134.1, 129.4, 128.6, 128.3, 126.8, 100.3 (d,  $J$  = 214.1 Hz), 88.3, 75.9, 61.5, 56.1 (d,  $J$  = 26.8 Hz), 26.9, 24.5, 24.3, 22.6, 7.5; <sup>19</sup>F NMR (282.4 MHz, CDCl<sub>3</sub>, ppm): -92.8 (d,  $J$  = 22.1 Hz); IR (film): 2970, 2361, 1786, 1732, 1705, 1485, 1327 cm<sup>-1</sup>; LRMS (ESI)  $m/z$  521.0 (M + Na<sup>+</sup>), HRMS (ESI)  $m/z$  565.1833 (M + Na<sup>+</sup>), calc. for C<sub>24</sub>H<sub>32</sub>ClFN<sub>2</sub>O<sub>6</sub><sup>23</sup>Na 521.1825.

The *ee* was determined by HPLC analysis. CHIRALCEL IC (4.6 mm i.d. x 250 mm); Hexane/2-propanol = 85/15; flow rate 1.0 ml/min; 25°C; 210 nm; retention time: major isomer: 6.9 min (minor), 8.2 min (major); minor isomer: 11.6 min (major), 15.2 min (minor).



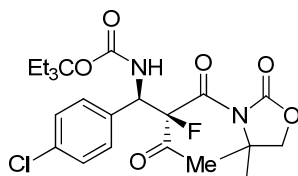
### 3-ethylpentan-3-yl

### (1R,2R)-2-(4,4-dimethyl-2-oxooxazolidine-3-carbonyl)-2-fluoro-1-(naphthalen-2-yl)-3-oxobutylcarbamate (129j)

Colorless oil; 98% *ee*, *dr* = 93:7;  $[\alpha]_D^{29}$  = +126.1 (*c* 1.54, CHCl<sub>3</sub>); <sup>1</sup>H NMR (500 MHz, CDCl<sub>3</sub>, ppm):  $\delta$  = 7.81 (t,  $J$  = 8.7, 4H), 7.52 - 7.48 (m, 3H), 6.00 (d,  $J$

= 7.6 Hz, 1H), 5.69 – 5.63 (m, 1H), 4.04 – 3.88 (m, 2H), 2.42, (br, 0.2H), 2.19 (br, 2.8H), 1.77 – 1.66 (m, 6H), 1.59 -1.40 (m, 3.8H), 1.25 - 1.16 (br, 2.3H), 0.80 – 0.65 (m, 9H);  $^{13}\text{C}$  NMR (75.5 MHz,  $\text{CDCl}_3$ , ppm):  $\delta$  = 200.0 (d,  $J$  = 25.0 Hz), 166.7 (d,  $J$  = 26.8 Hz), 154.4, 152.4, 133.3, 133.0, 132.9, 128.2, 127.9, 127.5, 126.4, 126.3, 125.8, 101.0 (d,  $J$  = 219.2 Hz), 88.0, 75.9, 61.5, 56.8 (d,  $J$  = 25.7 Hz), 26.9, 24.7, 24.3, 22.7, 7.5;  $^{19}\text{F}$  NMR (282.4 MHz,  $\text{CDCl}_3$ , ppm):  $-92.3$  (d,  $J$  = 22.7 Hz); IR (film): 3448, 2970, 1782, 1732, 1705, 1492, 1327, 1215  $\text{cm}^{-1}$ ; LRMS (ESI)  $m/z$  537.0 ( $\text{M} + \text{Na}^+$ ), HRMS (ESI)  $m/z$  537.2388 ( $\text{M} + \text{Na}^+$ ), calc. for  $\text{C}_{28}\text{H}_{35}\text{FN}_2\text{O}_6^{23}\text{Na}$  537.2371.

The *ee* was determined by HPLC analysis. CHIRALCEL IC (4.6 mm i.d. x 250 mm); Hexane/2-propanol = 80/20; flow rate 0.5 ml/min; 25°C; 230 nm; retention time: major isomer: 14.9 min (minor), 18.5 min (major); minor isomer: 26.2 min (minor), 28.7 min (major).



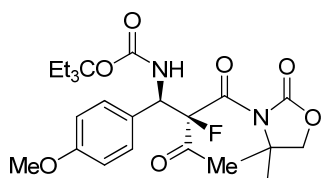
### 3-ethylpentan-3-yl

**(1*R*,2*R*)-1-(4-chlorophenyl)-2-(4,4-dimethyl-2-oxooxazolidine-3-carbonyl)-2-fluoro-3-oxobutylcarbamate (129k)**

Colorless oil; 97% *ee*, *dr* = 94:6;  $[\alpha]_{\text{D}}^{29} = +72.8$  ( $c$  1.63,  $\text{CHCl}_3$ );  $^1\text{H}$  NMR (500 MHz,  $\text{CDCl}_3$ , ppm):  $\delta$  = 7.35 - 7.29 (m, 4H), 5.87 (d,  $J$  = 8.9 Hz, 1H), 5.46 – 5.41

(m, 1H), 4.04 – 3.94 (m, 2H), 2.37, (br, 0.2H), 2.26 (br, 2.8H), 1.82 – 1.71 (m, 6H), 1.56 -1.43 (m, 3.5H), 1.25 - 1.21 (br, 2.5H), 0.80 – 0.68 (m, 9H);  $^{13}\text{C}$  NMR (75.5 MHz,  $\text{CDCl}_3$ , ppm):  $\delta$  = 199.7 (d,  $J$  = 25.2 Hz), 166.6 (d,  $J$  = 24.6 Hz), 154.4, 152.4, 134.6, 134.2, 129.9, 128.3, 100.4 (d,  $J$  = 213.7 Hz), 88.2, 75.9, 61.5, 56.0 (d,  $J$  = 26.7 Hz), 26.9, 24.6, 24.3, 22.7, 7.5;  $^{19}\text{F}$  NMR (282.4 MHz,  $\text{CDCl}_3$ , ppm):  $\delta$  = -92.7 (d,  $J$  = 24.5 Hz); IR (film): 3456, 2970, 2364, 1786, 1705, 1489, 1330, 1215  $\text{cm}^{-1}$ ; LRMS (ESI)  $m/z$  520.9 ( $\text{M} + \text{Na}^+$ ), HRMS (ESI)  $m/z$  521.1821 ( $\text{M} + \text{Na}^+$ ), calc. for  $\text{C}_{24}\text{H}_{32}\text{ClFN}_2\text{O}_6^{23}\text{Na}$  521.1825.

The *ee* was determined by HPLC analysis. CHIRALCEL AD-H (4.6 mm i.d. x 250 mm); Hexane/2-propanol = 85/15; flow rate 1.0 ml/min; 25°C; 210 nm; retention time: major isomer: 8.7 min (minor), 17.0 min (major); minor isomer: 19.6 min (major), 32.3 min (minor).



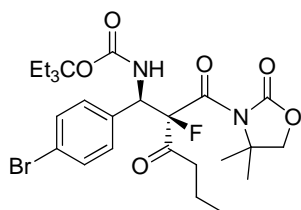
### 3-ethylpentan-3-yl

#### (1R,2R)-2-(4,4-dimethyl-2-oxooxazolidine-3-carbonyl)-2-fluoro-1-(4-methoxyphenyl)-3-oxobutylcarbamate (1291)

Colorless oil; 99% *ee*, *dr* = 98:2;  $[\alpha]_{\text{D}}^{20}$  = +103.8 ( $c$  1.32,  $\text{CHCl}_3$ );  $^1\text{H}$  NMR (500 MHz,  $\text{CDCl}_3$ , ppm):  $\delta$  = 7.29 – 7.19 (m, 2H), 6.84 (d,  $J$  = 8.7 Hz, 2H), 5.82 (br, 1H), 5.47 - 5.41 (m, 1H), 4.03 – 3.96 (m, 2H), 3.78 (s, 3H), 2.37, (br, 0.1H),

2.16 (d,  $J = 5.5$  Hz, 2.9H), 1.76 – 1.74 (m, 6H), 1.60 -1.45 (m, 3.9H), 1.25 (br, 2.2H), 0.79 – 0.70 (m, 9H);  $^{13}\text{C}$  NMR (125.8 MHz,  $\text{CDCl}_3$ , ppm):  $\delta = 200.2$  (d,  $J = 26.2$  Hz), 166.7 (d,  $J = 31.7$  Hz), 159.5, 154.3, 152.6 (d,  $J = 31.5$  Hz), 129.9, 129.7, 128.0, 115.3 (d,  $J = 242.8$  Hz), 113.6, 87.8, 75.9, 61.4, 56.2 (d,  $J = 24.8$  Hz), 52.2, 27.0, 24.7, 24.4, 22.8, 7.5;  $^{19}\text{F}$  NMR (282.4 MHz,  $\text{CDCl}_3$ , ppm):  $-93.0$  (d,  $J = 23.5$  Hz); IR (film): 3579, 2970, 1782, 1732, 1705, 1512, 1327, 1246  $\text{cm}^{-1}$ ; LRMS (ESI)  $m/z$  517.0 ( $\text{M} + \text{Na}^+$ ), HRMS (ESI)  $m/z$  517.2328 ( $\text{M} + \text{Na}^+$ ), calc. for  $\text{C}_{25}\text{H}_{35}\text{FN}_2\text{O}_7^{23}\text{Na}$  517.2321.

The *ee* was determined by HPLC analysis. CHIRALCEL IC (4.6 mm i.d. x 250 mm); Hexane/2-propanol = 80/20; flow rate 1.0 ml/min; 25°C; 210 nm; retention time: major isomer: 8.8 min (minor), 10.1 min (major); minor isomer: 13.2 min (minor), 17.7 min (major).



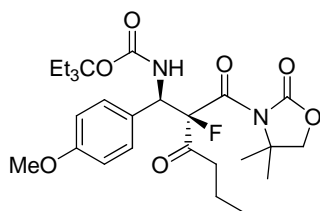
### 3-ethylpentan-3-yl

### (1*R*,2*R*)-1-(4-bromophenyl)-2-(4,4-dimethyl-2-oxooxazolidine-3-carbonyl)-2-fluoro-3-oxohexylcarbamate (129m)

Colorless oil; 97% *ee*, *dr* = 95:5;  $[\alpha]_{\text{D}}^{29} = +86.4$  ( $c$  2.34,  $\text{CHCl}_3$ );  $^1\text{H}$  NMR (500 MHz,  $\text{CDCl}_3$ , ppm):  $\delta = 7.44$  (d,  $J = 8.0$  Hz, 2H), 7.28 (d,  $J = 8.0$  Hz, 2H) 5.95

(d,  $J = 9.6$  Hz, 1H), 5.37 (t,  $J = 12.2$  Hz, 1H), 4.03 – 3.89 (m, 2H), 3.00 – 2.96 (m, 1H), 2.42 (br, 1H), 1.83 – 1.71 (m, 6H), 1.63 – 1.57 (m, 2H), 1.53 – 1.45 (m, 3.5H), 1.25 – 1.16 (br, 2.8H), 0.92 (t,  $J = 7.3$  Hz, 3H), 0.85 – 0.67 (m, 9H);  $^{13}\text{C}$  NMR (75.5 MHz,  $\text{CDCl}_3$ , ppm):  $\delta = 201.6$  (d,  $J = 23.5$  Hz), 167.2 (d,  $J = 25.7$  Hz), 154.3, 152.2, 135.3, 131.1, 130.2, 122.2, 100.2 (d,  $J = 213.5$  Hz), 88.2, 75.8, 61.5, 56.4 (d,  $J = 27.7$  Hz), 38.0, 26.9, 24.3, 22.7, 15.7, 13.5, 7.5;  $^{19}\text{F}$  NMR (282.4 MHz,  $\text{CDCl}_3$ , ppm):  $-95.1$ ,  $-95.2$ ; IR (film): 3445, 2970, 1786, 1705, 1589, 1327  $\text{cm}^{-1}$ ; LRMS (ESI)  $m/z$  592.9, 594.9 ( $\text{M} + \text{Na}^+$ ), HRMS (ESI)  $m/z$  593.1638, ( $\text{M} + \text{Na}^+$ ), calc. for  $\text{C}_{26}\text{H}_{36}\text{F}^{79}\text{BrN}_2\text{O}_6^{23}\text{Na}$ , 593.1633,  $m/z$ , 595.1626 ( $\text{M} + \text{Na}^+$ ), ,  $\text{C}_{26}\text{H}_{36}\text{F}^{81}\text{BrN}_2\text{O}_6^{23}\text{Na}$ , 595.1613

The *ee* was determined by HPLC analysis. CHIRALCEL AD-H (4.6 mm i.d. x 250 mm); Hexane/2-propanol = 90/10; flow rate 1.0 ml/min; 25°C; 230 nm; retention time: major isomer: 9.5 min (minor), 15.5 min (major); minor isomer: 17.4 min (major), 25.0 min (minor).

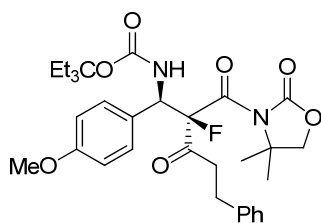


### 3-ethylpentan-3-yl

**(1R,2R)-2-(4,4-dimethyl-2-oxooxazolidine-3-carbonyl)-2-fluoro-1-(4-methoxyphenyl)-3-oxohexylcarbamate (129n)**

Colorless oil; 98% *ee*, *dr* = 97:3;  $[\alpha]_D^{29} = +84.6$  (*c* 2.05, CHCl<sub>3</sub>); <sup>1</sup>H NMR (500 MHz, CDCl<sub>3</sub>, ppm): δ = 7.29 (d, *J* = 8.3 Hz, 2H), 6.83 (d, *J* = 8.3 Hz, 2H), 5.92 (br, 1H), 5.38 (t, *J* = 12.6 Hz, 1H), 4.02 – 3.91 (m, 2H), 3.78 (s, 3H), 2.95 – 2.81 (m, 1H), 2.33 (m, 1H), 1.82 – 1.74 (m, 6H), 1.62 (br, 2H), 1.54 – 1.43 (m, 2.7H), 1.25 – 1.18 (br, 2.2H), 0.89 – 0.83 (m, 3H), 0.79 – 0.68 (m, 9H); <sup>13</sup>C NMR (75.5 MHz, CDCl<sub>3</sub>, ppm): δ = 202.0 (d, *J* = 23.8 Hz), 167.3 (d, *J* = 25.6 Hz), 159.4, 154.3, 152.4, 129.7, 128.2, 113.5, 100.8 (d, *J* = 210.4 Hz), 87.8, 75.8, 61.4, 56.7 (d, *J* = 27.0 Hz), 52.3, 38.1, 26.9, 24.7, 24.4, 22.7, 15.7, 13.5, 7.5; <sup>19</sup>F NMR (282.4 MHz, CDCl<sub>3</sub>, ppm): –95.4 (d, *J* = 19.7 Hz); IR (film): 3449, 2970, 2364, 1786, 1732, 1705, 1508, 1327 cm<sup>-1</sup>; LRMS (ESI) *m/z* 545.0 (M + Na<sup>+</sup>), HRMS (ESI) *m/z* 545.2652 (M + Na<sup>+</sup>), calc. for C<sub>27</sub>H<sub>39</sub>FN<sub>2</sub>O<sub>7</sub><sup>23</sup>Na 545.2634.

The *ee* was determined by HPLC analysis. CHIRALCEL IB (4.6 mm i.d. x 250 mm); Hexane/2-propanol = 85/15; flow rate 1.0 ml/min; 25°C; 230 nm; retention time: major isomer: 7.5 min (major), 8.9 min (minor); minor isomer: 10.2 min (major), 11.4 min (minor).



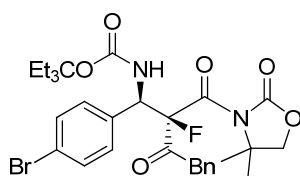
### 3-ethylpentan-3-yl

(1*R*,2*R*)-2-(4,4-dimethyl-2-oxooxazolidine-3-carbonyl)-2-fluoro-1-(4-methoxy

**phenyl)-3-oxo-5-phenylpentylcarbamate (129o)**

Colorless oil; 98% *ee*, *dr* = 96:4;  $[\alpha]_D^{29} = +66.0$  (*c* 5.08, CHCl<sub>3</sub>); <sup>1</sup>H NMR (500 MHz, CDCl<sub>3</sub>, ppm):  $\delta = 7.29 - 7.15$  (m, 7H), 6.84 (d, *J* = 8.8 Hz, 2H), 5.86 (br, 1H), 5.48 – 5.44 (m, 1H), 4.05 – 3.94 (m, 2H), 3.79 (s, 3H), 3.27 (br, 1H), 2.92 – 2.71 (m, 3H), 1.79 – 1.75 (m, 6H), 1.56 -1.45 (m, 4H), 1.26 – 1.24 (br, 2.5H), 0.81 – 0.69 (m, 9H); <sup>13</sup>C NMR (75.5 MHz, CDCl<sub>3</sub>, ppm):  $\delta = 201.4$  (d, *J* = 24.3 Hz), 166.8 (d, *J* = 23.0 Hz), 159.4, 154.3, 152.5, 141.0, 129.9, 129.7, 128.4, 128.3, 128.0, 125.9, 113.6, 101.2 (d, *J* = 205.8 Hz), 87.8, 75.9, 61.5, 56.5 (d, *J* = 25.7 Hz), 55.2, 38.6, 28.6, 26.9, 24.4, 22.7, 7.5; <sup>19</sup>F NMR (282.4 MHz, CDCl<sub>3</sub>, ppm): –94.8 (d, *J* = 19.7 Hz); IR (film): 3448, 2970, 1786, 1732, 1705, 1608, 1508, 1327, 1253 cm<sup>-1</sup>; LRMS (ESI) *m/z* 607.0 (M + Na<sup>+</sup>), HRMS (ESI) *m/z* 607.2805 (M + Na<sup>+</sup>), calc. for C<sub>32</sub>H<sub>41</sub>FN<sub>2</sub>O<sub>7</sub><sup>23</sup>Na 607.2790.

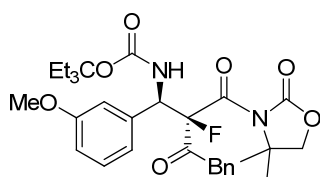
The *ee* was determined by HPLC analysis. CHIRALCEL IB (4.6 mm i.d. x 250 mm); Hexane/2-propanol = 85/15; flow rate 1.0 ml/min; 25°C; 230 nm; retention time: major isomer: 6.4 min (major), 7.5 min (minor); minor isomer: 9.7 min (minor), 10.8 min (major).

**3-ethylpentan-3-yl****(1R,2R)-1-(4-bromophenyl)-2-(4,4-dimethyl-2-oxooxazolidine-3-carbonyl)-2-fl**

**uoro-3-oxo-4-phenylbutylcarbamate (129p)**

Colorless oil; >99% *ee*, *dr* = 96:4;  $[\alpha]_D^{29} = +11.4$  (*c* 1.08, CHCl<sub>3</sub>); <sup>1</sup>H NMR (500 MHz, CDCl<sub>3</sub>, ppm):  $\delta$  = 7.48 (d, *J* = 8.2 Hz, 2H), 7.33 – 7.19 (m, 7H), 5.97 (d, *J* = 9.3 Hz, 1H), 5.53 – 5.48 (m, 1H), 4.44 – 4.40 (m, 1H), 3.99 – 3.80 (m, 2H), 1.84 – 1.73 (m, 6H), 1.60 (br, 1H), 1.51 -1.43 (m, 3.7), 1.21 (br, 2.4H), 0.85 – 0.72 (m, 9H); <sup>13</sup>C NMR (75.5 MHz, CDCl<sub>3</sub>, ppm):  $\delta$  = 199.0 (d, *J* = 23.7 Hz), 166.6 (d, *J* = 25.5 Hz), 154.3, 152.3, 135.1, 132.4, 131.5, 131.2, 130.4, 128.1, 126.7, 122.3, 100.4 (d, *J* = 213.9 Hz), 88.3, 75.9, 61.5, 56.3 (d, *J* = 27.2 Hz), 42.9, 26.9, 24.3, 22.7, 7.5; <sup>19</sup>F NMR (282.4 MHz, CDCl<sub>3</sub>, ppm): –97.1 (d, *J* = 31.0 Hz); IR (film): 3357, 2972, 1787, 1736, 1708, 1487, 1328, 1220, 1136 cm<sup>-1</sup>; LRMS (ESI) *m/z* 617.0, 619.0 (M - H<sup>+</sup>), HRMS (ESI) *m/z* 641.1643, (M + Na<sup>+</sup>), calc. for C<sub>30</sub>H<sub>36</sub>F<sup>79</sup>BrN<sub>2</sub>O<sub>6</sub><sup>23</sup>Na 641.1633; *m/z* 643.1642 (M + Na<sup>+</sup>), calc. for C<sub>30</sub>H<sub>36</sub>F<sup>81</sup>BrN<sub>2</sub>O<sub>6</sub><sup>23</sup>Na 643.1613.

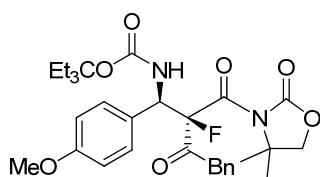
The *ee* was determined by HPLC analysis. CHIRALCEL IB (4.6 mm i.d. x 250 mm); Hexane/2-propanol = 80/20; flow rate 1.0 ml/min; 25°C; 210 nm; retention time: major isomer: 5.1 min (major), 6.3 min (minor); minor isomer: 8.3 min (major), 11.0 min (minor).

**3-ethylpentan-3-yl**

**(1R,2R)-2-(4,4-dimethyl-2-oxooxazolidine-3-carbonyl)-2-fluoro-1-(3-methoxyphenyl)-3-oxo-4-phenylbutylcarbamate (129q)**

Colorless oil; 95% *ee*, *dr* = 92:8;  $[\alpha]_{\text{D}}^{29} = +85.2$  (*c* 1.42,  $\text{CHCl}_3$ );  $^1\text{H}$  NMR (500 MHz,  $\text{CDCl}_3$ , ppm):  $\delta = 7.29 - 6.86$  (m, 9H), 5.90 (br, 1H), 5.60 – 5.54 (m, 1H), 4.44 – 4.37 (m, 1H), 4.10 – 3.95 (m, 2H), 3.80 (s, 3H), 1.79 – 1.75 (m, 6H), 1.60 (br, 1H), 1.52 -1.42 (m, 3.4), 1.26 (br, 2.5H), 0.76 – 0.73 (m, 9H);  $^{13}\text{C}$  NMR (75.5 MHz,  $\text{CDCl}_3$ , ppm):  $\delta = 199.3$  (d,  $J = 24.1$  Hz), 166.4 (d,  $J = 21.9$  Hz), 159.5, 154.4, 152.5, 137.6, 132.6, 130.5, 128.0, 126.8, 120.8, 114.4, 113.8, 101.1 (d,  $J = 225.4$  Hz), 88.0, 75.9, 61.5, 56.9 (d,  $J = 25.3$  Hz), 55.3, 43.0, 26.9, 24.3, 22.7, 7.5;  $^{19}\text{F}$  NMR (282.4 MHz,  $\text{MeOH-d}_4$ , ppm):  $-97.6$  (d,  $J = 30.2$  Hz); IR (film): 3449, 2970, 2361, 1782, 1735, 1705, 1600, 1492, 1327  $\text{cm}^{-1}$ ; LRMS (ESI)  $m/z$  569.1 ( $\text{M} - \text{H}^+$ ), HRMS (ESI)  $m/z$  593.2625 ( $\text{M} + \text{Na}^+$ ), calc. for  $\text{C}_{31}\text{H}_{39}\text{FN}_2\text{O}_7^{23}\text{Na}$  593.2634.

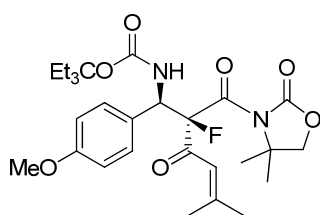
The *ee* was determined by HPLC analysis. CHIRALCEL IA (4.6 mm i.d. x 250 mm); Hexane/2-propanol = 70/30; flow rate 1.0 ml/min; 25°C; 210 nm; retention time: major isomer: 6.7 min (minor), 8.6 min (major); minor isomer: 12.6 min (major), 21.5 min (minor).

**3-ethylpentan-3-yl**

**(1*R*,2*R*)-2-(4,4-dimethyl-2-oxooxazolidine-3-carbonyl)-2-fluoro-1-(4-methoxyphenyl)-3-oxo-4-phenylbutylcarbamate (129r)**

Colorless oil; 98% *ee*, *dr* = 94:6;  $[\alpha]_{\text{D}}^{29} = +42.9$  (*c* 2.99, CHCl<sub>3</sub>); <sup>1</sup>H NMR (500 MHz, CDCl<sub>3</sub>, ppm):  $\delta = 7.35 - 7.15$  (m, 7H), 6.89 – 6.80 (m, 2H), 5.90 (br, 1H), 5.55 – 5.50 (m, 1H), 4.39 (d, *J* = 17.9 Hz, 1H), 4.06 – 3.94 (m, 2H), 3.81 (s, 3H), 1.80 – 1.73 (m, 6H), 1.64 (br, 1H), 1.56 -1.41 (m, 3.4H), 1.24 (br, 2.6H), 0.75 – 0.72 (m, 9H); <sup>13</sup>C NMR (75.5 MHz, CDCl<sub>3</sub>, ppm):  $\delta = 199.4$  (d, *J* = 24.3 Hz), 166.6 (d, *J* = 26.1 Hz), 159.5, 154.4, 152.7, 132.6, 130.4, 129.9, 128.2, 128.0, 126.8, 113.6, 101.2 (d, *J* = 200.8 Hz), 88.0, 75.9, 61.5, 56.5 (d, *J* = 26.3 Hz), 55.3, 43.0, 26.9, 24.3, 22.7, 7.5; <sup>19</sup>F NMR (282.4 MHz, MeOH-d<sub>4</sub>, ppm): –98.4 (d, *J* = 31.3 Hz); IR (film): 3449, 2970, 2372, 1782, 1705, 1493, 1331, 1253 cm<sup>-1</sup>; LRMS (ESI) *m/z* 593.0 (M + Na<sup>+</sup>), HRMS (ESI) *m/z* 593.2616 (M + Na<sup>+</sup>), calc. for C<sub>31</sub>H<sub>39</sub>FN<sub>2</sub>O<sub>7</sub><sup>23</sup>Na 593.2634.

The *ee* was determined by HPLC analysis. CHIRALCEL IA (4.6 mm i.d. x 250 mm); Hexane/2-propanol = 75/25; flow rate 1.0 ml/min; 25°C; 210 nm; retention time: major isomer: 7.6 min (minor), 10.3 min (major); minor isomer: 12.9 min (major), 17.4 min (minor).



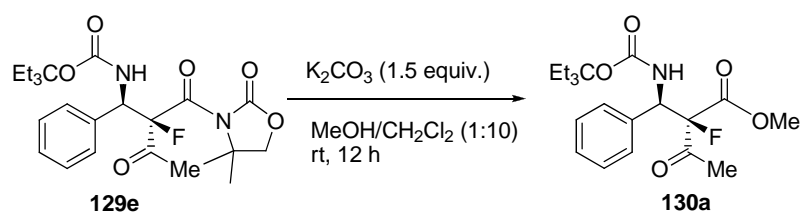
### 3-ethylpentan-3-yl

#### **(1R,2R)-2-(4,4-dimethyl-2-oxooxazolidine-3-carbonyl)-2-fluoro-1-(4-methoxyphenyl)-5-methyl-3-oxohex-4-enylcarbamate (129s)**

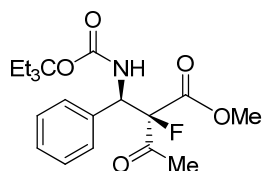
Colorless oil; 97% *ee*, *dr* = 98:2;  $[\alpha]_D^{29} = +162.0$  (*c* 1.34, CHCl<sub>3</sub>); <sup>1</sup>H NMR (500 MHz, CDCl<sub>3</sub>, ppm):  $\delta$  = 7.28 (d, *J* = 8.0 Hz, 2H), 6.80 (d, *J* = 8.0 Hz, 2H), 6.34 (br, 1H), 6.00 (br, 1H), 5.43 – 5.34 (m, 1H), 4.01 – 3.91 (m, 2H), 3.81 (s, 3H), 2.08 (br, 3H), 1.89, (br, 3H), 1.77 – 1.68 (m, 6H), 1.56 (br, 3.2H), 1.41, (br, 0.7H), 1.23 (br, 2.4H), 0.77 – 0.67 (m, 9H); <sup>13</sup>C NMR (75.5 MHz, CDCl<sub>3</sub>, ppm):  $\delta$  = 190.1 (d, *J* = 19.6 Hz), 167.6 (d, *J* = 25.5 Hz), 160.7, 159.3, 154.2, 152.3, 129.7, 128.6, 117.7, 113.4, 100.5 (d, *J* = 214.4 Hz), 87.4, 75.8, 61.4, 56.8 (d, *J* = 26.9 Hz), 55.2, 28.3, 26.9, 24.4, 22.8, 21.1, 7.5; <sup>19</sup>F NMR (282.4 MHz, CDCl<sub>3</sub>, ppm): –94.3 (d, *J* = 19.2 Hz); IR (film): 3449, 2970, 1786, 1717, 1616, 1508, 1327 cm<sup>-1</sup>; LRMS (ESI) *m/z* 557.0 (M + Na<sup>+</sup>), HRMS (ESI) *m/z* 557.2639 (M + Na<sup>+</sup>), calc. for C<sub>28</sub>H<sub>39</sub>FN<sub>2</sub>O<sub>7</sub><sup>23</sup>Na 557.2634.

The *ee* was determined by HPLC analysis. CHIRALCEL IA (4.6 mm i.d. x 250 mm); Hexane/2-propanol = 85/15; flow rate 1.0 ml/min; 25°C; 254 nm; retention time: major isomer: 10.9 min (minor), 15.8 min (major); minor isomer: 19.1 min (major), 45.7 min (minor).

#### **4.3.3 Experimental procedure for the conversion of oxazolidione moiety to ester**



Mannich product **129e** (23.0 mg, 0.05 mmol, 1.0 equiv. *dr* = 96:4, *ee* = 98%) was dissolved in the solvent mixture of MeOH and CH<sub>2</sub>Cl<sub>2</sub> (v/v, 1:10), followed by adding K<sub>2</sub>CO<sub>3</sub> (10.4 mg, 0.075 mmol, 1.5 equiv.) in one portion. The reaction mixture was stirred at room temperature and monitored by TLC. After 12 hours, upon complete consumption of **129e**, the reaction solvent was removed *in vacuo* and the crude product was directly loaded onto a short silica gel column, followed by gradient elution with hexane/EA mixtures (15/1-6/1 ratio). After removing the solvent, product **130a** (14.2 mg) was obtained as colorless oil in 73% yield.



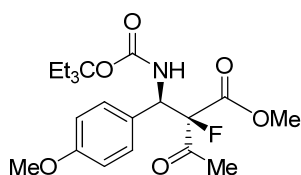
**(R)-methyl**

**2-((R)-((3-ethylpentan-3-yl)oxy)carbonylamino)(phenyl)methyl-2-fluoro-3-oxobutanoate (130a)**

Colorless oil; 73% yield, 95% *ee*, *dr* = 96:4;  $[\alpha]_{\text{D}}^{29} = -6.1$  (*c* 0.75, CHCl<sub>3</sub>); <sup>1</sup>H NMR (500 MHz, CDCl<sub>3</sub>, ppm): δ = 7.31 (br, 5H), 5.67 – 5.19 (m, 2H), 3.82 – 3.64 (br, m, 3H), 2.34 (d, *J* = 4.4 Hz, 0.14H), 1.99 (d, *J* = 4.5 Hz, 2.88H), 1.78 – 1.71 (m, 6H), 0.77 – 0.64 (m, 9H); <sup>13</sup>C NMR (75.5 MHz, CDCl<sub>3</sub>, ppm): δ =

199.9 (d,  $J = 28.2$  Hz), 164.9 (d,  $J = 26.2$  Hz), 154.0, 135.5, 128.6, 128.5, 128.3, 101.9 (d,  $J = 203.3$  Hz), 88.1, 57.0 (d,  $J = 18.9$  Hz), 53.5, 26.9, 26.3, 7.5;  $^{19}\text{F}$  NMR (282.4 MHz,  $\text{CDCl}_3$ , ppm): -98.6 (d,  $J = 25.9$  Hz), -103.2 (d,  $J = 27.2$  Hz); LRMS (ESI)  $m/z$  404.0 ( $\text{M} + \text{Na}^+$ ), HRMS (ESI)  $m/z$  404.1861 ( $\text{M} + \text{Na}^+$ ), calc. for  $\text{C}_{20}\text{H}_{28}\text{FNO}_5^{23}\text{Na}$  404.1844.

The *ee* was determined by HPLC analysis. CHIRALCEL IC (4.6 mm i.d. x 250 mm); Hexane/2-propanol = 95/5; flow rate 0.5 ml/min; 25°C; 210 nm; retention time: major isomer: 20.9 min (major), 30.8 min (minor); minor isomer: 34.2 min (minor), 45.0 min (major).



**(R)-methyl**

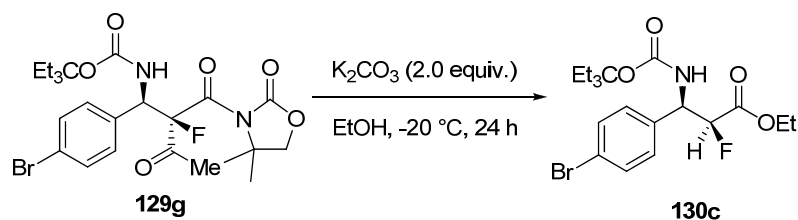
**2-((R)-((3-ethylpentan-3-yl)oxy)carbonylamino)(4-methoxyphenyl)methyl-2-fluoro-3-oxobutanoate (130b)**

Colorless oil; 75% yield, 98% *ee*, *dr* = 96:4;  $[\alpha]_{\text{D}}^{29} = -13.2$  (*c* 2.02,  $\text{CHCl}_3$ );  $^1\text{H}$  NMR (500 MHz,  $\text{CDCl}_3$ , ppm):  $\delta = 7.22$  (d,  $J = 7.5$  Hz, 2H), 6.83 (d,  $J = 8.5$  Hz, 2H), 5.61 – 5.14 (m, 2H), 3.82 – 3.64 (m, 6H), 2.33 (d,  $J = 4.4$  Hz, 0.1H), 2.00 (d,  $J = 4.3$  Hz, 2.9H), 1.82 – 1.68 (m, 6H), 0.77 – 0.66 (m, 9H);  $^{13}\text{C}$  NMR (75.5 MHz,  $\text{CDCl}_3$ , ppm):  $\delta = 199.9$  (d,  $J = 28.4$  Hz), 164.9 (d,  $J = 27.2$  Hz), 159.6, 154.0, 129.4, 128.4 (d,  $J = 112.6$  Hz), 114.0, 102.0 (d,  $J = 203.4$  Hz), 88.0,

56.6 (d,  $J = 18.8$  Hz), 55.2, 53.4, 26.9, 26.4, 7.5;  $^{19}\text{F}$  NMR (282.4 MHz,  $\text{CDCl}_3$ , ppm): -99.1 (d,  $J = 26.1$  Hz), -103.4 (d,  $J = 27.9$  Hz); IR (film): 3356, 2970, 2360, 1759, 1705, 1612, 1585, 1354, 1250, 1138  $\text{cm}^{-1}$ ; LRMS (ESI)  $m/z$  434.0 ( $\text{M} + \text{Na}^+$ ), HRMS (ESI)  $m/z$  434.1949 ( $\text{M} + \text{Na}^+$ ), calc. for  $\text{C}_{21}\text{H}_{30}\text{FNO}_6^{23}\text{Na}$  434.1949.

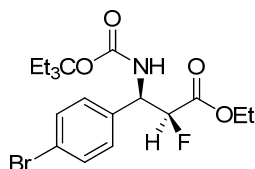
The *ee* was determined by HPLC analysis. CHIRALCEL IC (4.6 mm i.d. x 250 mm); Hexane/2-propanol = 90/10; flow rate 1.0 ml/min; 25°C; 210 nm; retention time: major isomer: 8.6 min (major), 10.3 min (minor); minor isomer: 11.8 min (minor), 19.4 min (major).

#### 4.3.4 Experimental procedure for the deacylation of **129g** to **130c**



Mannich product **129g** (27.2 mg, 0.05 mmol, 1.0 equiv.  $dr = 99:1$ ,  $ee = 98\%$ ) was dissolved in EtOH (0.5 ml). After it was stirred at  $-20^\circ\text{C}$  for 30 min,  $\text{K}_2\text{CO}_3$  (13.8 mg, 0.10 mmol, 2.0 equiv.) was added. The reaction mixture was stirred at  $-20^\circ\text{C}$  and monitored by TLC. After 24 hours, the reaction solvent was removed *in vacuo* and the crude product was directly loaded onto a short silica gel column, followed by gradient elution with hexane/EA mixtures (15/1-6/1 ratio). After removing the solvent, mixture of the two diastereomers

(14.2 mg) was obtained as colorless oil in 65% yield.



**(2S,3R)-ethyl**

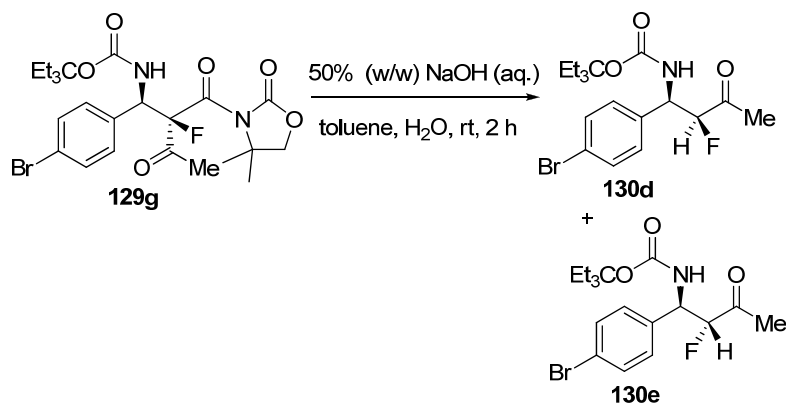
**3-(4-bromophenyl)-3-((3-ethylpentan-3-yl)oxy)carbonylamino-2-fluoropropionate (130c)**

Colorless oil; 95% *ee* (*syn*, major), *dr* = 4:1; Characterization of the isolated *syn* isomer  $[\alpha]_D^{29} = -9.5$  (*c* 0.20,  $\text{CHCl}_3$ );  $^1\text{H}$  NMR (500 MHz,  $\text{MeOH-d}_4$ , ppm):  $\delta = 7.53$  (d,  $J = 8.1$  Hz, 2H), 7.35 (d,  $J = 8.0$  Hz, 2H), 5.28 (d,  $J = 6.7$  Hz, 1H), 5.20 (d,  $J = 7.6$  Hz, 1H), 4.26 – 4.21 (m, 2H), 1.82 (q,  $J = 7.2, 14.6$  Hz, 6H), 1.28 (t,  $J = 7.0$  Hz, 3H), 0.85 – 0.71 (m, 9H);  $^{13}\text{C}$  NMR (75.5 MHz,  $\text{CDCl}_3$ , ppm):  $\delta = 167.2$  (d,  $J = 22.2$  Hz), 154.4, 136.9, 131.9, 128.4, 122.2, 90.2 (d,  $J = 192.0$  Hz), 88.1, 62.2, 54.8 (d,  $J = 19.1$  Hz), 26.9, 14.0, 7.6;  $^{19}\text{F}$  NMR (282.4 MHz,  $\text{CDCl}_3$ , ppm): -127.2 (dd,  $J = 28.5, 47.1$  Hz); IR (film) (mixture of the two diastereomers) : 3353, 2972, 1764, 1710, 1490, 1376, 1297, 1242, 1137  $\text{cm}^{-1}$ ; LRMS (ESI)  $m/z$  453.9 ( $\text{M} + \text{Na}^+$ ), HRMS (ESI)  $m/z$  454.1004, 456.0980 ( $\text{M} + \text{Na}^+$ ), calc. for  $\text{C}_{19}\text{H}_{27}\text{F}^{79}\text{BrNO}_4^{23}\text{Na}$  454.1000,  $\text{C}_{19}\text{H}_{27}\text{F}^{81}\text{BrNO}_4^{23}\text{Na}$ , 456.0979.

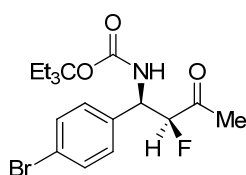
The *ee* was determined by HPLC analysis. CHIRALCEL AD-H (4.6 mm i.d. x 250 mm); Hexane/2-propanol = 90/10; flow rate 1.0 ml/min; 25°C; 230 nm; retention time: *syn* isomer: 10.4 min (minor), 19.4 min (major); *anti* isomer: 11.2

min (major), 14.4 min (minor).

#### 4.3.5 Experimental procedure for the decarboxylation of **129g** to **130d** and **130e**

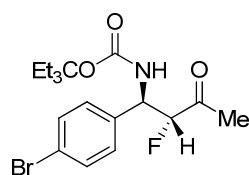


Mannich product **129g** (54.2 mg, 0.1 mmol, 1.0 equiv.  $dr = 99:1$ ,  $ee = 98\%$ ) was dissolved in toluene (1.0 ml), which was followed by adding H<sub>2</sub>O (0.5 ml). Then 0.5 ml of 50% (w/w) NaOH aqueous solution was added. The reaction mixture was stirred at room temperature and monitored by TLC. After 2 hours, upon complete consumption of **129g**, the reaction mixture was directly loaded onto a short silica gel column, followed by gradient elution with hexane/EA mixtures (20/1-8/1 ratio). After removing the solvent, product **130d** and **130e** (totally 24 mg) was obtained as white solid in 60% yield. **130d** and **130e** were separated by flash chromatography.



**3-ethylpentan-3-yl (1*R*,2*S*)-1-(4-bromophenyl)-2-fluoro-3-oxobutylcarbamate (130d)**

White solid, Mp 147.2 °C; 96% *ee*;  $[\alpha]_D^{29} = -24.2$  (*c* 0.56, CHCl<sub>3</sub>); <sup>1</sup>H NMR (500 MHz, MeOH-d<sub>4</sub>, ppm):  $\delta = 7.53$  (d, *J* = 8.4 Hz, 2H), 7.35 (d, *J* = 8.3 Hz, 2H), 5.29 – 5.08 (m, 2H), 2.29 (d, *J* = 4.2 Hz, 3H), 1.81 (q, *J* = 7.4 Hz, 6H), 0.84 – 0.71 (m, 9H); <sup>13</sup>C NMR (75.5 MHz, CDCl<sub>3</sub>, ppm):  $\delta = 205.9$  (d, *J* = 23.8 Hz), 154.4, 136.9, 131.9, 128.5, 122.2, 95.8 (d, *J* = 192.8 Hz), 88.3, 54.4 (d, *J* = 19.7 Hz), 29.7, 27.0, 7.6; <sup>19</sup>F NMR (282.4 MHz, CDCl<sub>3</sub>, ppm): -121.8 (dd, *J* = 24.9, 47.8 Hz)

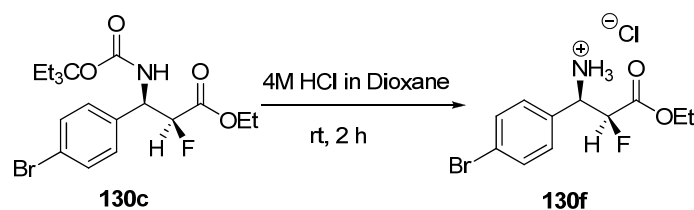
**3-ethylpentan-3-yl (1*R*,2*R*)-1-(4-bromophenyl)-2-fluoro-3-oxobutylcarbamate (130e)**

White solid, Mp 114.1 °C; 96% *ee*;  $[\alpha]_D^{29} = +8.6$  (*c* 0.15, CHCl<sub>3</sub>); <sup>1</sup>H NMR (500 MHz, MeOH-d<sub>4</sub>, ppm):  $\delta = 7.47$  (d, *J* = 8.5 Hz, 2H), 7.23 (d, *J* = 8.0 Hz, 2H), 5.09 – 4.99 (m, 2H), 1.92 (d, *J* = 4.4 Hz, 3H), 1.80 – 1.76 (m, 6H), 0.80 – 0.67 (m, 9H); <sup>13</sup>C NMR (75.5 MHz, CDCl<sub>3</sub>, ppm):  $\delta = 205.4$  (d, *J* = 22.5 Hz), 154.3, 135.1, 131.9, 129.6, 122.6, 96.5 (d, *J* = 192.7), 88.3, 55.2 (d, *J* = 19.2 Hz), 27.0, 26.8, 7.6; <sup>19</sup>F NMR (282.4 MHz, CDCl<sub>3</sub>, ppm): -124.8 (dd, *J* = 29.5, 49.4 Hz)

IR (film): (mixture of the two diastereomers) 3342, 2972, 1704, 1490, 1358, 1240, 1137  $\text{cm}^{-1}$ ; LRMS (ESI)  $m/z$  423.9, 425.9 ( $M + \text{Na}^+$ ), HRMS (ESI)  $m/z$  424.0882, 426.0875 ( $M + \text{Na}^+$ ), calc. for  $\text{C}_{18}\text{H}_{25}\text{FNO}_3$   $^{79}\text{Br}^{23}\text{Na}$  424.0894,  $\text{C}_{18}\text{H}_{25}\text{FNO}_3$   $^{81}\text{Br}^{23}\text{Na}$  426.0874.

The *ee* was determined by HPLC analysis. CHIRALCEL IC (4.6 mm i.d. x 250 mm); Hexane/2-propanol = 95/5; flow rate 0.5 ml/min; 25°C; 230 nm; retention time: *anti* isomer: 14.2 min (major), 18.2 min (minor); *syn* isomer: 15.9 min (major), 23.2 min (minor).

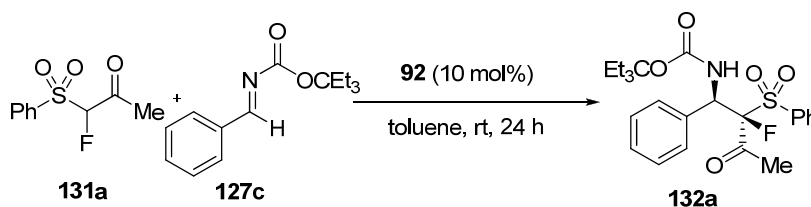
#### 4.3.6 Typical experimental procedure for the cleavage of *N*-Eoc group



A 5 ml round bottom flask was charged with racemic product **130d** (21.6 mg, 0.05 mmol, *d.r.* = 1:1), followed by adding 4M HCl of dioxane solution (0.5 ml). The reaction mixture was stirred at room temperature 2 hours. Upon complete consumption of **130d**, the solvent was removed *in vacuo* to leave a white solid, which was washed with 3 ml hexane 3 times, followed by a simple filtration. The residue was dried under vacuum to give product **130f** as a white solid (15.0 mg, 92% yield, *dr* = 1:1).  $^1\text{H}$  NMR (300 MHz,  $\text{MeOH-d}_4$ , ppm):  $\delta$  = 7.69 –

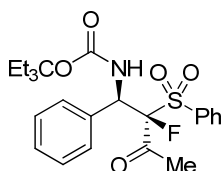
7.63 (m, 2H), 7.45 – 7.40, (m, 2H), 5.68 – 5.31, (m, 1H), 5.01 – 4.88, (m, 1H), 4.22 – 4.09, (m, 2H), 1.18 – 1.10, (m, 3H);  $^{13}\text{C}$  NMR (75.5 MHz, MeOH- $d_4$ , ppm):  $\delta$  = 167.4, 167.1, 166.9, 166.6, 133.7, 133.4, 133.0, 132.9, 131.8, 131.2, 125.5, 125.4, 90.1 (d,  $J$  = 191.0 Hz, *anti* isomer), 89.3 (d,  $J$  = 193.3 Hz, *syn* isomer), 63.6, 63.5, 56.6, 56.4, 56.4, 56.1, 14.3, 14.1;  $^{19}\text{F}$  NMR (282.4 MHz, MeOH- $d_4$ , ppm): -121.6 (dd,  $J$  = 16.7, 47.2 Hz, *syn* isomer), -129.7 (dd,  $J$  = 27.9, 48.8 Hz, *anti* isomer); LRMS (ESI)  $m/z$  289.9, 291.9 ( $M - \text{Cl}^-$ )

#### 4.3.7 Experimental procedure for the reaction between 1-fluoro-1-(phenylsulfonyl)propan-2-one **131a** and *N*-3-ethylpentan-3-yloxycarbonyl (Eoc) imine **127c** catalyzed by **92**



*N*-3-ethylpentan-3-yloxycarbonyl (Eoc) imine **127c** (24.7 mg, 0.1 mmol, 2.0 equiv.) and **92** (1.12 mg, 0.005 mmol, 0.1 equiv) were dissolved in toluene (0.5 ml) and stirred at room temperature for 10 min, then 1-fluoro-1-(phenylsulfonyl)propan-2-one **131a** (10.1 mg, 0.05 mmol, 1.0 equiv.) was added. The reaction mixture was stirred at room temperature and monitored by TLC. After 24 hours, upon complete consumption of **131a**, the reaction mixture was directly loaded onto a short silica gel column, followed by gradient elution with hexane/EA mixtures (10/1 - 2/1 ratio). After removing the solvent,

product **132a** (22.7 mg) was obtained as colorless oil in 98% yield.



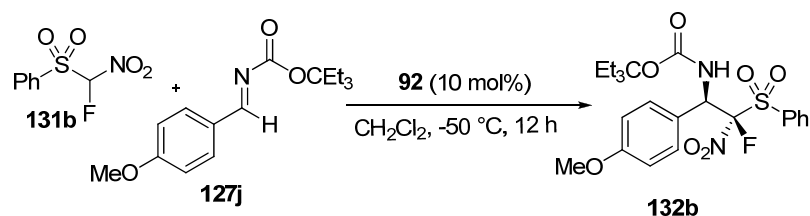
### 3-ethylpentan-3-yl

#### (1*R*,2*S*)-2-fluoro-3-oxo-1-phenyl-2-(phenylsulfonyl)butylcarbamate (**132a**)

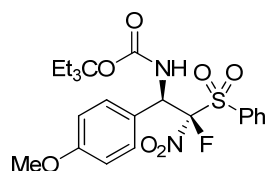
Colorless oil; 90% *ee*, *dr* = 86:14;  $[\alpha]_D^{29} = -67.3$  (*c* 0.79, CHCl<sub>3</sub>); <sup>1</sup>H NMR (500 MHz, CDCl<sub>3</sub>, ppm):  $\delta = 7.94$  (d, *J* = 7.2 Hz, 2H), 7.83 – 7.53 (m, 3H), 5.69 – 5.19 (m, 2H), 1.97 (d, *J* = 4.9 Hz, 0.5H), 1.83 – 1.74 (m, 6H), 1.63 (d, *J* = 5.4 Hz, 2.5H), 0.85 – 0.59 (m, 9H); <sup>13</sup>C NMR (75.5 MHz, CDCl<sub>3</sub>, ppm):  $\delta = 199.9$  (d, *J* = 25.8 Hz), 153.7, 135.2, 130.8, 130.4, 129.2, 128.6, 128.5, 128.4, 110.4 (d, *J* = 239.1 Hz), 88.2, 55.9 (d, *J* = 17.1 Hz), 27.1, 27.0, 7.6; <sup>19</sup>F NMR (282.4 MHz, CDCl<sub>3</sub>, ppm): -94.5 (d, *J* = 29.7 Hz), -96.1 (d, *J* = 29.3 Hz); IR (film): 2970, 2365, 1709, 1497, 1454, 1331, 1223, 1153 cm<sup>-1</sup>; LRMS (ESI) *m/z* 485.9 (M + Na<sup>+</sup>), HRMS (ESI) *m/z* 486.1721 (M + Na<sup>+</sup>), calc. for C<sub>24</sub>H<sub>30</sub>FSNO<sub>5</sub><sup>23</sup>Na 486.1721.

The *ee* was determined by HPLC analysis. CHIRALCEL IC (4.6 mm i.d. x 250 mm); Hexane/2-propanol = 70/30; flow rate 1.0 ml/min; 25°C; 230 nm; retention time: major isomer: 8.5 min (minor), 12.0 min (major); minor isomer: 18.2 min (major), 21.3 min (minor).

**4.3.8 Experimental procedure for the reaction between (fluoro(nitro)methylsulfonyl)benzene **131b** and *N*-3-ethylpentan-3-yloxycarbonyl (Eoc) imine **127j** catalyzed by **92**.**



*N*-3-ethylpentan-3-yloxycarbonyl (Eoc) imine **127j** (27.7 mg, 0.10 mmol, 2.0 equiv.) and **92** (1.12 mg, 0.005 mmol, 0.1 equiv) were dissolved in dichloromethane (0.5 ml). Stirred at  $-50^{\circ}\text{C}$  for 30 min, then (fluoro(nitro)methylsulfonyl)benzene **131b** (10.5 mg, 0.05 mmol, 1.0 equiv) was added. The reaction mixture was stirred at  $-50^{\circ}\text{C}$  and monitored by TLC. After 12 hours, upon complete consumption of **131b**, the reaction solvent was removed *in vacuo* and the crude product was directly loaded onto a short silica gel column, followed by gradient elution with hexane/EA mixtures (10/1 - 2/1 ratio). After removing the solvent, product **132b** (20.5 mg) was obtained as colorless oil in 83% yield.



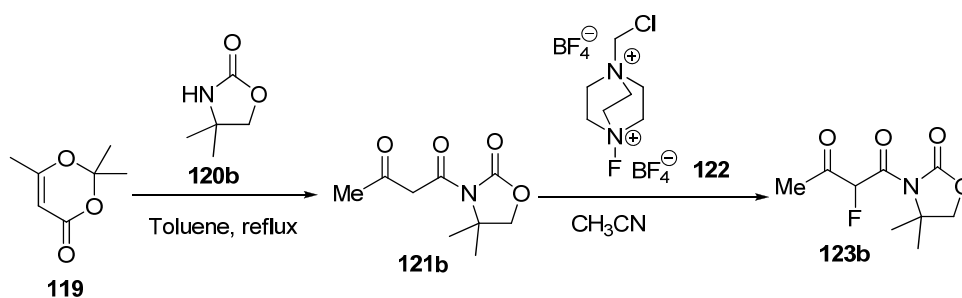
**3-ethylpentan-3-yl**

**(1*R*,2*S*)-2-fluoro-1-(4-methoxyphenyl)-2-nitro-2-(phenylsulfonyl)ethylcarbam**

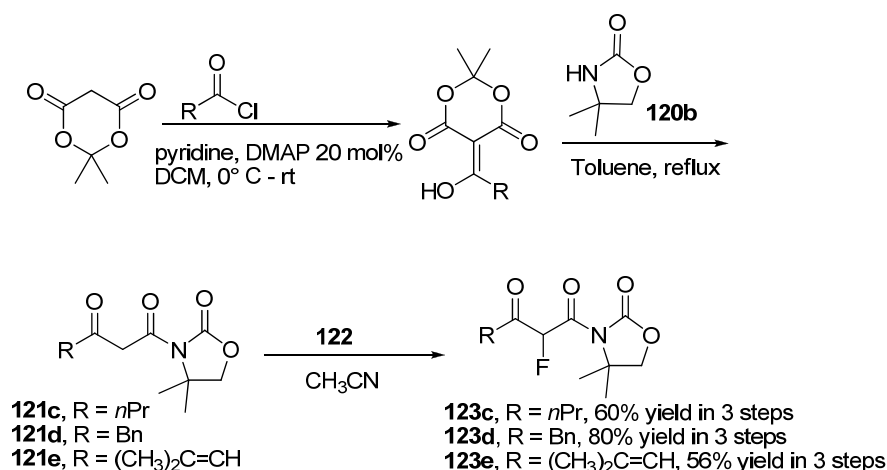
**ate (132b)**

Colorless oil; 85% *ee*, *dr* = 85:15;  $[\alpha]_D^{29} = -9.0$  (*c* 0.96, CHCl<sub>3</sub>); <sup>1</sup>H NMR (500 MHz, CDCl<sub>3</sub>, ppm):  $\delta = 7.97$  (d, *J* = 7.9 Hz, 2H), 7.79 – 7.50 (m, 3H), 7.22 – 7.15 (m, 2H), 6.82 – 6.80 (m, 2H), 6.07 – 6.02 (m, 1H), 5.43 (d, *J* = 6.4 Hz, 1H), 3.79 (minor) 3.76 (major) (s, 3H), 1.81 – 1.77 (m, 6H), 0.85 – 0.77 (m, 9H); <sup>13</sup>C NMR (75.5 MHz, CDCl<sub>3</sub>, ppm):  $\delta = 160.4, 153.4, 136.2, 132.5$  (d, *J* = 32.1 Hz), 131.0, 129.5, 129.3, 124.5, 114.4, 89.1, 55.6 (d, *J* = 14.1 Hz), 55.2, 26.9, 7.5; <sup>19</sup>F NMR (282.4 MHz, CDCl<sub>3</sub>, ppm): -46.5, -57.7 (d, *J* = 26.7 Hz), -59.1 (d, *J* = 12.2 Hz); IR (film): 3375, 2970, 2365, 1705, 1585, 1512, 1454, 1350, 1246, 1157 cm<sup>-1</sup>; LRMS (ESI) *m/z* 518.9 (M + Na<sup>+</sup>), HRMS (ESI) *m/z* 519.1558 (M + Na<sup>+</sup>), calc. for C<sub>23</sub>H<sub>29</sub>FSN<sub>2</sub>O<sub>7</sub><sup>23</sup>Na 519.1572.

The *ee* was determined by HPLC analysis. CHIRALCEL IC (4.6 mm i.d. x 250 mm); Hexane/2-propanol = 85/15; flow rate 1.0 ml/min; 25°C; 254 nm; retention time: major isomer: 8.7 min (major), 12.9 min (minor); minor isomer: 16.4 min (major), 20.4 min (minor).

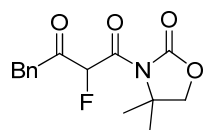
**4.3.9 Procedures for the preparation of  $\alpha$ -fluoro- $\beta$ -keto acyloxazolidinones**

**Method A<sup>13</sup>:** To a 50 ml clean round bottom flask was added 2,2,6-trimethyl-4H-1,3-dioxin-4-one **119** (664.3  $\mu$ l, 5.0 mmol, 1.0 equiv.), 5,5-dimethyloxazolidin-2-one **120b** (862.5 mg, 7.5 mmol, 1.5 equiv.) and toluene (10 ml). The mixture was stirred under reflux conditions for 5 hours. The reaction solvent was removed *in vacuo* and the crude product was directly loaded onto a silica gel column, followed by gradient elution with hexane/EA mixtures (10/1 - 2/1 ratio). After removing the solvent, the product 1-(4,4-dimethyl-2-oxooxazolidin-3-yl)butane-1,3-dione **121b** was directly dissolved in 10 ml CH<sub>3</sub>CN, followed by adding Selectfluor **122** (2.1 g, 6.0 mmol, 1.2 equiv.). The reaction mixture was stirred under room temperature for 24 hours. The solvent was removed *in vacuo* and the crude product was directly loaded onto a silica gel column, followed by gradient elution with hexane/EA mixtures (10/1 - 2/1 ratio). After removing the solvent, product 1-(4,4-dimethyl-2-oxooxazolidin-3-yl)-2-fluorobutane-1,3-dione **123b** (922 mg, totally 85% yield in two steps) was obtained as white solid. <sup>1</sup>H NMR (500 MHz, CDCl<sub>3</sub>, ppm):  $\delta$  = 6.17 (d, *J* = 48.0 Hz, 1H), 4.08 (q, *J* = 5.9 Hz, 2H), 2.34 (d, *J* = 3.1 Hz, 3H), 1.58 (s, 3H), 1.55 (s, 3H); <sup>13</sup>C NMR (125.8 MHz, CDCl<sub>3</sub>, ppm):  $\delta$  = 198.9 (d, *J* = 23.0 Hz), 164.8 (d, *J* = 22.1 Hz), 153.9, 90.6 (d, *J* = 190.3 Hz), 76.1, 60.7, 26.8, 24.8, 24.0; <sup>19</sup>F NMR (282.4 MHz, CDCl<sub>3</sub>, ppm): -119.4 (m, d, *J* = 48.0 Hz); LRMS (FAB) *m/z* 218.0 (M + H<sup>+</sup>).



**Method B**<sup>14a</sup>: Meldrum's acid (200 mg, 1.38 mmol, 1.0 equiv.), DMAP (34 mg, 0.27 mmol, 0.2 equiv.), pyridine (0.023 ml, 2.76 mmol, 2.0 equiv.), were dissolved in anhydrous DCM (5 ml) with stirring under nitrogen atmosphere. The solution was cooled to 0°C and butyryl chloride was added slowly. The mixture was stirred at 0°C for 2 hours and for 15 hours at room temperature. The solvent was removed *in vacuo* and dissolved in 3 ml toluene, followed by adding 5,5-dimethyl-2-oxo-1,3-dioxolane **120b** (238.1 mg, 2.07 mmol, 1.5 equiv.). The mixture was stirred under reflux conditions for 5 hours. The reaction solvent was removed *in vacuo* and the crude product was directly loaded onto a silica gel column, followed by gradient elution with hexane/EA mixtures (10/1-2/1 ratio). After removing the solvent, the product 1-(4,4-dimethyl-2-oxooxazolidin-3-yl)hexane-1,3-dione **121c** was directly dissolved in 3 ml CH<sub>3</sub>CN, followed by adding Selectfluor **92** (586.7 mg, 1.7 mmol, 1.2 equiv.). The reaction mixture was stirred under room temperature for 24 hours. The solvent was removed *in vacuo* and the crude product was directly

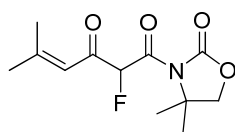
loaded onto a silica gel column, followed by gradient elution with hexane/EA mixtures (10/1-2/1 ratio). After removing the solvent, product 1-(4,4-dimethyl-2-oxooxazolidin-3-yl)-2-fluorohexane-1,3-dione **123c** (202 mg, totally 60% yield in three steps.) was obtained as white solid.  $^1\text{H}$  NMR (300 MHz,  $\text{CDCl}_3$ , ppm):  $\delta$  = 6.24 (d,  $J$  = 48.1 Hz, 1H), 4.12 (q,  $J$  = 5.5 Hz, 2H), 2.80 – 2.63 (m, 2H), 1.68 – 1.58 (m, 8H), 0.94, (t,  $J$  = 7.4 Hz, 3H);  $^{13}\text{C}$  NMR (75.5 MHz,  $\text{CDCl}_3$ , ppm):  $\delta$  = 201.3 (d,  $J$  = 22.1 Hz), 165.2 (d,  $J$  = 21.8 Hz), 154.1, 90.5 (d,  $J$  = 189.9 Hz), 76.3, 60.8, 41.3, 25.1, 24.1, 16.2, 13.4;  $^{19}\text{F}$  NMR (282.4 MHz,  $\text{CDCl}_3$ , ppm): -120.5 (d,  $J$  = 48.0 Hz); LRMS (FAB)  $m/z$  246.0 ( $\text{M} + \text{H}^+$ ).



**1-(4,4-dimethyl-2-oxooxazolidin-3-yl)-2-fluoro-4-phenylbutane-1,3-dione**

**(123d)**

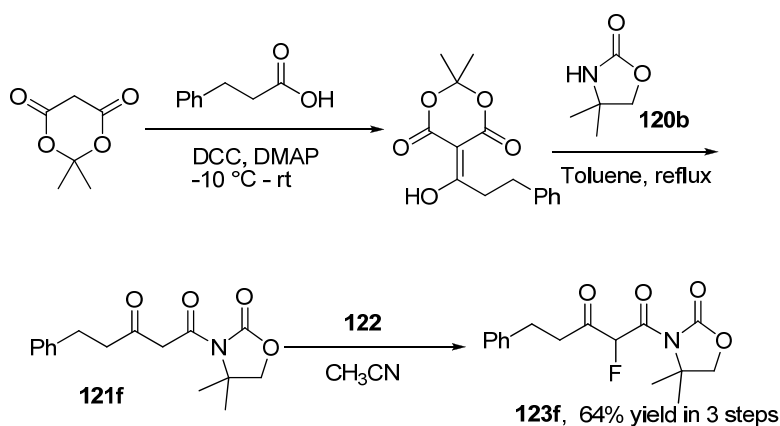
Following **Method B**, 80% yield. Pale yellow solid;  $^1\text{H}$  NMR (300 MHz,  $\text{CDCl}_3$ , ppm):  $\delta$  = 7.43 – 7.21 (m, 5H), 6.29 (d,  $J$  = 48.0 Hz, 1H), 4.17, (s, 2H), 4.05 (br, 2H), 1.63 (s, 3H), 1.59, (s, 3H);  $^{13}\text{C}$  NMR (75.5 MHz,  $\text{CDCl}_3$ , ppm):  $\delta$  = 198.6 (d,  $J$  = 22.1 Hz), 164.8 (d,  $J$  = 21.8 Hz), 154.0, 132.0, 130.0, 128.6, 127.3, 90.3 (d,  $J$  = 190.8 Hz), 76.3, 60.8, 46.1, 25.0, 24.1;  $^{19}\text{F}$  NMR (282.4 MHz,  $\text{CDCl}_3$ , ppm): -119.6 (d,  $J$  = 48.0 Hz); LRMS (ESI)  $m/z$  316.0 ( $\text{M} + \text{Na}^+$ ).



**1-(4,4-dimethyl-2-oxooxazolidin-3-yl)-2-fluoro-5-methylhex-4-ene-1,3-dione**

**(123e)**

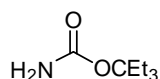
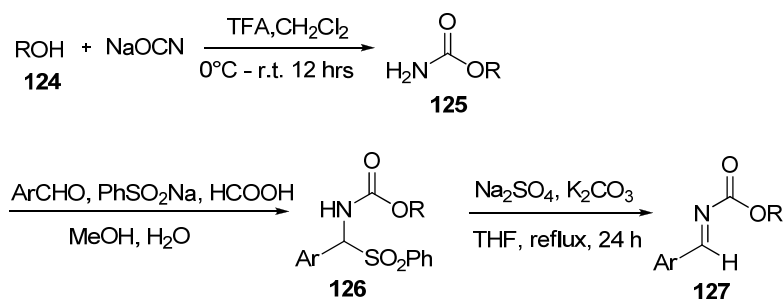
Following **Method B**, 56% yield. Colorless oil;  $^1\text{H}$  NMR (300 MHz,  $\text{CDCl}_3$ , ppm):  $\delta = 6.39 - 6.21$  (m, 2H), 4.11 (q,  $J = 6.2$  Hz, 2H), 2.17 (s, 3H), 1.98 (s, 3H), 1.63 (s, 3H), 1.63, (s, 3H);  $^{13}\text{C}$  NMR (75.5 MHz,  $\text{CDCl}_3$ , ppm):  $\delta = 189.5$  (d,  $J = 19.9$  Hz), 165.8 (d,  $J = 22.3$  Hz), 162.4, 154.0, 119.5, 90.9 (d,  $J = 191.3$  Hz), 76.2, 60.7, 28.1, 25.1, 24.2, 21.4;  $^{19}\text{F}$  NMR (282.4 MHz,  $\text{CDCl}_3$ , ppm): -119.0 (d,  $J = 48.5$  Hz); LRMS (ESI)  $m/z$  257.9 ( $\text{M} + \text{H}^+$ ).



**Method C<sup>14b</sup>**: DCC (2.3 mmol, 480 mg, 1.1 equiv.) was dissolved in 3ml DCM and stirred for 30min at 0°C. Then Meldrum's acid (2.3 mmol, 1.0 g, 1.1 equiv.), DMAP (3.37 mmol, 410 mg, 1.5 equiv.) and 3-phenylpropanoic acid (2.1 mmol, 315.3 mg, 1.0 equiv.) was dissolved in 15 ml DCM and stirred at -10°C for 45 min. To this solution was added the DCC solution dropwise over 1.5 hours at -10°C. Then the mixture was allowed to warm to room temperature and stirred

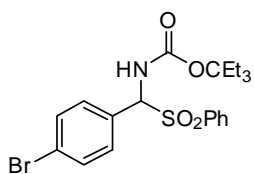
overnight.  $\text{KHSO}_4$  (6% aqueous) was added and the resulting precipitate was filtered off. The crude intermediate 5-(1-hydroxy-3-phenylpropylidene)-2,2-dimethyl-1,3-dioxane-4,6-dione was obtained. The next steps were the same as **Method B**. 1-(4,4-dimethyl-2-oxooxazolidin-3-yl)-2-fluoro-5-phenylpentane-1,3-dione **123f** was obtained as white solid (411.8 mg, totally 64% yield in three steps).  $^1\text{H}$  NMR (300 MHz,  $\text{CDCl}_3$ , ppm):  $\delta$  = 6.16 (d,  $J$  = 48.1 Hz, 1H), 4.03 – 3.97 (m, 2H), 3.09 – 2.82 (m, 4H), 1.53 (s, 3H), 1.49 (s, 3H);  $^{13}\text{C}$  NMR (75.5 MHz,  $\text{CDCl}_3$ , ppm):  $\delta$  = 200.1 (d,  $J$  = 22.1 Hz), 164.7 (d,  $J$  = 22.1 Hz), 153.9, 140.0, 128.3, 128.0, 126.1, 90.3 (d,  $J$  = 189.7 Hz), 76.0, 60.5, 40.7, 28.3, 24.7, 23.8;  $^{19}\text{F}$  NMR (282.4 MHz,  $\text{CDCl}_3$ , ppm): -120.4 (d,  $J$  = 48.1 Hz); LRMS (ESI)  $m/z$  307.9 ( $\text{M} + \text{H}^+$ ).

#### 4.3.10 Typical experimental procedure for the synthesis of *N*-Eoc imines



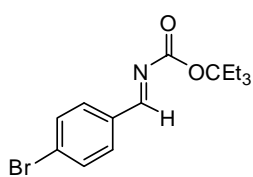
To a  $0^\circ\text{C}$  suspension of sodium cyanate (2.6 g, 40 mmol, 2.0 equiv.) in 20 ml  $\text{CH}_2\text{Cl}_2$  was added 2.75 ml 3-ethylpentan-3-ol (20 mmol, 1.0 equiv.), followed by adding 3.3 ml TFA (42 mmol, 2.1 equiv.)

dropwise with stirring. The reaction mixture was allowed to warm to room temperature slowly. After stirred at room temperature 12 hours, 20 ml H<sub>2</sub>O was added. The aqueous layer was extracted with 60 ml CH<sub>2</sub>Cl<sub>2</sub> 3 times. The combined organic layer was dried over anhydrous Na<sub>2</sub>SO<sub>4</sub> and evaporated to leave a white solid (2.3 g, 71% yield), which was pure enough for the next step. <sup>1</sup>H NMR (300 MHz, CDCl<sub>3</sub>, ppm): δ = 4.43 (br, 2H), 1.81 (q, *J* = 7.6 Hz, 2H), 0.83 (t, *J* = 7.6 Hz, 3H); <sup>13</sup>C NMR (75.5 MHz, CDCl<sub>3</sub>, ppm): δ = 156.4, 87.1, 26.9, 7.5.



To a suspension of benzenesulfonic acid sodium salt (820 mg, 5 mmol, 2.0 equiv.) in the mixture solvent of 10 ml MeOH/H<sub>2</sub>O (v/v, 1:1), was added 4-bromobenzaldehyde (694 mg, 3.75 mmol, 1.5 equiv.) and 3-ethylpentan-3-yl carbamate (398 mg, 2.5 mmol, 1.0 equiv.), followed by formic acid (189 μl, 5 mmol, 2.0 equiv.). The reaction was allowed to stir at room temperature 4 days. During which time the product precipitated as a white solid. The imine precursor **126** was isolated *via* Büchner funnel filtration and washed with water and diethyl ether. After drying in vacuo, it was obtained as a white solid (1.73 g, 74% yield). <sup>1</sup>H NMR (300 MHz, CDCl<sub>3</sub>, ppm): δ = 7.89, (d, *J* = 7.5 Hz, 2H), 7.68 – 7.52 (m, 5H), 7.30, (d, *J* = 8.3 Hz, 2H), 5.90 (br, d, *J* = 10.7 Hz, 1H), 5.72

(br, d,  $J = 11.8$  Hz, 1H), 1.67 – 1.61 (m, 6H), 0.69 (t,  $J = 7.2$  Hz, 9H);  $^{13}\text{C}$  NMR (75.5 MHz,  $\text{CDCl}_3$ , ppm):  $\delta = 153.2, 136.7, 134.1, 132.0, 130.4, 129.3, 129.2, 127.0, 124.3, 89.4, 73.3, 26.8, 7.6$ ; LRMS (ESI)  $m/z$  489.7, 491.7 (M +  $\text{Na}^+$ ).

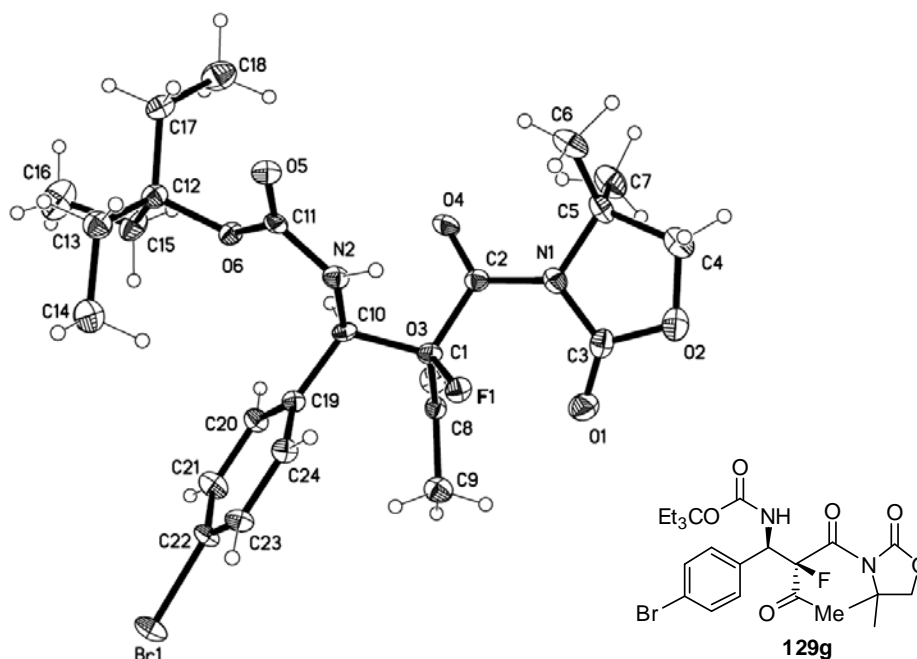


A 50 ml round bottom flask was charged with anhydrous potassium carbonate (828 mg, 6.0 mmol, 6.0 equiv.) and anhydrous sodium sulfate (852 mg, 6.0 mmol, 6.0 equiv.). The flask was capped with a water-cooled reflux condenser. The solids were placed under vacuum and flame-dried. Once cool, imine precursor **126** (467 mg, 1.0 mmol, 1.0 equiv.) was added under a positive stream of nitrogen, followed by anhydrous THF (10 ml). After 24 hours, the reaction mixture was cooled down to room temperature and the solids were removed *via* simple filtration. The filtrate was concentrated in *vacuo* and dried under vacuum to give imine **127e** as colorless oil (293 mg, 90% yield).  $^1\text{H}$  NMR (300 MHz,  $\text{CDCl}_3$ , ppm):  $\delta = 8.76$  (s, 1H), 7.77, (d,  $J = 8.5$  Hz, 2H), 7.61, (d,  $J = 8.5$  Hz, 2H), 1.94 (q,  $J = 7.5$  Hz, 6H), 0.89 (t,  $J = 7.5$  Hz, 9H);  $^{13}\text{C}$  NMR (75.5 MHz,  $\text{CDCl}_3$ , ppm):  $\delta = 167.5, 162.1, 133.0, 132.1, 131.3, 128.2, 90.4, 26.6, 7.7$ .

#### 4.3.11 Determination of the absolute configurations of adducts

- i. Absolute configurations of **129a-s**, were determined by X-ray structure

analysis of the product **129g**



X-ray structure of **129g**

- ii. Absolute configurations of **132a** and **132b** were deduced by comparing the structure of compound **129g**.
- iii. Determination of the absolute configurations of **139d** and **130e** were based on **129g** and the H-F coupling constant of  $^{19}\text{F}$  NMR as well as reference 19.
- iv. The absolute configuration of **130c** was deduced from the H-F coupling constant and the comparison of the  $^{19}\text{F}$  NMR and  $^1\text{H}$  NMR with compounds **130d** and **130e**.

#### X-ray report of compound **129g**

The crystal is orthorhombic, space group P2(1). The asymmetric unit contains

one molecule of the compound C. As the space group is chiral and the absolute parameter = -0.003 with esd 0.007, the reported structure is the correct hand. Final R values are: R1= 0.0411 and wR2=0.0871 for two-theta up to 55°.

Table. Crystal data and structure refinement for 9387.

Identification code	9387	
Empirical formula	C <sub>24</sub> H <sub>32</sub> Br F N <sub>2</sub> O <sub>6</sub>	
Formula weight	543.43	
Temperature	100(2) K	
Wavelength	0.71073 Å	
Crystal system	Monoclinic	
Space group	P2(1)	
Unit cell dimensions	a = 6.1411(8) Å	α = 90°.
	b = 9.2639(13) Å	β =
	90.215(4)°.	
	c = 22.411(3) Å	γ = 90°.
Volume	1275.0(3) Å <sup>3</sup>	
Z	2	
Density (calculated)	1.416 Mg/m <sup>3</sup>	
Absorption coefficient	1.660 mm <sup>-1</sup>	
F(000)	564	
Crystal size	0.90 x 0.10 x 0.02 mm <sup>3</sup>	
Theta range for data collection	1.82 to 27.48°.	
Index ranges	-7<=h<=7, -12<=k<=11, -29<=l<=27	
Reflections collected	8965	
Independent reflections	5595 [R(int) = 0.0338]	
Completeness to theta = 27.48°	99.8 %	
Absorption correction	Semi-empirical from equivalents	
Max. and min. transmission	0.9676 and 0.3166	
Refinement method	Full-matrix least-squares on F <sup>2</sup>	

---

Data / restraints / parameters	5595 / 1 / 317
Goodness-of-fit on $F^2$	0.984
Final R indices [ $I > 2\sigma(I)$ ]	R1 = 0.0411, wR2 = 0.0871
R indices (all data)	R1 = 0.0471, wR2 = 0.0892
Absolute structure parameter	-0.003(7)
Largest diff. peak and hole	1.354 and -0.406 e.Å <sup>-3</sup>

**References:**

---

- (1) Ojima I., *Fluorine in Medicinal Chemistry and Chemical Biology*, Wiley-Blackwell, **2009**.
- (2) (a) J. A. Wilkinson, *Chem. Rev.* **1992**, *92*, 50; (b) Banchet, J.; Lefebvre, P.; Legay, R.; Lasne, M.-A.; Rouden, J. *Green Chem.* **2010**, *12*, 252.
- (3) (a) Taylor, S. D.; Kotoris, C. C.; Hum, G. *Tetrahedron* **1999**, *55*, 12431; (b) Singh, R. P.; Shreeve, J. n. M. *Acc. Chem. Res.* **2003**, *37*, 31.
- (4) (a) Fukuzumi, T.; Shibata, N.; Sugiura, M.; Yasui, H.; Nakamura, S.; Toru, T.; *Angew. Chem. Int. Ed.* **2006**, *45*, 4973; (b) Mizuta, S.; Shibata, N.; Goto, Y.; Furukawa, T.; Nakamura, S.; Toru, T., *J. Am. Chem. Soc.* **2007**, *129*, 6394; (c) Furukawa, T.; Shibata, N.; Mizuta, S.; Nakamura, S.; Toru, T.; Shiro, M., *Angew. Chem. Int. Ed.* **2008**, *47*, 8051; (d) Ullah, F.; Zhao, G.-L.; Deiana, L.; Zhu, M.; Dziedzic, P.; Ibrahim, I.; Hammar, P.; Sun J.; Córdova, A. *Chem. Eur. J.* **2009**, *15*, 10013; (e) Moon, H. W.; Cho, M. J.; Kim, D. Y. *Tetrahedron Lett.* **2009**, *50*, 4896.
- (5) Prakash, G. K. S.; Wang, F.; Stewart, T.; Mathew, T.; Olah, G. A., *Proc. Natl. Acad. Sci. USA.* **2009**, *106*, 4090.
- (6) Han, X.; Kwiatkowski, J.; Xue, F.; Huang, K.-W.; Lu, Y. *Angew. Chem. Int. Ed.* **2009**, *48*, 7604.
- (7) (a) Han, X.; Luo, J.; Liu C.; Lu, Y. *Chem. Commun.*, **2009**, 2044; (b) Han, X.; Zhong, F.; Lu, Y. *Adv. Synth. Catal.* **2010**, *352*, 2778.

- (8) (a) Li, H.; Zhang, S.; Yu, C.; Song X.; Wang, W. *Chem. Commun.* **2009**, 2136; (b) Oh, Y.; Kim, S. M.; Kim, D. Y. *Tetrahedron Lett.* **2009**, 50, 4674.
- (9) Ding, C.; Maruoka, K. *Synlett*, **2009**, 664.
- (10) Jiang, Z.; Pan, Y.; Zhao, Y.; Ma, T.; Lee, R.; Yang, Y.; Huang, K.-W.; Wong, M. W.; Tan, C.-H. *Angew. Chem. Int. Ed.* **2009**, 48, 3627.
- (11) Sutherland, A.; Willis, C. L. *Nat. Prod. Rep.* **2000**, 17, 621.
- (12) For selected reviews, see: (a) Ting, A.; Schaus, S. E. *Eur. J. Org. Chem.* **2007**, 5797; (b) Verkade, J. M. M.; Hermert, L. J. C. v.; P. Quaedflieg, J. L. M.; Rutjes, F. P. J. T. *Chem. Soc. Rev.* **2008**, 37, 29; (c) Palomo, C.; Oiarbide, M.; López, R. *Chem. Soc. Rev.* **2008**, 38, 632.
- (13) Rosa, M. D.; Palombi, L.; Acocella, M. R.; Fruilo, M.; Vallano, R.; Soriente, A.; Scettri, A. *Chirality* **2003**, 15, 579.
- (14) (a) Marchi, C.; Trepát, E.; M-M, M.; Vallribera, A.; Molins, E. *Tetrahedron*, **2002**, 58, 5699; (b) Åberg, V.; Norman, F.; Chorell, E.; Westmark, A.; Olofsson, A.; S.-E., A. E.; Almqvist, F. *Org. Biomol. Chem.*, **2005**, 3, 2817.
- (15) Wenzel, A. G.; Jacobsen, E. N. *J. Am. Chem. Soc.* **2002**, 124, 12964–12965.
- (16) Gupta, S. K. *J. Org. Chem.* **1973**, 38, 4081.
- (17) Kawata, A.; Takata, K.; Kuninobu, Y.; Takai, K. *Angew. Chem. Int. Ed.* **2007**, 46, 7793.
- (18) Burnner, H.; Baur, M. A. *Eur. J. Org. Chem.* **2003**, 2854.

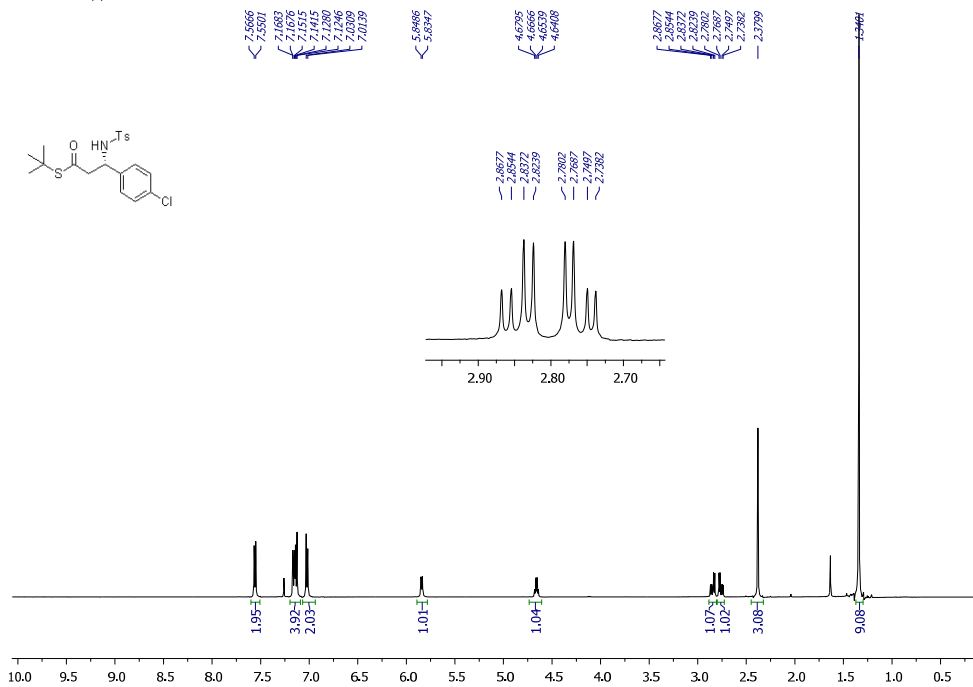
(19) Andrews, P. C.; Bhaskar, V.; Bromfield, K. M.; Dodd, A. M.; Duggan, P. J.;

Duggan, S. A. M.; McCarthy, T. M. *Synlett* **2004**, 791.

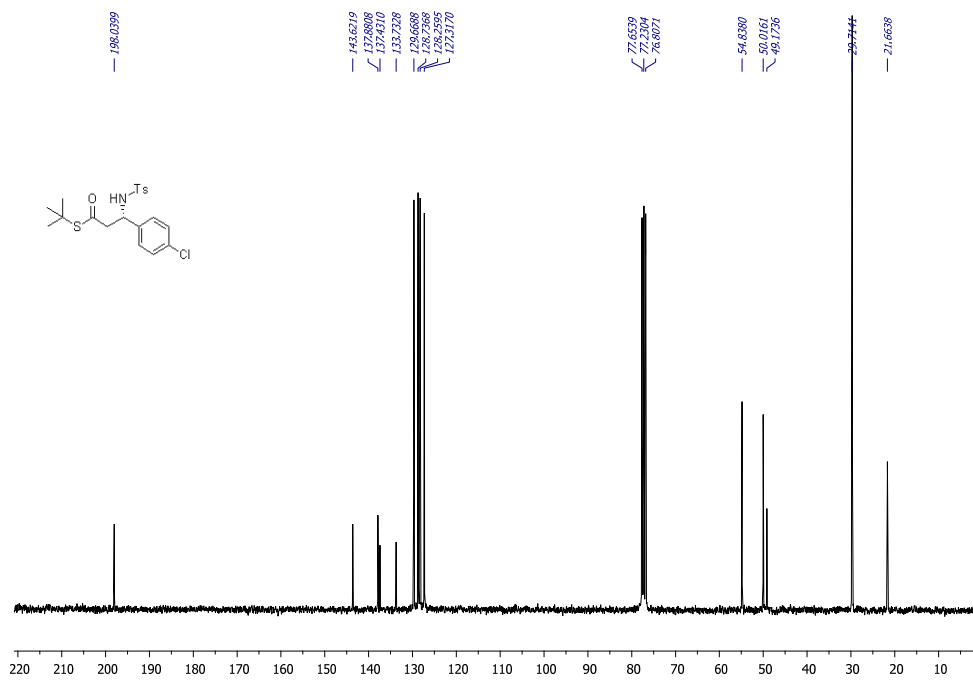
# Appendix

## Copies of NMR Spectra

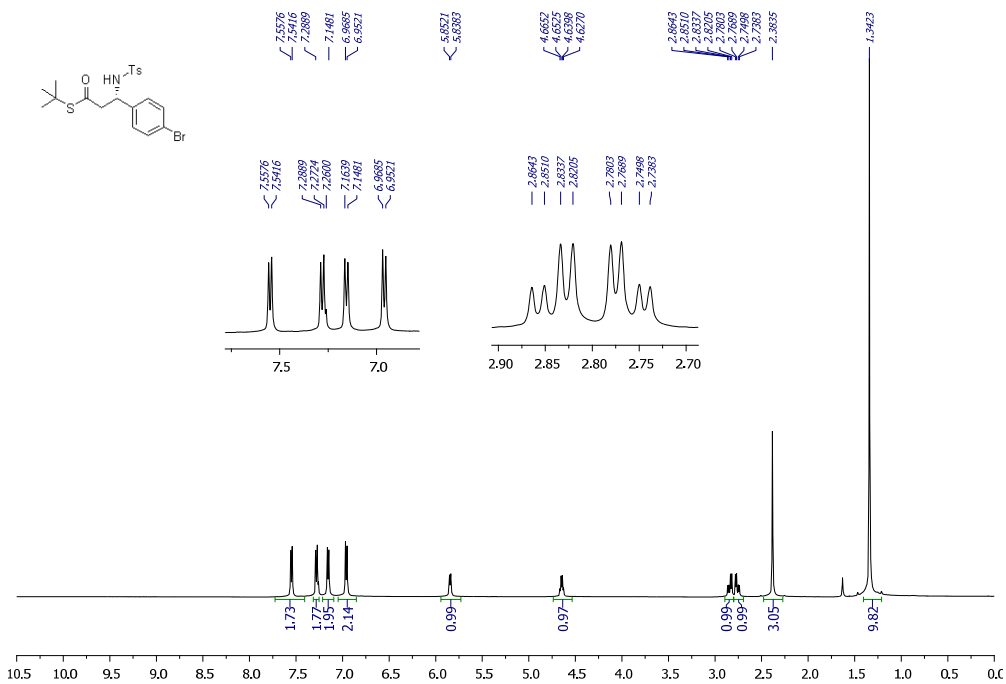
DRX500 1H pyh0513 1.1 WL1001



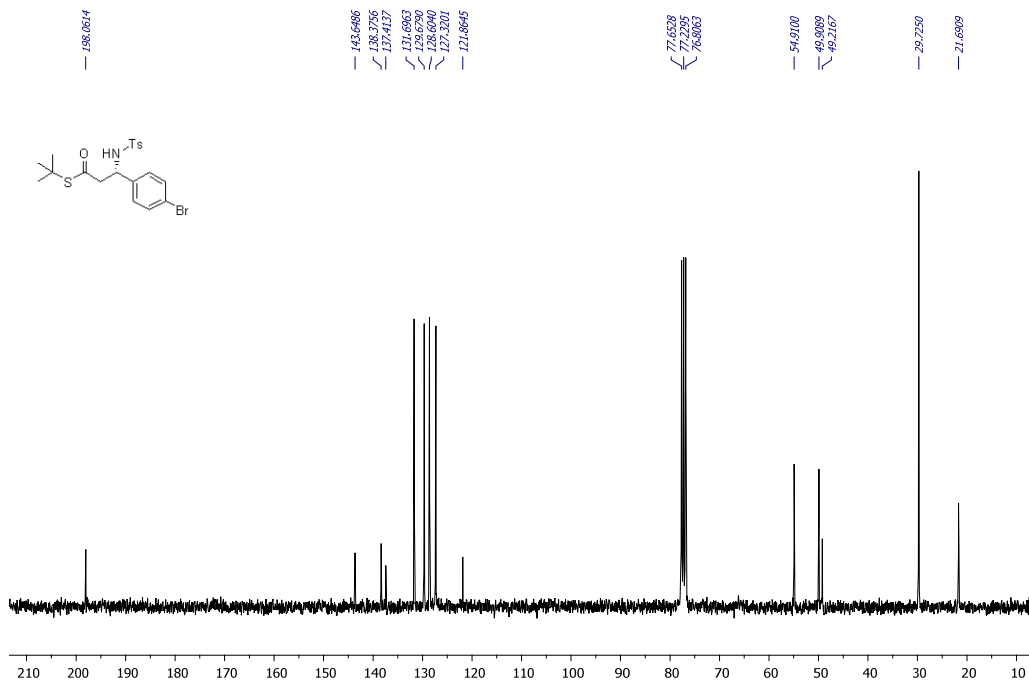
dpx300 13C my13pyh4.1 CWL1001



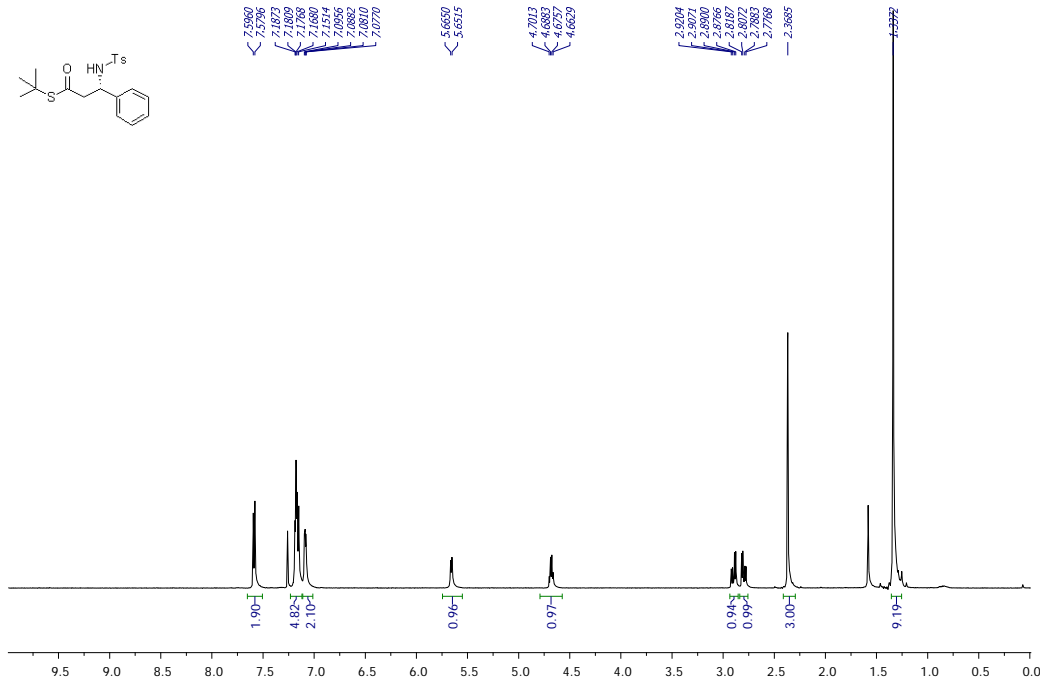
drx 500 1H pyh0601 1.1 pyh7025A 4-Br



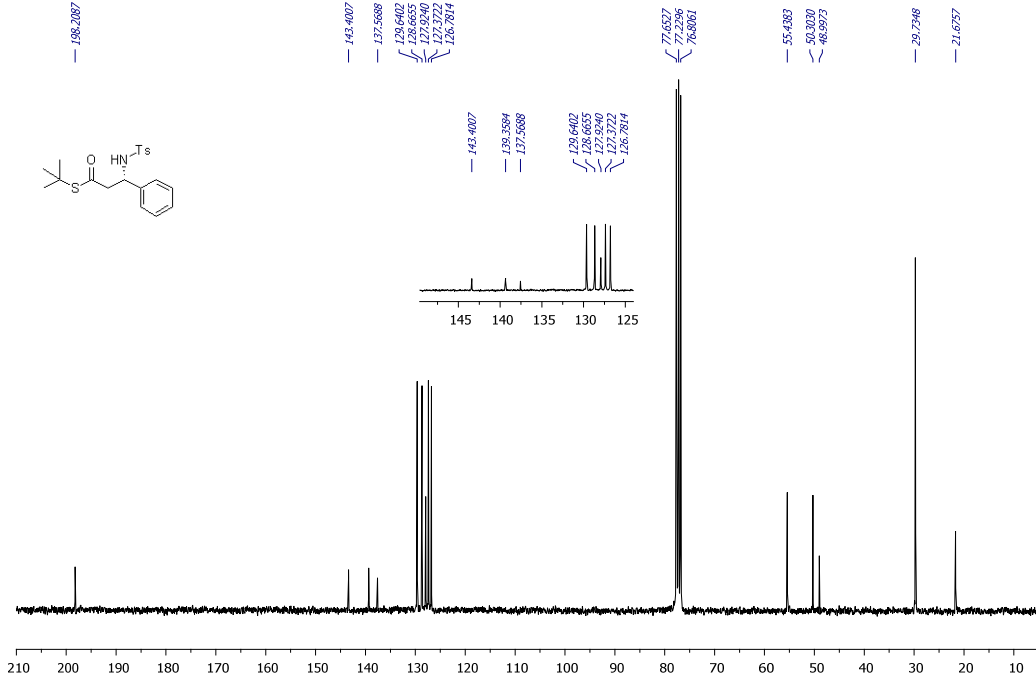
dpx300 13C my31pyh4.1 pyh7023C



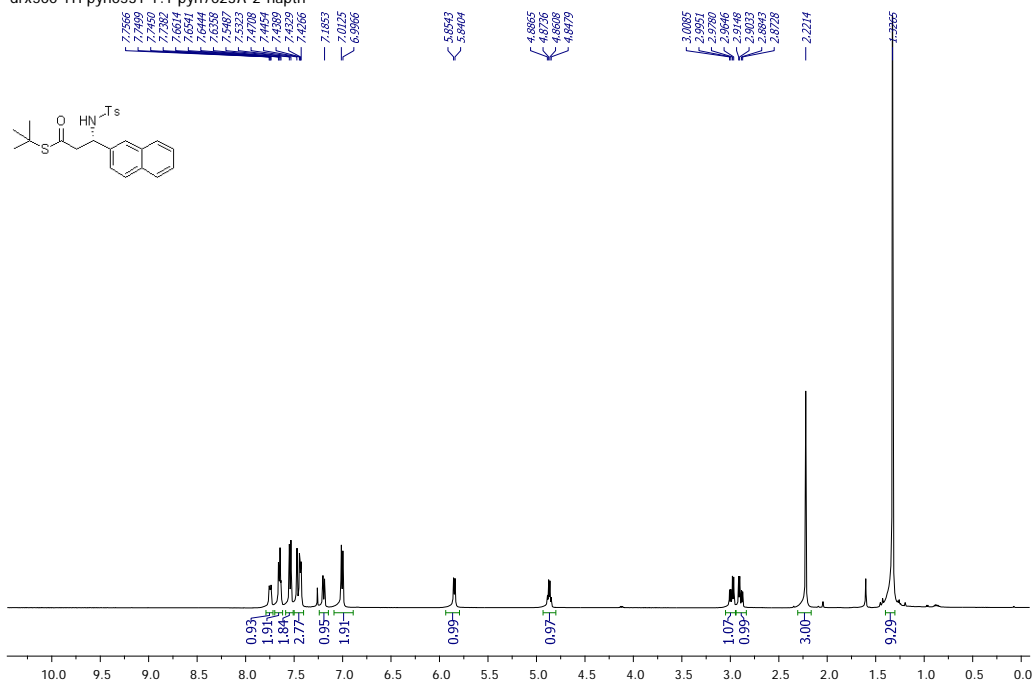
DRX500 1H pyh0514 1.1 PZW1002



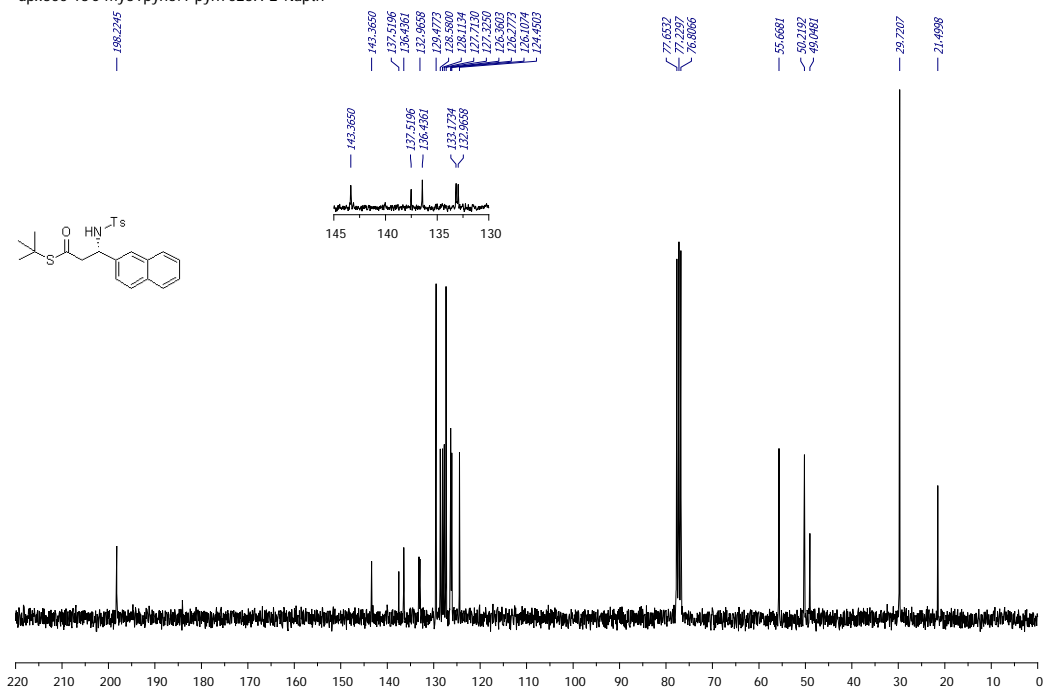
dpx300 13C my13pyh 5.1 PZW1002



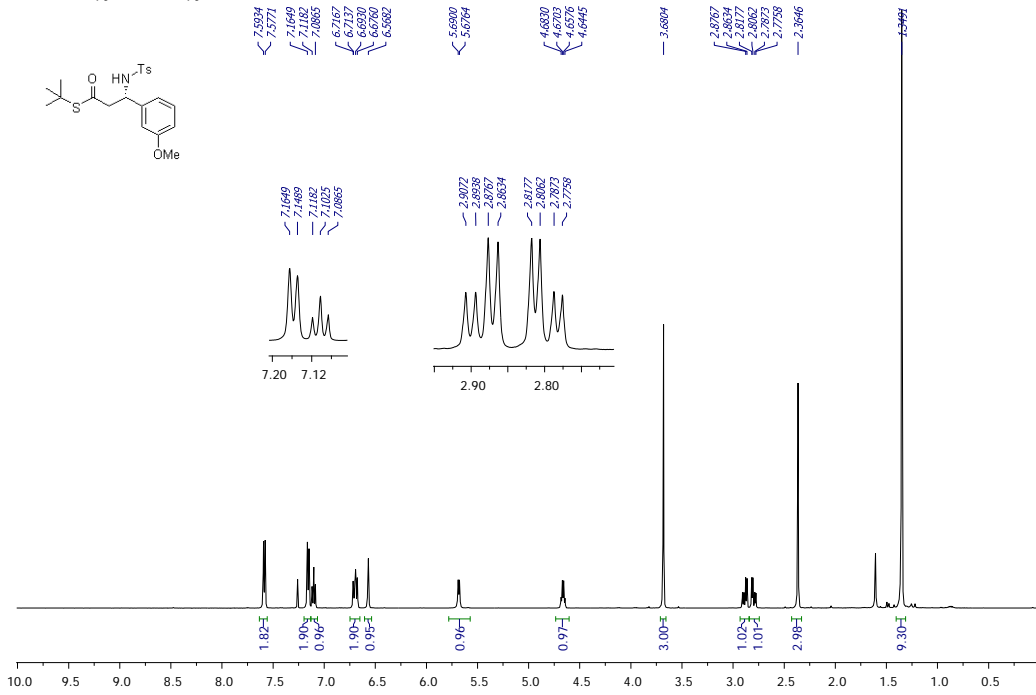
drx500 1H pyh0531 1.1 pyh7023A 2-naph



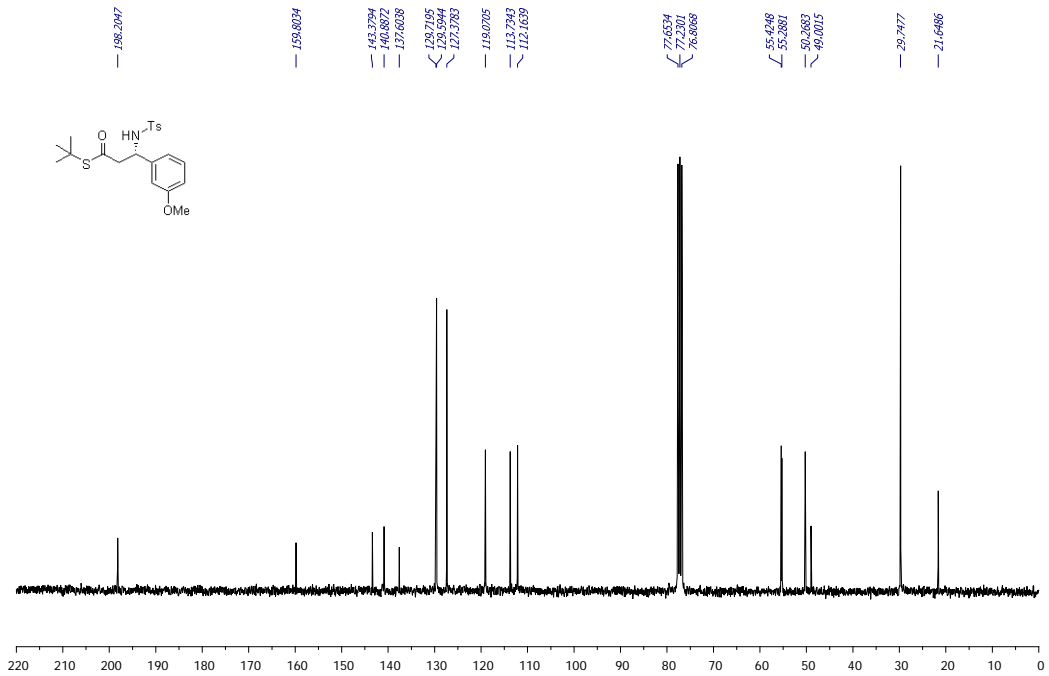
dpx300 13C my31pyh6.1 pyh7023A 2-Napth



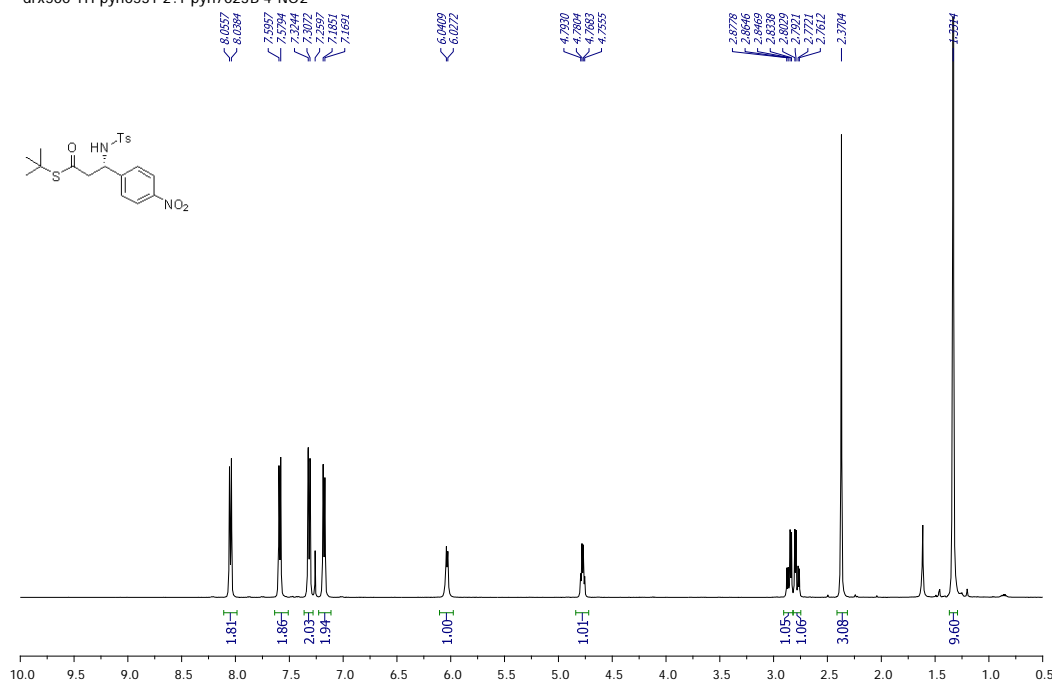
drx500 1H pyh0612 2.1 pyh7053A 3OMe,H



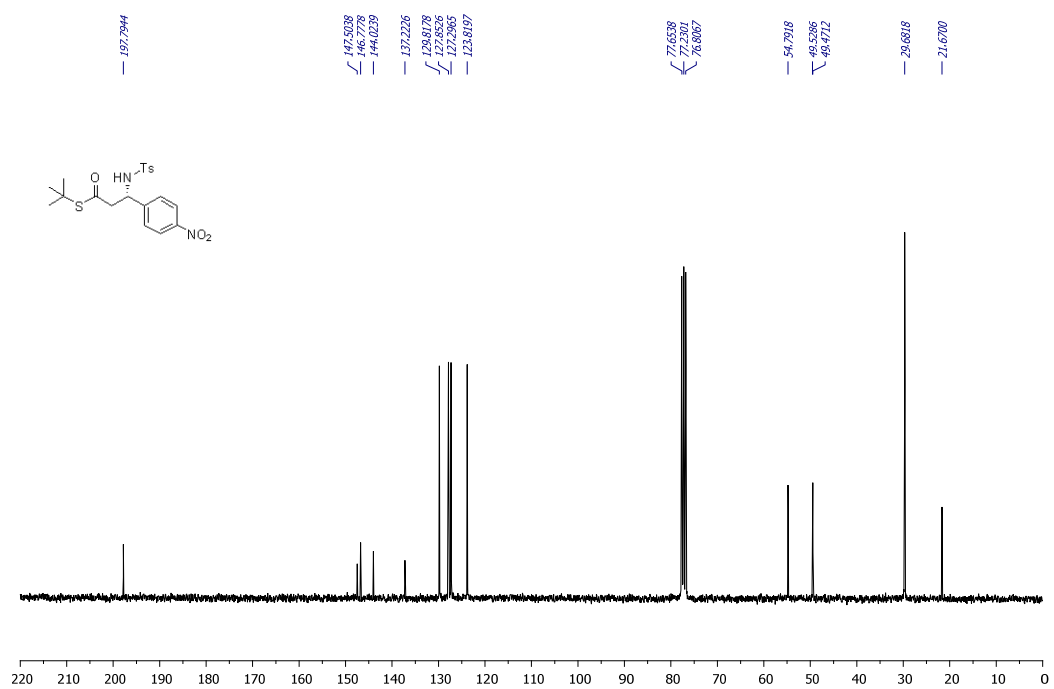
dpx300 13C ju12pyh2.1 pyh7053S 3MOe,H



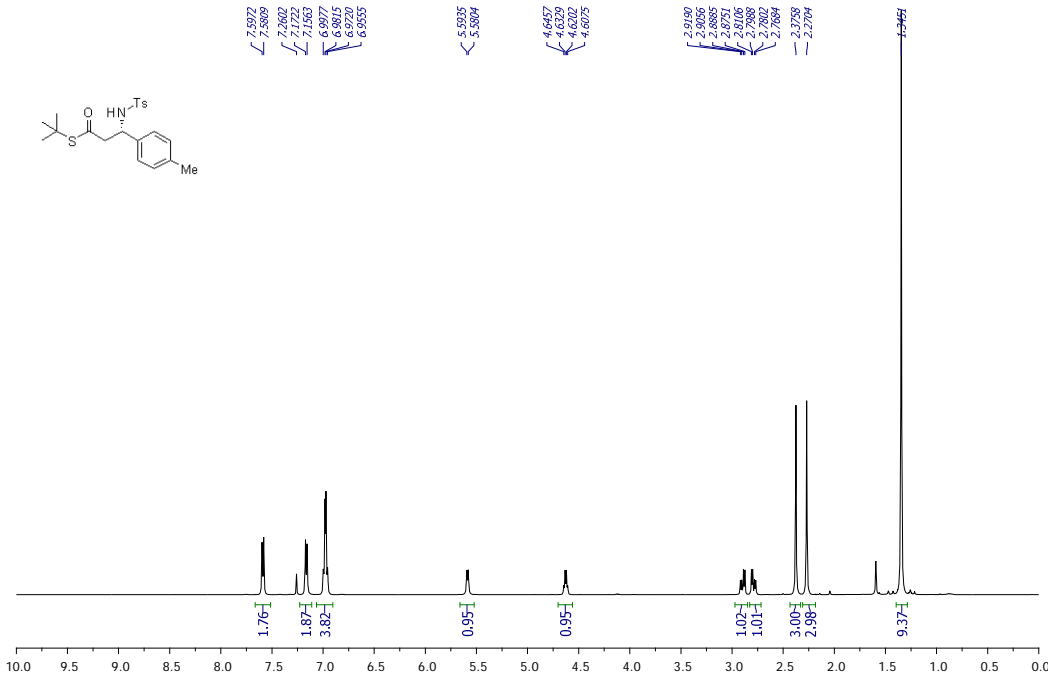
drx500 1H pyh0531 2.1 pyh7023B 4-NO2



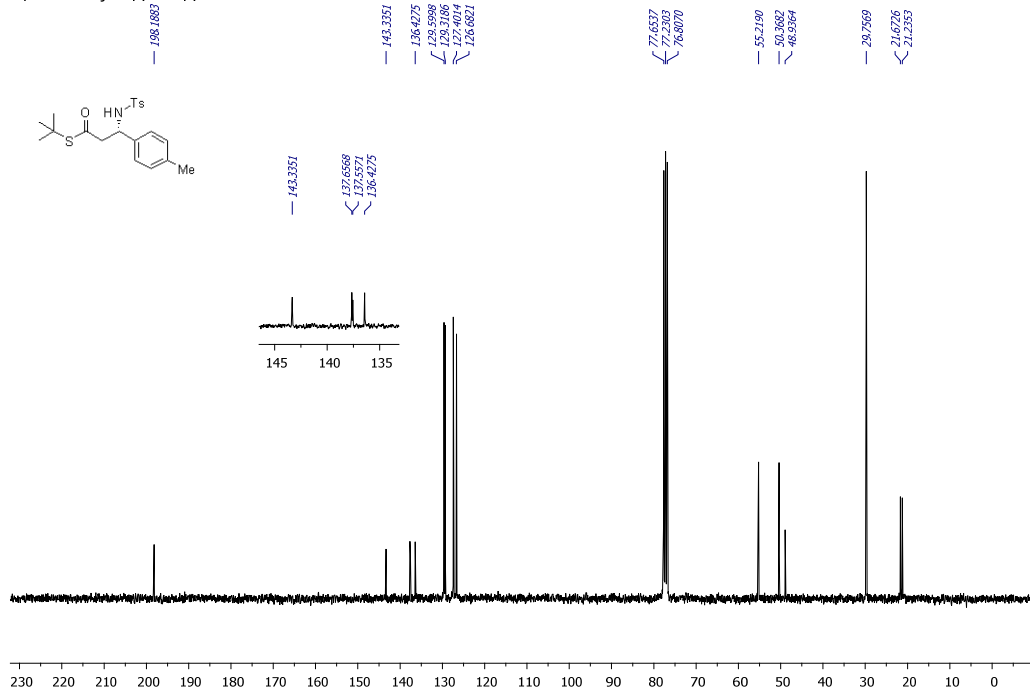
dpx300 13C ju02pyh 1.1 pyh7023B 4-NO2



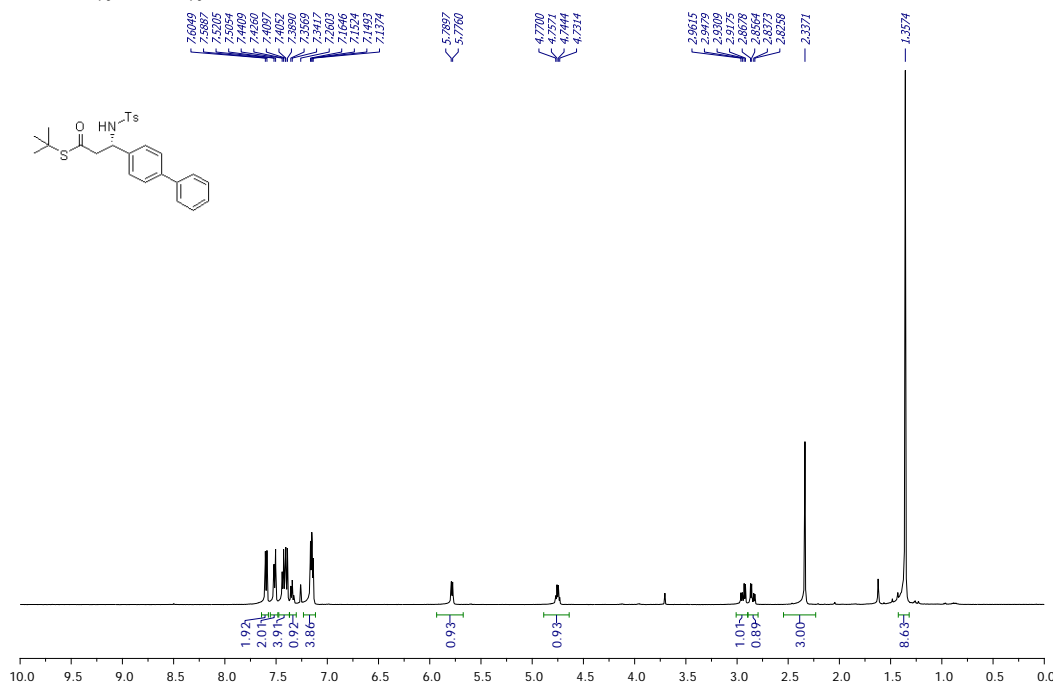
drx500 1H pyh0623 5.1 pyh7068A



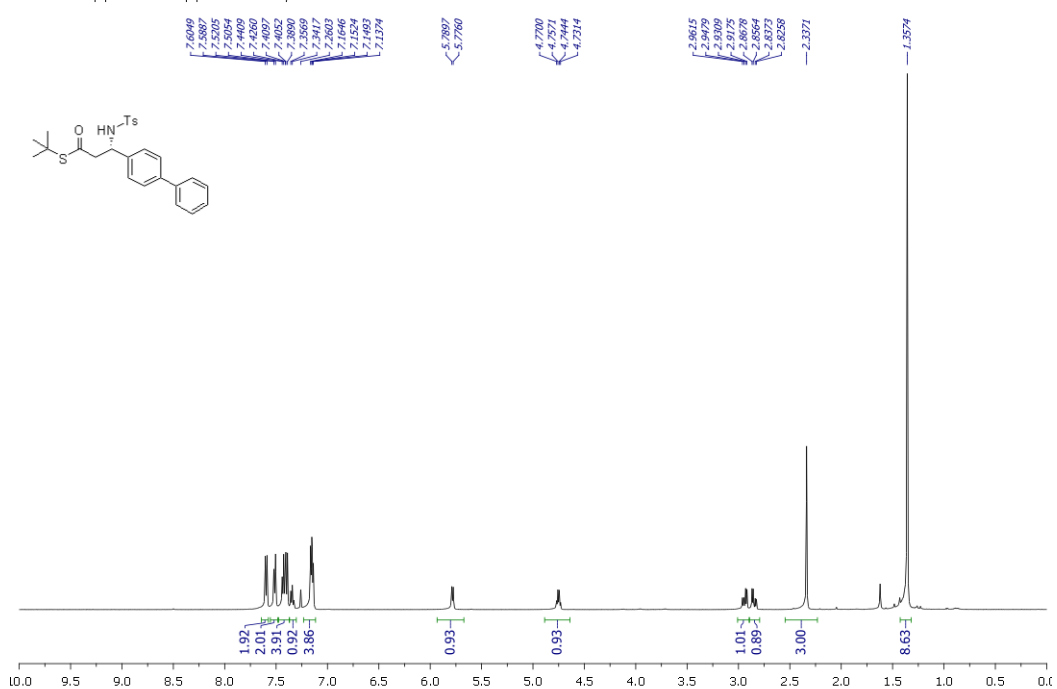
dpx300 13C ju22pyh4.1 pyh7068A



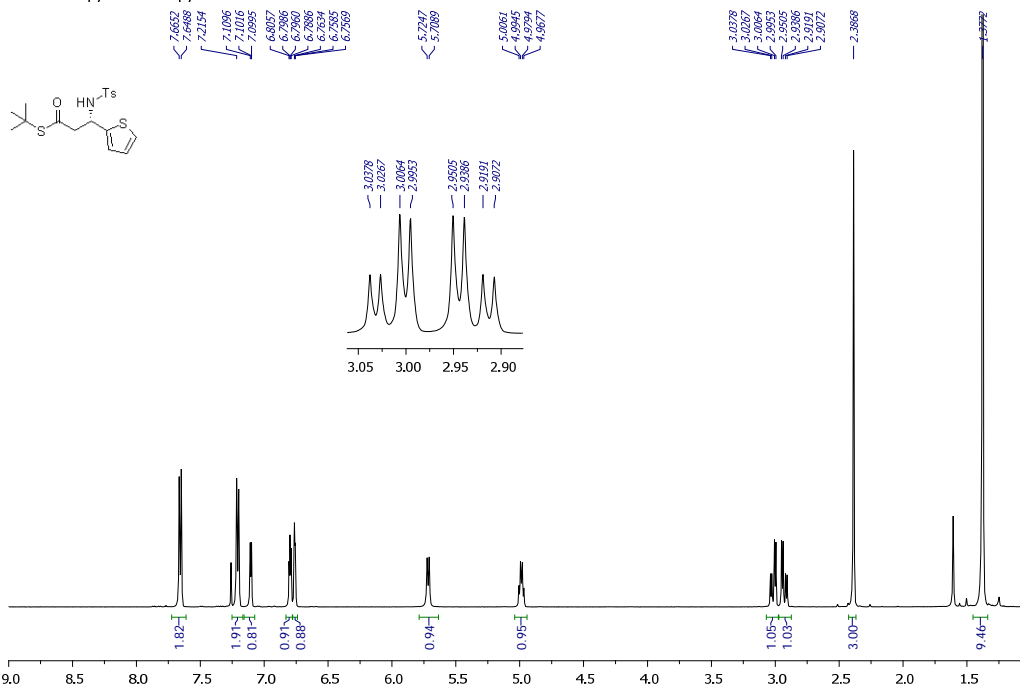
drx500 1H pyh0618 1.1 pyh7068B 4Ph, H



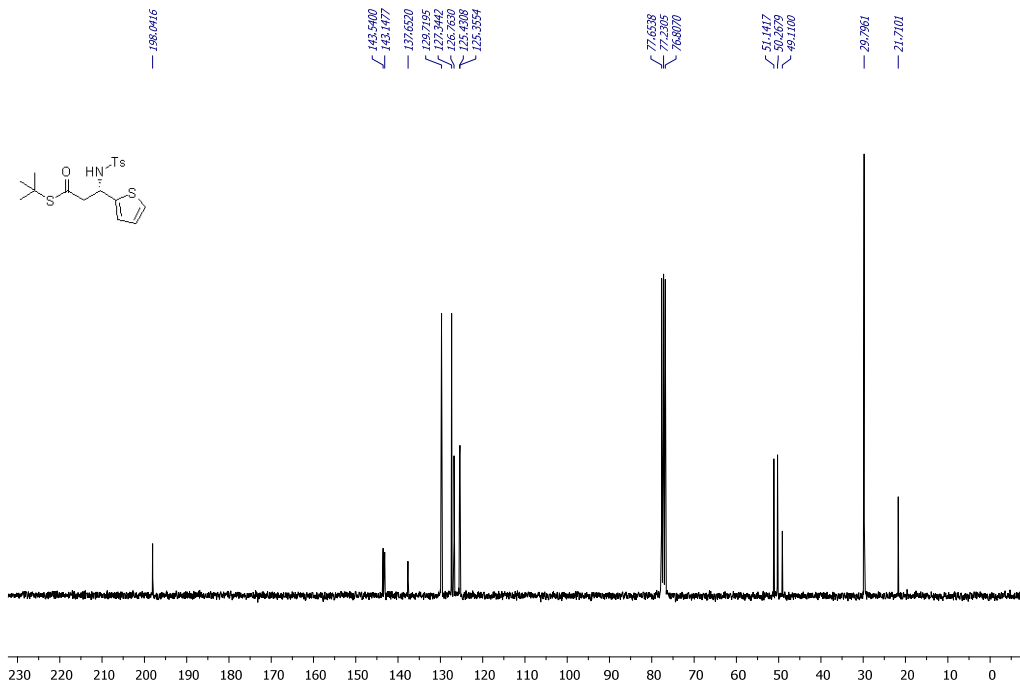
drx500 1H pyh0618 1.1 pyh7068B 4Ph, H



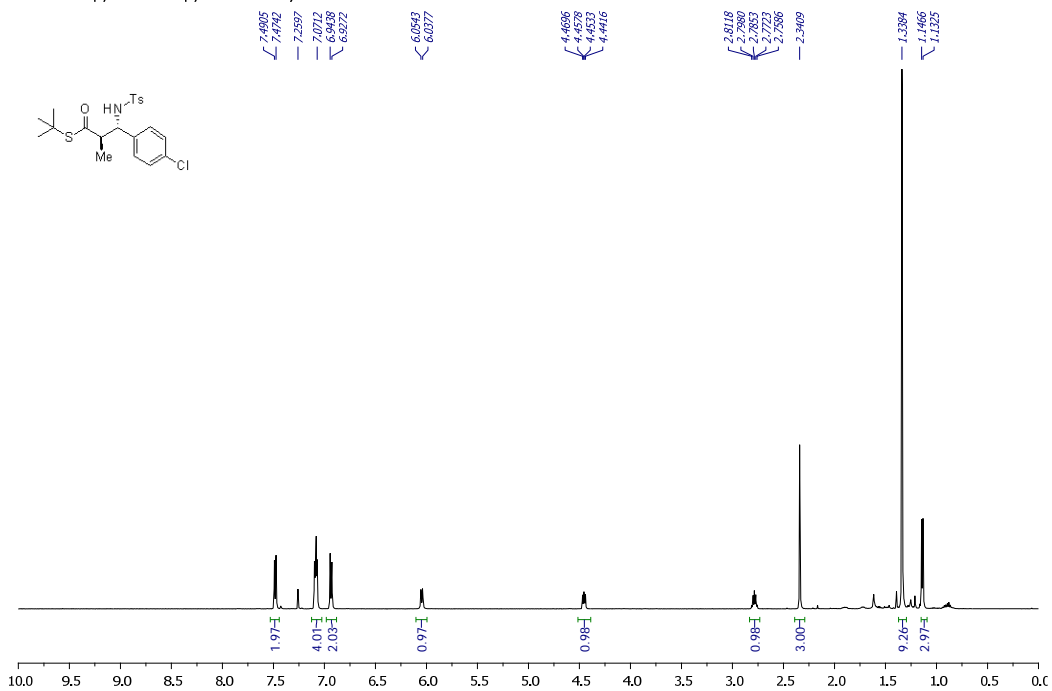
drx500 1H pyh0612 3.1 pyh7053B



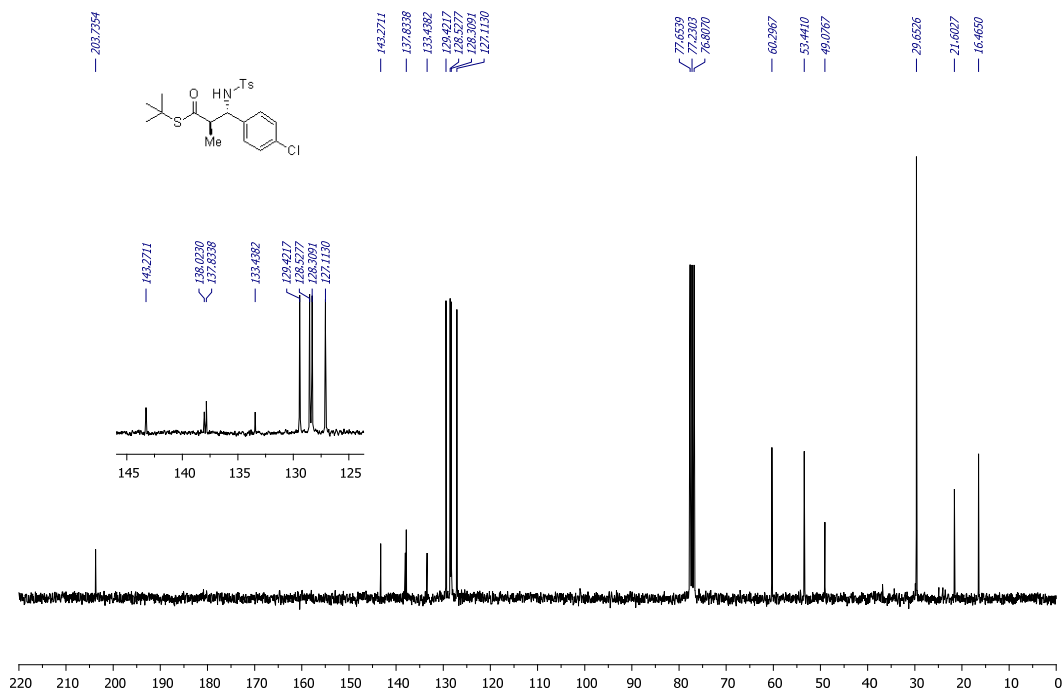
dpx300 13CH ju14pyh3.1 pyh7053B



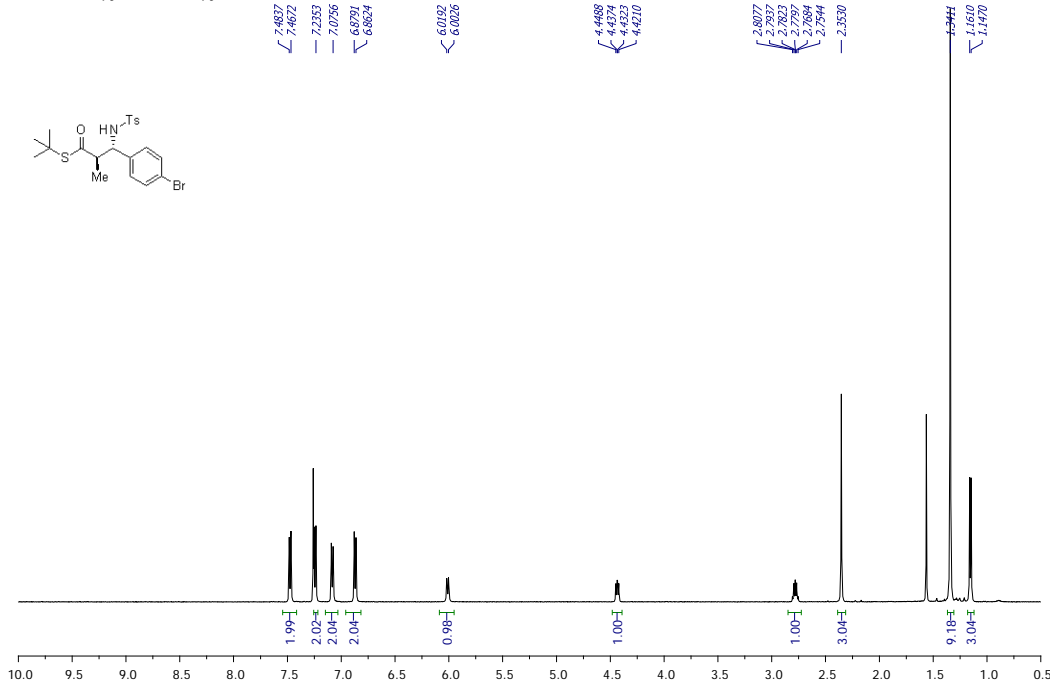
drx500 1H pyh0617 1.1 pyh7070-1 4-Cl<sub>1</sub>Me



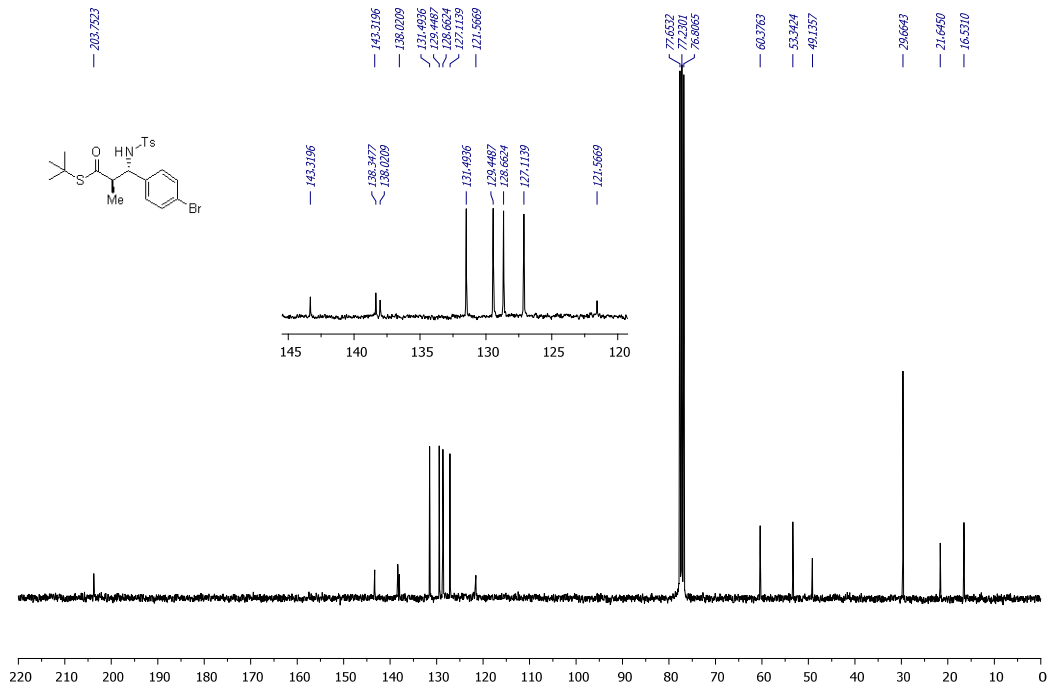
dpx300 13C ju18pyh1.1 pyh7070-1 4Cl<sub>1</sub>Me



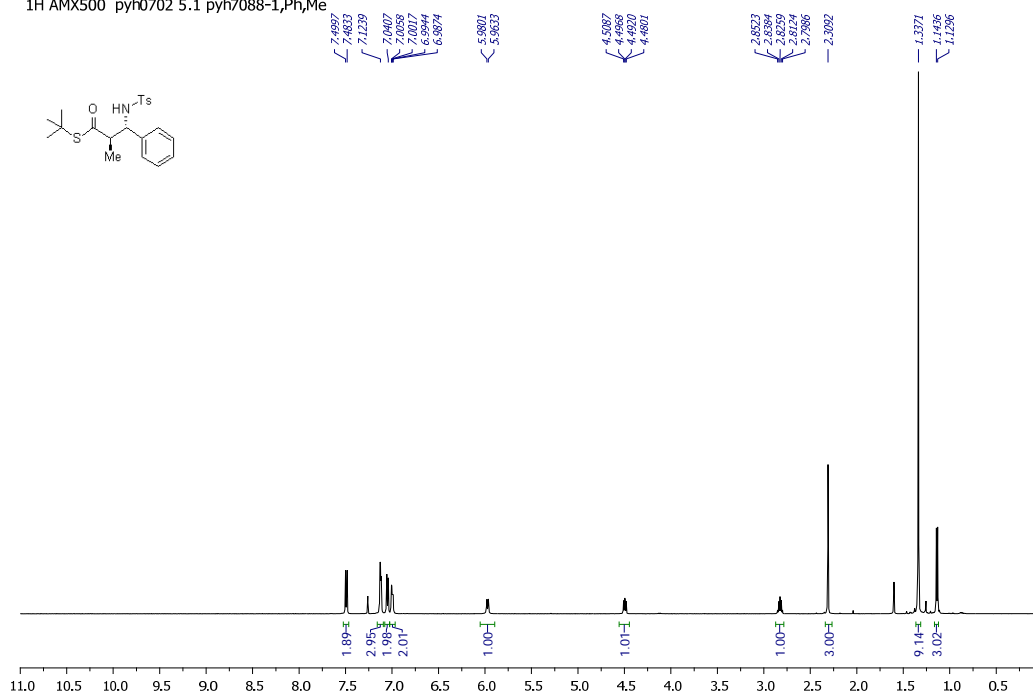
drx500 1H pyh06261 1.1 pyh7075A1 4Br,Me



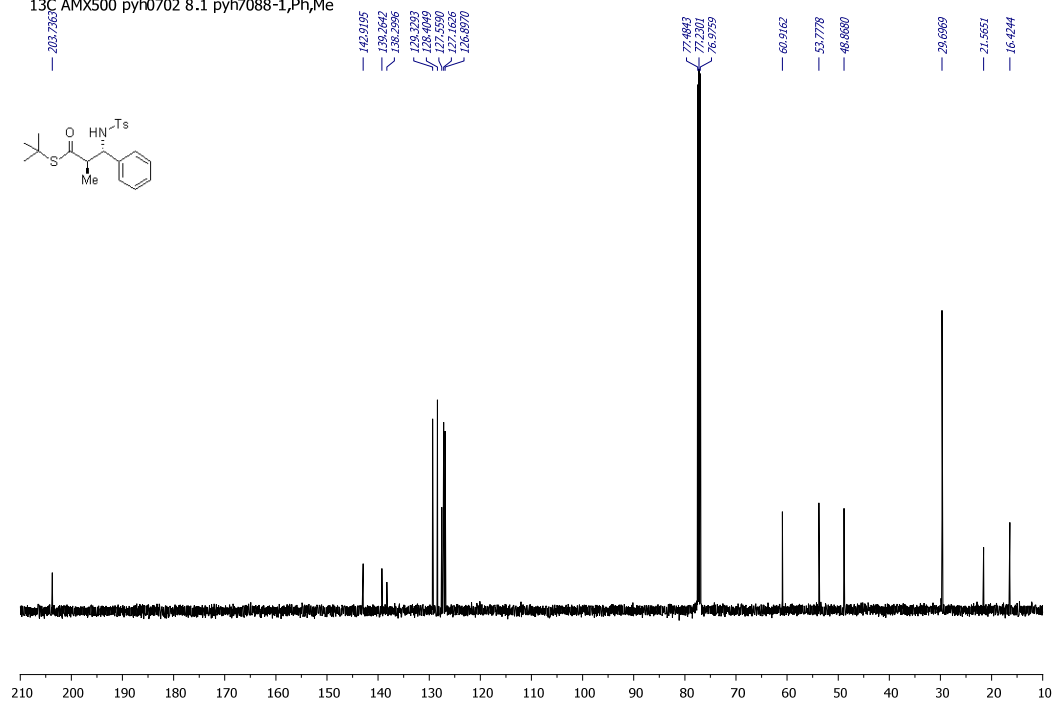
dpx300 13C ju28pyh1.1 pyh7075A1,4Br, Me



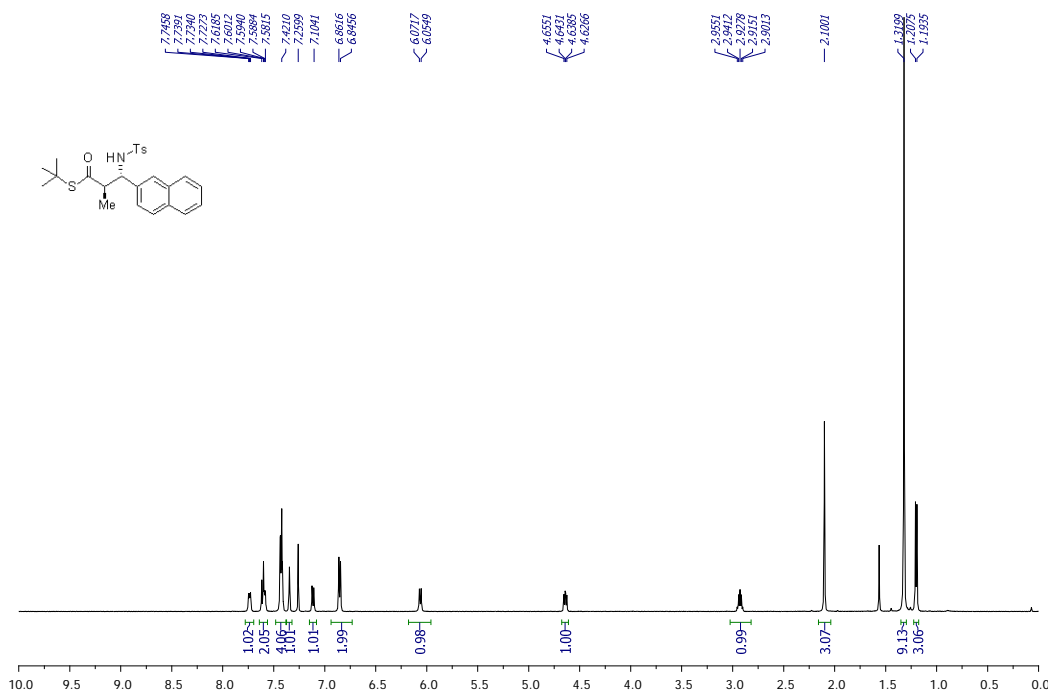
1H AMX500 pyh0702 5.1 pyh7088-1,Ph,Me



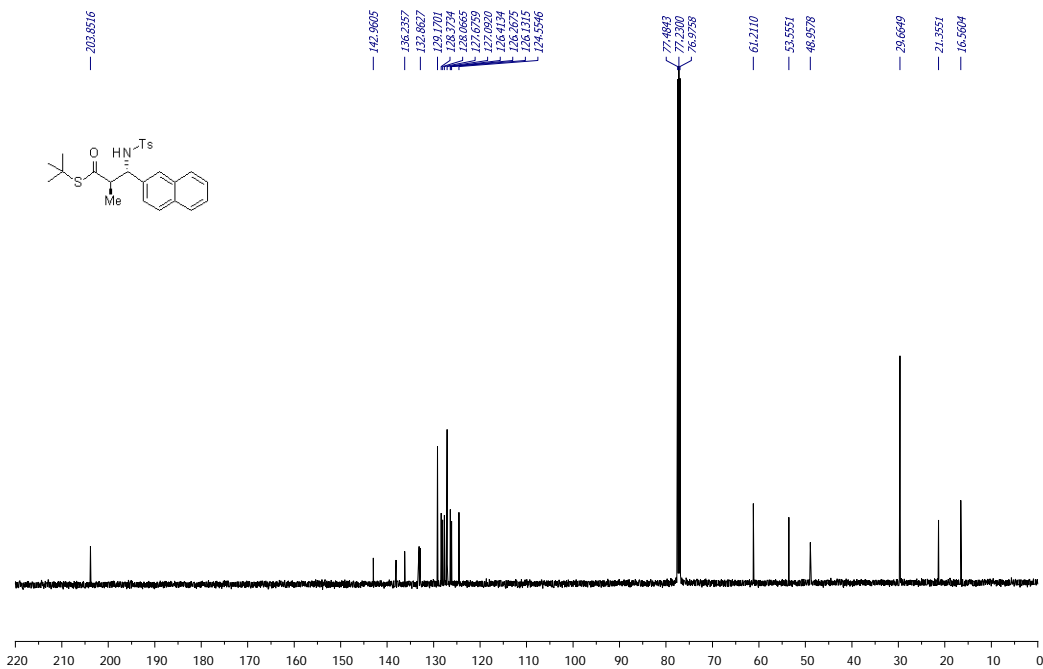
13C AMX500 pyh0702 8.1 pyh7088-1,Ph,Me



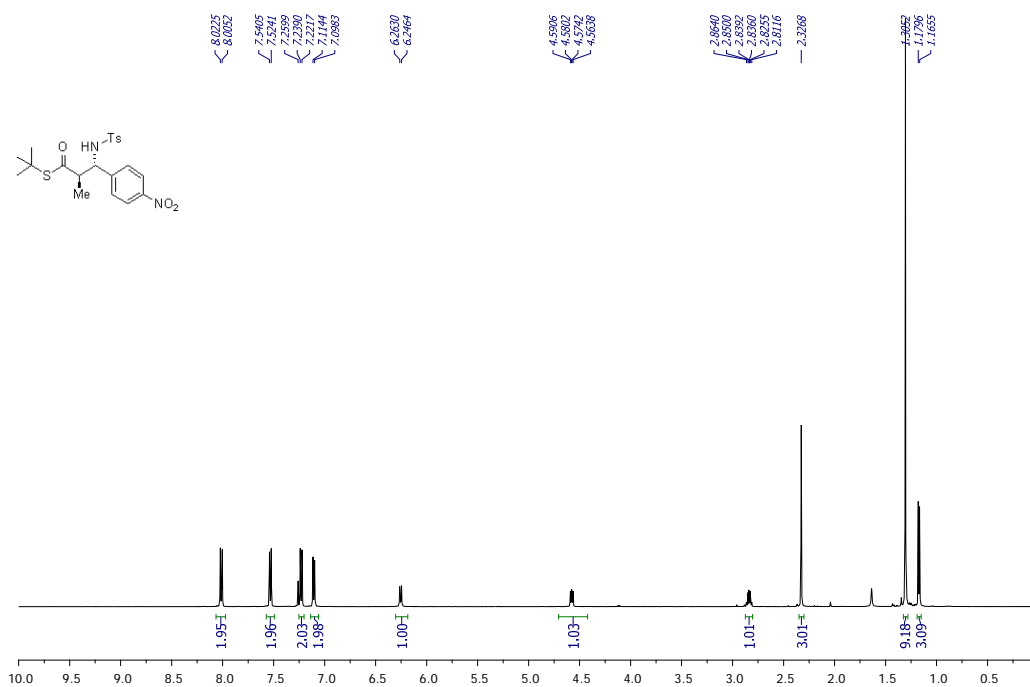
drx500 1H pyh0628 2.1 pyh7075B1 2Naph,Me



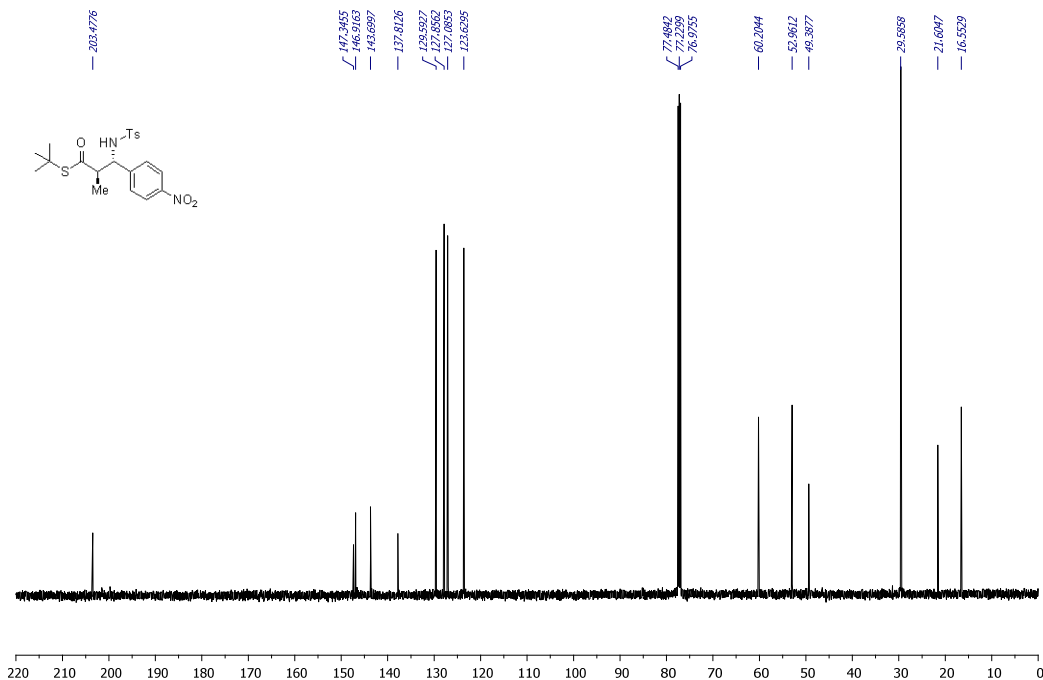
13C AMX500 pyh0630 7.1 pyh7075B1, 2Naph, Me



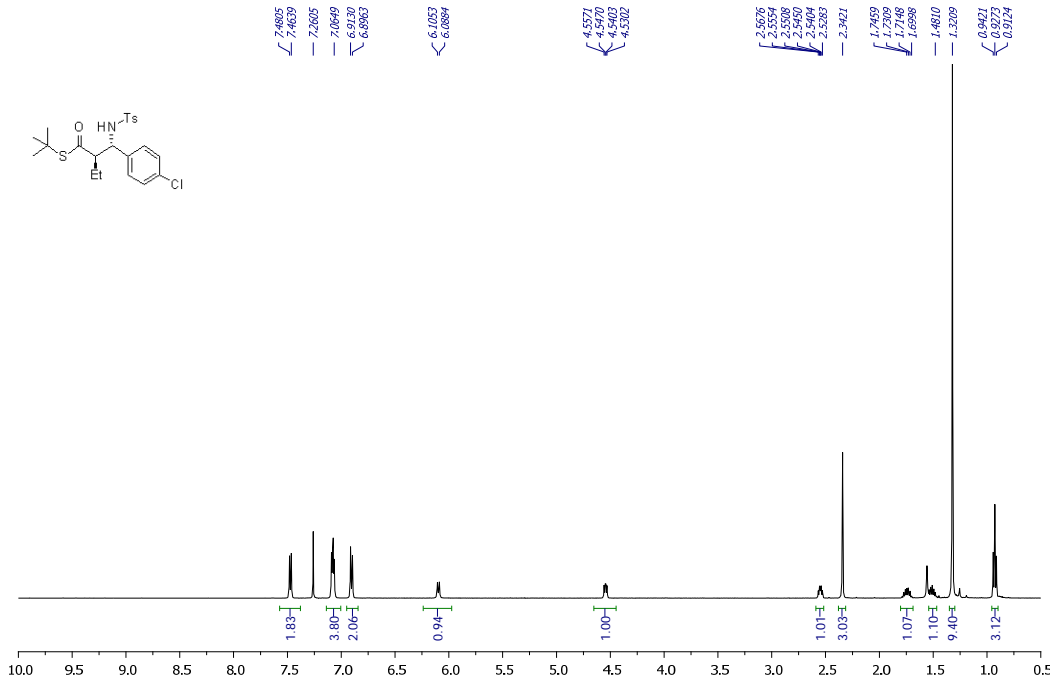
1H AMX500 pyh0706 1.1 pyh7090A1 4NO2,Me



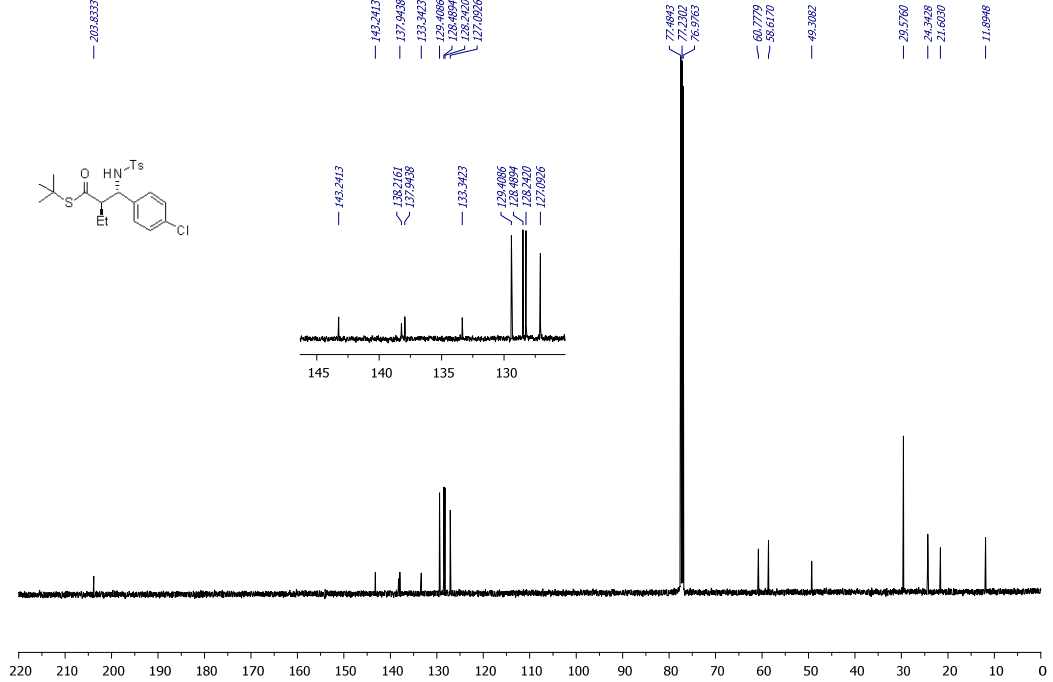
13C AMX500 pyh0706 2.1 pyh7090A1 4NO2,Me



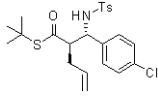
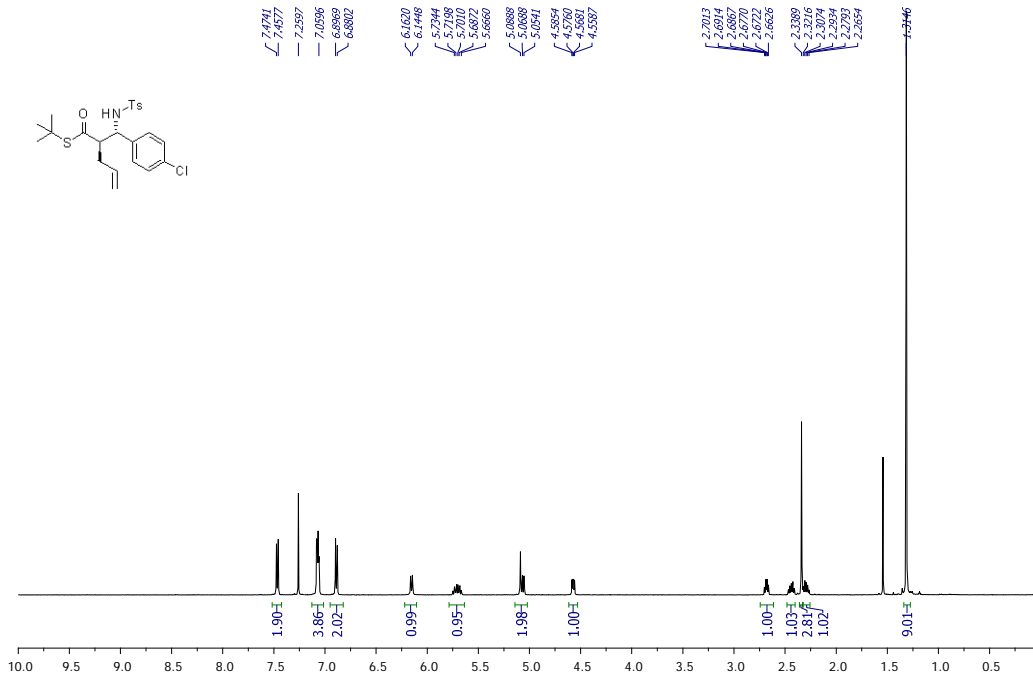
drx500 1H pyh0629 3.1 pyh7083A1 4Cl,Et



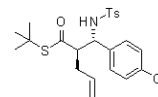
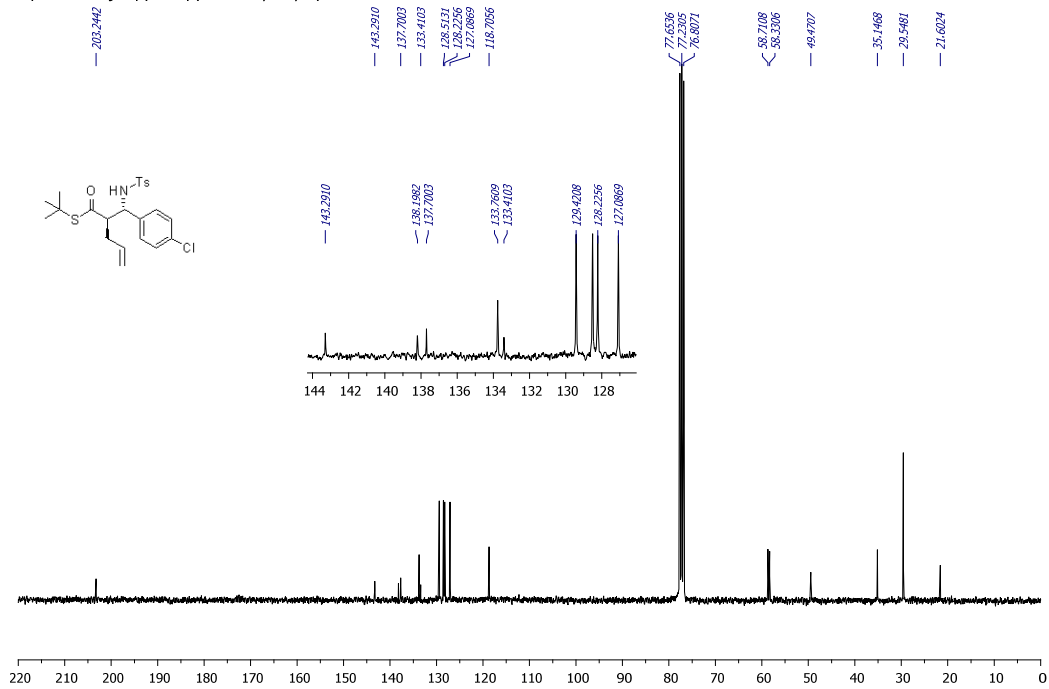
13C AMX500 pyh0630 9.1 pyh7083A1,4Cl, Et



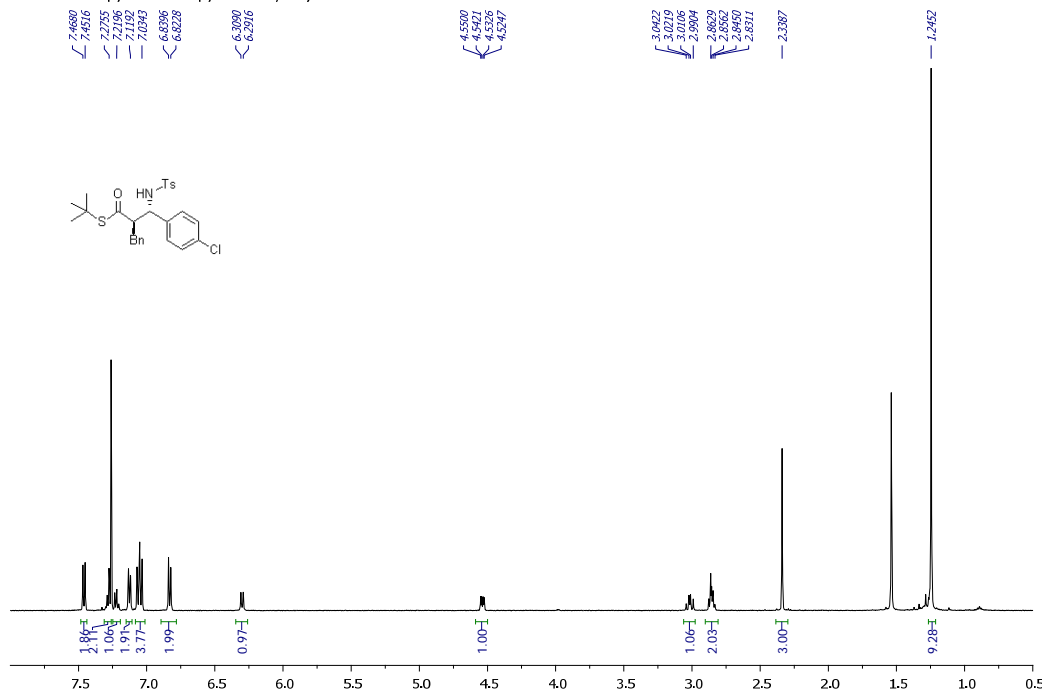
1H AMX500 pyh0702 1.1 pyh7083B1, 4Cl, ally



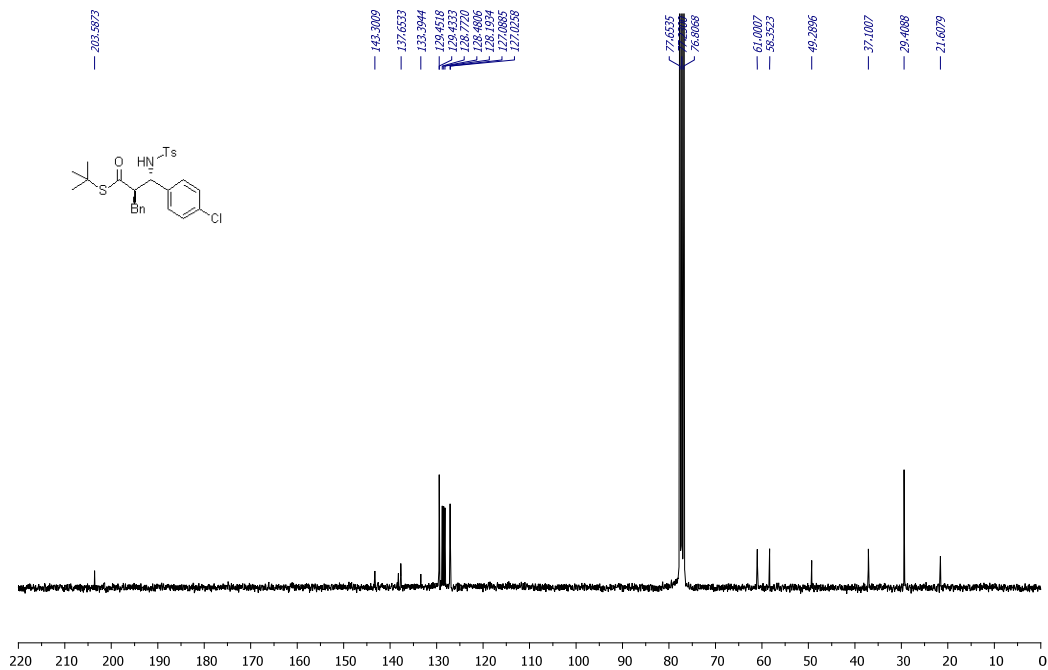
dpx300 13C j102pyh1.1 pyh7083B1, 4Cl, ally



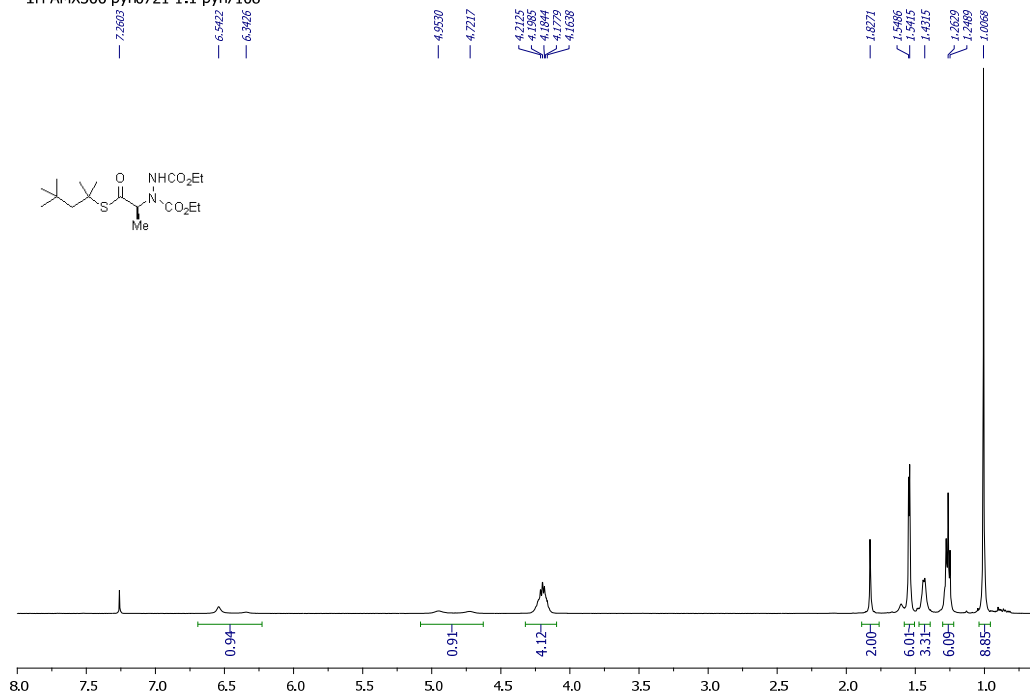
1H AMX500 pyh0702 3.1 pyh7083C1, 4Cl, Bn



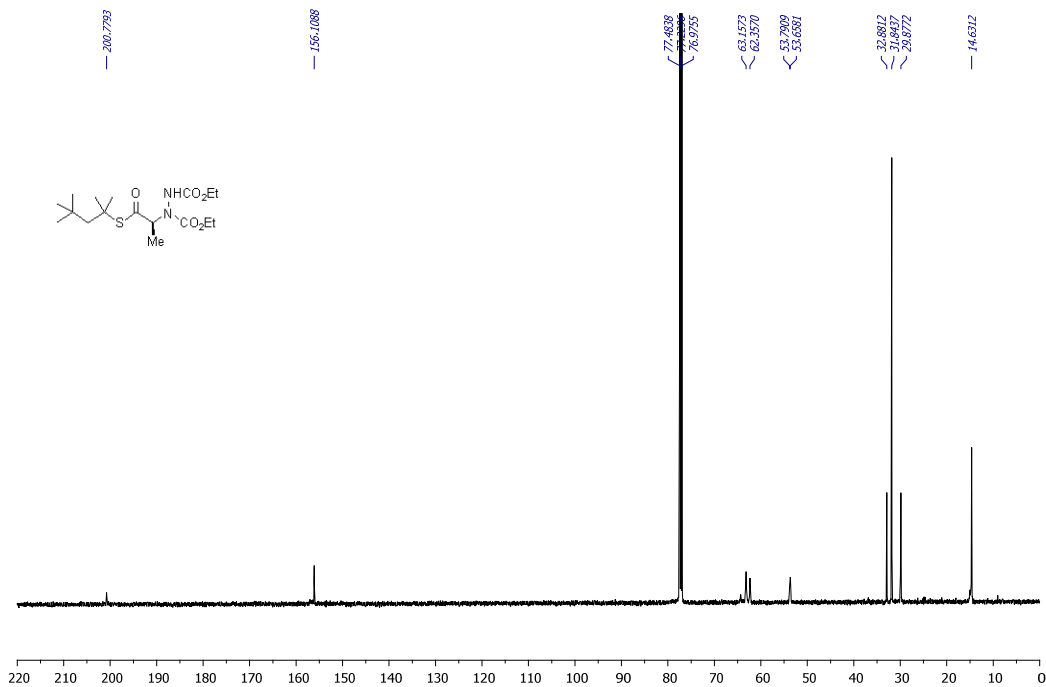
dpx300 13C j102pyh3.1 pyh7083C1 4Cl,Bn



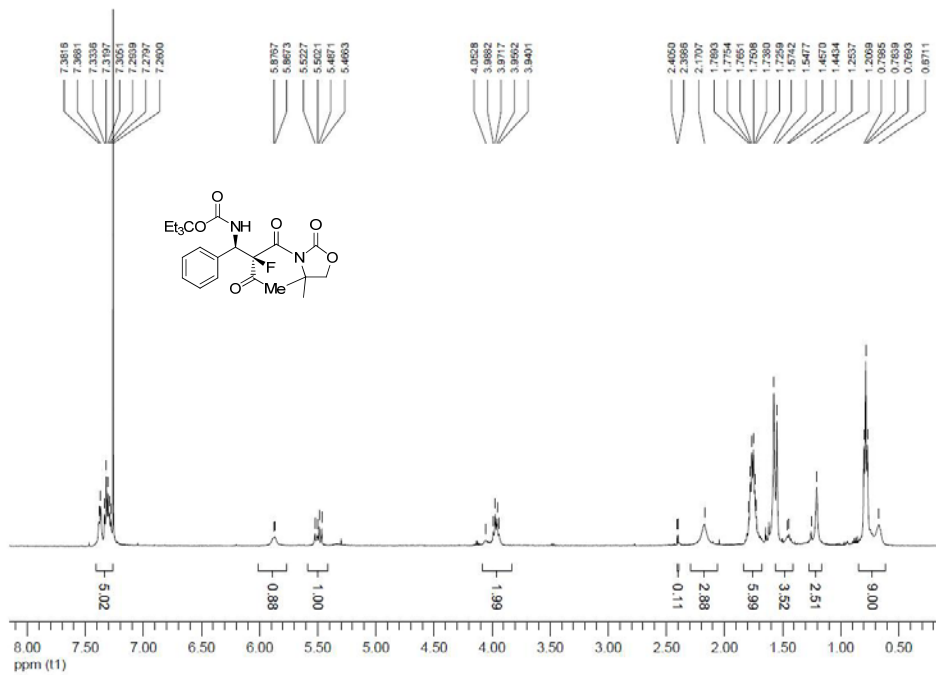
1H AMX500 pyh0721 1.1 pyh7108



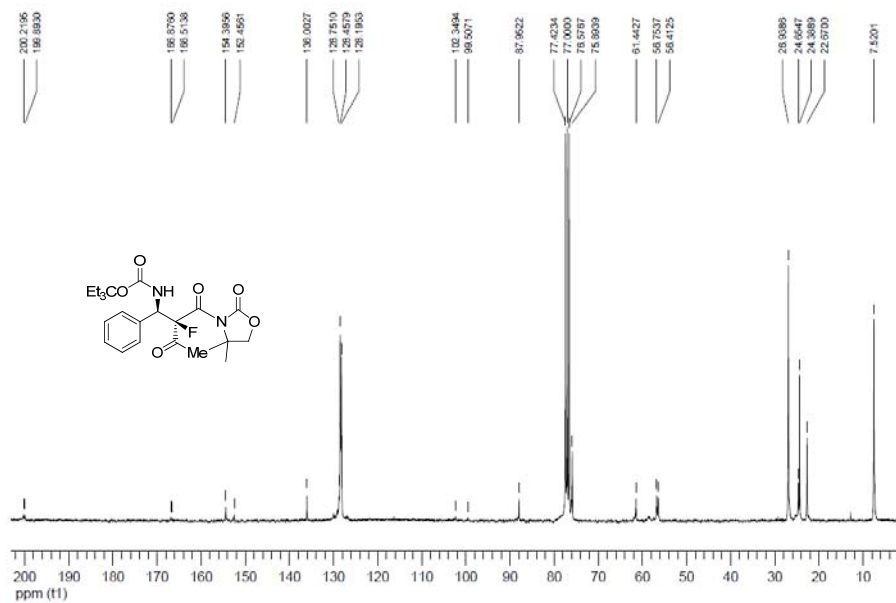
13C AMX500 pyh0720 3.1 pyh7108



1H AMX500 pyh250409 1.1 pyh4163A Ph

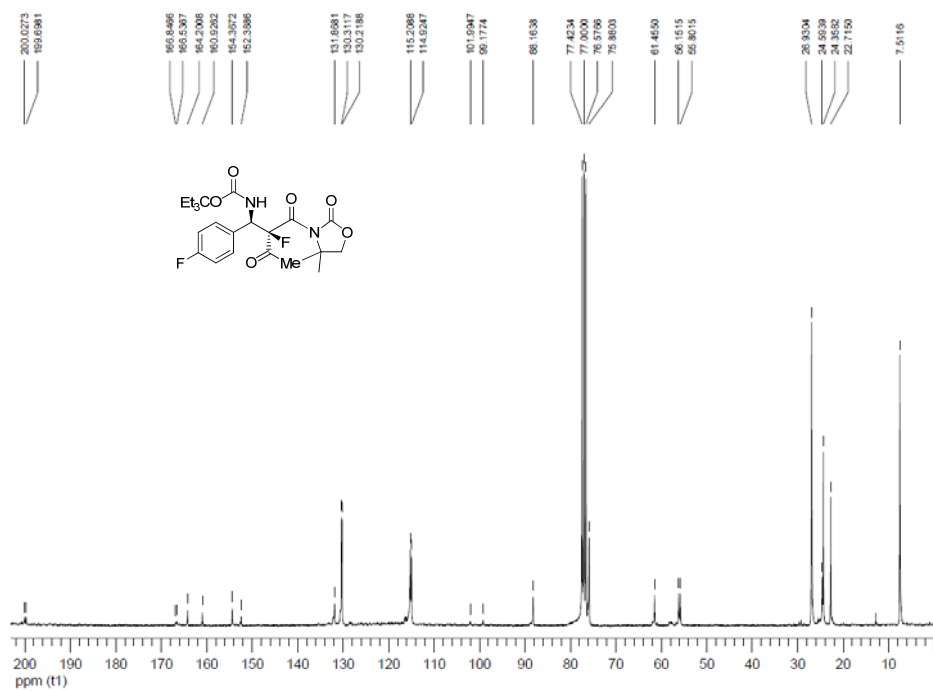


dpx300 pyh0410 2.1 pyh4163A Ph 13C

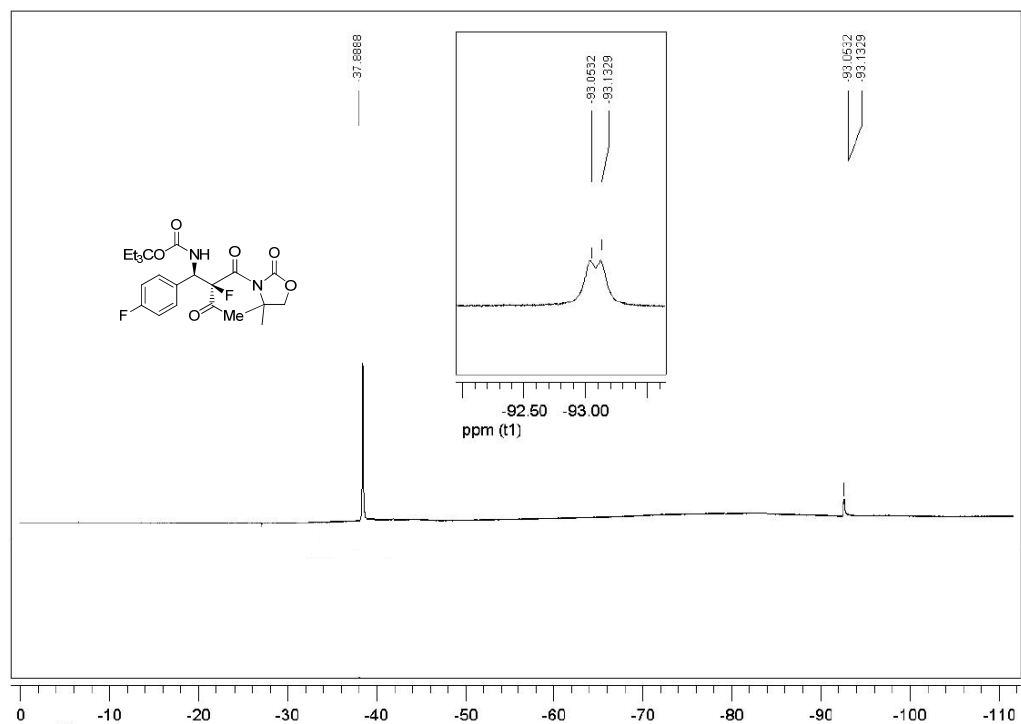




dpx300 ap11pyh4.1 pyh4163B 4F 13C



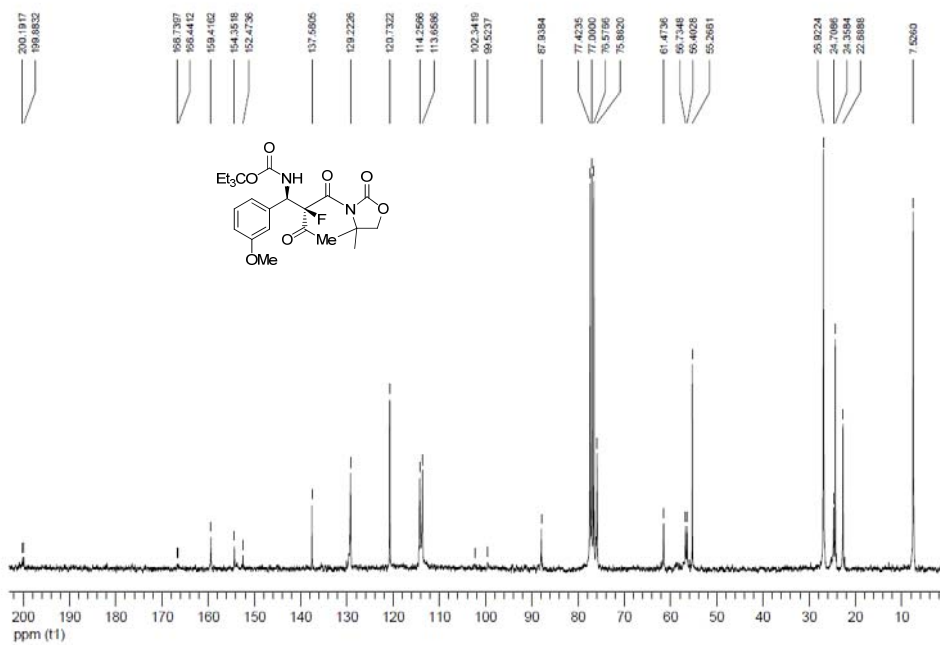
F19 ( no decoupled) jl24pyh8.1 4F



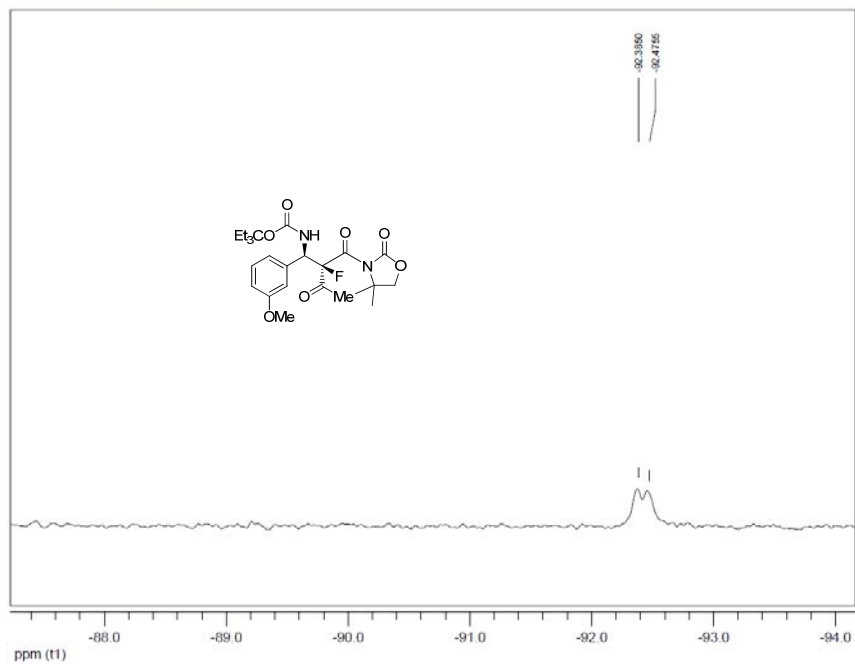




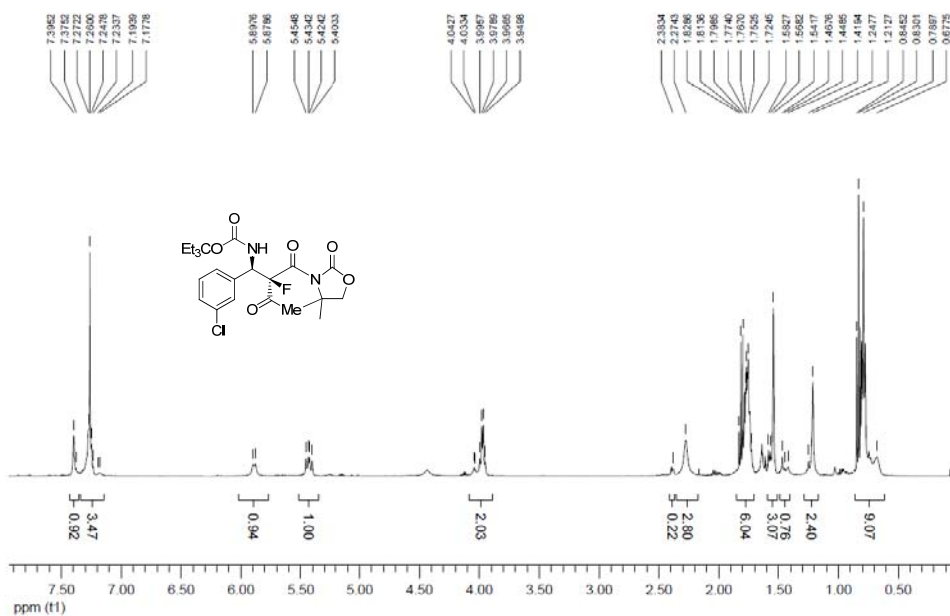
dpx300 ap25pyh1.1 pyh4184B 3OMe 13C



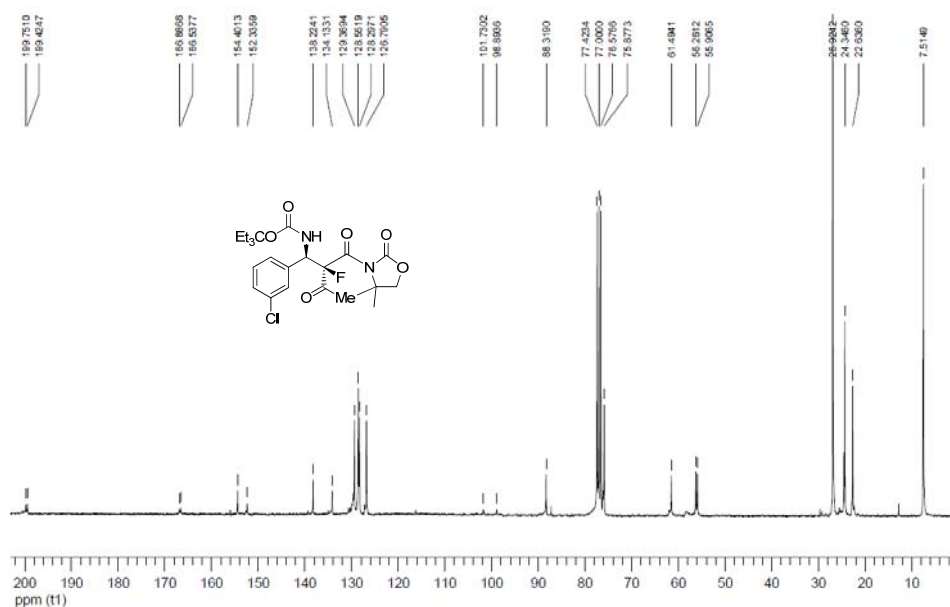
F19 (no decoupled) j124pyh3.1 3OMe



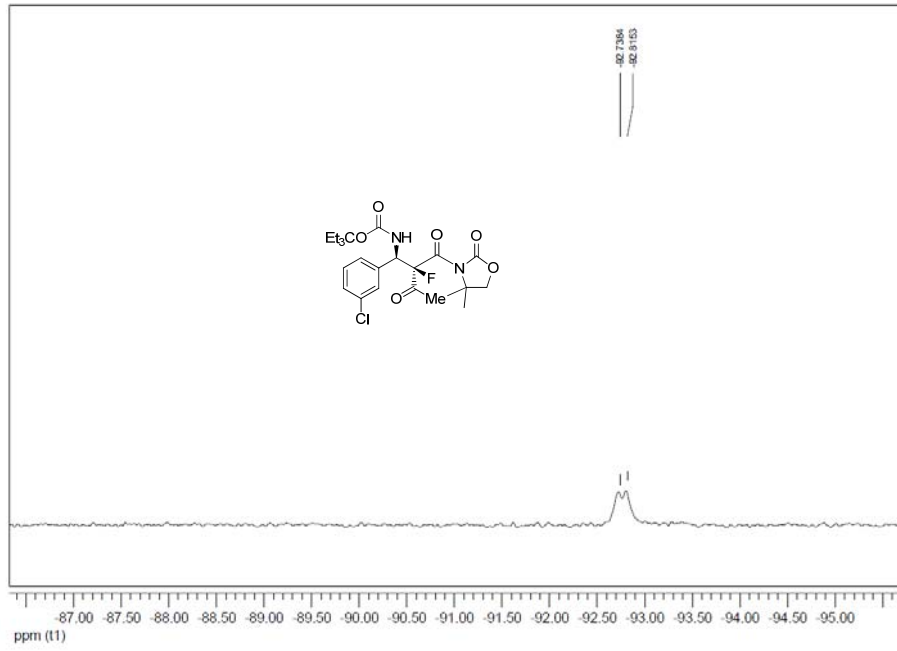
1H AMX500 pyh250409 3.1 pyh4186 3Cl



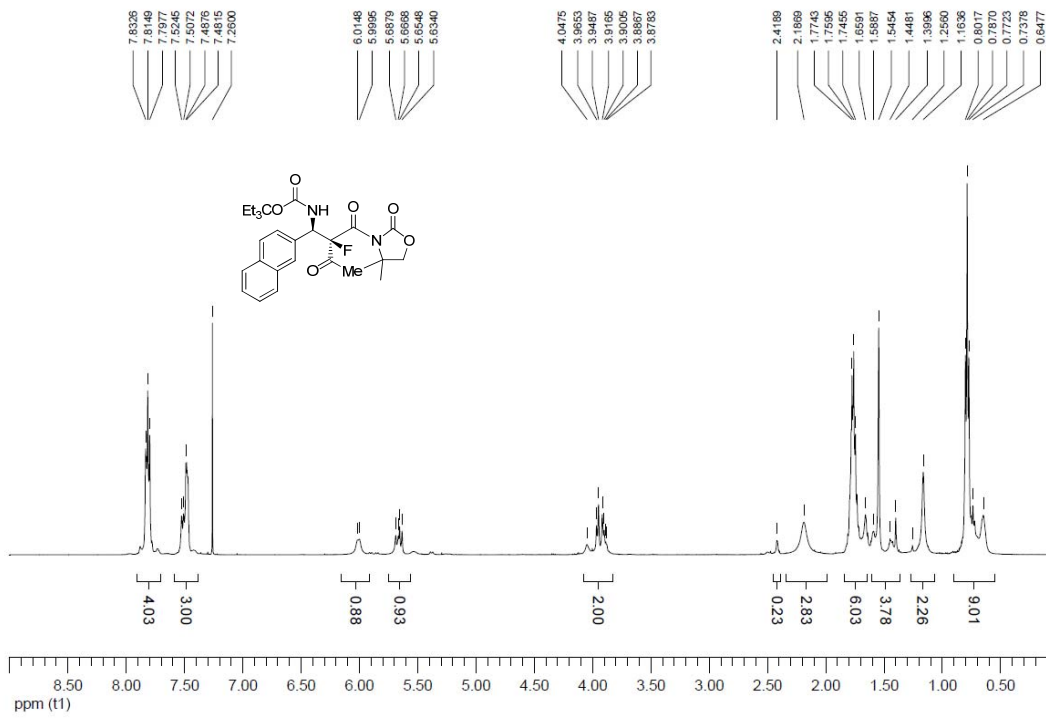
dpX300 ap24pyh4.1 pyh4186 3Cl 13C



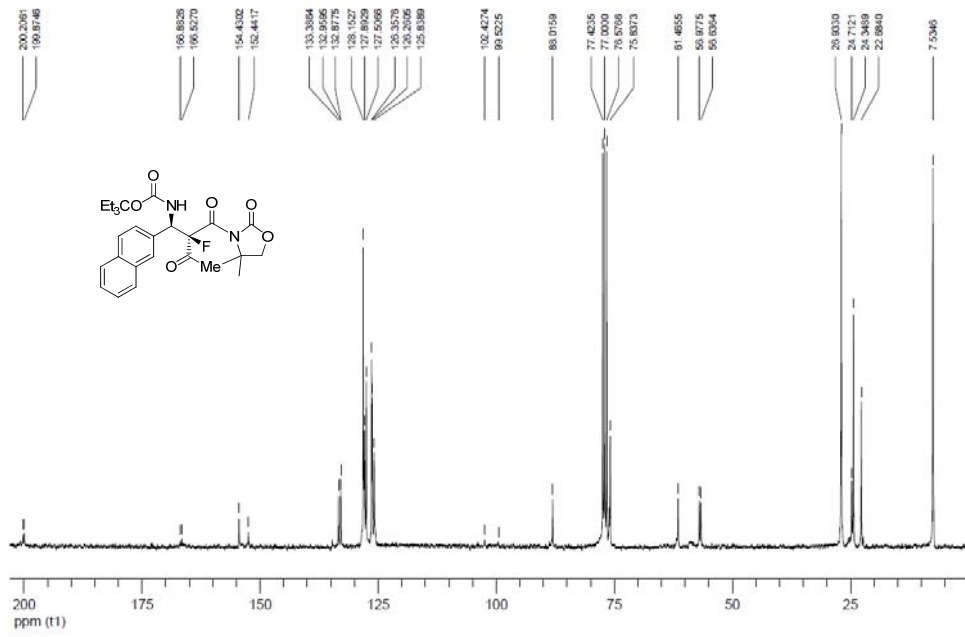
F19 (no decoupled) ap20pyh1 5.1 pyh4186 3Cl



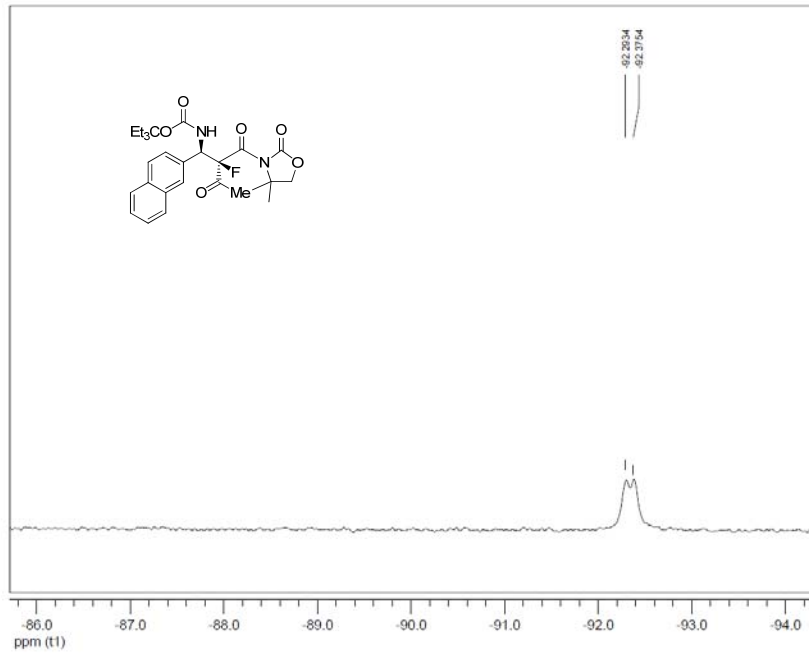
1H AMX500 pyh270409 2.1 pyh4189 2Naph



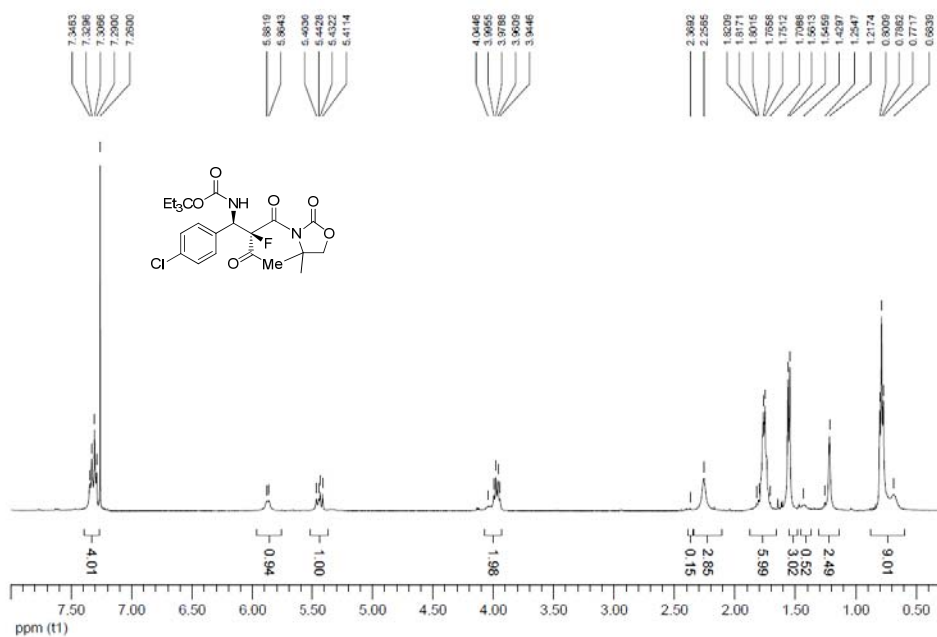
dpx300 my08pyh19.1 pyh4189 2naph 13C



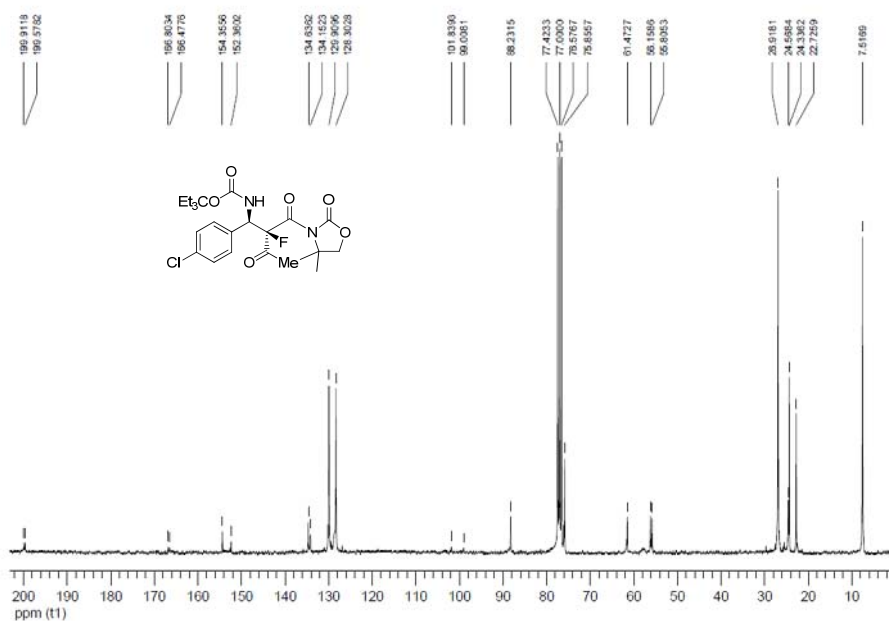
F19 (no decoupled) j124pyh4.1 2Naph



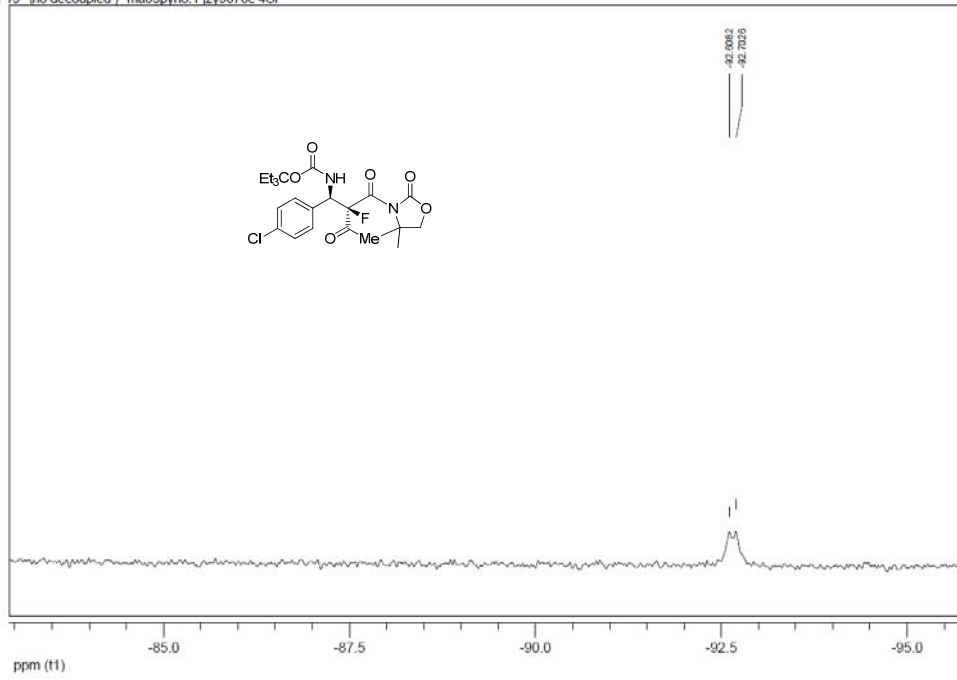
1H AMX500 pyh090409 1.1 pyh4157B 1 4Cl Tol 1H



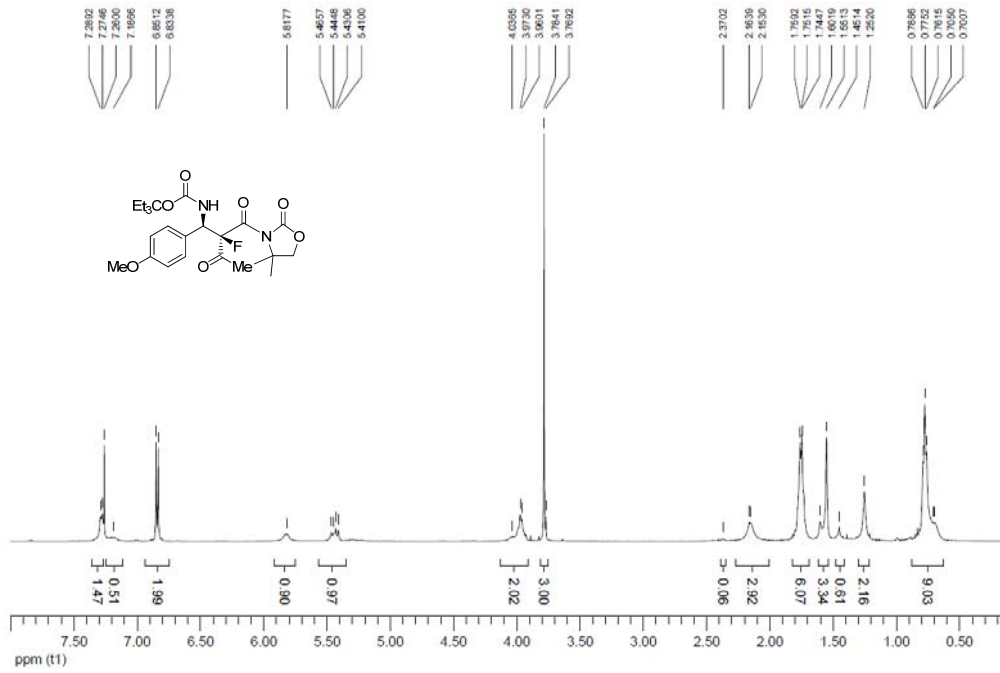
dpx300 ap02pyh3.1 pyh4155 4-Cl 13C



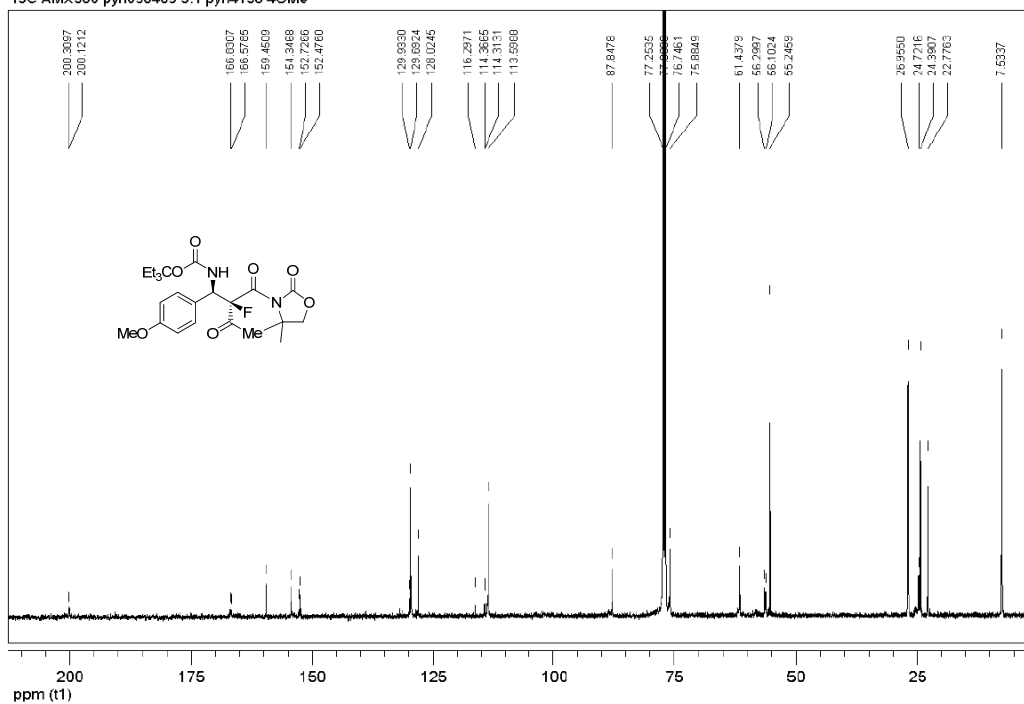
F19 (no decoupled) ma09pyh8.1 jzy9070c 4Cl



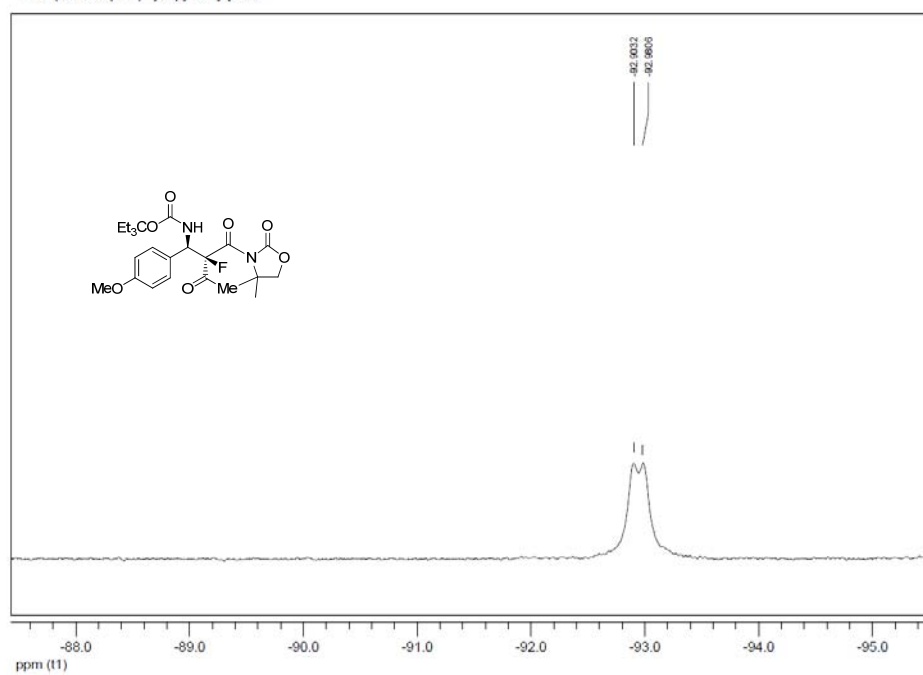
1H AMX500 pyh270409 7.1 jzy9138 4OMe



13C AMX500 pyh090409 5.1 pyh4158 4OMe

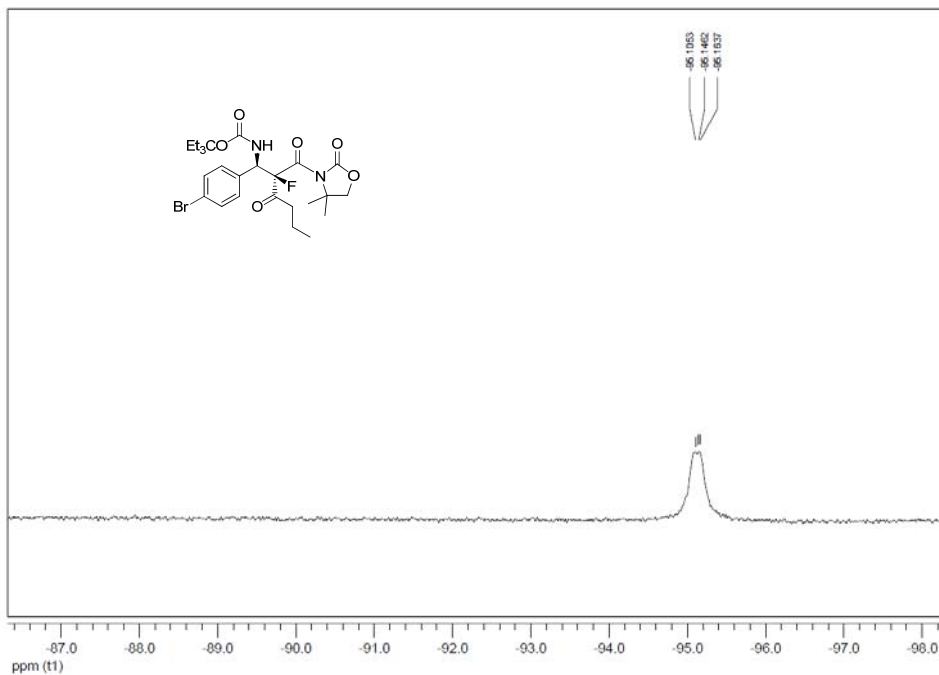


F19 (no decoupled) j124pyh2.1 jzy9138

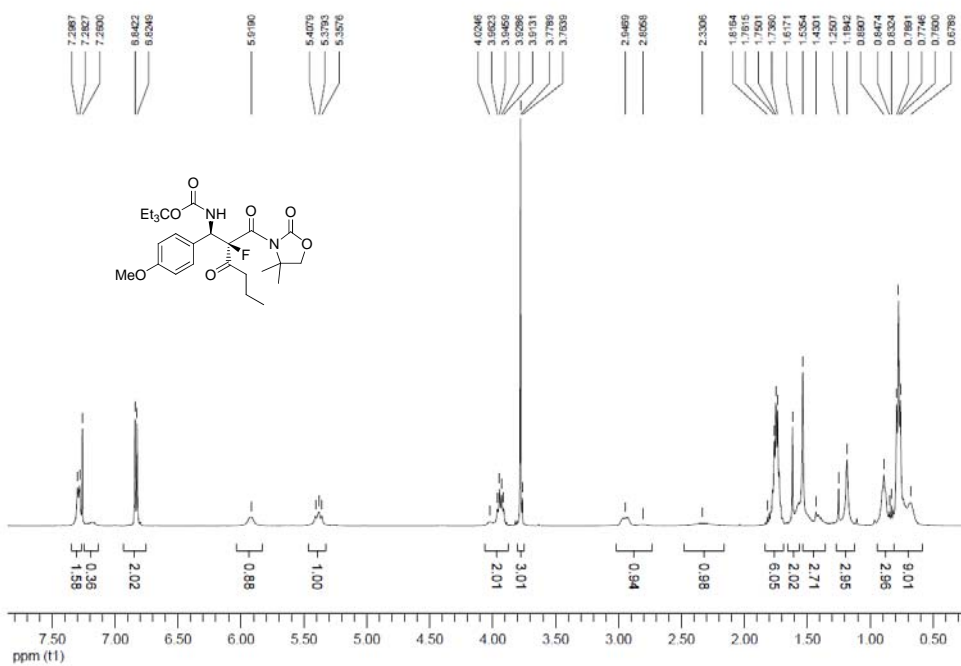




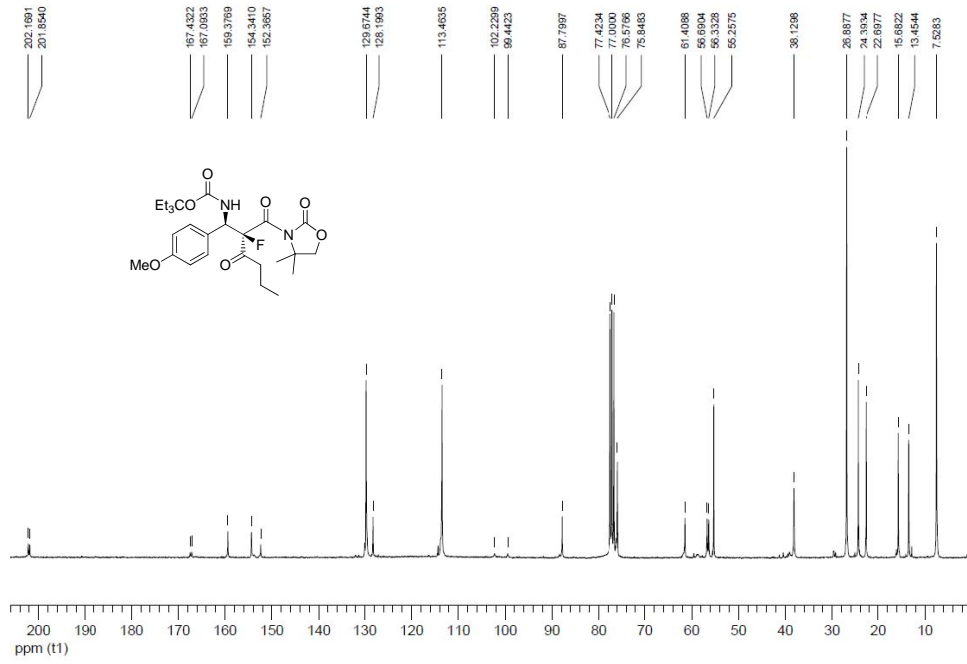
F19 (no decoupled) j124pyh5.1 4241B nPr+4Br



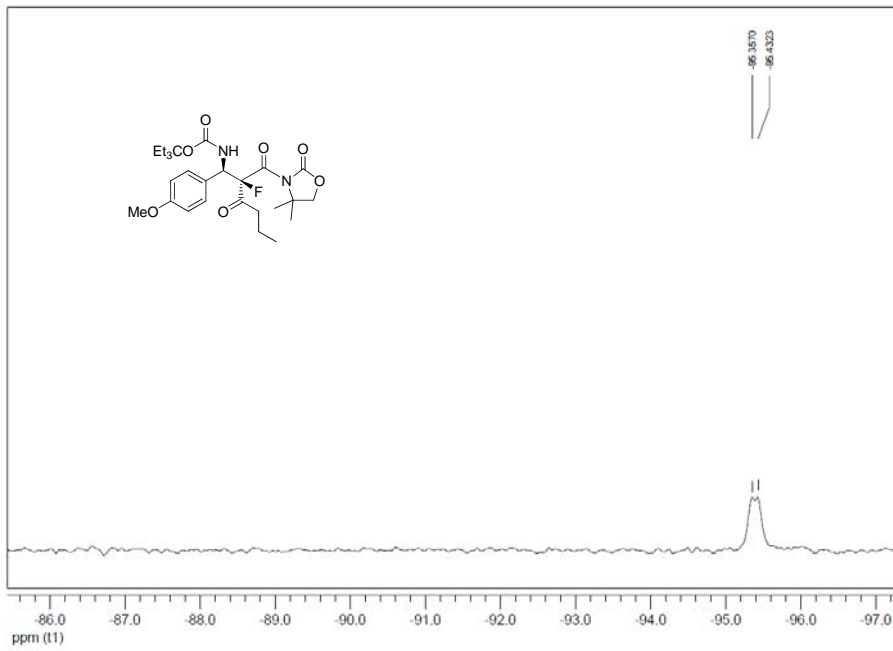
1H AMX500 pyh260509 1.1 pyh4240 n-Pr+4OMe



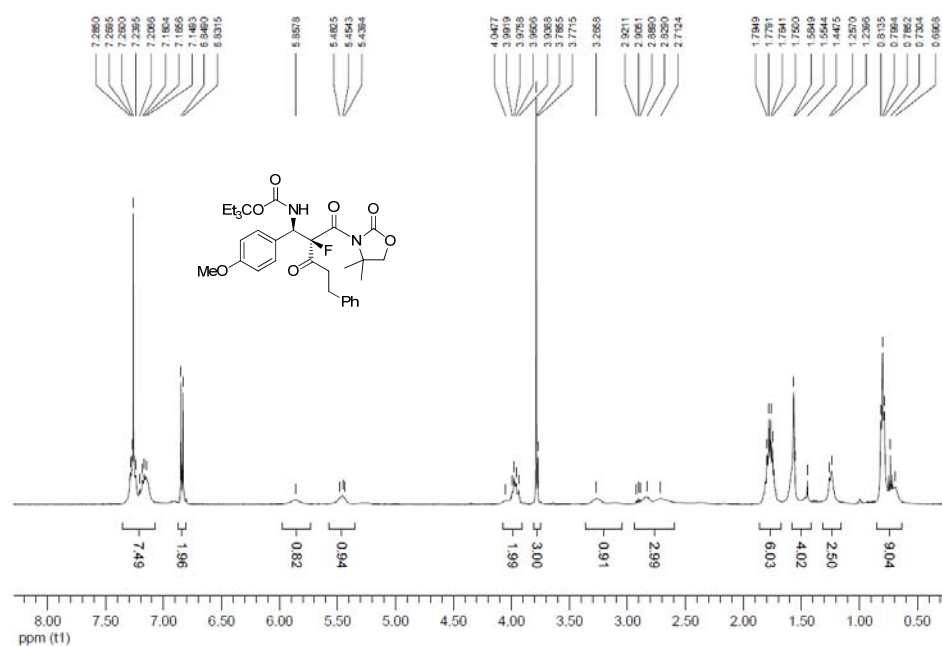
dpx300 my30pyh1.1 pyh4240 n-Pr+4OMe 13C



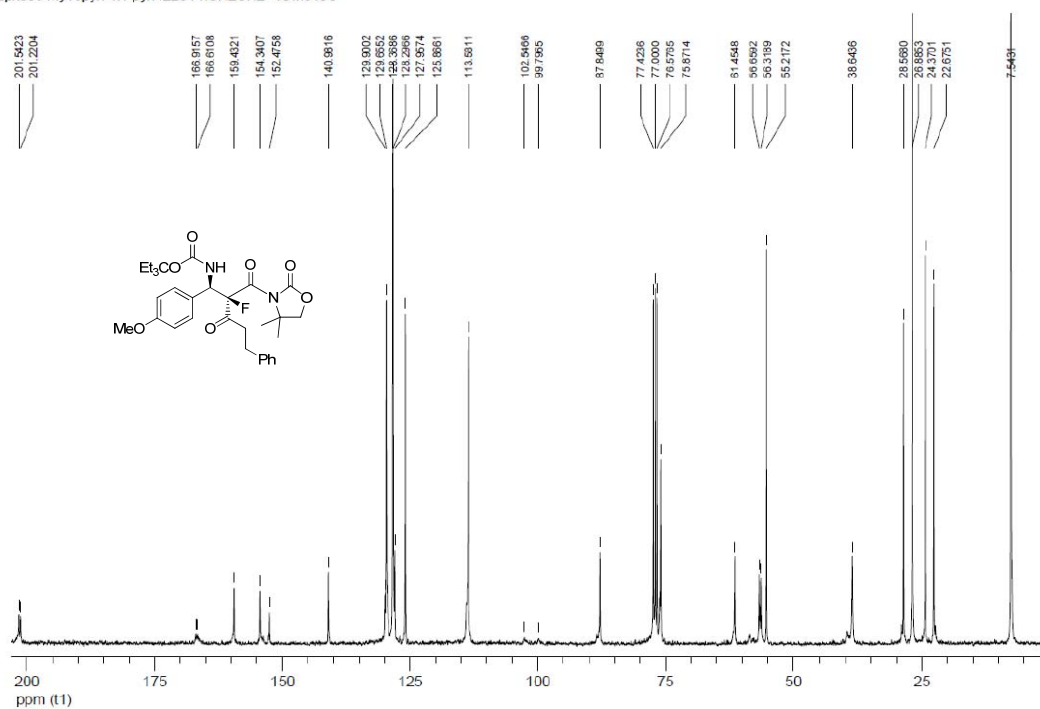
F19 (no decoupled) j127pyh7.1 4240 npr+4OMe



1H AMX500 pyh180409 7.1 pyh4176 PhCH2CH2+ 4OMe

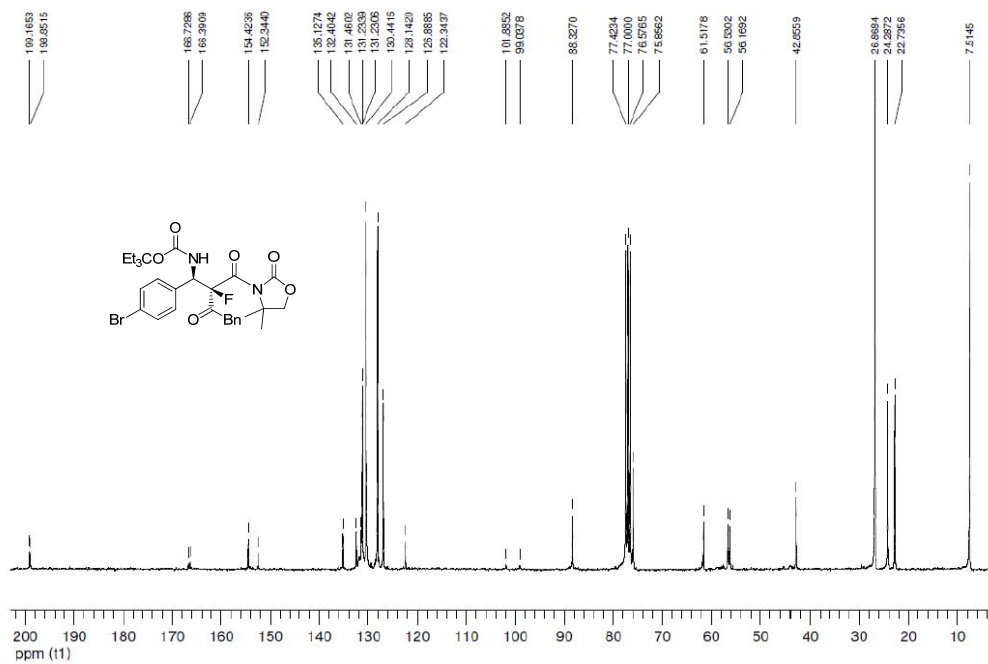


dpx300 my16pyh 4.1 pyh4226 PhCH2CH2+4OMe13C

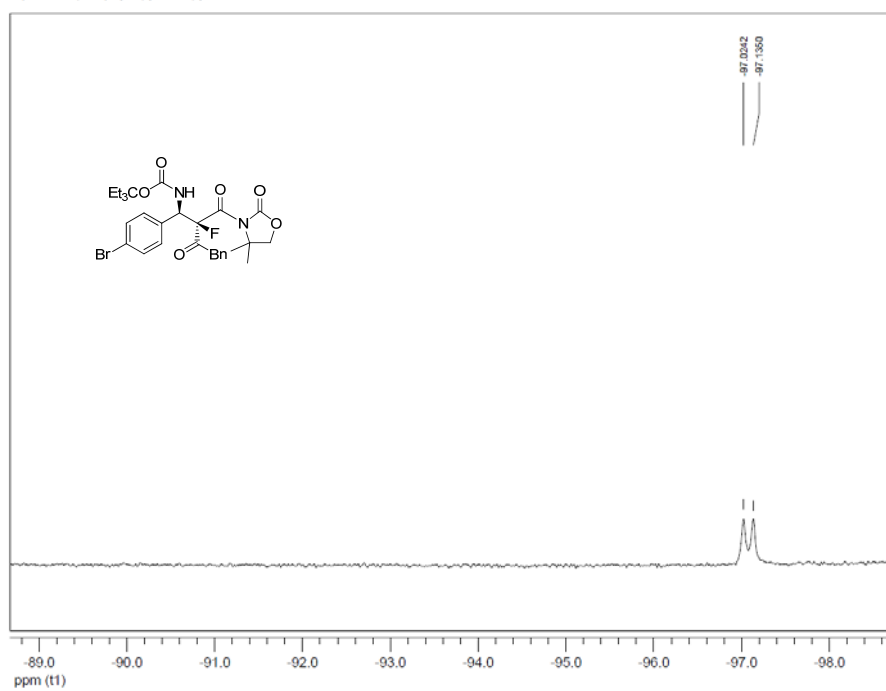




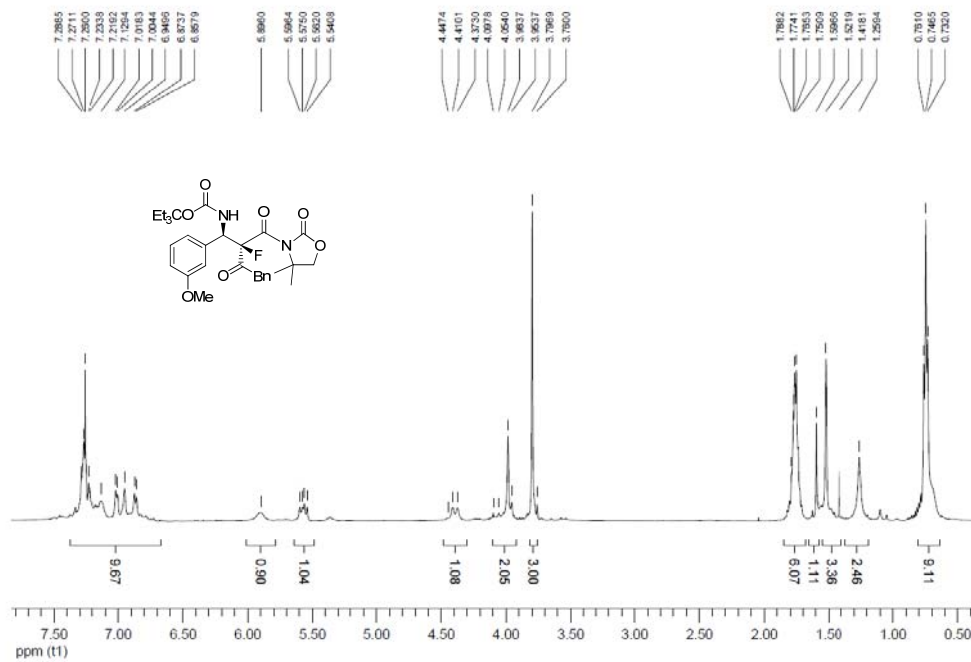
dpx300 my22pyh9 1 pyh4234B Bn+4Br 13C



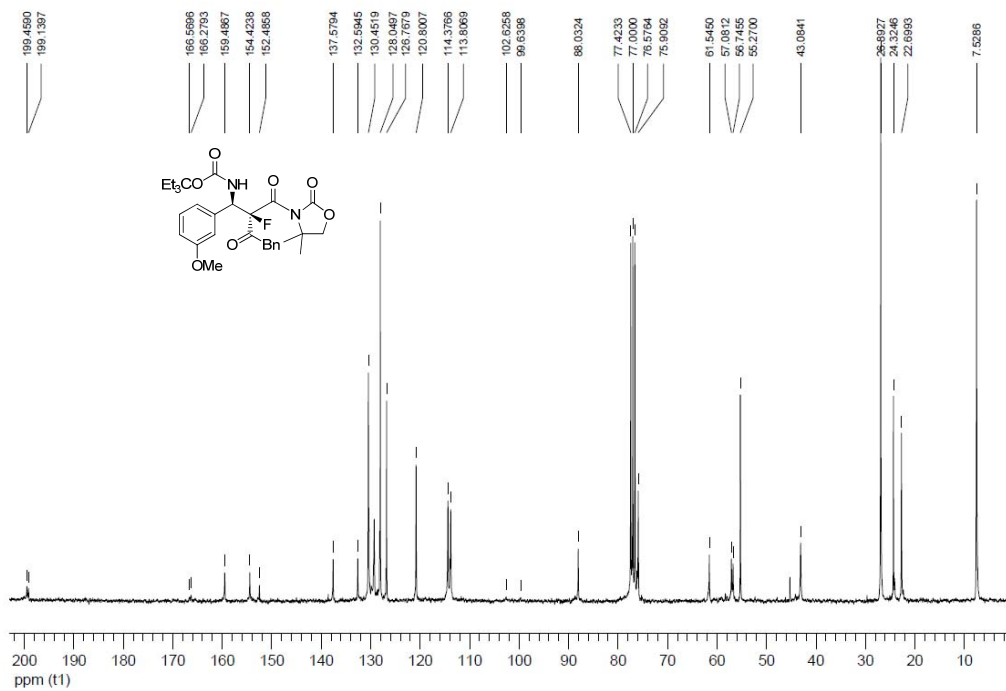
F19 (no decoupled) j124pyh12.1 pyh4234



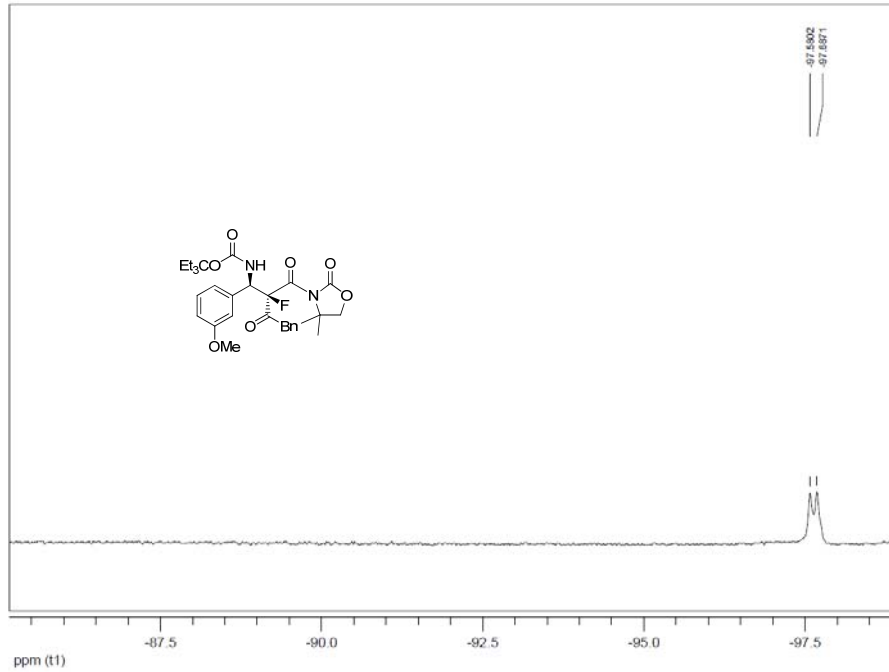
1H AMX500 pyh250509 2.1 pyh4235B Bn+3OMe



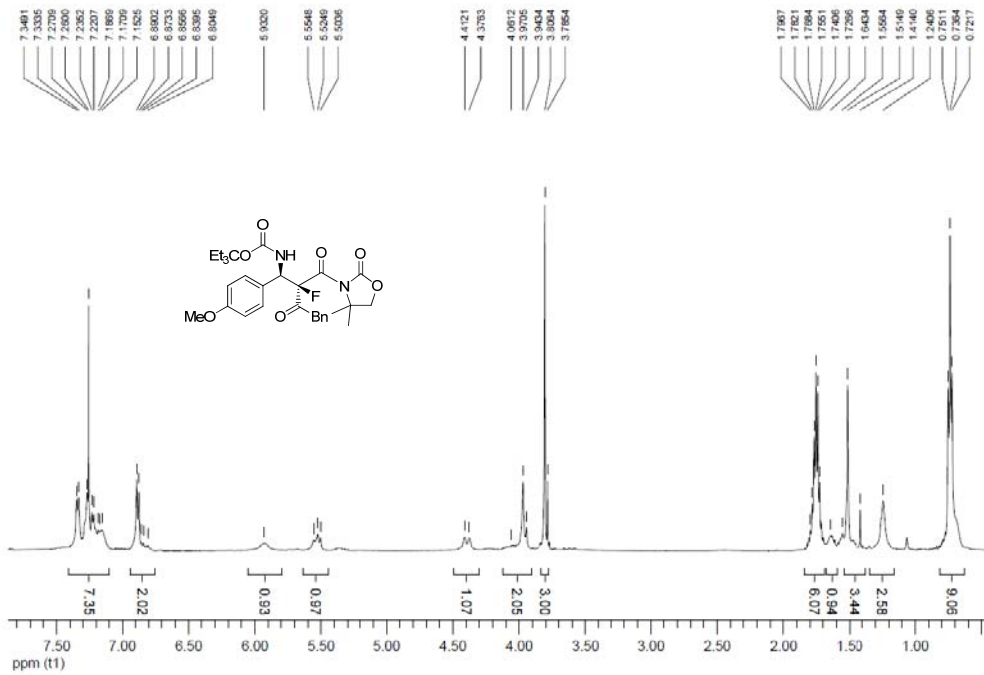
dpx300 my23pyh 4.1 pyh4235B Bn+3OMe 13C



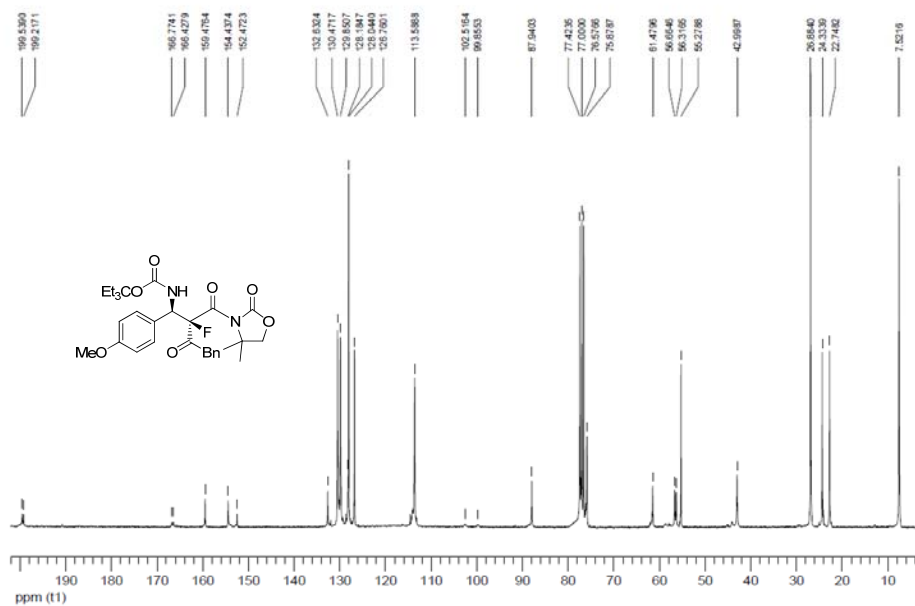
F19 (no decoupled) J124pyh10.1 pyh4235B MeOD



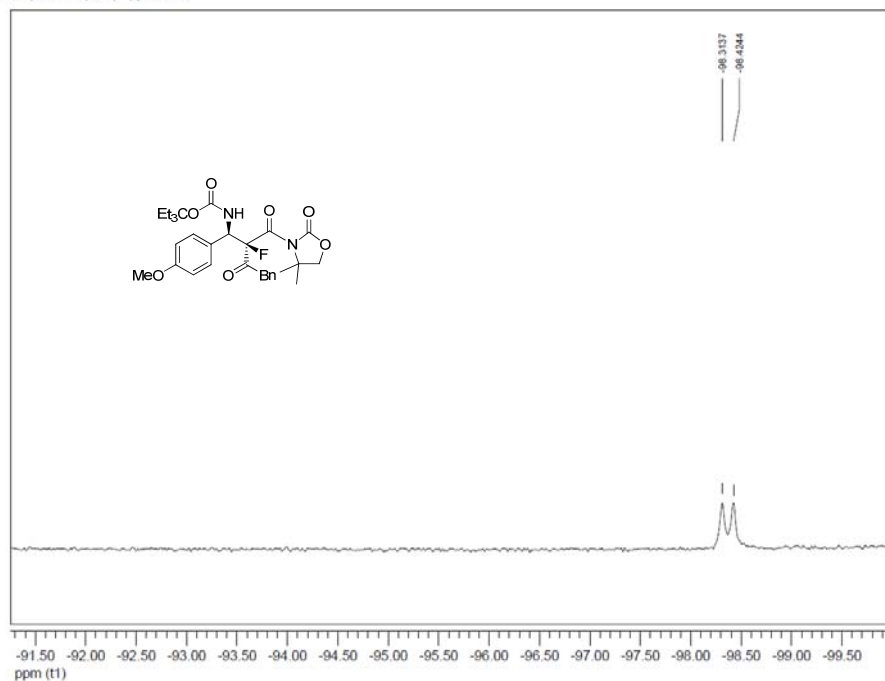
1H AMX500 pyh250409 6.1 pyh4192A Bn+4OMe



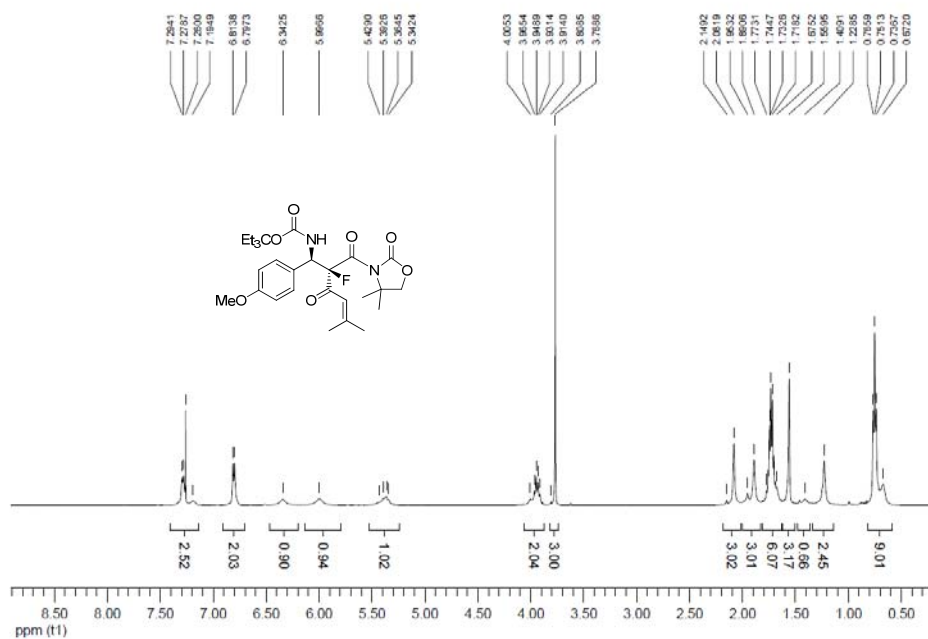
dpx300 ap25pyh 2.1 pyh4192A Bn+4OMe 13C



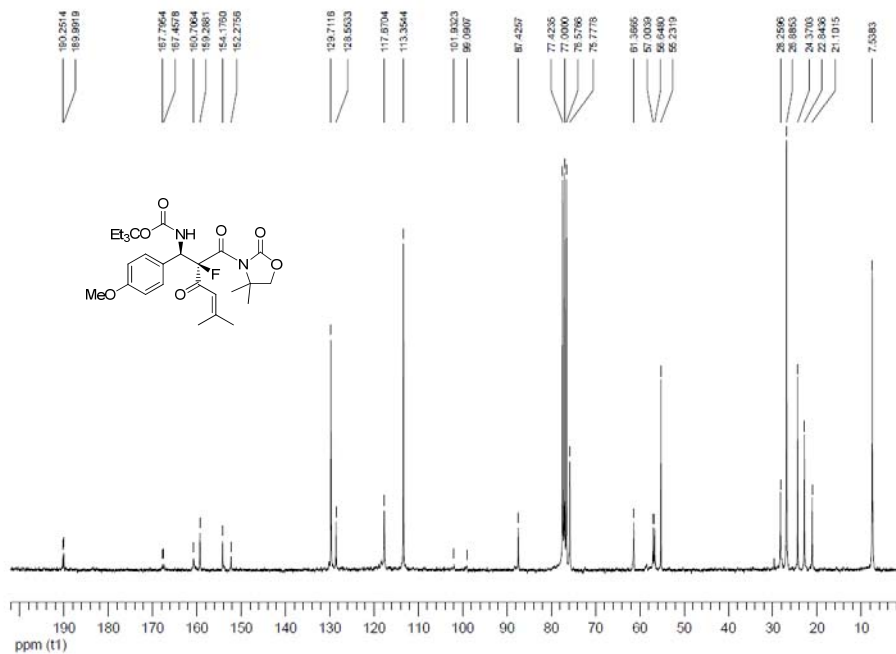
F19 (no decoupled) pyh4192A



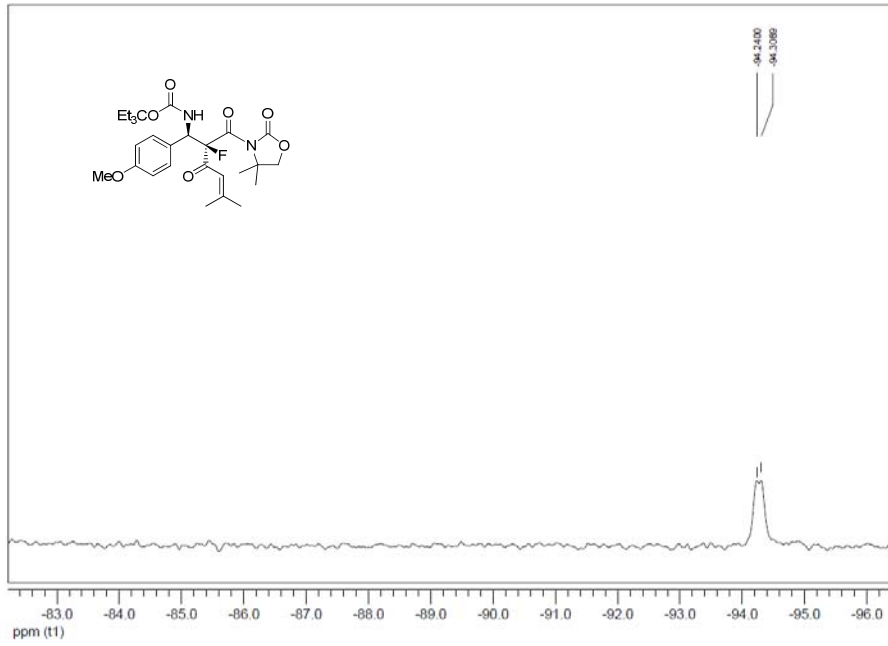
1H AMX500 pyh270409 3.1 pyh4 192B =+4OMe



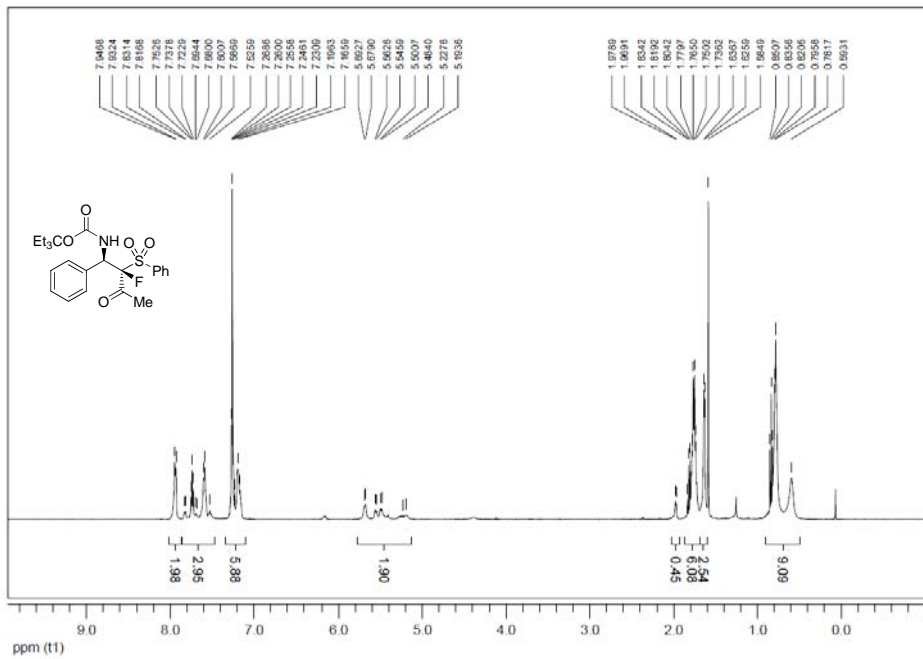
dpx300 my09pyh3.1 pyh4 192B =+4OMe 13C



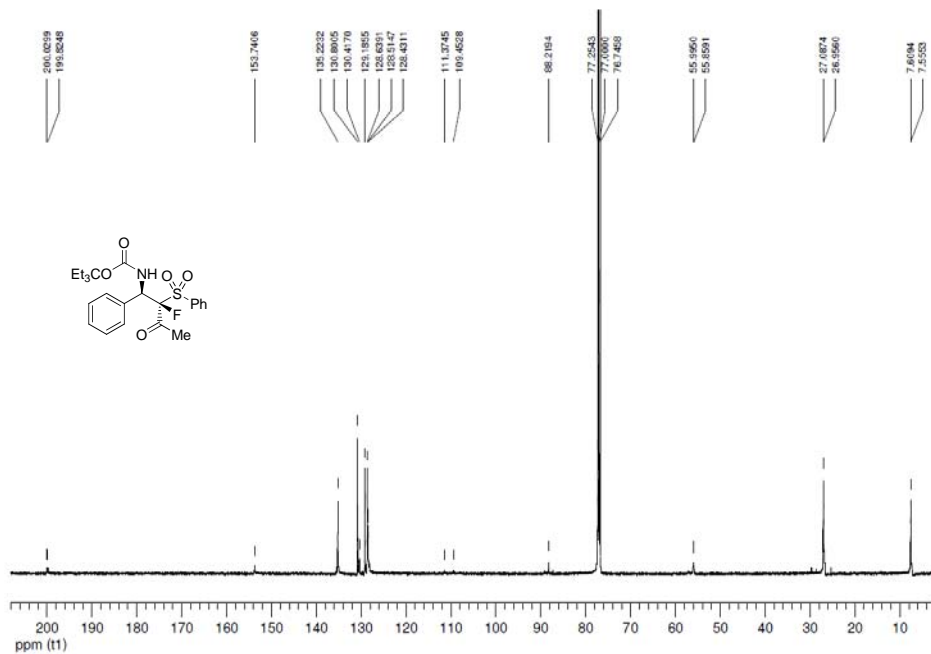
F19 (no decoupled) j127pyh1 2.1 (CH3) 2= + 4OMe



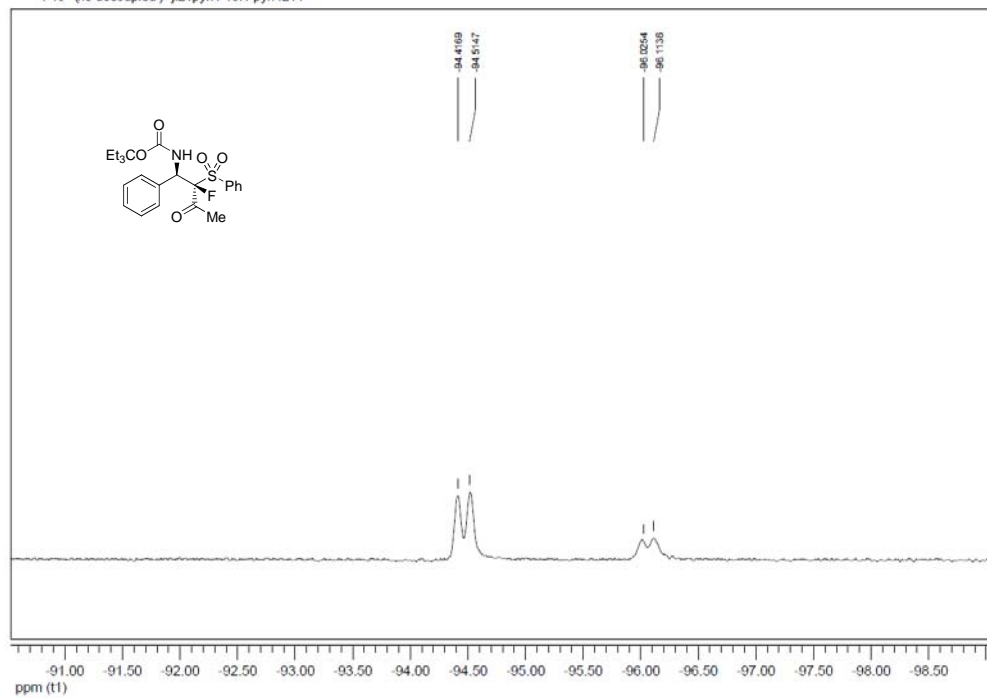
1H AMX500 pyh130509 2.1 pyh4211



13C AMX500 pyh200509 2.1 pyh4211

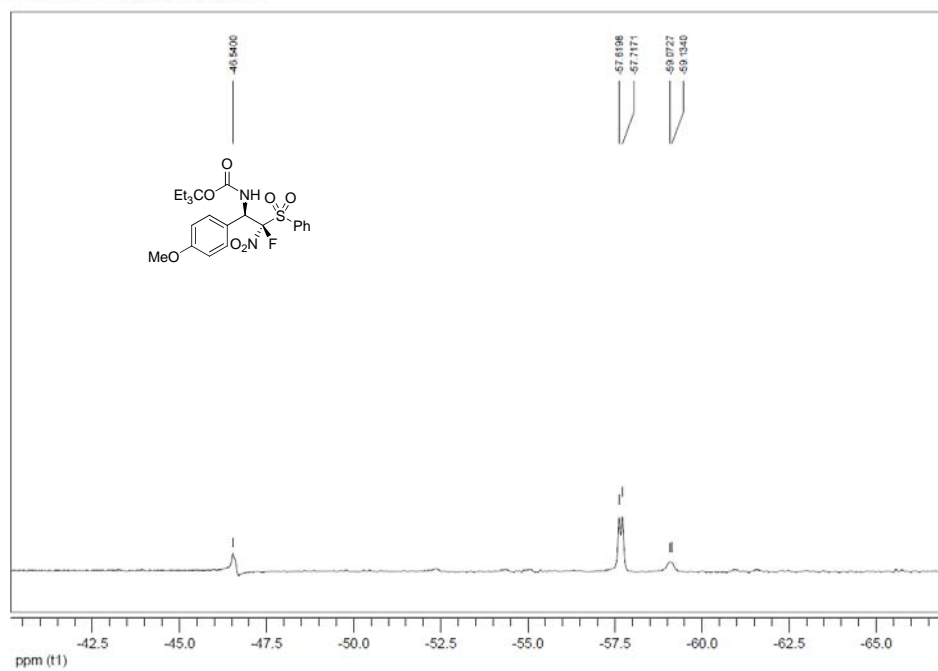


F19 (no decoupled) j121pyh1 10.1 pyh4211

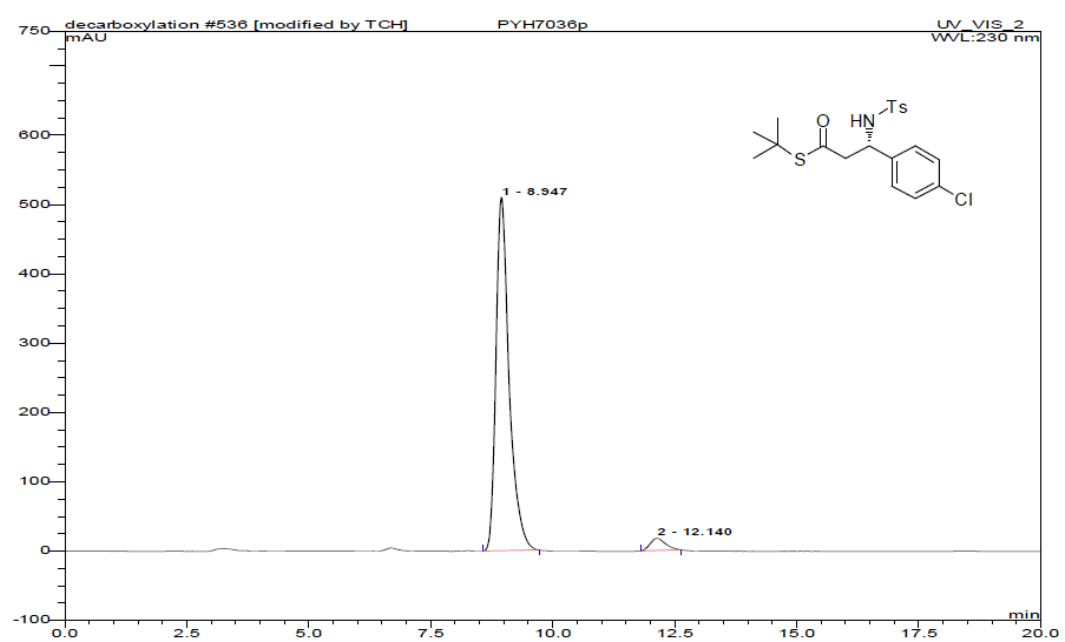
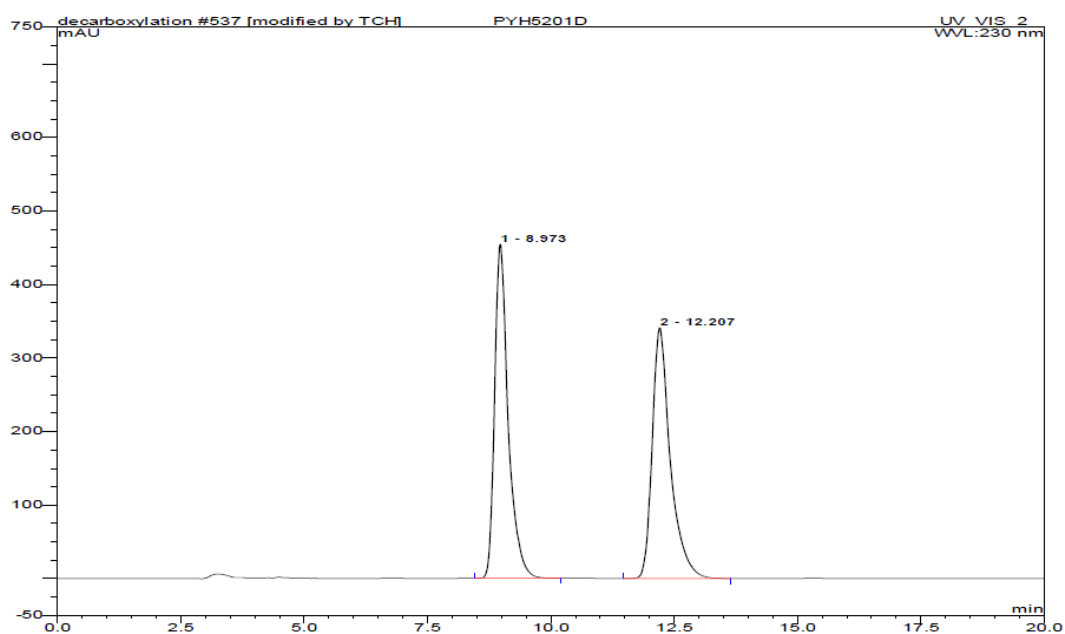


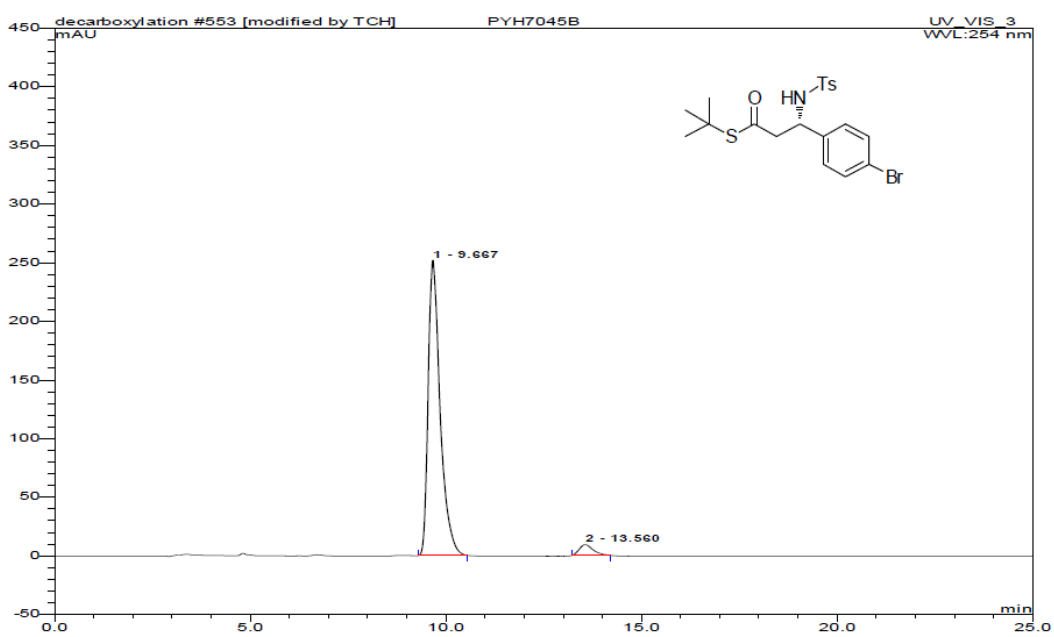
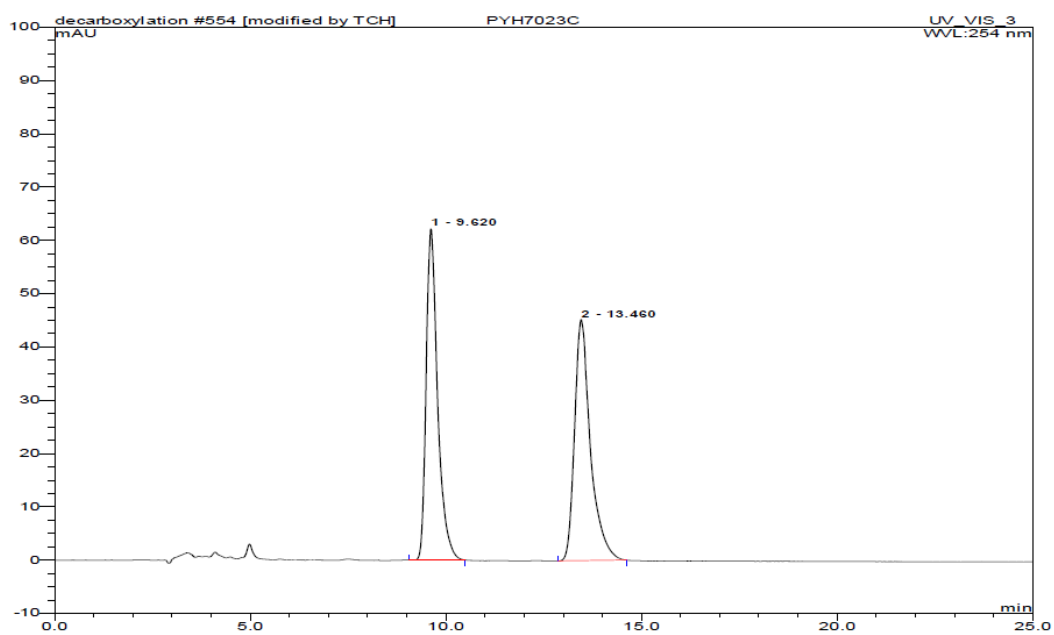


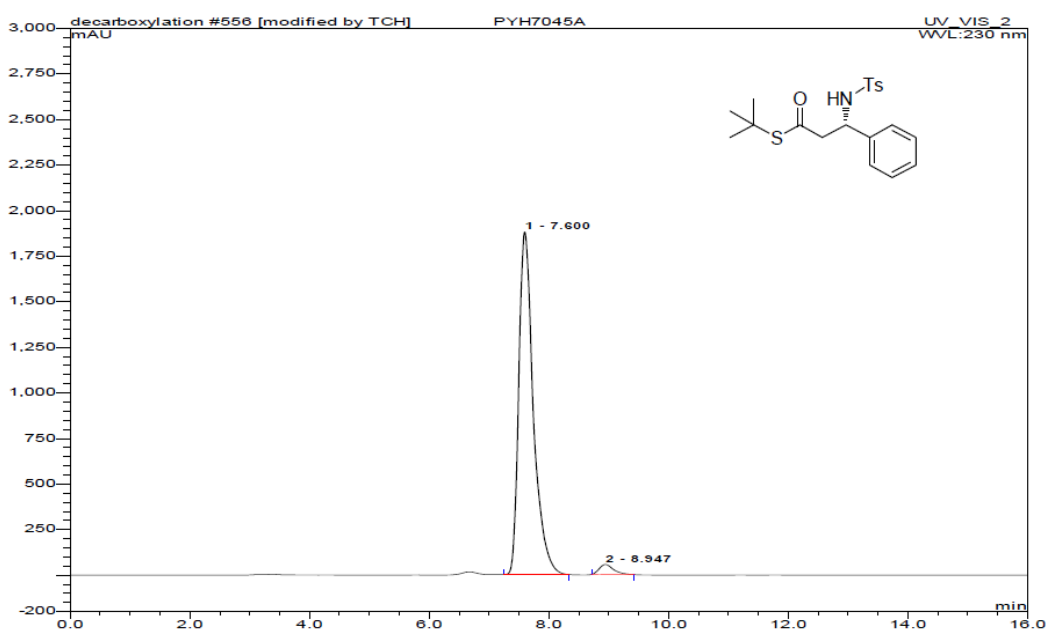
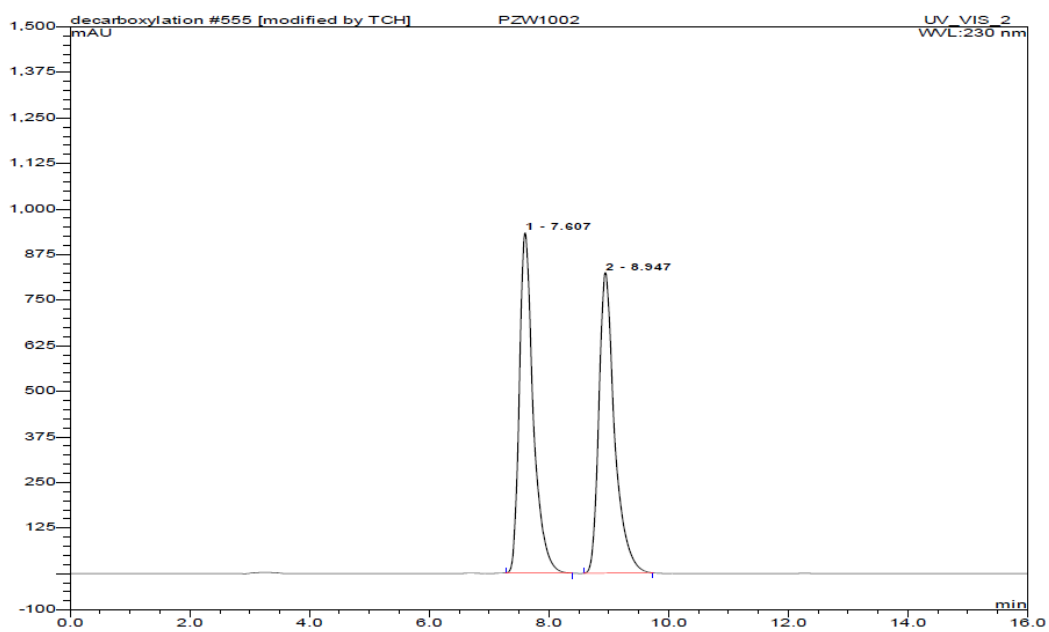
F19 (no decoupled) j121pyh1 9.1 pyh4212

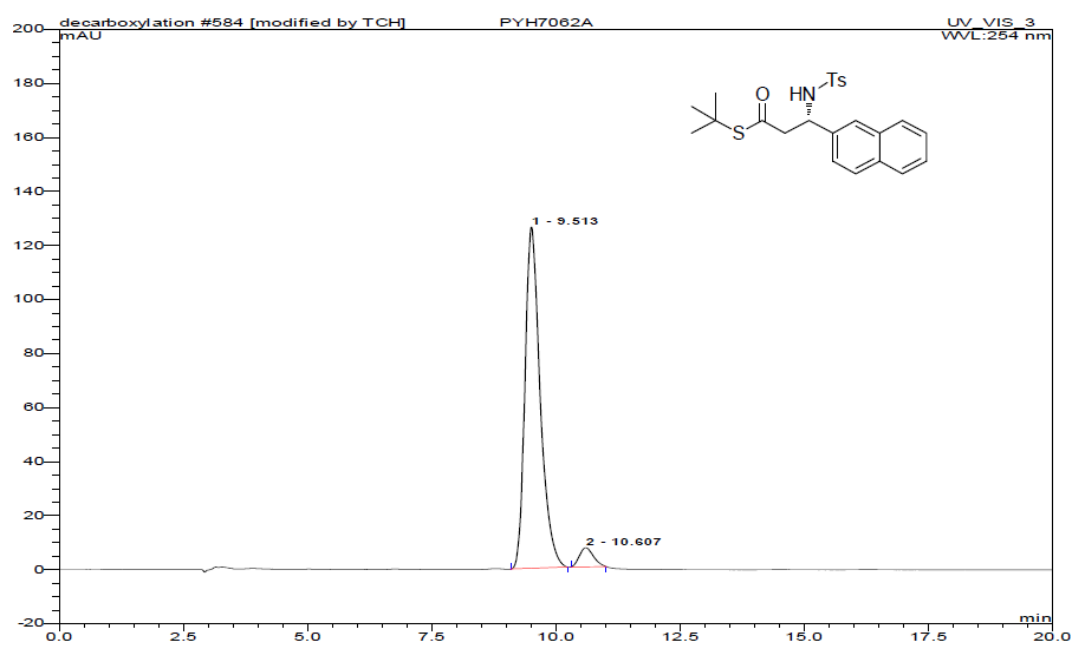
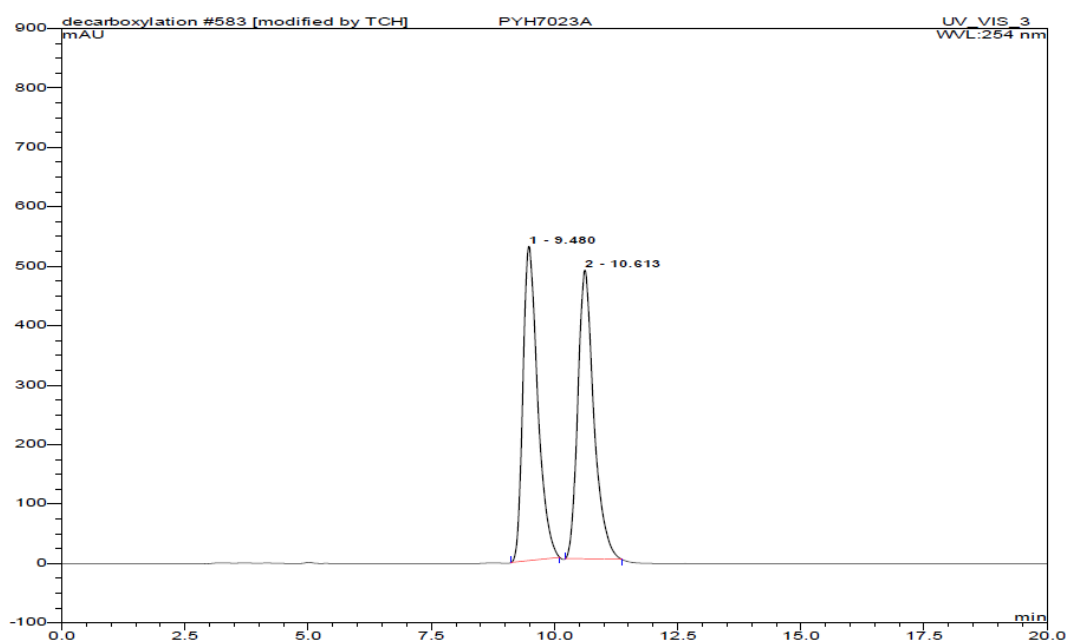


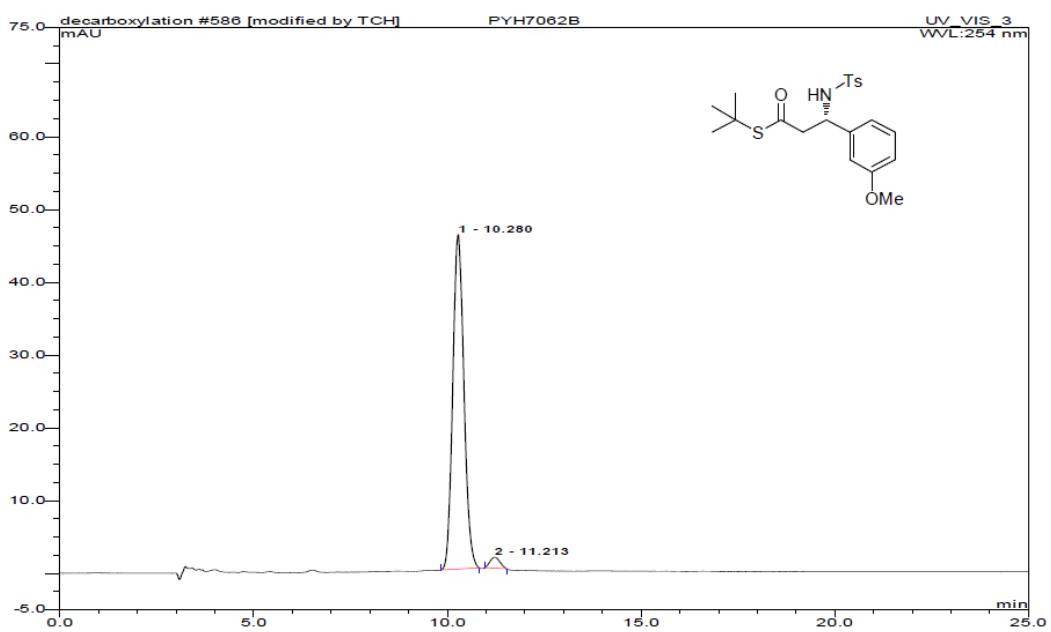
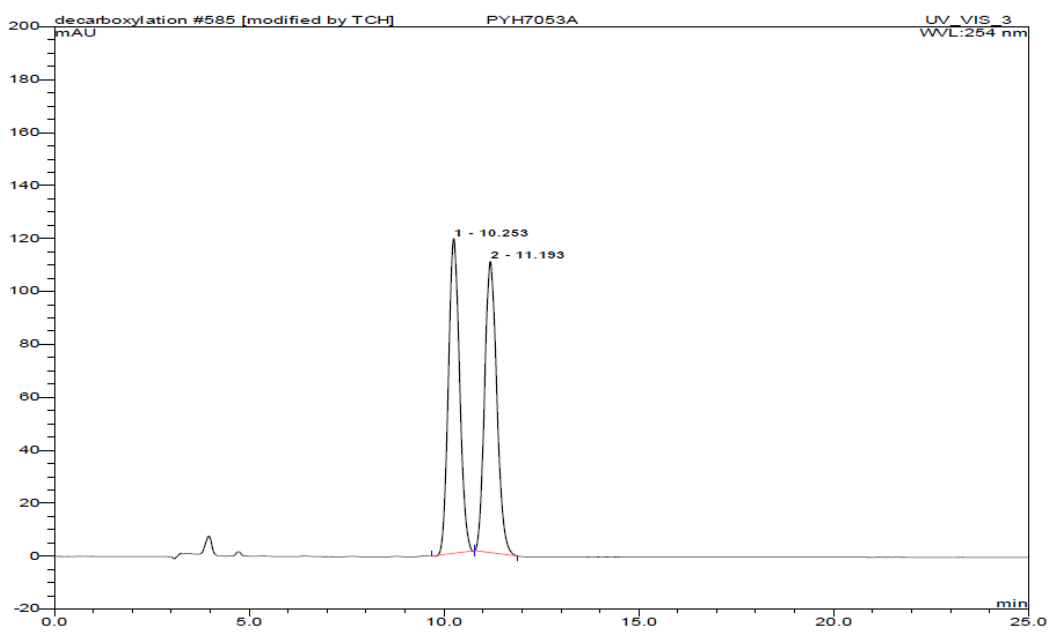
# Chiral HPLC Spectra

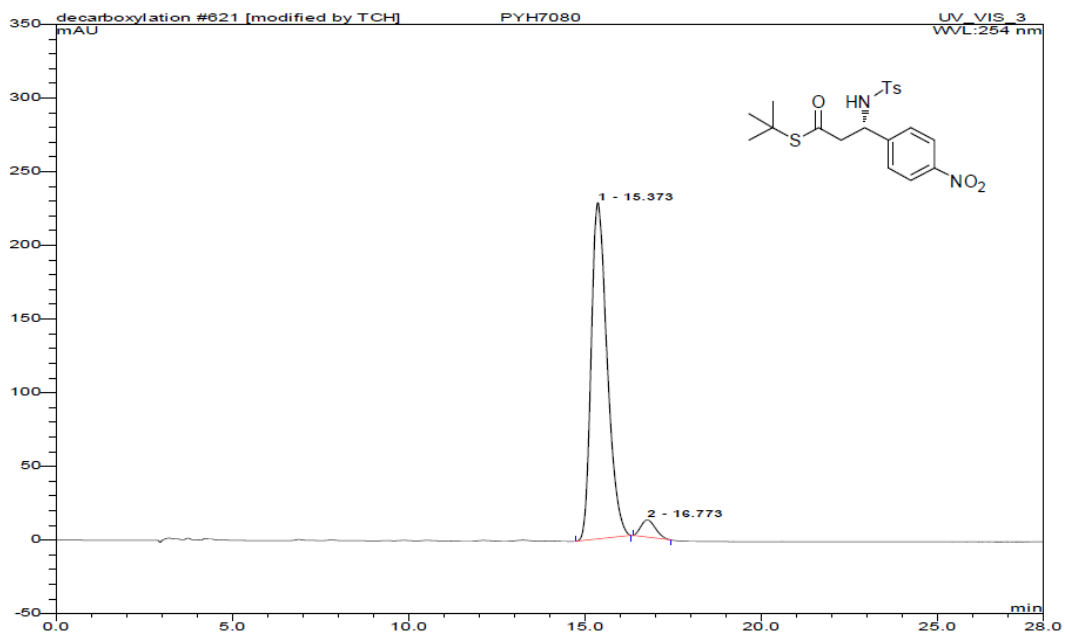
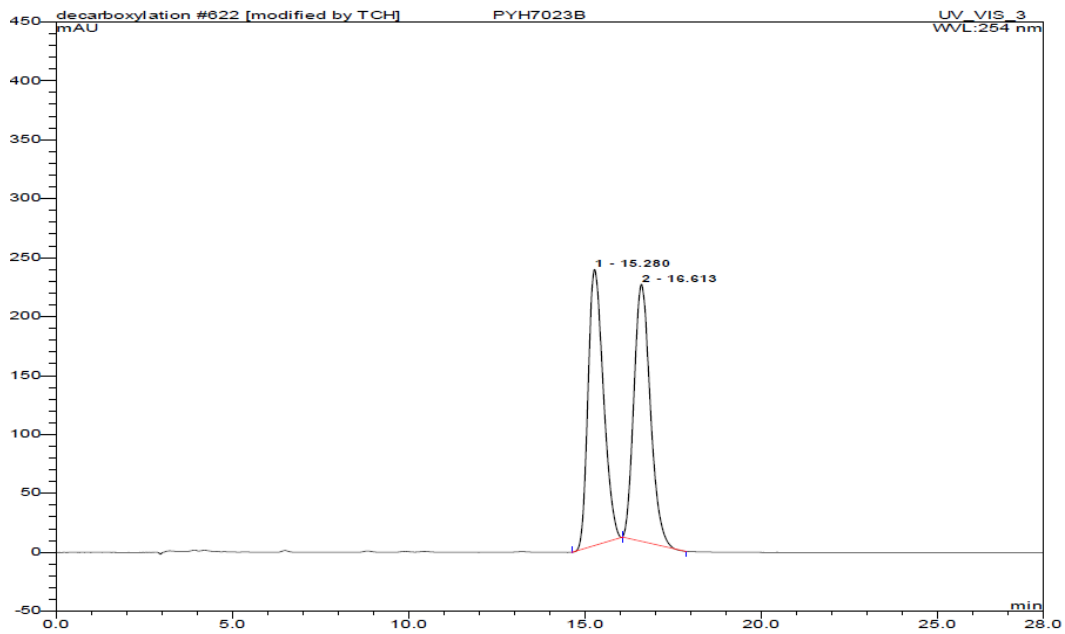


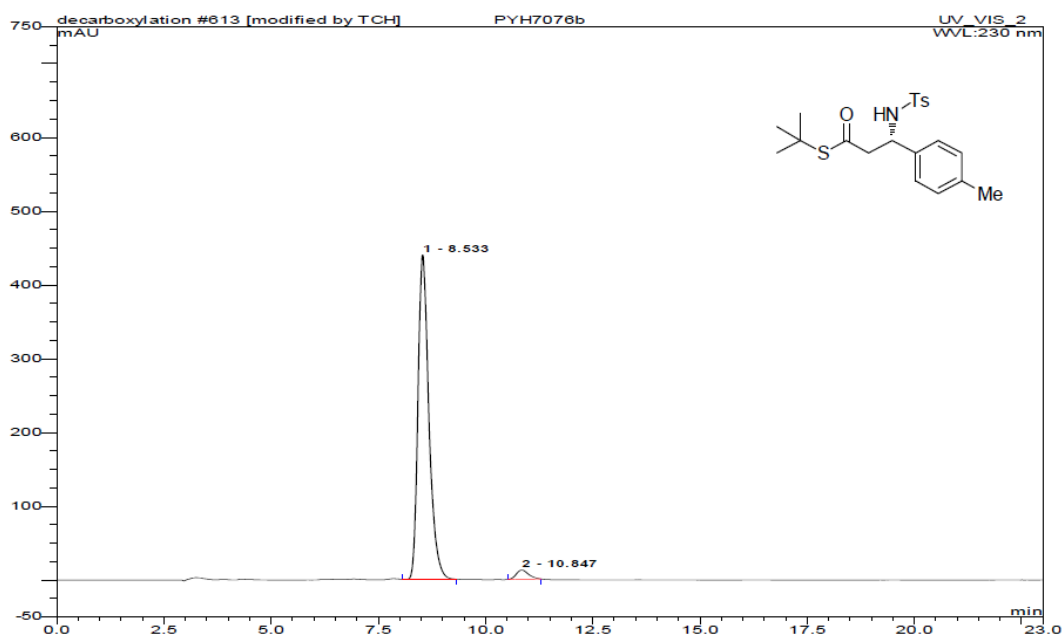
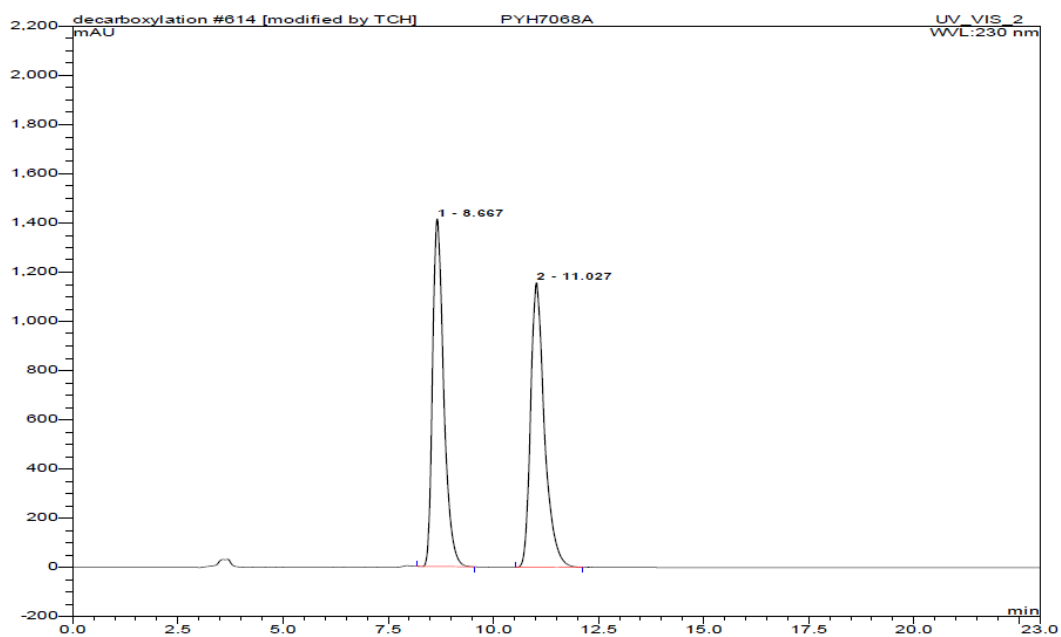


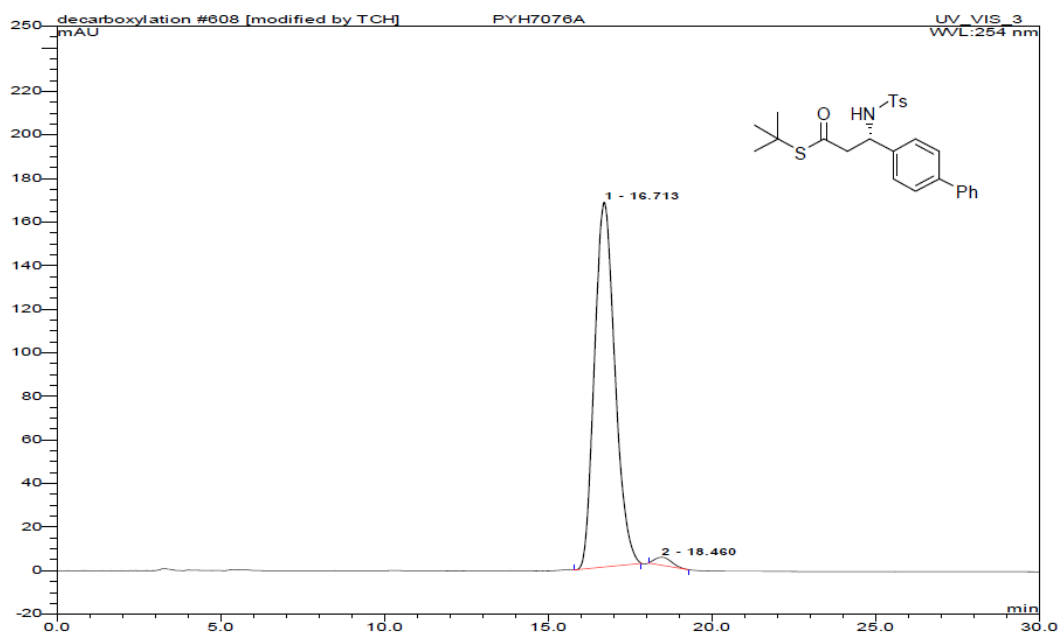
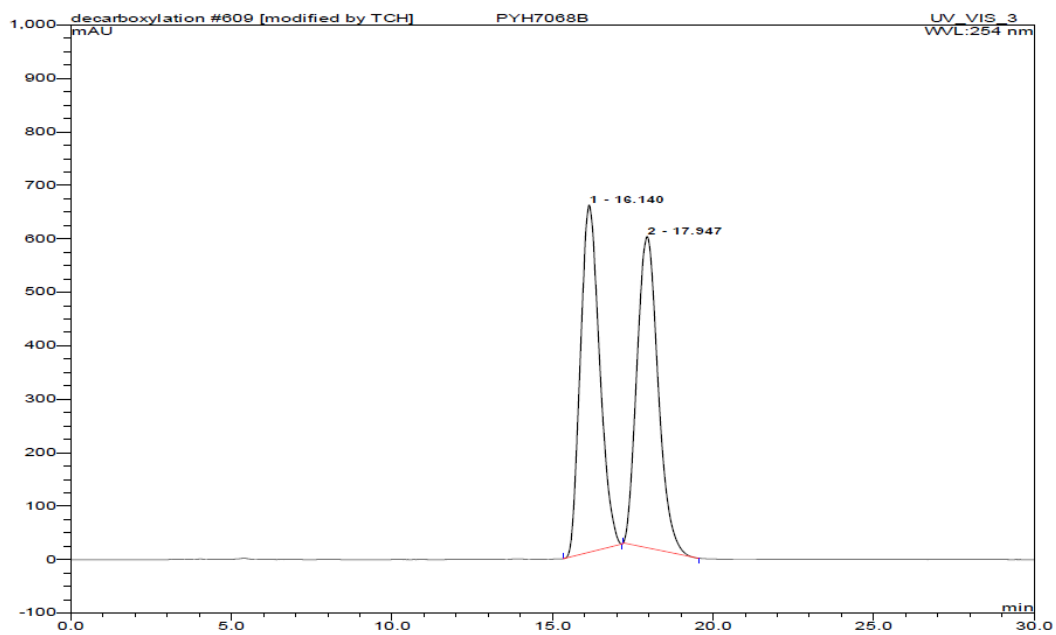


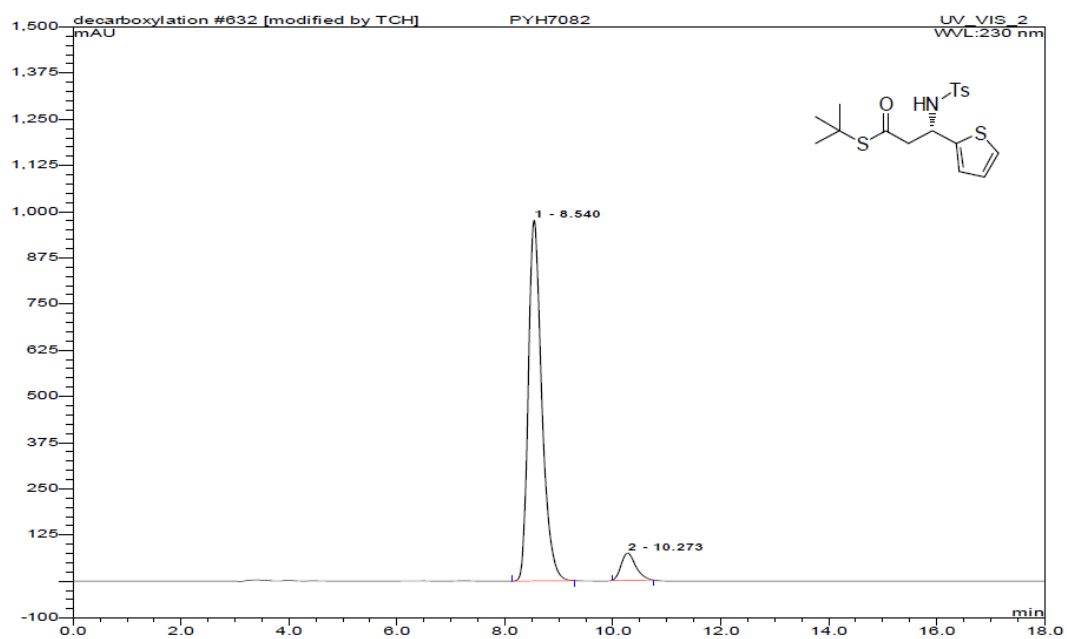
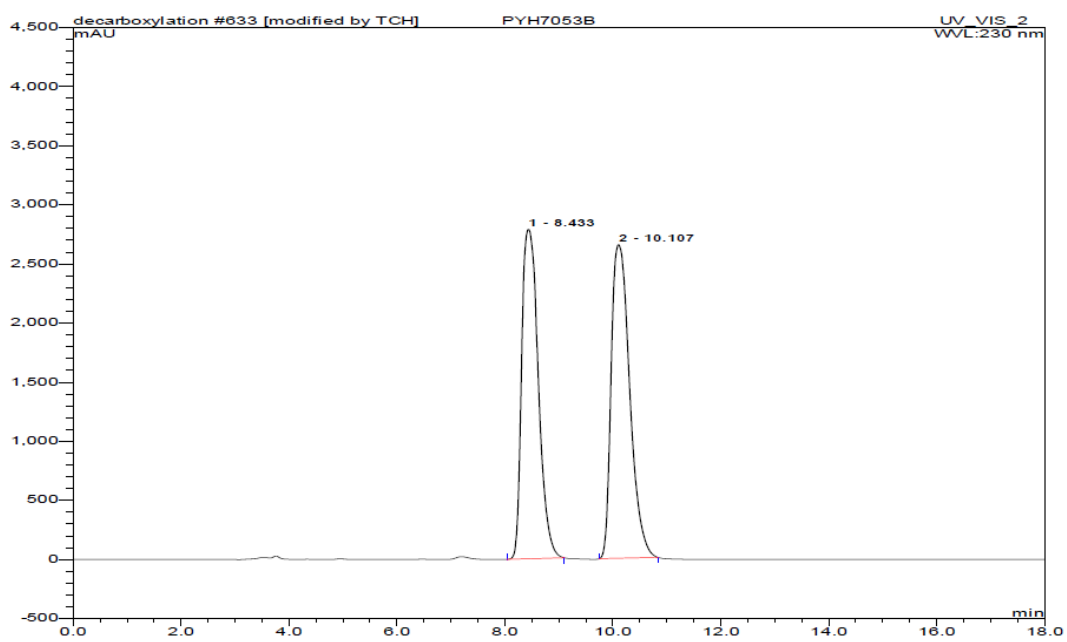


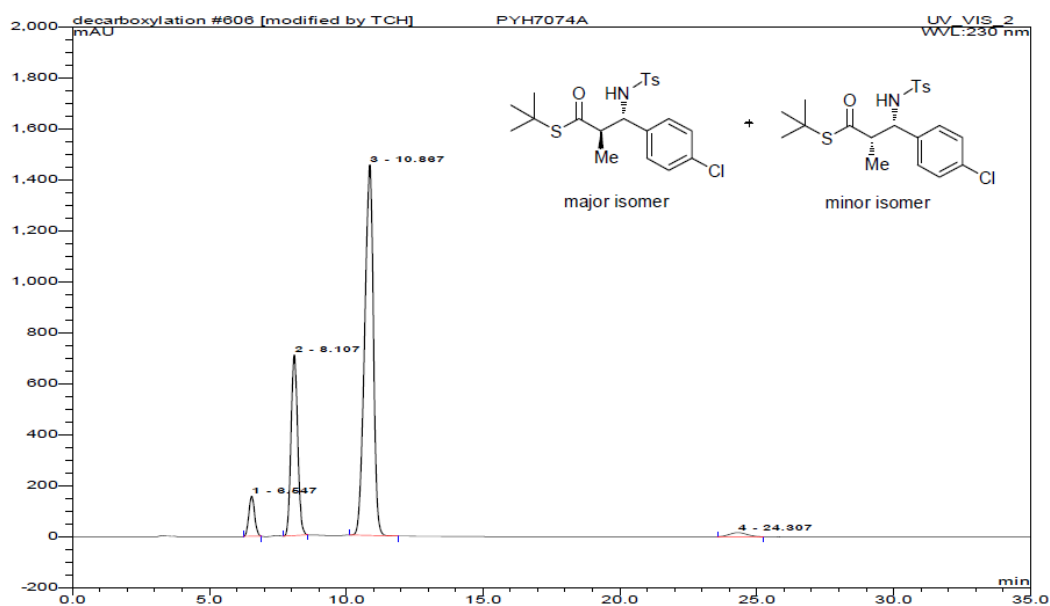
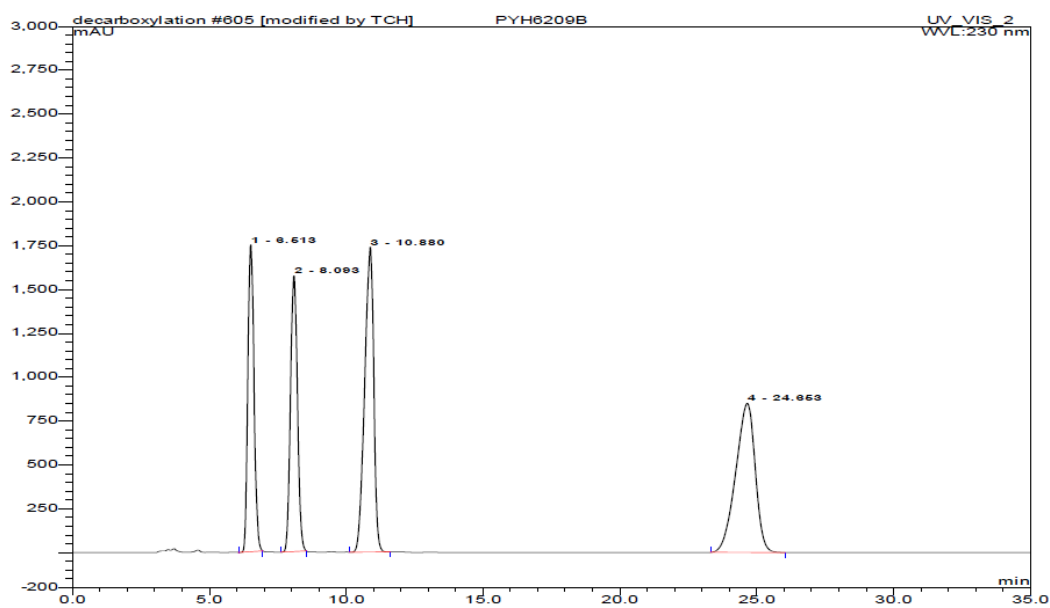


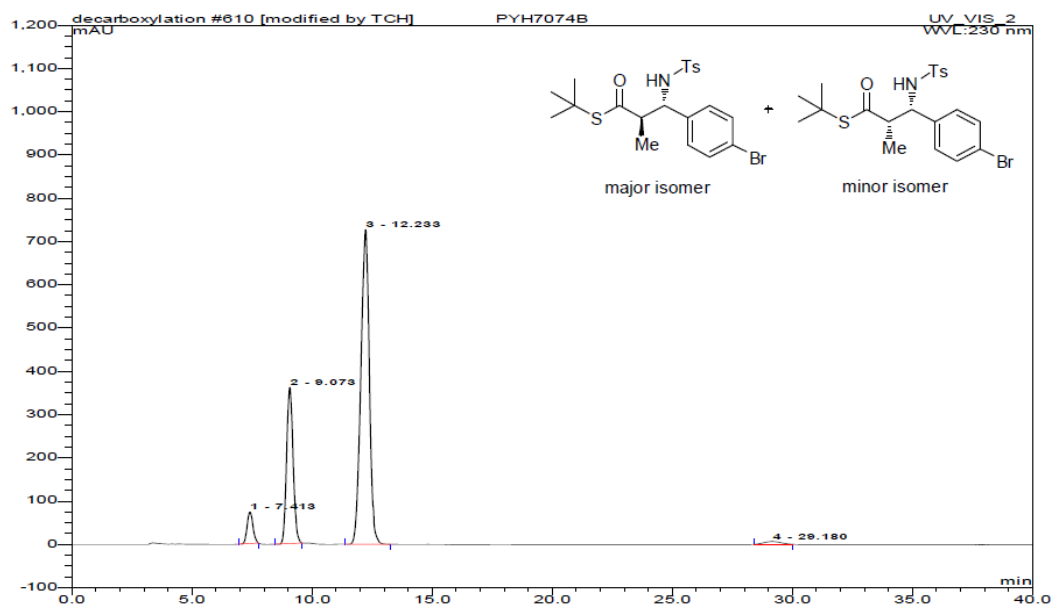
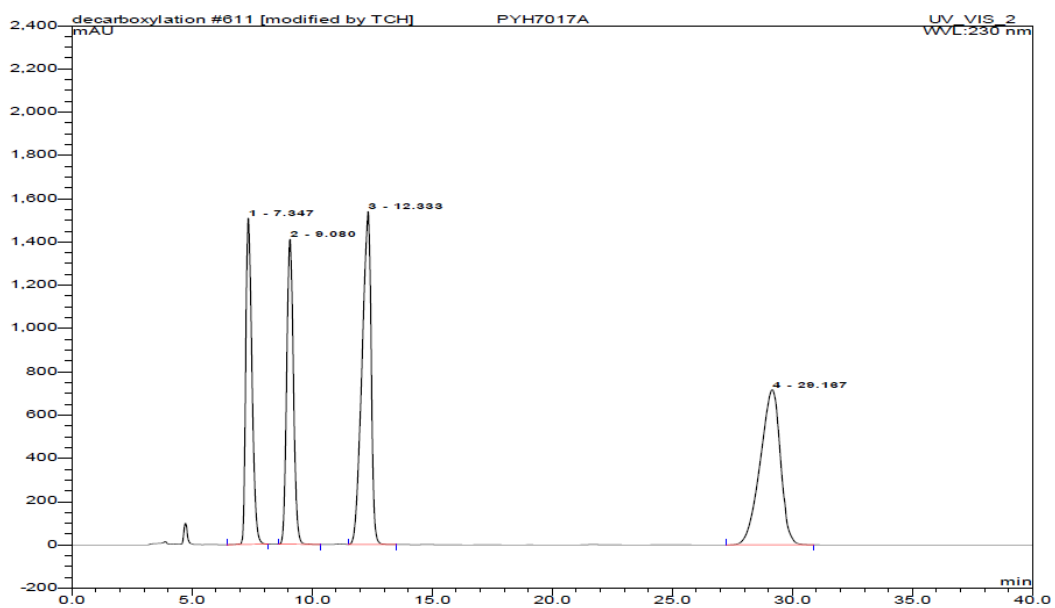


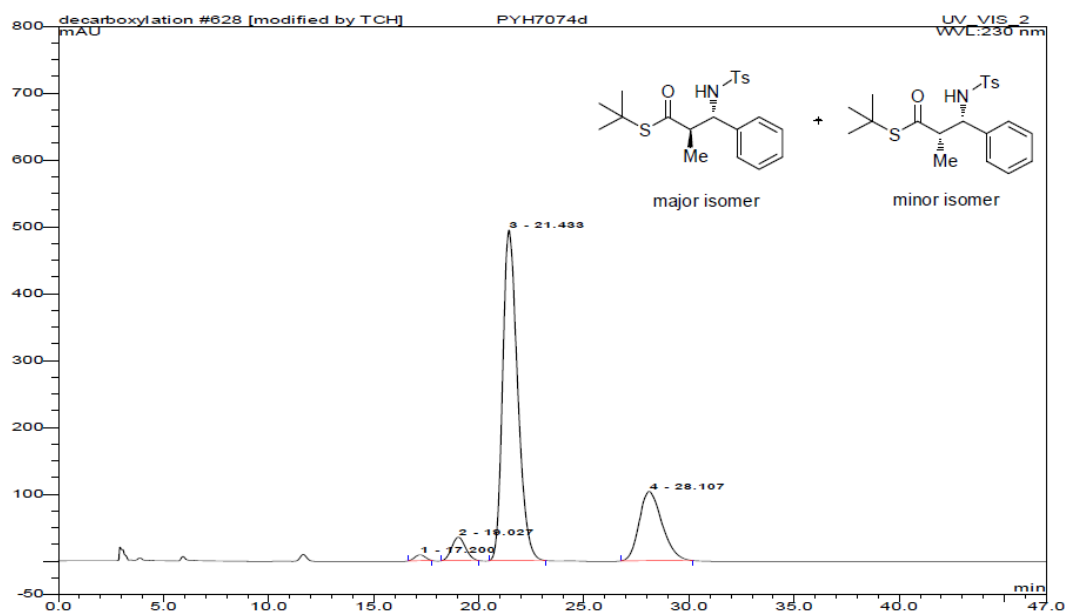
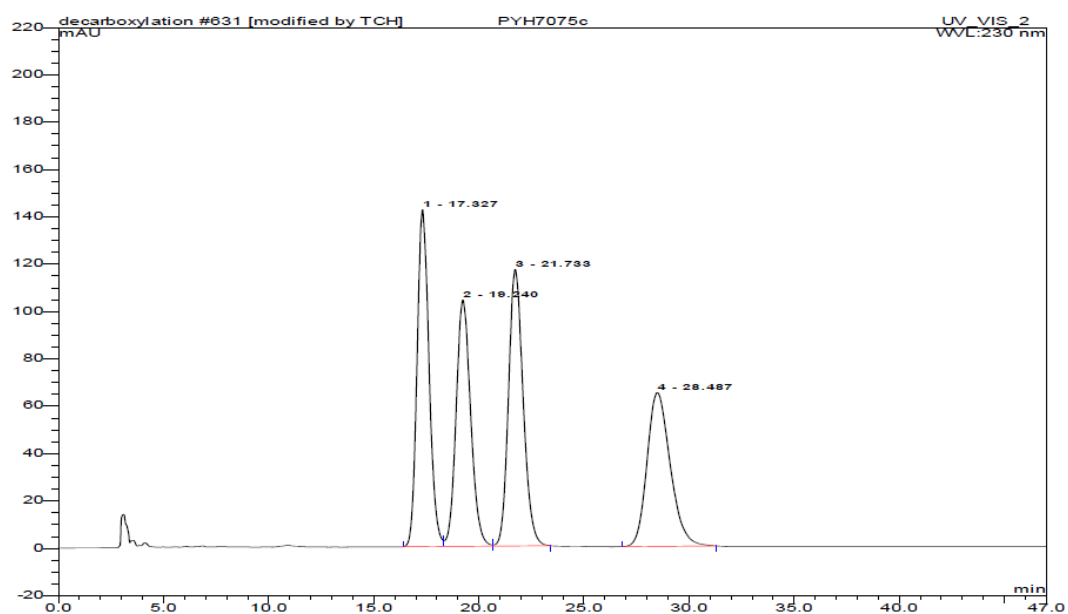


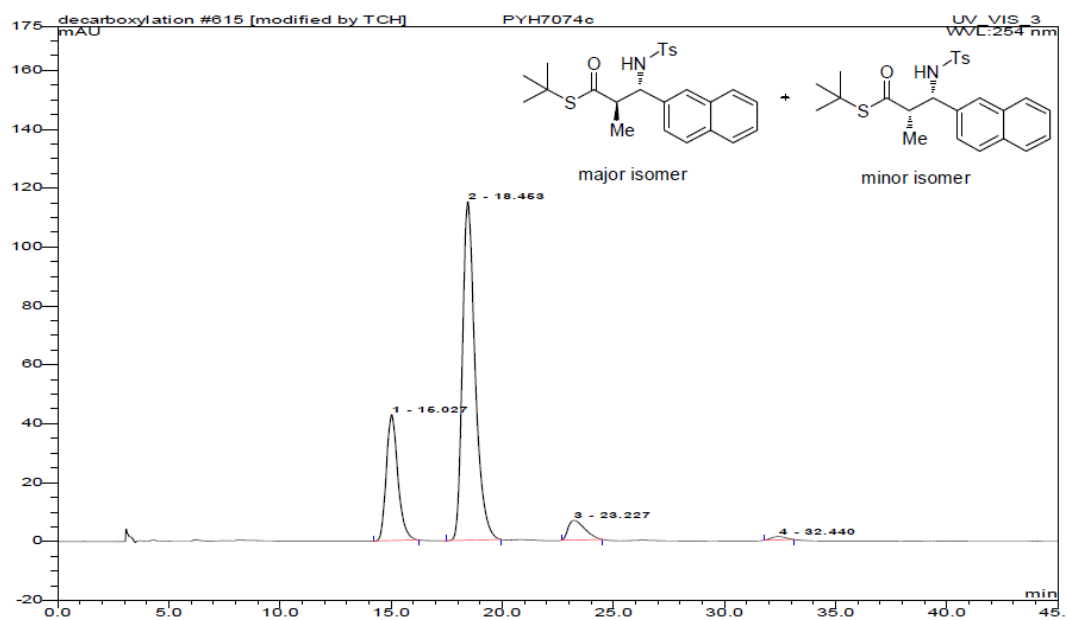
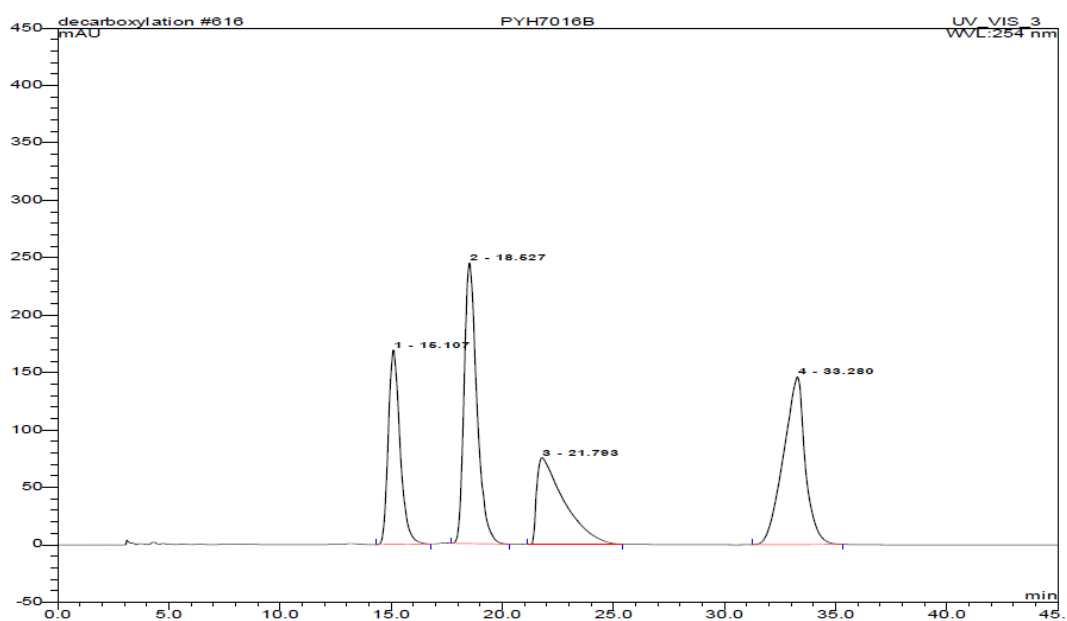


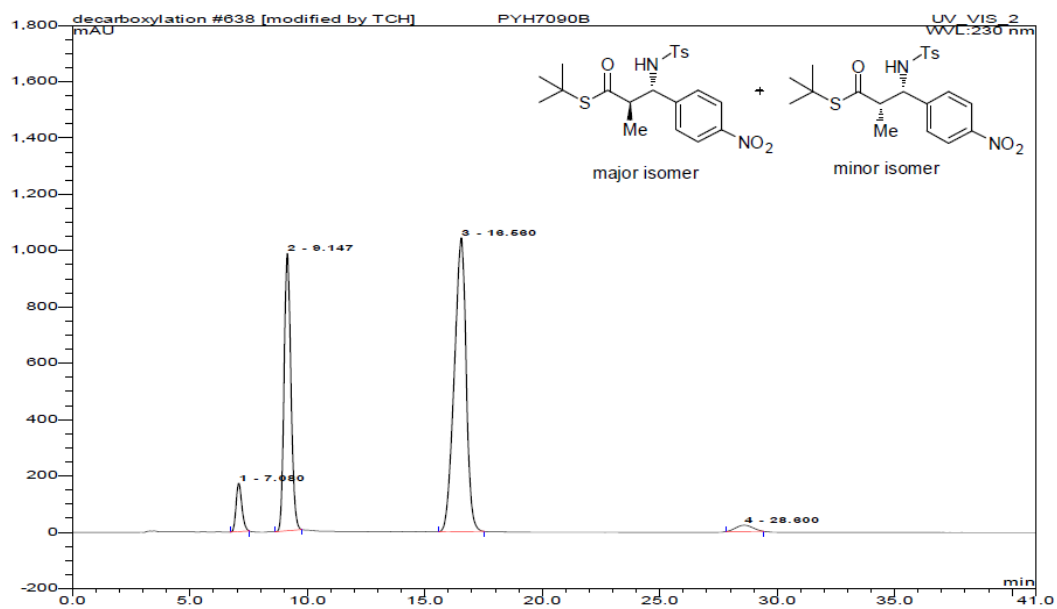
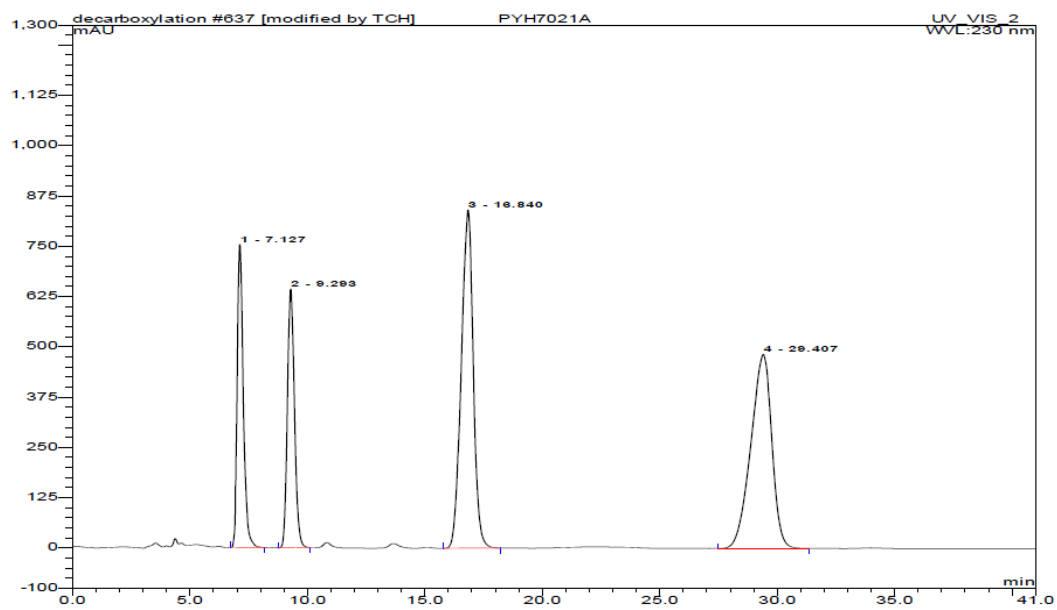


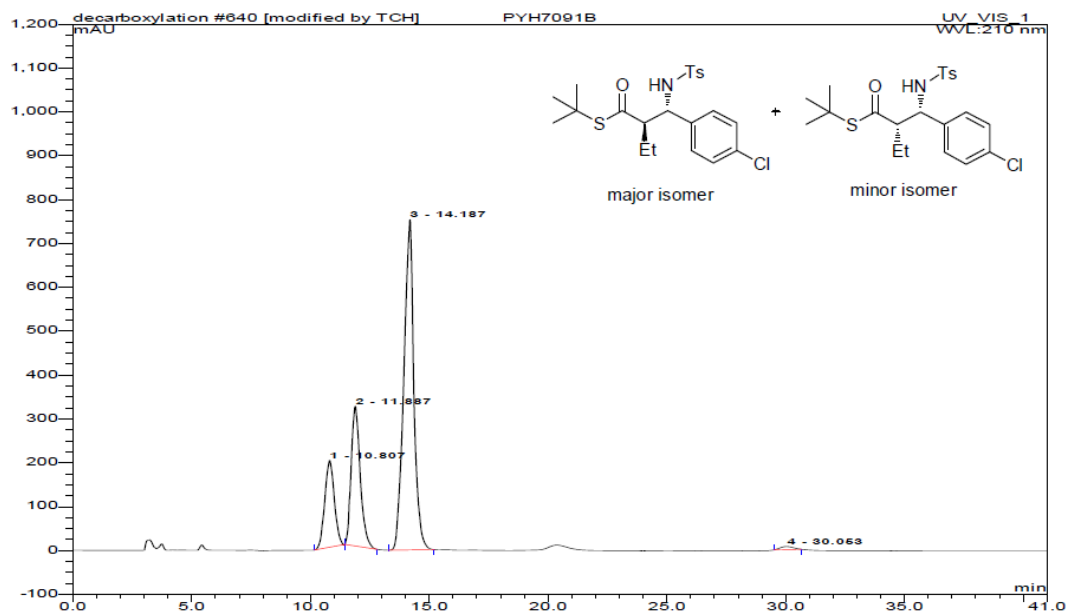
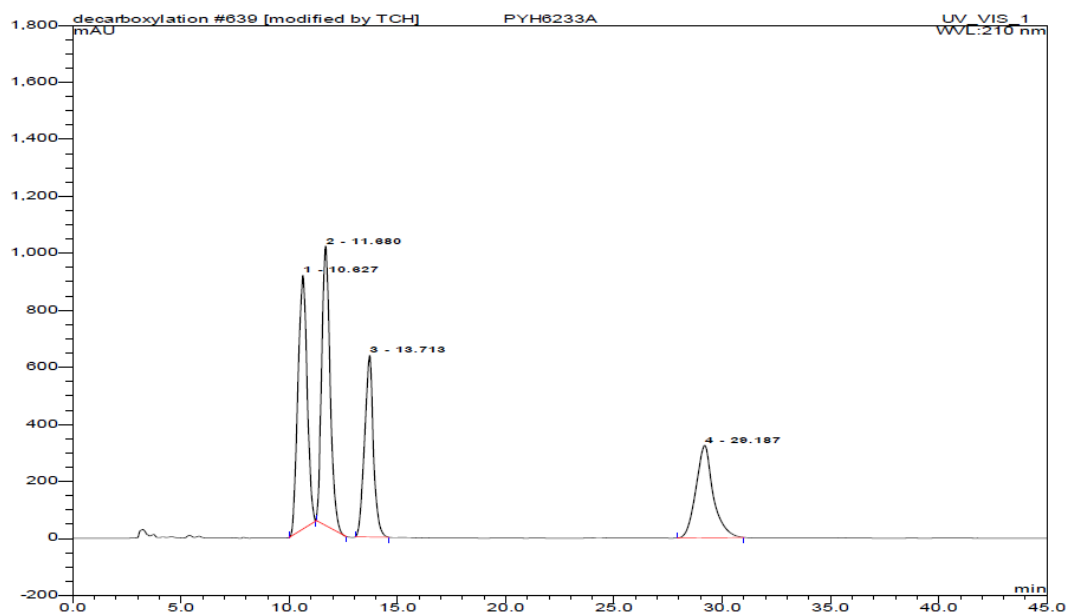


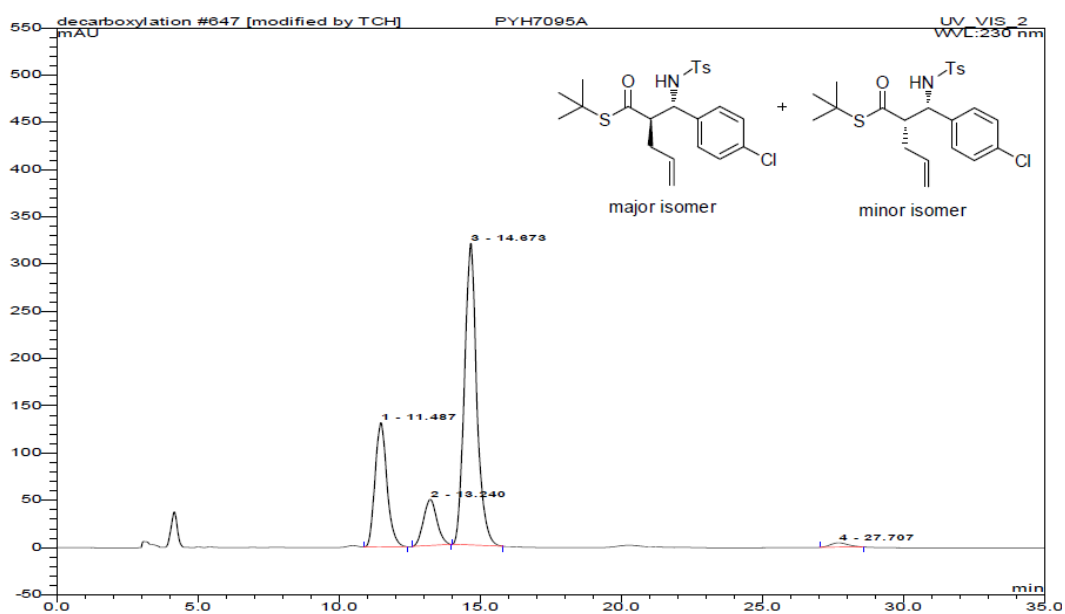
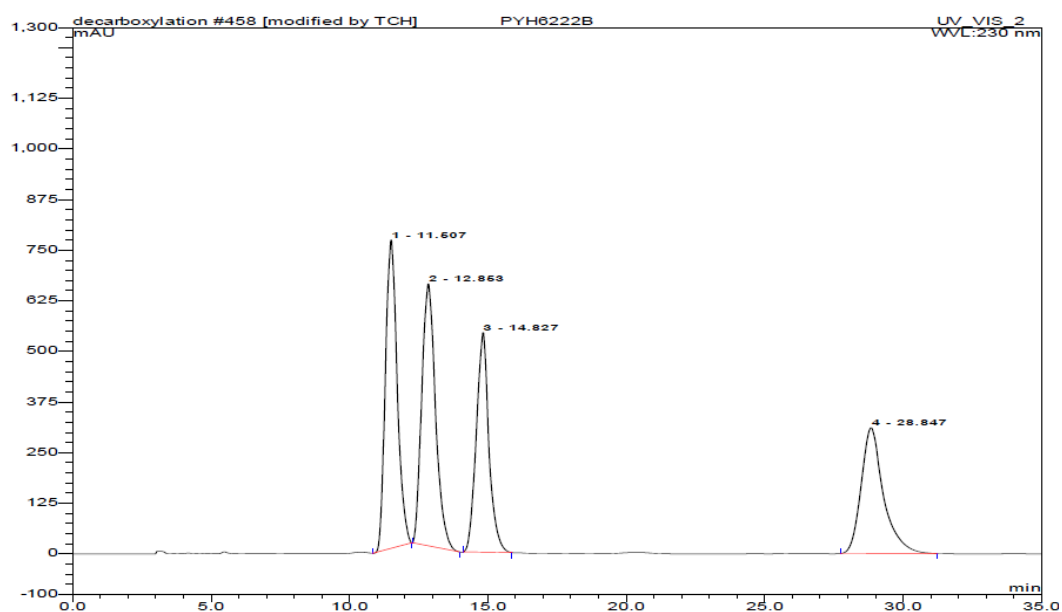


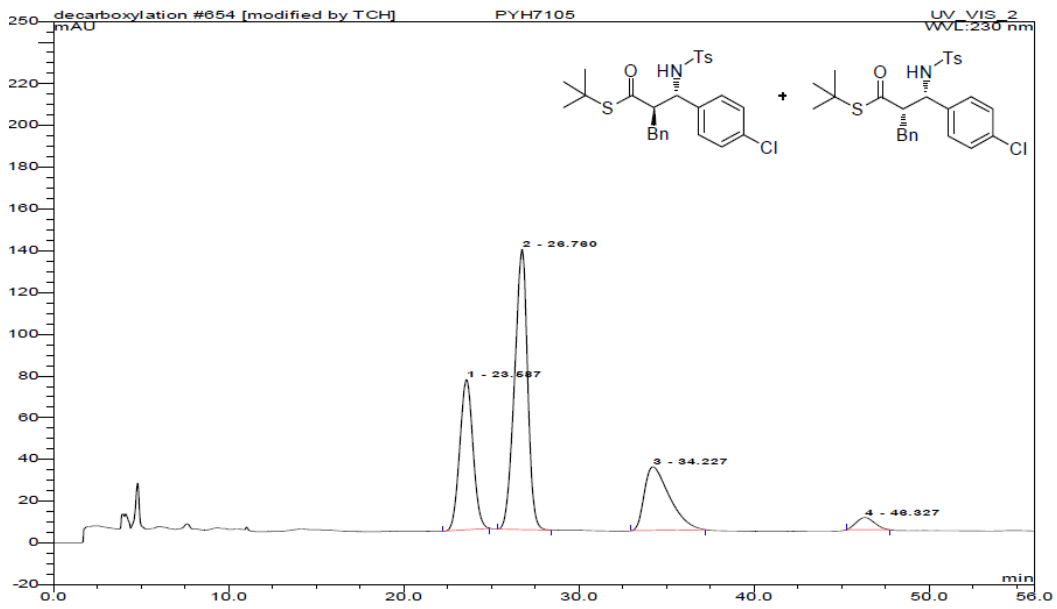
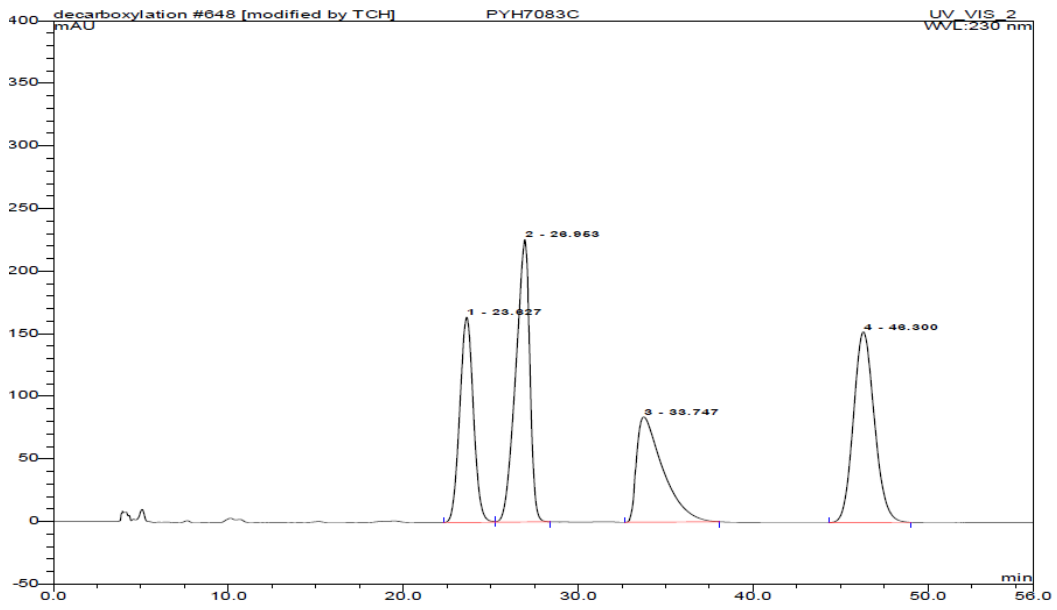


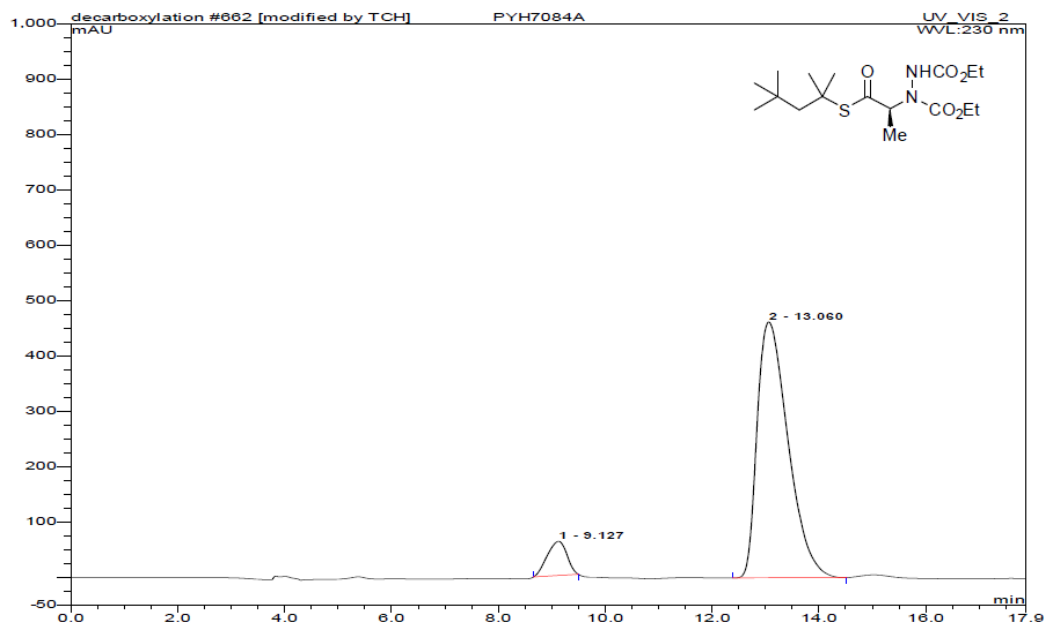
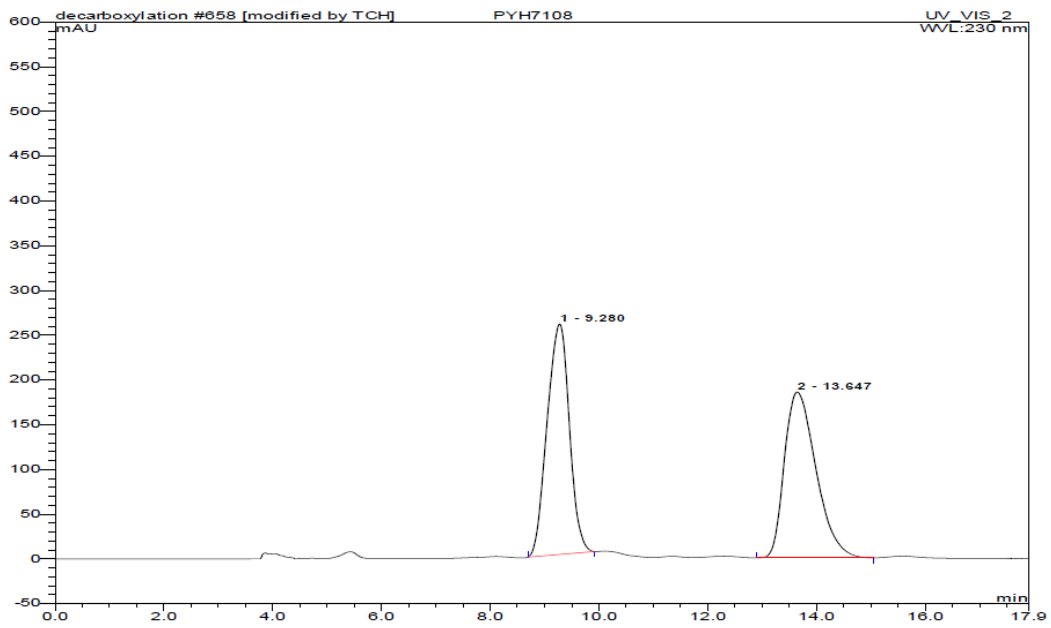


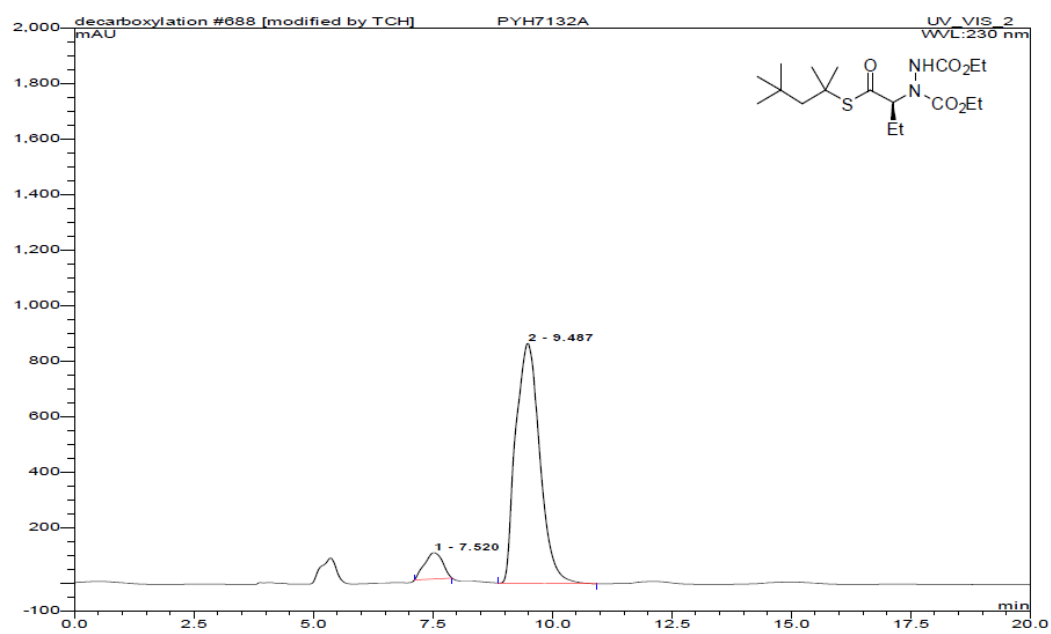
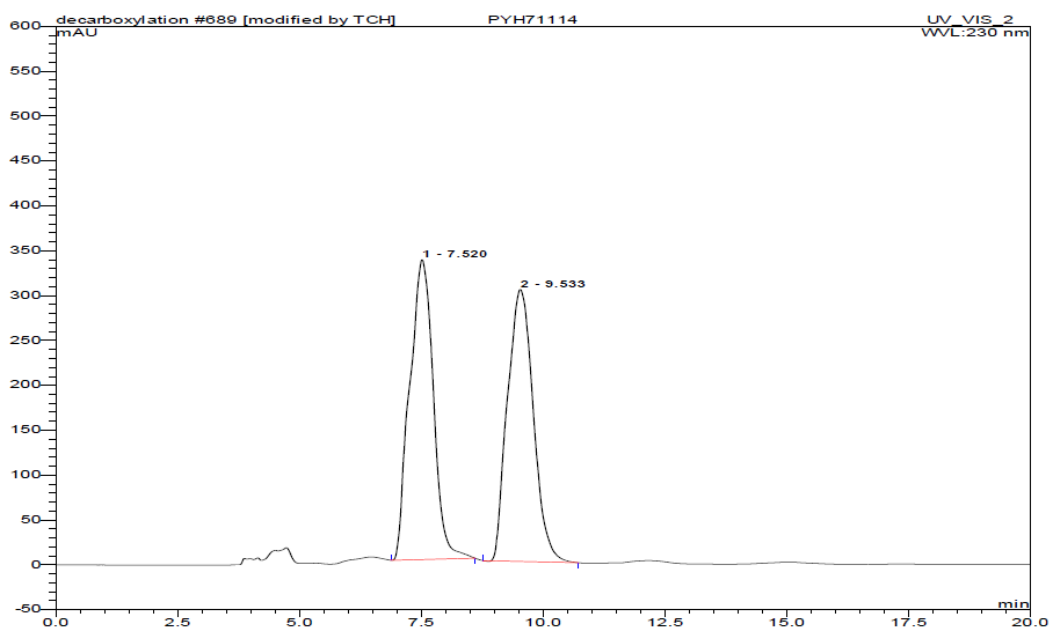


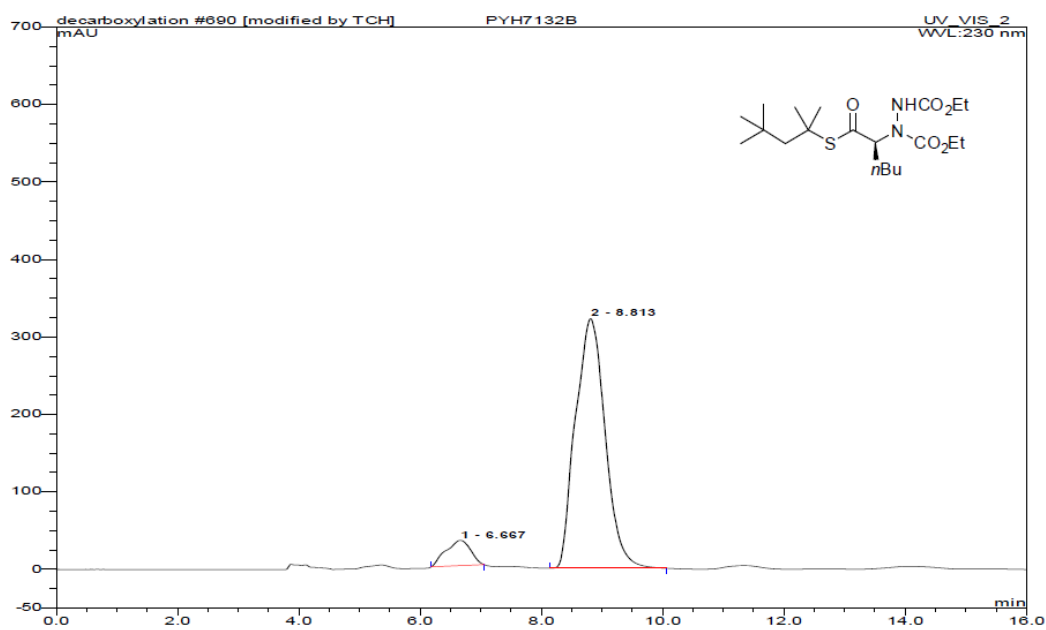
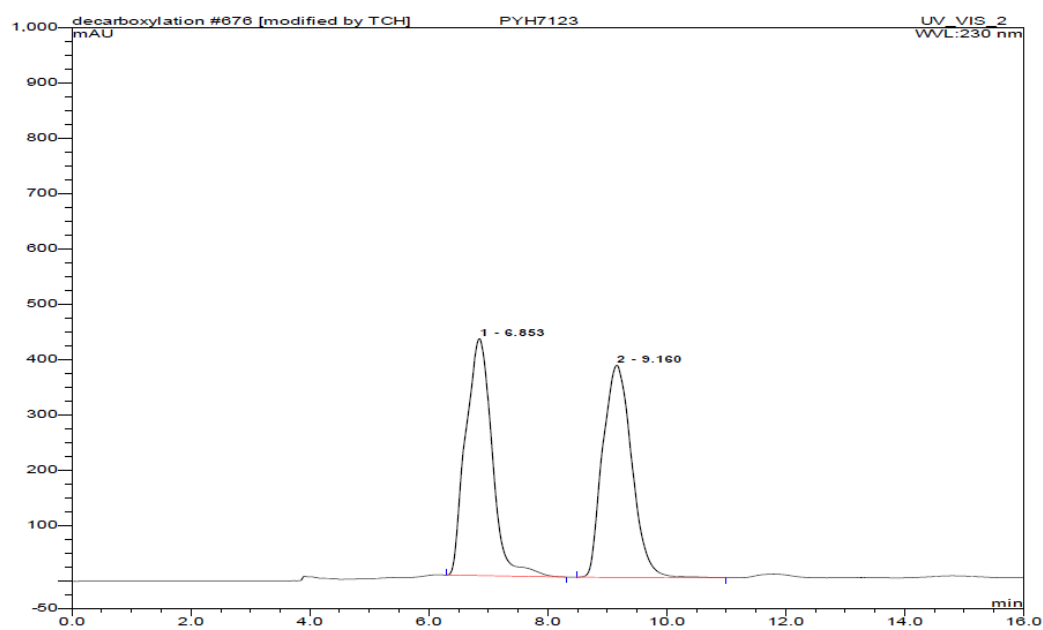


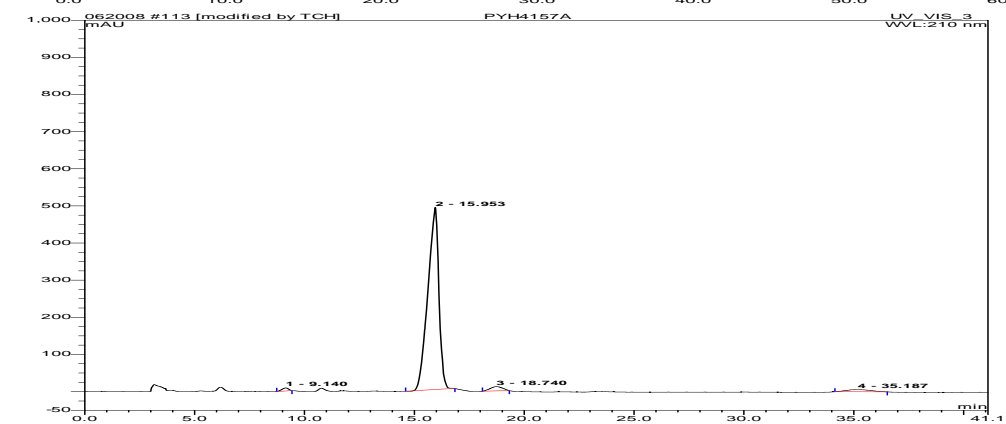
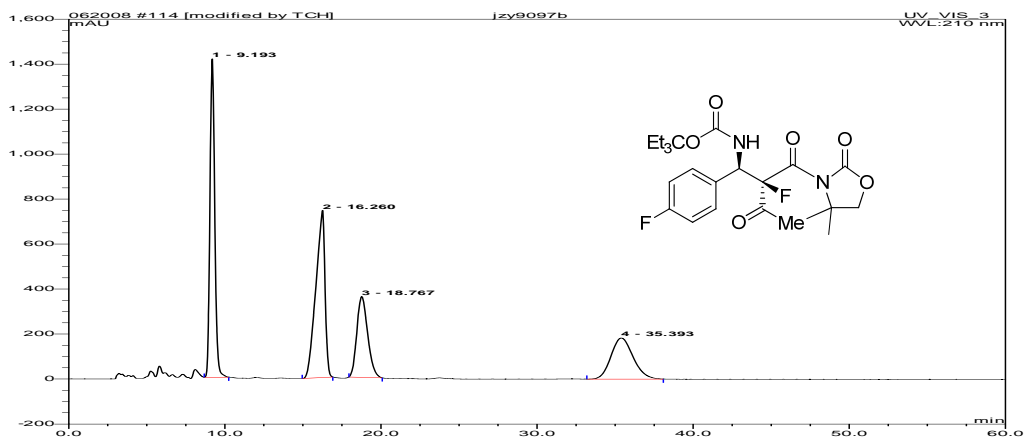
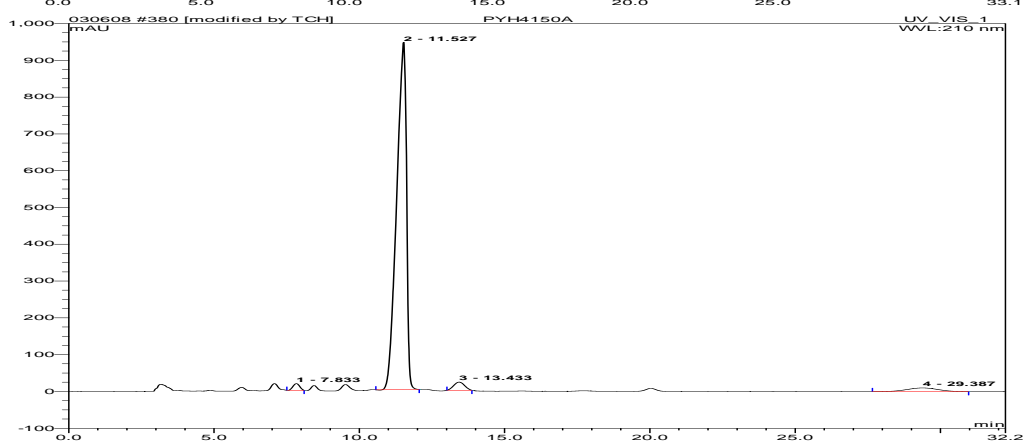
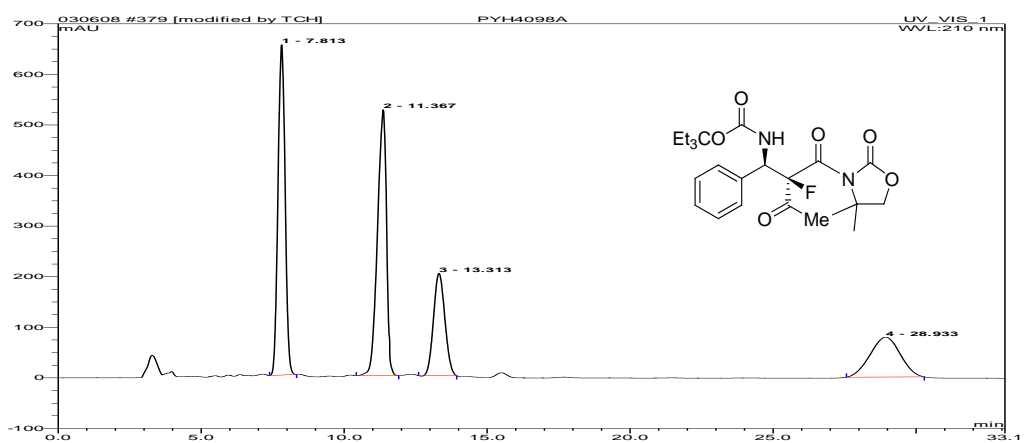


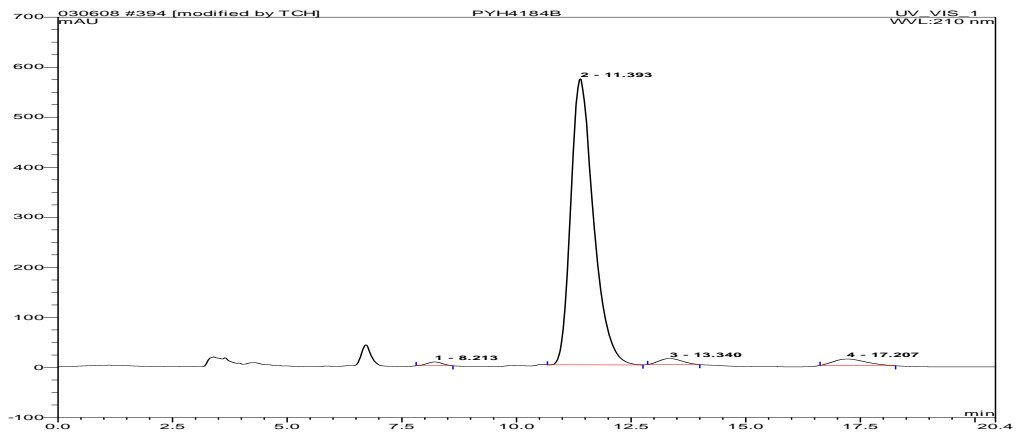
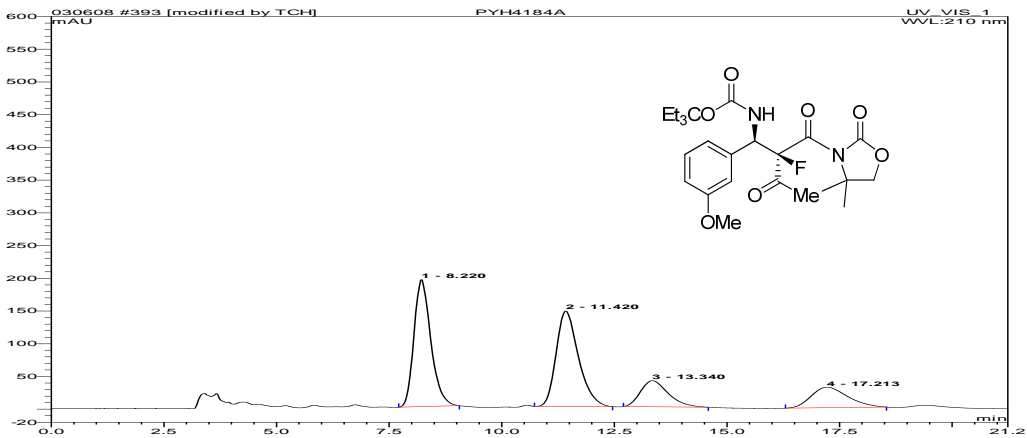
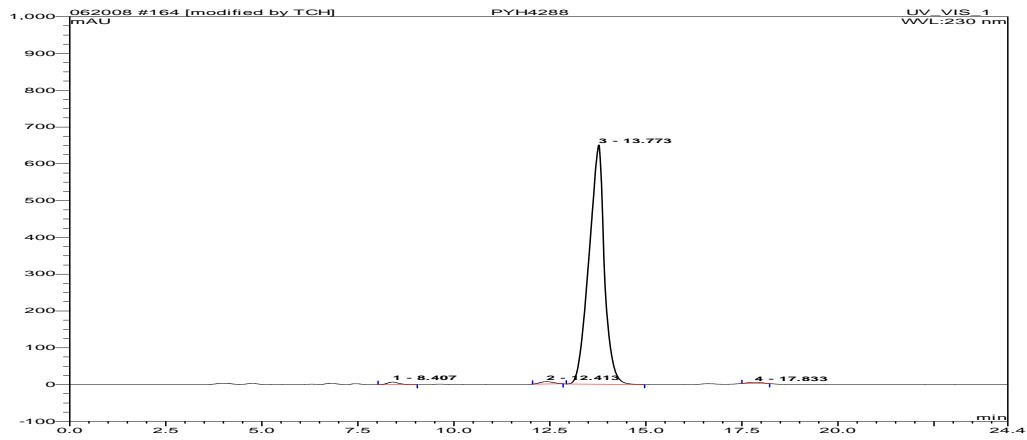
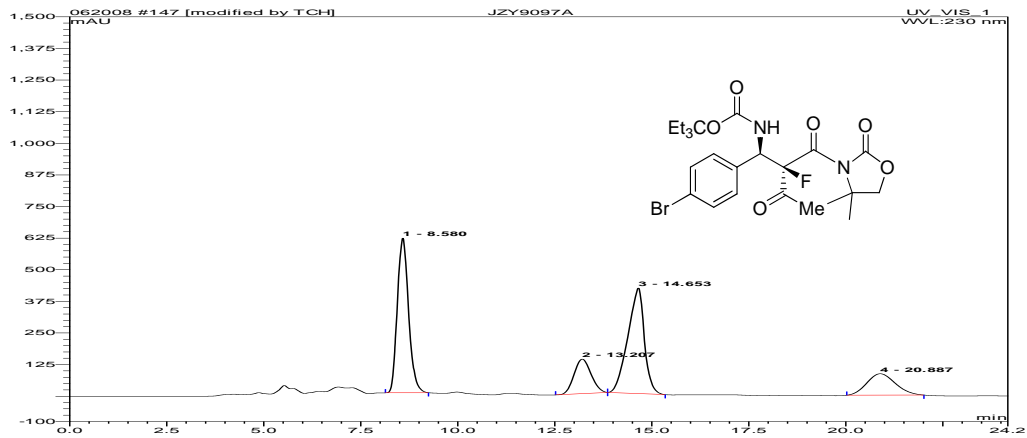


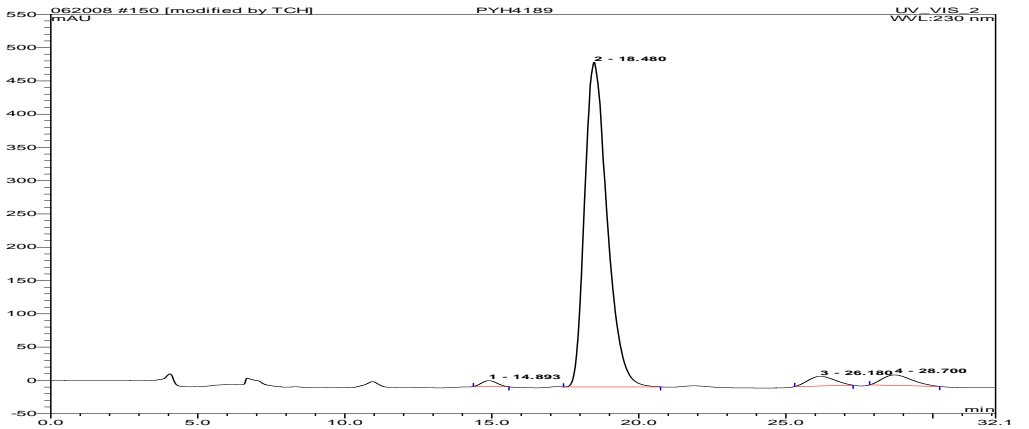
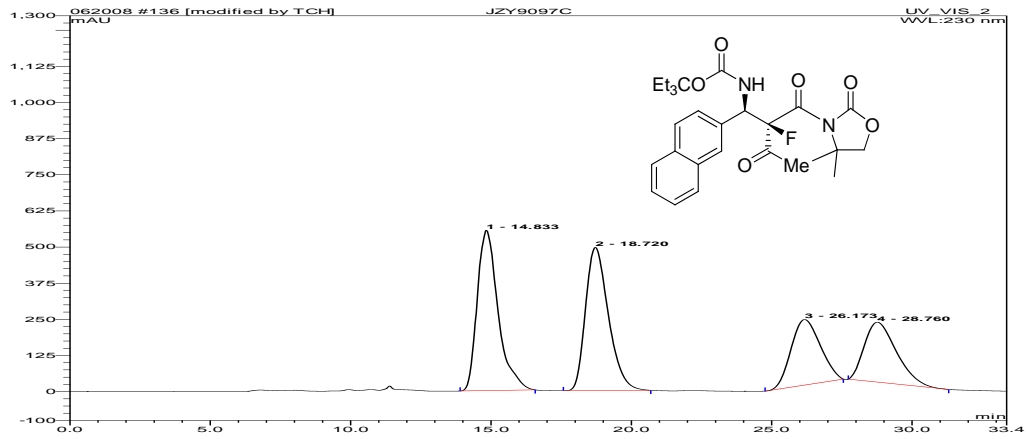
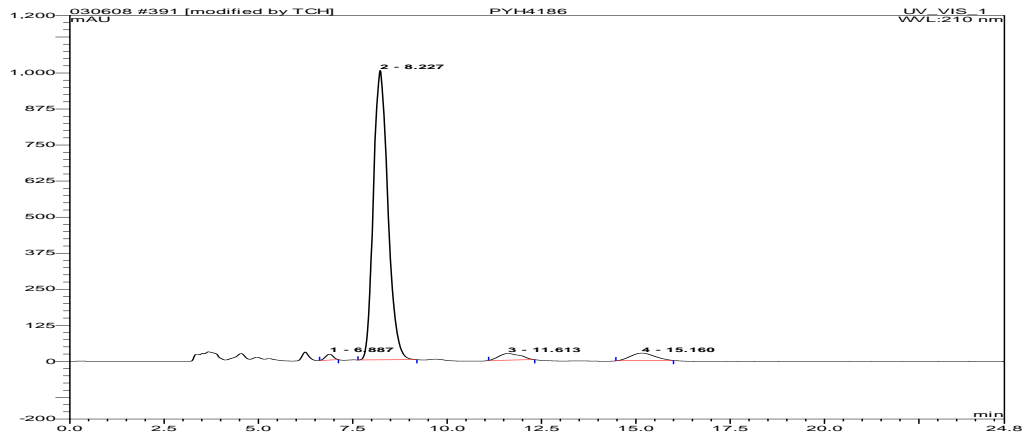
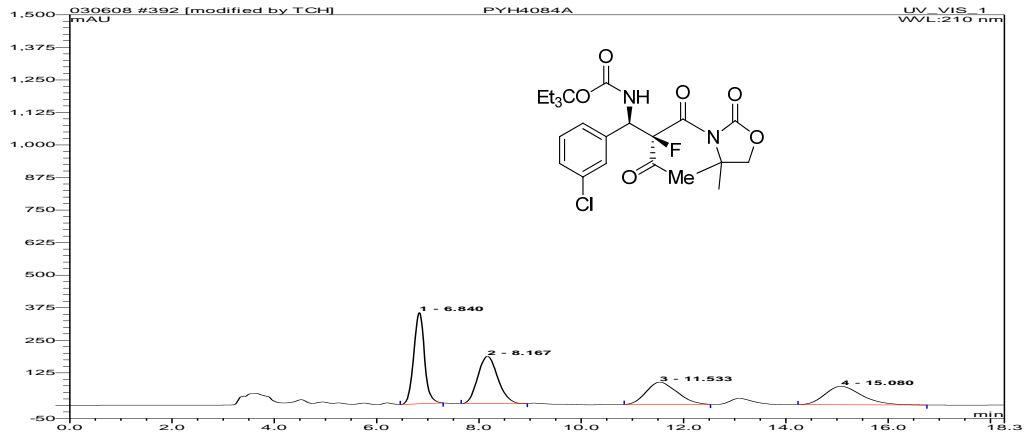


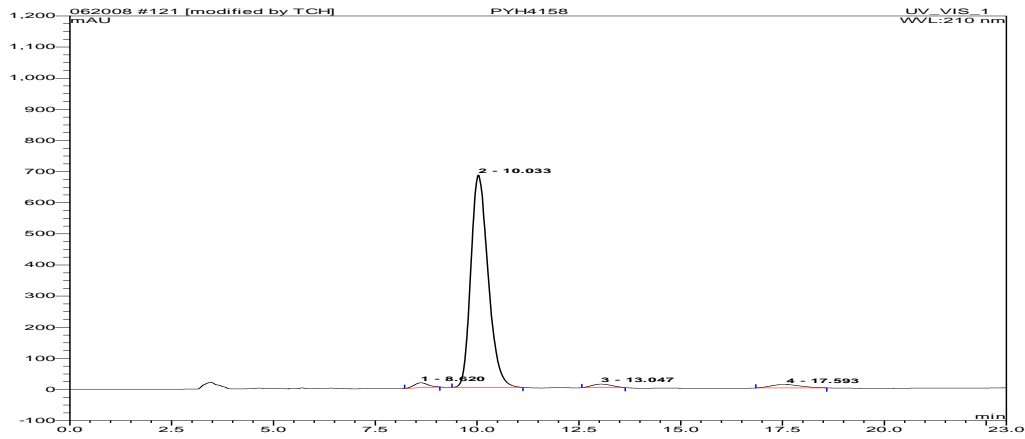
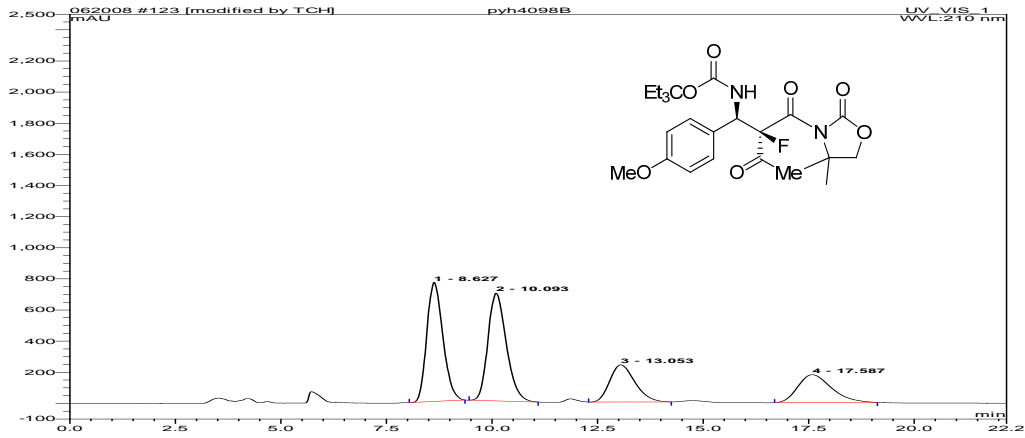
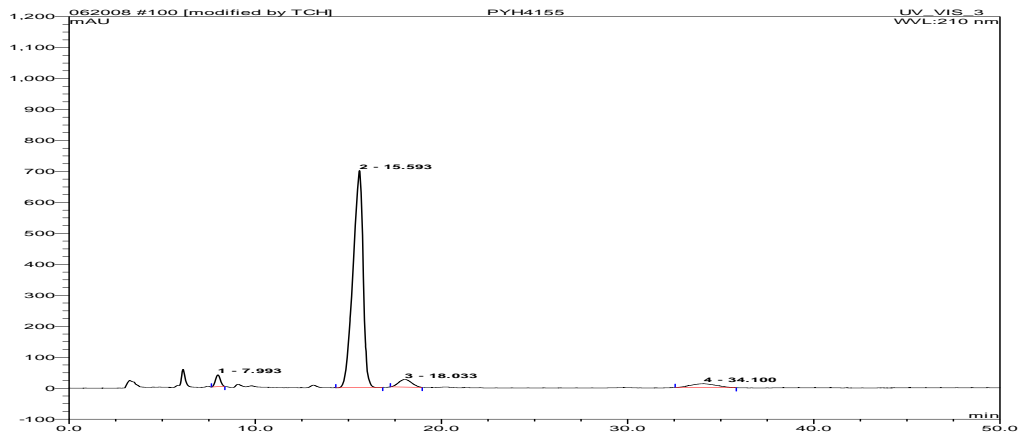
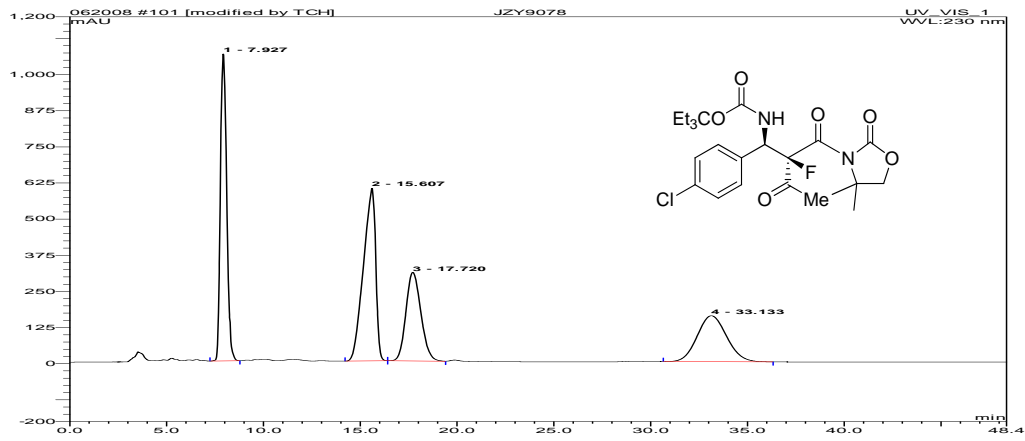


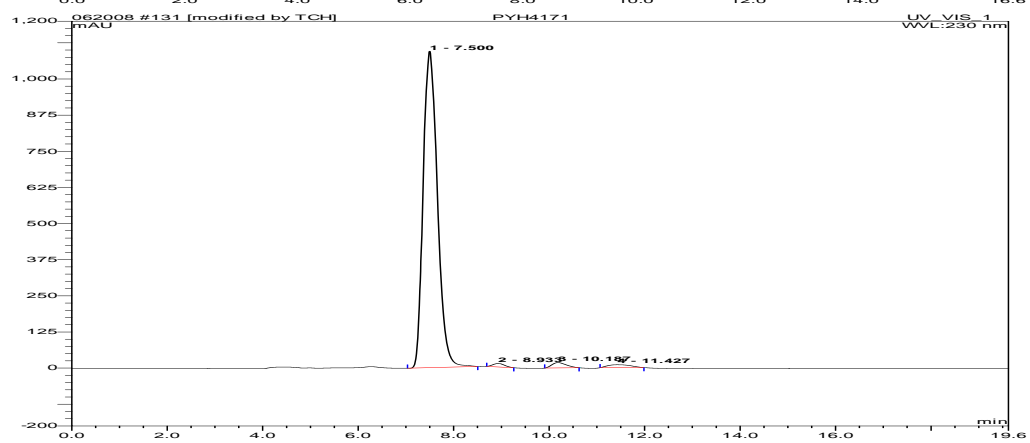
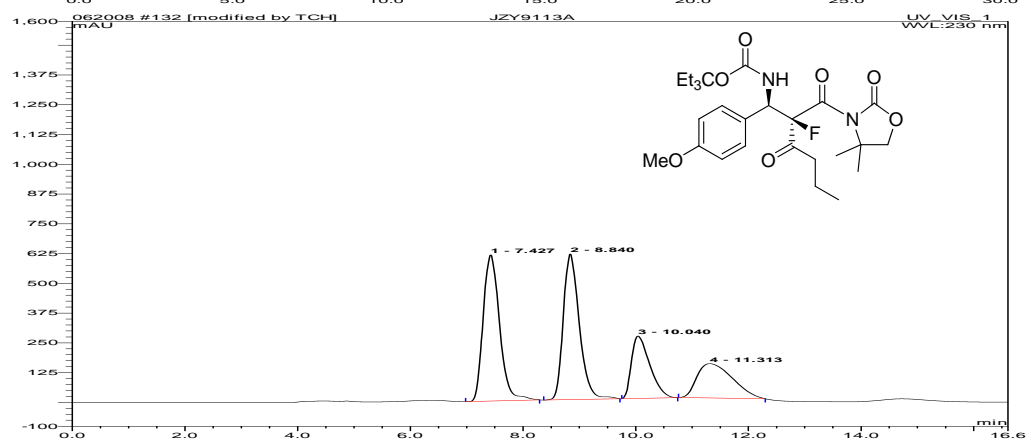
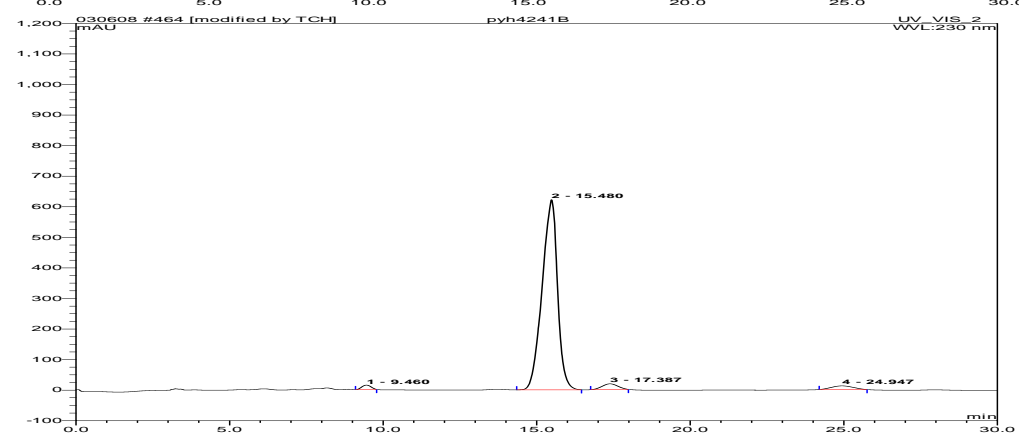
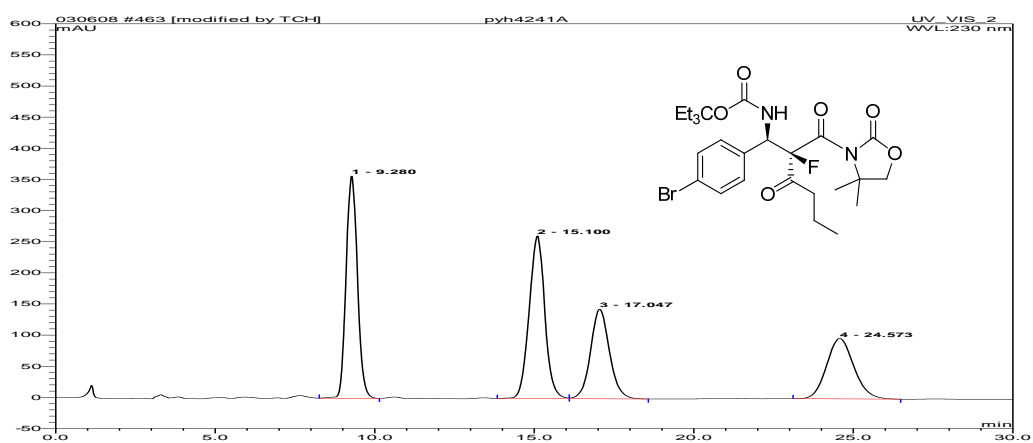


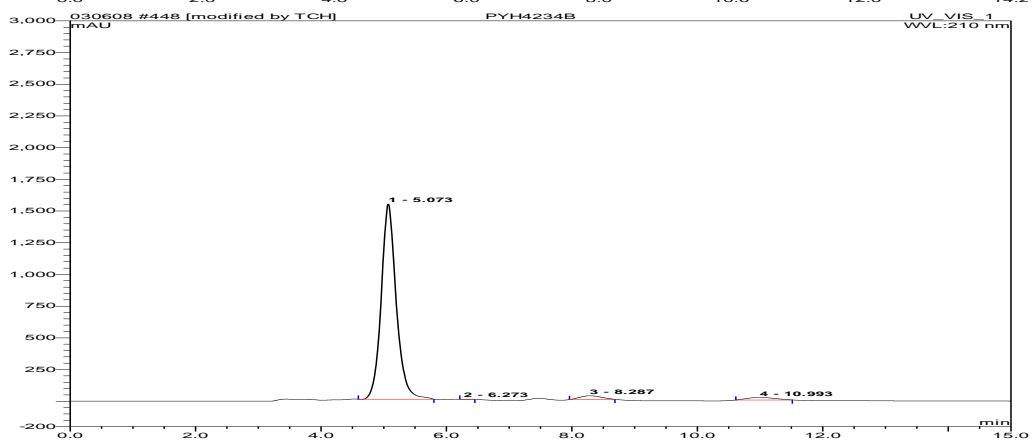
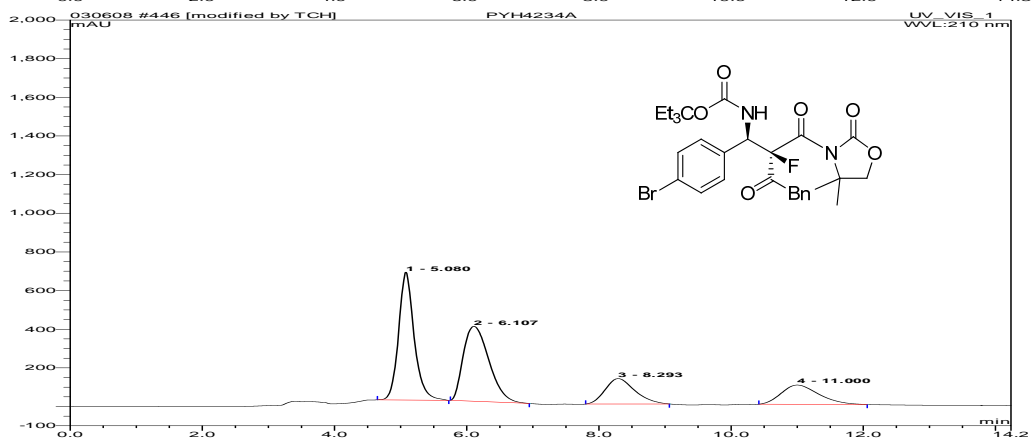
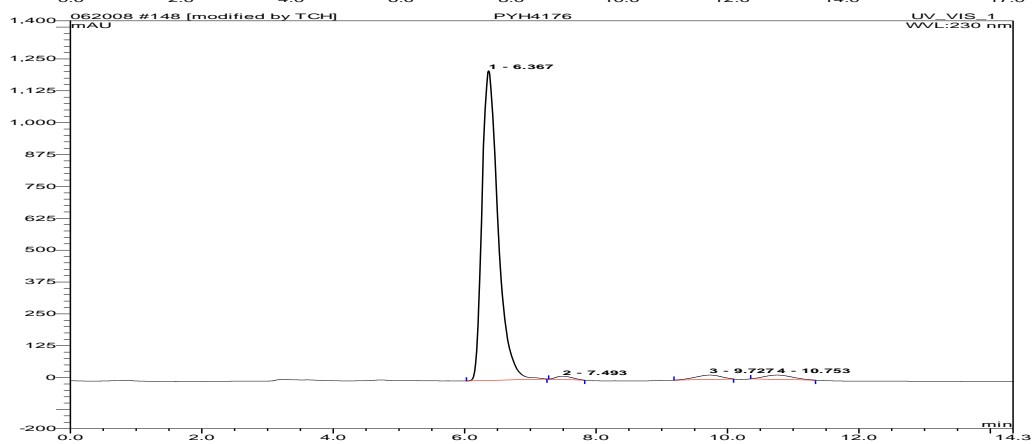
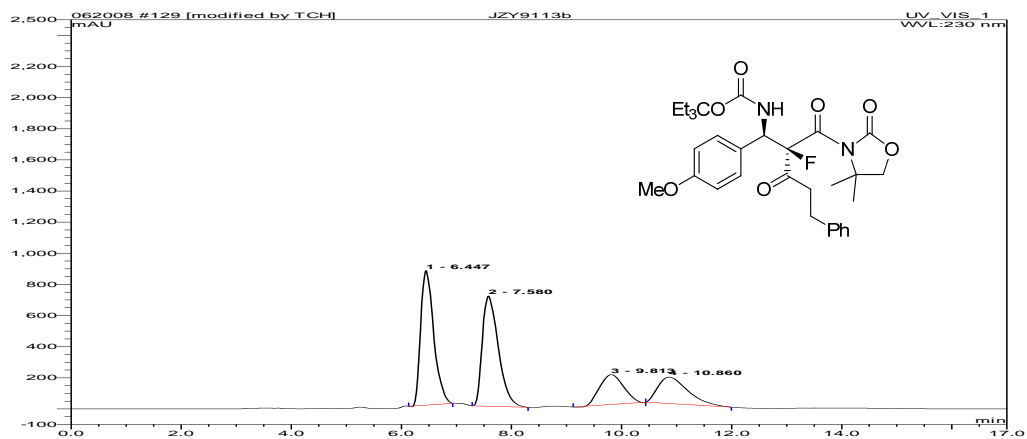


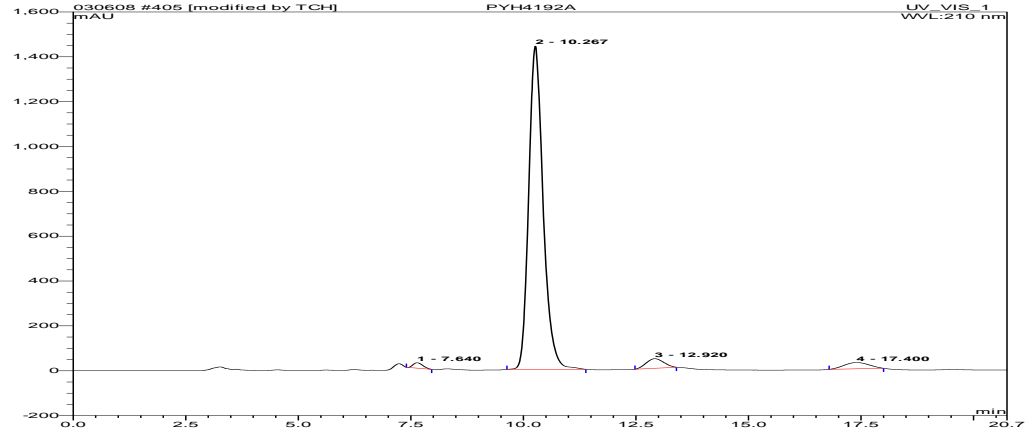
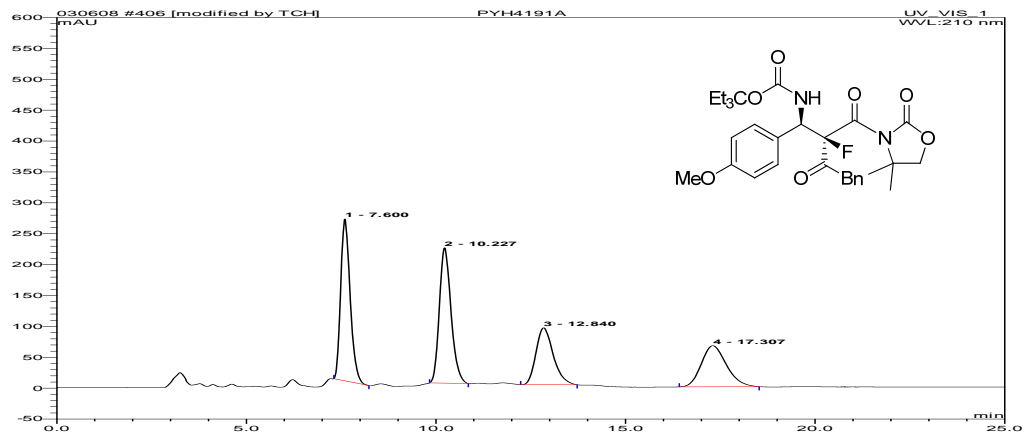
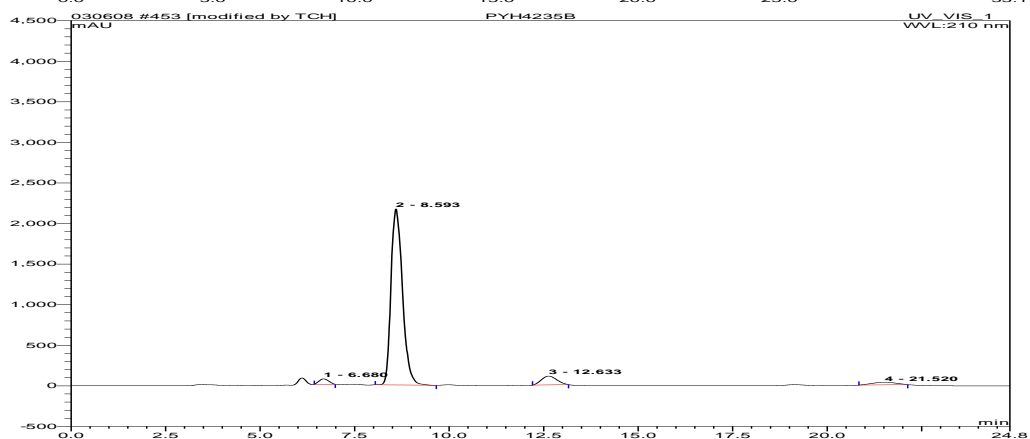
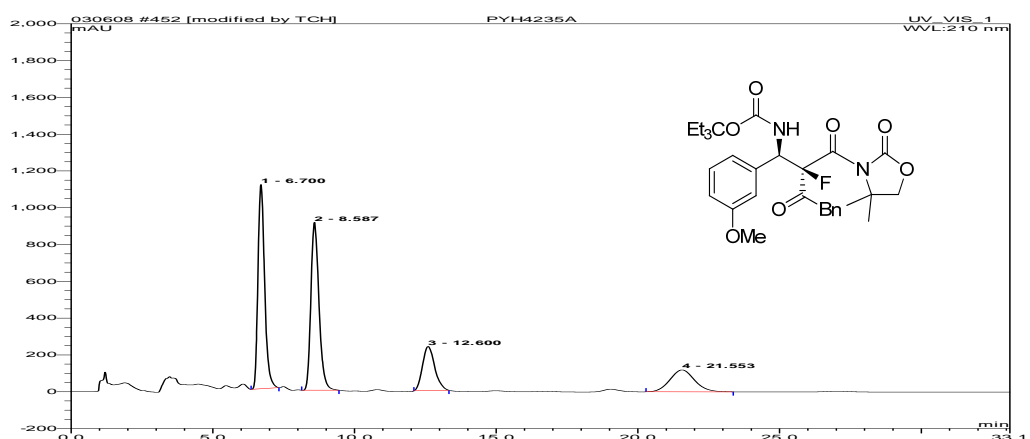


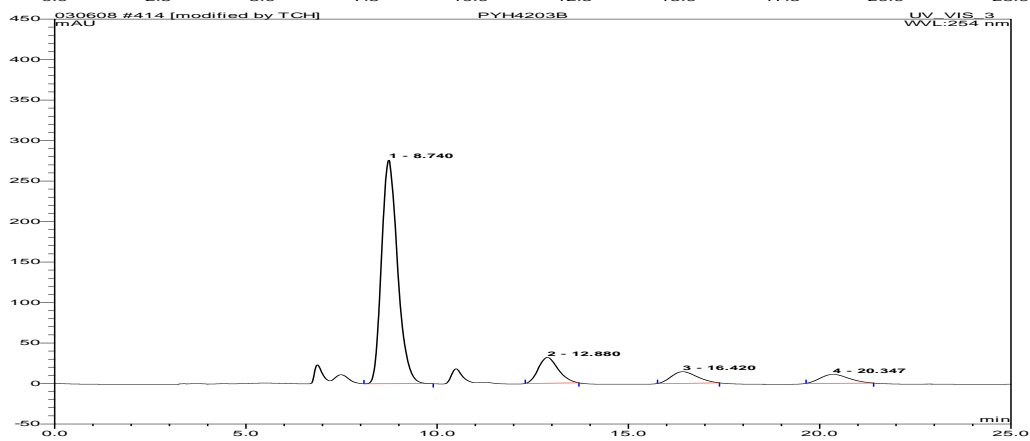
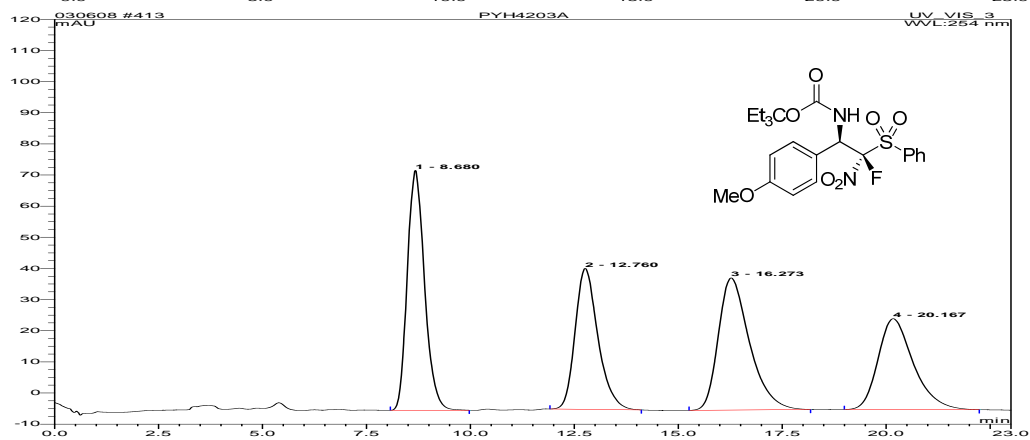
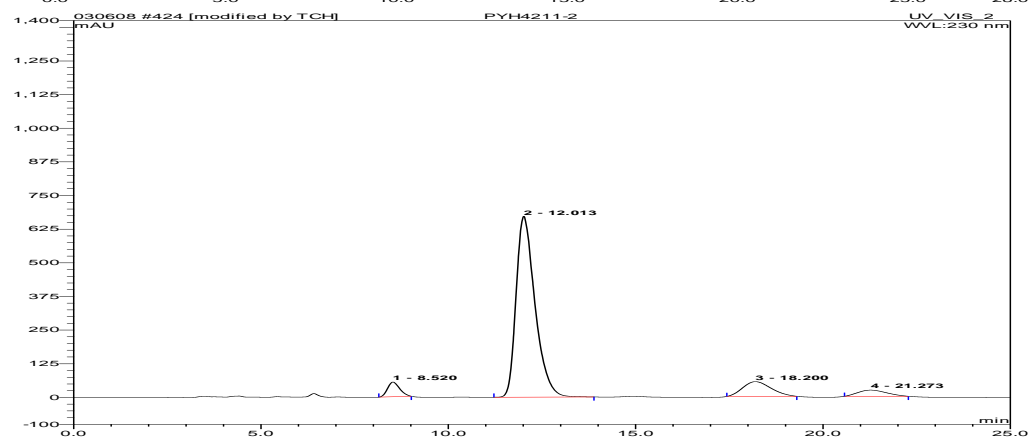
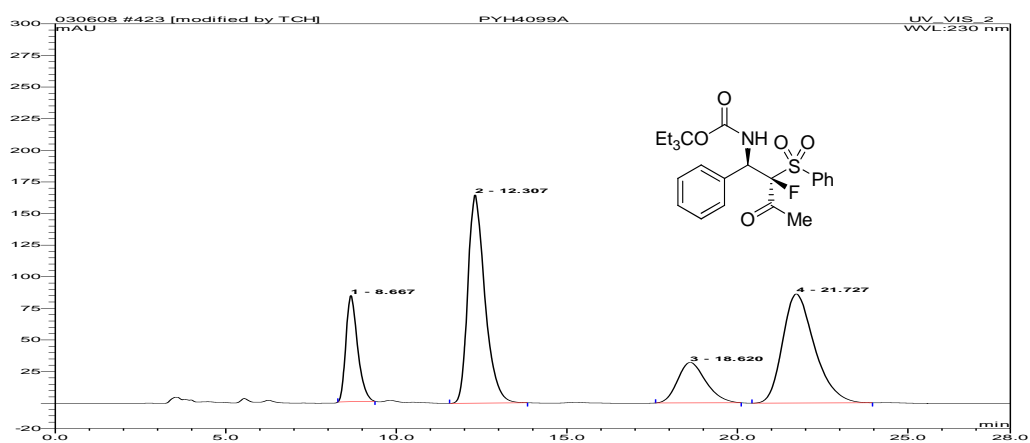












## Publications

1. **Pan Yuanhang**, Wang Shuai, Kee Choon Wee, Loh Kian Ping, Tan Choon-Hong\* “Graphene Oxide and Rose Bengal: Oxidative C-H Functionalization of Tertiary Amines using Visible Light” *Green Chem.* **2011**, *13*, 3341.
2. **Pan Yuanhang**, Kee Choon Wee, Chen Li, Tan Choon-Hong\* “Dehydrogenative Coupling Reactions Catalyzed by Rose Bengal Using Visible Light Irradiation” *Green Chem.* *13*, 2682.
3. **Pan Yuanhang**, Tan Choon-Hong\* “Catalytic Decarboxylative Reactions, A Biomimetic Approach Inspired from Polyketides Biosynthesis” *Synthesis* **2011**, *13*, 2044. (invited review)
4. **Pan Yuanhang**, Kee Choon Wee, Jiang Zhiyong, Ma Ting, Zhao Yujun, Yang Yuanyong, Xue Hansong, Tan Choon-Hong\* “Expanding the Utility of Brønsted Base Catalysis: Biomimetic Enantioselective Decarboxylative Reactions” *Chem. Eur. J.* **2011**, *17*, 8363.
5. **Pan Yuanhang**, Zhao Yujun, Ma Ting, Yang Yuanyong, Liu Hongjun, Jiang Zhiyong\*, Tan Choon-Hong\* “Enantioselective Synthesis of  $\alpha$ -Fluorinated  $\beta$ -Amino Acid Derivatives by An Asymmetric Mannich Reaction and Selective Deacylation/Decarboxylation Reactions” *Chem. Eur. J.* **2010**, *16*, 779.
6. Zhao, Y., Lim, X., **Pan, Y.**, Zong, L., Feng, W., Tan, C.-H.\*, Huang, K.-W.\* “Asymmetric H/D Exchange Reactions of Fluorinated Aromatic Ketones” *Chem. Comm.* **2012**, DOI: 10.1039/c1cc00000x.
7. Li, L., Chen, W., Yang, W., **Pan, Y.**, Liu, H., Tan, C.-H.\*, Jiang, Z.\* “Bicyclic Guanidine-Catalyzed Asymmetric Michael Additions of 3-Benzyl Substituted Oxindoles to N-Maleimides” *Chem. Comm.* **2012**, DOI: 10.1039/c1cc00000x.
8. Yang, W., Tan, D., Lee, R., Li, L., **Pan, Y.**, Huang, K.-W., Tan, C.-H.\*, Jiang, Z.\* “Catalytic Diastereoselective Tandem Conjugate Addition–Elimination Reaction of Morita–Baylis–Hillman Adducts by C-C Bond Cleavage” *Chem. Asian J.* **2012**, *7*, 771.
9. Zhao, Y., **Pan, Y.**, Sim, S.-B., Tan, C.-H.\* “Enantioselective Organocatalytic Fluorination Using Organofluoro Nucleophiles” *Org. Biomol. Chem.*, **2012**, *10*, 479. (invited review)
10. Zhao, Y., **Pan, Y.**, Liu, H., Yang, Y., Jiang, Z.\*, Tan, C.-H.\* “Fluorinated Aromatic Ketones as Nucleophiles in the Asymmetric Organocatalytic Formation

- of C-C and C-N Bonds: A Facile Route to the Construction of Fluorinated Quaternary Stereogenic Centers” *Chem. Eur. J.* **2011**, *17*, 3571.
11. Yang, W., Wei, X., **Pan, Y.**, Lee, R., Zhu, B., Liu, H., Yan, L., Huang, K.-W\*, Jiang, Z.\*, Tan, C.-H.\* “Highly Enantio- and Diastereoselective Synthesis of  $\beta$ -Methyl- $\gamma$ -monofluoromethyl Substituted Alcohols” *Chem. Eur. J.* **2011**, *17*, 8066.
  12. Zhu, B., Yan, L., **Pan, Y.**, Lee, R., Liu, H., Han, Z., Huang, K.-W., Jiang, Z.\*, Tan, C.-H.\* “Lewis Base Catalyzed Enantioselective Allylic Hydroxylation of Morita Baylis Hillman Carbonates with Water” *J. Org. Chem.* **2011**, *76*, 6894.
  13. Ma, T., Fu, X., Kee, C., Zong, L., **Pan, Y.**, Huang, K.-W., Tan, C.-H.\* “Pentamidium-Catalyzed Enantioselective Phase-Transfer Conjugate Addition Reactions” *J. Am. Chem. Soc.*, **2011**, *133*, 2828.
  14. Zhao, F., Zhang, W., Yang, Y., **Pan, Y.**, Chen, W., Liu, H., Yan, L.\*, Tan, C.-H.\*, Jiang, Z.\* “Synthesis of Sulfur-Substituted  $\alpha$ -Stereogenic Amides and Ketones: Highly Enantioselective Sulfa-Michael Additions of 1,4-Dicarbonyl but-2-enes” *Adv. Synth. Catal.* **2011**, *353*, 2624.
  15. Liu, H., Feng, W., Kee, C. W., Zhao, Y., Leow, D., **Pan, Y.**, Tan, C.-H.\* “Organic Dye Photocatalyzed  $\alpha$ -Oxyamination through Irradiation with Visible Light” *Green Chem.* **2010**, *12*, 953.
  16. Jiang, Z., **Pan, Y.**, Zhao, Y., Ma, T., Lee, Richmond, Yang, Y., Huang, K.-W., Wong, M. W.\*, Tan, C.-H.\* “Synthesis of Chiral Quaternary Carbon Centre Bearing A Fluorine Atom: Enantio- and Diastereoselective Guanidine-Catalyzed Addition of Fluorocarbon Nucleophiles” *Angew. Chem. Int. Ed.* **2009**, *48*, 3627. (*Hot paper Chosen by Angewandte Chemie*)
  17. Jiang, Z., Yang, Y., **Pan, Y.**, Zhao, Y., Liu, H., Tan, C.-H.\* “Synthesis of  $\alpha$ -Stereogenic Amides and Ketones via Enantioselective Conjugate Addition of 1,4-Dicarbonyl but-2-enes” *Chem. Eur. J.* **2009**, *15*, 4925.
  18. Liu, H., **Pan, Y.**, Tan, C.-H.\* “Sodium Nitrite (NaNO<sub>2</sub>) Catalyzed Iodo-Cyclization of Alkenes and Alkynes Using Molecular Oxygen” *Tetrahedron Lett.* **2008**, *49*, 4424.